

**WIDE AREA DAMPING CONTROLLER  
DESIGN AND IMPLEMENTATION**

BY

**ABDULMOHSEN FAHAD AL-MULHIM**

A Thesis Presented to the  
DEANSHIP OF GRADUATE STUDIES

**KING FAHD UNIVERSITY OF PETROLEUM & MINERALS**

DHAHRAN, SAUDI ARABIA

In Partial Fulfillment of the  
Requirements for the Degree of

**MASTER OF SCIENCE**

In

**ELECTRICAL ENGINEERING**

**MAY 2013**

KING FAHD UNIVERSITY OF PETROLEUM & MINERALS

DHAHRAN- 31261, SAUDI ARABIA

DEANSHIP OF GRADUATE STUDIES

This thesis, written by

ABDULMOHSEN FAHAD AL-MULHIM

under the direction his thesis advisor and approved by his thesis committee, has been presented and accepted by the Dean of Graduate Studies, in partial fulfillment of the requirements for the degree of

MASTER OF SCIENCE IN ELECTRICAL ENGINEERING

Thesis Committee



Dr. Mohammad A. Abido  
(Advisor)



Dr. Ali A. Al-Shaikhi  
Department Chairman



Dr. Zakariya Al-Hamouz  
(Member)



Dr. Salam A. Zummo  
Dean of Graduate Studies



Dr. Ibrahim O. Habiballah  
(Member)

25/12/13

Date



© Abdulmohsen Al-Mulhim

2013

Dedicated to  
My Beloved Parents,  
My Sincere Wife  
and  
My Lovely Daughters, Shada and Aljawhara



## ACKNOWLEDGMENTS

In the name of Allah, the Most Gracious and the Most Merciful. Prayers and peace be upon Him prophet Mohammed, the last messenger for all humankind.

First and foremost, all praise and deep thanks are due to Allah, who helped and guided me through the challenges of my study. Glory is to Allah who has given me the strength, patience and knowledge to continue and complete my thesis.

Allah said:

*“He is the Ever-Living; there is no god except Him, so call upon Him, being sincere to Him in religion. All praise is due to Allah, Lord of the worlds” (Qur’an 40:65)*

I would like to acknowledge all those who help me to complete this thesis. I would like to express my sincere gratitude to my advisor, Prof. Mohammad Abido for his guidance and constant support in helping me to conduct and complete this research. I would like also to thank my thesis committee members, Prof. Zakariya Al-Hamouz and Dr. Ibrahim Habiballah for their involvement and the time they spare to review this thesis.

Acknowledge is due to my company, Saudi Aramco for giving me the opportunity and the support to obtain this achievement.

My deepest gratitude goes to my beloved parents for their endless care, love, prayers and encouragement. May almighty God give you health and wellness, happiness, and long life of obedience to God.

I reserve this last acknowledge to my wife for her emotional support, encouragement and patience throughout the long journey of this thesis. The completion of this thesis wouldn't have been possible without her monumental support and love. Nawarh, with you my life became different.

وآخر دعوانا أن الحمد لله رب العالمين.

والصلاة والسلام على سيد المرسلين وعلى آله وصحبه أجمعين.

# TABLE OF CONTENTS

<b>ACKNOWLEDGMENTS .....</b>	<b>VII</b>
<b>LIST OF TABLES .....</b>	<b>XIII</b>
<b>LIST OF FIGURES .....</b>	<b>XV</b>
<b>LIST OF ABBREVIATIONS .....</b>	<b>XIX</b>
<b>LIST OF SYMBOLS .....</b>	<b>XX</b>
<b>ABSTRACT (ENGLISH) .....</b>	<b>XXII</b>
<b>ABSTRACT (ARABIC) .....</b>	<b>XXIII</b>
<b>CHAPTER 1 INTRODUCTION .....</b>	<b>1</b>
1.1 Overview .....	1
1.2 Thesis Motivation .....	2
1.3 Thesis Objectives .....	4
1.4 Thesis Organization.....	5
<b>CHAPTER 2 LITERATURE REVIEW .....</b>	<b>7</b>
2.1 Low Frequency Oscillations.....	7
2.2 Power System Stabilizer .....	10
2.3 Wide-Area Damping Controller .....	12
2.4 Modal Analysis as Design Technique.....	19
2.5 Real Time Digital Simulator (RTDS).....	21
2.5.1 Introduction .....	21
2.5.2 RTDS Applications .....	22
<b>CHAPTER 3 POWER SYSTEM MODELING AND ANALYSIS .....</b>	<b>26</b>



3.1	Introduction .....	26
3.2	Power System Model .....	27
3.2.1	Synchronous Generator and Exciter Models .....	27
3.2.2	Power System Stabilizer Structure .....	29
3.3	Modal Analysis.....	30
3.3.1	Participation Factors and Mode Shape .....	33
3.3.2	Controllability, Observability and Residue .....	34
3.4	Summary .....	36
<b>CHAPTER 4 WIDE AREA DAMPING CONTROL DESIGN .....</b>		<b>37</b>
4.1	Introduction .....	37
4.2	Local PSSs Placement .....	37
4.3	Design of Wide Area Damping Controller .....	39
4.3.1	WADC Placement.....	41
4.3.2	WADC With a Combination Input Signal.....	41
4.4	Controller Parameters Tuning .....	43
4.5	Summary .....	46
<b>CHAPTER 5 DESIGN OF LOCAL PSS FOR MULTIMACHINE TWO-AREA SYSTEM.....</b>		<b>47</b>
5.1	Introduction .....	47
5.2	Case Study.....	48
5.3	Modal Analysis.....	49
5.4	Local PSSs Design.....	54
5.4.1	Local PSSs Placement .....	54
5.4.2	PSSs Parameters Tuning.....	58
5.5	Non-Linear Time Domain Simulation .....	59

5.6	Summary .....	69
<b>CHAPTER 6 ANALYSIS AND DESIGN OF WADC .....</b>		<b>70</b>
6.1	Introduction .....	70
6.2	Case Study .....	71
6.3	Modal Analysis.....	72
6.4	WADC Design .....	73
6.4.1	WADC Placement.....	73
6.4.2	WADC Input Signals Selection.....	74
6.4.3	WADC Parameters Tuning .....	75
6.5	Non-Linear Time Domain Simulation .....	77
6.6	Comparison Between Local Based PSS and WADC .....	87
6.6.1	Using Typical Values for The Controller Parameters .....	87
6.6.2	WADC Parameters Optimization Using PSO Technique .....	93
6.7	Summary .....	100
<b>CHAPTER 7 REAL-TIME IMPLEMENTATION.....</b>		<b>101</b>
7.1	Introduction .....	101
7.2	Real Time Digital Simulator (RTDS) Overview .....	101
7.3	Laboratory Setup for RTDS Simulation .....	104
7.4	RTDS Simulation.....	110
7.4.1	Simulation Results .....	112
7.4.1.1	Case-1: Fault Disturbance.....	112
7.4.1.2	Case-2: Load Change Disturbance.....	121
7.4.2	RUNTIME Interface (On-Line) Results.....	127
7.4.2.1	Case-1: Fault Disturbance.....	127
7.4.2.2	Case-2: Load Change Disturbance.....	128

<b>7.5</b>	<b>RTDS Comparison Between Local Based PSS and WADC.....</b>	<b>133</b>
<b>7.5.1</b>	<b>Using Typical Values for The Controller Parameters .....</b>	<b>133</b>
<b>7.5.2</b>	<b>Using WADC Parameters Optimized By PSO Technique .....</b>	<b>138</b>
<b>7.6</b>	<b>Comparison Between Simulation and RTDS Results .....</b>	<b>141</b>
<b>7.7</b>	<b>Summary .....</b>	<b>143</b>
<b>CHAPTER 8</b>	<b>CONCLUSIONS AND FUTURE WORK .....</b>	<b>145</b>
<b>8.1</b>	<b>Conclusions .....</b>	<b>145</b>
<b>8.2</b>	<b>Future Work .....</b>	<b>148</b>
<b>APPENDICES</b>	<b>.....</b>	<b>150</b>
<b>BIBLIOGRAPHY</b>	<b>.....</b>	<b>166</b>
<b>VITAE</b>	<b>.....</b>	<b>177</b>

## LIST OF TABLES

Table 5-1: Oscillatory modes of the system without control.....	49
Table 5-2: Participation factor magnitudes of oscillatory modes .....	51
Table 5-3: Right-eigenvector elements (Corresponding to $\Delta\delta$ ).....	52
Table 5-4: Oscillatory modes shape for the system without control .....	52
Table 5-5: Oscillatory modes for the system with PSS .....	57
Table 5-6: Information required to use phase compensation technique for local PSSs....	58
Table 5-7: Local PSSs parameters .....	59
Table 5-8: Oscillatory modes for the system with tuned PSSs at G2 and G4 .....	59
Table 6-1: Oscillatory modes for the system with local PSSs .....	72
Table 6-2: Controllability measure for interarea mode (normalized, 100 % ).....	73
Table 6-3: Information required to use phase compensation technique for WADC .....	76
Table 6-4: WADC parameters .....	76
Table 6-5: Oscillatory modes for the system with local PSSs and WADC .....	77
Table 6-6: Oscillatory modes for the system with controller placed at G3 .....	88
Table 6-7: PSO Parameters .....	94
Table 6-8: WADC optimized parameters .....	95
Table 6-9: Oscillatory modes for the system with optimized WADC placed at G3.....	95
Table A-1: Generator Dynamic Data .....	150
Table A-2: System Bus Data .....	150
Table A-3: System Transmission Lines Data (in pu. Value) .....	151
Table A-4: System Load Flow Results .....	151
Table D-1: Generator parameters .....	159
Table D-2: Transformer parameters .....	159
Table D-3: Speed governor parameters.....	160
Table D-4: Exciter parameters .....	161
Table D-5: PSS2 parameters .....	162
Table D-6: PSS3 parameters .....	163
Table D-7: PSS4 parameters .....	164
Table D-8: Load parameters .....	165

Table D-9: Transmission line data .....	165
---	-----

## LIST OF FIGURES

Figure 2-1: Classification of Power System Stability .....	9
Figure 3-1: IEEE type-ST1 excitation system with PSS.....	29
Figure 3-2: Linearized model of the $i$ th machine in multimachine power system.....	32
Figure 4-1: Wide Area Damping Control System Structure .....	40
Figure 4-2: Wide Area Damping Controller .....	44
Figure 5-1: Two area four machine system .....	48
Figure 5-2: Mode shape of rotor angle (Mode-7) - System without control.....	53
Figure 5-3: Mode shape of rotor angle (Mode-9) - System without control.....	53
Figure 5-4: Mode shape of rotor angle (Mode-11) - System without control.....	54
Figure 5-5: Controllability, observability and residue of Mode-7 .....	56
Figure 5-6: Controllability, observability and residue of Mode-9 .....	57
Figure 5-7: Rotor angle $\delta_{21}$ response with local PSSs at G2 and G4 .....	60
Figure 5-8: Rotor angle $\delta_{31}$ response with local PSSs at G2 and G4 .....	61
Figure 5-9: Rotor angle $\delta_{41}$ response with local PSSs at G2 and G4 .....	61
Figure 5-10: Rotor speed $\omega_1$ response with local PSSs at G2 and G4 .....	62
Figure 5-11: Rotor speed $\omega_2$ response with local PSSs at G2 and G4 .....	62
Figure 5-12: Rotor speed $\omega_3$ response with local PSSs at G2 and G4.....	63
Figure 5-13: Rotor speed $\omega_4$ response with local PSSs at G2 and G4.....	63
Figure 5-14: Control response of PSS at G2.....	64
Figure 5-15: Control response of PSS at G4.....	64
Figure 5-16: Electric power output $P_{e1}$ response with local PSSs at G2 and G4 .....	65
Figure 5-17: Electric power output $P_{e2}$ response with local PSSs at G2 and G4 .....	65
Figure 5-18: Electric power output $P_{e3}$ response with local PSSs at G2 and G4 .....	66
Figure 5-19: Electric power output $P_{e4}$ response with local PSSs at G2 and G4 .....	66
Figure 5-20: Terminal voltage $V_{t1}$ response with local PSSs at G2 and G4 .....	67
Figure 5-21: Terminal voltage $V_{t2}$ response with local PSSs at G2 and G4 .....	67
Figure 5-22: Terminal voltage $V_{t3}$ response with local PSSs at G2 and G4 .....	68
Figure 5-23: Terminal voltage $V_{t4}$ response with local PSSs at G2 and G4 .....	68
Figure 6-1: Two area four machine system equipped with WADC.....	71
Figure 6-2: Interarea mode controllability measure.....	74
Figure 6-3: Wide Area Damping Controller connected to G3.....	75

Figure 6-4: Rotor angle $\delta_{21}$ response.....	78
Figure 6-5: Rotor angle $\delta_{31}$ response.....	79
Figure 6-6: Rotor angle $\delta_{41}$ response.....	79
Figure 6-7: Rotor speed $\omega_1$ response.....	80
Figure 6-8: Rotor speed $\omega_2$ response.....	80
Figure 6-9: Rotor speed $\omega_3$ response.....	81
Figure 6-10: Rotor speed $\omega_4$ response.....	81
Figure 6-11: Control response at G2.....	82
Figure 6-12: Control response at G3.....	82
Figure 6-13: Control response at G4.....	83
Figure 6-14: Electric power output $P_{e1}$ response .....	83
Figure 6-15: Electric power output $P_{e2}$ response .....	84
Figure 6-16: Electric power output $P_{e3}$ response .....	84
Figure 6-17: Electric power output $P_{e4}$ response .....	85
Figure 6-18: Terminal voltage $V_{t1}$ response .....	85
Figure 6-19: Terminal voltage $V_{t2}$ response .....	86
Figure 6-20: Terminal voltage $V_{t3}$ response .....	86
Figure 6-21: Terminal voltage $V_{t4}$ response .....	87
Figure 6-22: Rotor angle $\delta_{21}$ response with controller placed at G3 .....	89
Figure 6-23: Rotor angle $\delta_{31}$ response with controller placed at G3 .....	89
Figure 6-24: Rotor angle $\delta_{41}$ response with controller placed at G3 .....	90
Figure 6-25: Rotor speed $\omega_1$ response with controller placed at G3 .....	90
Figure 6-26: Rotor speed $\omega_2$ response with controller placed at G3 .....	91
Figure 6-27: Rotor speed $\omega_3$ response with controller placed at G3 .....	91
Figure 6-28: Rotor speed $\omega_4$ response with controller placed at G3 .....	92
Figure 6-29: Electric power output $P_{e1}$ response with controller placed at G3 .....	92
Figure 6-30: Electric power output $P_{e3}$ response with controller placed at G3 .....	93
Figure 6-31: Convergence of the objective function .....	95
Figure 6-32: Rotor angle $\delta_{21}$ response with controller placed at G3 (Optimized WADC) .....	96
Figure 6-32: Rotor angle $\delta_{21}$ response with controller placed at G3 (Optimized WADC) .....	96
Figure 6-33: Rotor angle $\delta_{31}$ response with controller placed at G3 (Optimized WADC).....	97
Figure 6-34: Rotor angle $\delta_{41}$ response with controller placed at G3 (Optimized WADC).....	97
Figure 6-35: Rotor speed $\omega_1$ response with controller placed at G3 (Optimized WADC).....	98
Figure 6-36: Rotor speed $\omega_2$ response with controller placed at G3 (Optimized WADC).....	98

Figure 6-37: Rotor speed $\omega_3$ response with controller placed at G3 (Optimized WADC).....	99
Figure 6-38: Rotor speed $\omega_4$ response with controller placed at G3 (Optimized WADC).....	99
Figure 7-1: Synchronous generator Model in RSCAD .....	106
Figure 7-2: IEEE type 1 speed governor block diagram.....	106
Figure 7-3: IEEE type AC4 exciter block diagram.....	107
Figure 7-4: IEEE type ST stabilizer block diagram.....	107
Figure 7-5: PMUs model in RSCAD .....	108
Figure 7-6: WADC scheme in RSCAD .....	108
Figure 7-7: Load and transmission line models in RSCAD.....	109
Figure 7-8: Fault point model at RSCAD (connected at Bus 8) .....	109
Figure 7-9: Two-area power system as modeled in RSCAD .....	111
Figure 7-10: Two-area power system represented graphically at RunTime .....	112
Figure 7-11: Rotor Speed response of G1 for a 3-phase fault at Bus 8 (RTDS).....	114
Figure 7-12: Rotor Speed response of G2 for a 3-phase fault at Bus 8 (RTDS).....	114
Figure 7-13: Rotor Speed response of G3 for a 3-phase fault at Bus 8 (RTDS).....	115
Figure 7-14: Rotor Speed response of G4 for a 3-phase fault at Bus 8 (RTDS).....	115
Figure 7-15: Control responses for 3-phase fault at Bus 8 (RTDS).....	116
Figure 7-16: Electric power output response of G1 for 3-phase fault at Bus 8 (RTDS).....	117
Figure 7-17: Electric power output response of G2 for 3-phase fault at Bus 8 (RTDS).....	117
Figure 7-18: Electric power output response of G3 for 3-phase fault at Bus 8 (RTDS).....	118
Figure 7-19: Electric power output response of G4 for 3-phase fault at Bus 8 (RTDS).....	118
Figure 7-20: Terminal voltage response of G1 for 3-phase fault at Bus 8 (RTDS).....	119
Figure 7-21: Terminal voltage response of G2 for 3-phase fault at Bus 8 (RTDS).....	119
Figure 7-22: Terminal voltage response of G3 for 3-phase fault at Bus 8 (RTDS).....	120
Figure 7-23: Terminal voltage response of G4 for 3-phase fault at Bus 8 (RTDS).....	120
Figure 7-24: Power transfer across one of the tie lines for 3-phase fault at Bus 8 (RTDS).....	121
Figure 7-25: Rotor speed response of G1 for sudden decreased in LOAD 8 (RTDS).....	123
Figure 7-26: Rotor speed response of G2 for sudden decreased in LOAD 8 (RTDS).....	123
Figure 7-27: Rotor speed response of G3 for sudden decreased in LOAD 8 (RTDS).....	124
Figure 7-28: Rotor speed response of G4 for sudden decreased in LOAD 8 (RTDS).....	124
Figure 7-29: Electric power output response of G1 for sudden decreased in LOAD 8 (RTDS) .	125
Figure 7-30: Electric power output response of G2 for sudden decreased in LOAD 8 (RTDS) .	125
Figure 7-31: Electric power output response of G3 for sudden decreased in LOAD 8 (RTDS) .	126
Figure 7-32: Electric power output response of G4 for sudden decreased in LOAD 8 (RTDS) .	126



Figure 7-33: Power transfer across one of the tie lines for sudden decreased in LOAD 8 (RTDS) .	127
Figure 7-34: System responses for 3-phase fault at Bus 8 (without controller, RunTime).....	129
Figure 7-35: System responses for 3-phase fault at Bus 8 (with PSSs at G2 & G4, RunTime) .	129
Figure 7-36: System responses for 3-phase fault at Bus 8 (with PSSs at G2, G3 & G4, RunTime)	130
Figure 7-37: System responses for 3-phase fault at Bus 8 (with PSSs at G2 & G4 and WADC at G3,)..	130
Figure 7-38: System responses for sudden decreased in LOAD 8 (without controller, RunTime)..	131
Figure 7-39: System responses for sudden decreased in LOAD 8 (with PSSs at G2 & G4, RunTime)	131
Figure 7-40: System responses for sudden decreased in LOAD 8 (with PSSs at G2, G3 & G4, RunTime) .....	132
Figure 7-41: System responses for sudden decreased in LOAD 8 (with PSSs at G2 & G4 and WADC at G3, RunTime) .....	132
Figure 7-42: Rotor speed $\omega_1$ response with controller placed at G3 (RTDS) .....	134
Figure 7-43: Rotor speed $\omega_2$ response with controller placed at G3 (RTDS) .....	134
Figure 7-44: Rotor speed $\omega_3$ response with controller placed at G3 (RTDS) .....	135
Figure 7-45: Rotor speed $\omega_4$ response with controller placed at G3 (RTDS) .....	135
Figure 7-46: Electric power output Pe1 response with controller placed at G3 (RTDS).....	136
Figure 7-47: Electric power output Pe2 response with controller placed at G3 (RTDS).....	136
Figure 7-48: Electric power output Pe3 response with controller placed at G3 (RTDS).....	137
Figure 7-49: Power transfer through one of the tie lines response with controller placed at G3 (RTDS) .....	137
Figure 7-50: Rotor speed $\omega_1$ response with controller placed at G3 (Optimized RTDS) .....	138
Figure 7-51: Rotor speed $\omega_3$ response with controller placed at G3 (Optimized RTDS).....	139
Figure 7-52: Electric power output Pe1 response with controller placed at G3 (Optimized RTDS) .....	139
Figure 7-53: Electric power output Pe2 response with controller placed at G3 (Optimized RTDS) .....	140
Figure 7-54: Power transfer through one of the tie lines response with controller placed at G3 (Optimized RTDS).....	140
Figure 7-55: Electric power output Pe1 response with controller placed at G3 (MATLAB and RTDS) .	142
Figure 7-56: Electric power output Pe3 response with controller placed at G3 (MATLAB and RTDS) .	142
Figure 7-57: Terminal voltage Vt1 response with controller placed at G3 (MATLAB and RTDS) ....	143

## **LIST OF ABBREVIATIONS**

<b>PSS</b>	Power System Stabilizer
<b>CPSS</b>	Conventional Power System Stabilizer
<b>WAMS</b>	Wide Area Measurement System
<b>WADC</b>	Wide Area Damping Controller
<b>PMU</b>	Phasor Measurement Unit
<b>GPS</b>	Global Positioning System
<b>CSG</b>	China's Southern Power Grid
<b>RTDS</b>	Real Time Digital Simulator
<b>LFO</b>	Low Frequency Oscillation
<b>FACTS</b>	Flexible AC Transmission Systems
<b>AVR</b>	Automatic Voltage Regulator
<b>ASC</b>	Adaptive Supervisory Controller
<b>PF</b>	Participating Factor
<b>PLC</b>	Programmable Logic Controller
<b>DSP</b>	Digital Signal Processor
<b>SVP</b>	Synchrophasor Vector Processor

## LIST OF SYMBOLS

Symbol	Description
$\omega$	Rotor speed
$\delta$	Rotor angle
$T_e$	Electromagnetic torque
$T_S$	Synchronizing torque
$T_D$	Damping torque
$\omega_b$	Synchronous speed
$M$	Machine inertia constant
$D$	Damping Coefficient
$P_m$	Mechanical input power
$P_e$	Electrical output power
$E'_q$	Generator internal voltage
$E_{fd}$	Equivalent excitation voltage
$T'_{d0}$	Open-circuit time constant
$i_d, i_q$	d- and q-axis armature current
$V_d, V_q$	d- and q-axis armature voltage
$V$	Generator terminal voltage
$V_{ref}$	Reference voltage
$x_d, x_q$	d- and q-axis generator reactance
$x'_d, x'_q$	d- and q-axis generator transient reactance
$u_{PSS}$	PSS output signal

$K_A, T_A$	Gain and time constant of the excitation system
$K_{PSS}$	Stabilizer gain
$T_W$	PSS washout filter time constant
$T_i$	PSS phase compensation time constant ( $i = 1,2,...,4$ )
$u_{PSS-max}$	PSS output signal upper limit
$u_{PSS-min}$	PSS output signal lower limit
$E_{fd-max}, E_{fd-min}$	Upper and lower limit of the excitation voltage
$\lambda$	Eigenvalue
$\Phi$	Right-eigenvector
$\Psi$	Left-eigenvector
$\zeta$	Damping ratio
$B'$	Mode controllability matrix
$C'$	Mode observability matrix
$R$	Residue
$f$	System frequency
$K$	Control system input signals selection vector

## ABSTRACT

**Full Name** : ABDULMOHSEN FAHAD AL-MULHIM

**Thesis Title** : WIDE AREA DAMPING CONTROLLER  
DESIGN AND IMPLEMENTATION

**Degree** : MASTER OF SCIENCE

**Major Field** : ELECTRICAL ENGINEERING

**Date of Degree** : MAY 2013

As power systems grow-up and continue to be interconnected and more power is transmitted over weak (or limited capacity) transmission lines, low frequency oscillation becomes a major concern for secure and reliable operation of large power systems. Small disturbance at poorly damped Low Frequency Oscillation (LFO) system may affect the stability or lead to unstable the system. So damping controllers are required to damped out these oscillations and improve the dynamic performance of the power system. Conventionally, Power System Stabilizers (PSSs) are used to provide supplementary control action through the excitation system. But these controllers are using local measurements as inputs and this not effective enough to damp out the inter-area oscillations. Recently, availability of remote signals provided by Wide Area Measurement System (WAMS), gives researchers possibilities to design Wide Area Damping Controller (WADC).

In this thesis, power system stabilizer based on WAMS is proposed and designed. Modal analysis including controllability, observability and residue analysis are carried out in order to identify the best location and the combination of input signals of WADC. The controller location is selected based on Controllability measurements, and the input signals to the controller will be a combination of all machines that participate in the concern mode. Locations of local PSS are determined based on residue analysis of certain oscillation mode.

A multi-machine two-area power system is used to test the performance of the proposed wide area damping control scheme. Eigenvalue analysis and time domain simulation are performed to the two area system in order to evaluate the performance of the controller.

It is also aimed for implementing the tested power system equipped with wide area damping controller (WADC), on Real Time Digital Simulator (RTDS®). The simulation results are verified and the effectiveness of the proposed wide area damping controller are assessed.

## ملخص الرسالة

الاسم الكامل : عبدالمحسن فهد ملحم الملحم  
عنوان الرسالة : تصميم مثبت شبكة الطاقة المُستند على نظام القياس واسع المدى  
الدرجة : الماجستير في العلوم  
التخصص : الهندسة الكهربائية  
تاريخ الدرجة العلمية : مايو 2013 م

مع ازدياد إتساع شبكات الطاقة الكهربائية و إستمرار الربط الكهربائي بينها لهدف نقل الطاقة عبر خطوط النقل و التي عادةً ما تكون محدودية القدرة، ذلك يجعل خطر الذبذبات ذات التردد المنخفض أكبر على أداء و موثوقية أنظمة الشبكة الكهربائية. فأى اضطراب بسيط في الشبكة يمكن أن يؤثر على ثبات النظام أو يؤدي الى عدم إستقراره. لهذا السبب إن وجود المُثبتات ضروري لإخماد الذبذبات منخفضة التردد مما يُحسن الأداء الديناميكي للنظام الكهربائي. في العادة يتم استخدام مثبت شبكة الطاقة كُضبط مُساعد من خلال تأثيره على النظام المُحفز للمُولد. ولكن هذه المُثبتات تعتمد على القياسات المحلية المتاحة في موقع المُثبت والتي عادةً ما تكون فعالة على نمط الذبذبات الناتجة بين المولدات في نفس المنطقة أو القريبة نسبياً، أما فعاليتها في نمط الذبذبات المتداخلة بين منطقتين تكون ضعيفة. حديثاً مع توافر إمكانية الحصول على القياسات البعيدة من خلال نظام القياس واسع المدى، أتاح للباحثين إمكانية تصميم مُثبتات شبكة الطاقة تعتمد على نظام القياس واسع المدى.

هذا البحث يعرض مُقترح تصميم مثبت شبكة الطاقة الكهربائية بالاعتماد على نظام القياس واسع المدى. للحصول على أفضل أداء للمُثبت المُقترح، يتم تطبيق طريقة التحليل الخطي في تفاصيل تصميم المُثبت لتحديد أمثل موقع للمُثبت، ويتم اختيار مجموعة الإشارات المُدخلة بالاعتماد على المُولدات ذات المشاركة المؤثرة في النطاق.

لتقدير مدى قدرة و كفاءة المُثبت المُقترح، يتم دراسة نظام طاقة متعدد المكاتن و يجري اختبار المُثبت عن طريق تحليل معامل التحول الخطي و مضائلة الشكل الكهروميكانيكي، إضافة الى المحاكاة الزمنية غير الخطية لإشارات الشبكة.

يهدف هذا البحث أيضاً لتطبيق النظام المُختبر و المُجهز بالُمثبت المُقترح على منصة محاكاة بالزمن الحقيقي. جهاز المحاكاة بالزمن الحقيقي يعكس ديناميكية النظام و يعطي السلوك أو الإستجابات الحقيقية لمكونات النظام في حال تعرض النظام الى اضطراب بسيط أو خطأ. بعد الحصول على نتائج المحاكاة بالزمن الحقيقي يتم التحقق من صحتها و فعاليتها و ذلك عن طريق مقارنتها بالبحوث السابقة.

# **CHAPTER 1**

## **INTRODUCTION**

### **1.1 Overview**

Power system networks now a days are became very complex, interconnected and have long transmission lines with limited capacity. To satisfy the grown-up loads demand, more power needs to be transferred across the transmission lines. As the systems loaded more and more, power systems operate closer to their stability limits. Stressed operating conditions can increase the possibility of power oscillations. One of the major problems in power system operation is the oscillations which caused by insufficient damping in the system. These oscillations include local modes and inter-area modes. Local modes are associated with the swinging of the machine with respect to the rest of the power system. Inter-area modes are associated with swinging of many machines in one part of the system against machines in other parts [1]. Inter-area modes may be caused by either high-gain exciters or heavy power transfers across weak tie lines. With the increasing of the interconnections and power transfer in the networks, inter-area oscillations become more poorly damped and power system stability becomes more and more of concern [2].

Damping of inter-area oscillations, as well as the local modes, is normally tackled by installing power system stabilizers (PSSs). Each installed PSS receives a local signal such as generator speed or power as an input and provides a supplementary signal to the generator excitation system. The local measurements based PSSs can provide sufficient damping for local mode oscillations, on the other hand their effectiveness in damping inter-area mode oscillations is very limited [3]. It has been proved that under certain operating conditions an inter-area mode may be controllable from one area and be observable from different area. So measured signals from different area in the system are required in order to make the system observable.

In recent years, wide area measurement system (WAMS) has been greatly developed and it becomes widely used in power system monitoring and control applications. Wide area measurement systems are using phasor measurement unit (PMU) technology which is a global positioning system (GPS) base device. With this technology, dynamic data of the systems such as voltage, current, angle and frequency can be precisely measured, synchronized and transferred over the whole network [5]. Providing this, wide area damping control (WADC) can be applied.

## **1.2 Thesis Motivation**

Recently, the concept of wide area measurement and control systems has been widely used. The idea is mainly based on data collection over the whole network by means of time synchronized phasor measurements. With the availability of these measurements, dynamic behavior of the system can be understood, the system becomes highly



observable and most of the important signals will be accessible. Remote signals (global signals) provided by WAMS give new opportunities for designing WADCs.

Because of economic constraints, electric utilities are being forced to operate power system networks under very stringent conditions. Moreover, deregulation has forced more power transfers over a limited transmission lines. As a result, power systems are being driven closer to their capacity limits which may lead to system instability problems [6]. So the main objectives of the power systems are to improve dynamic performance (stability improvement) and to enhance transfer capacity in weak tie lines. Several studies were conducted and their results confirmed that due to the lack of the observability in local measurements for certain inter-area oscillation modes, WADC using remote signals may be more effective and gives better performance than local control [7]-[10].

Recently, a WADC has been implemented on China's Southern Power Grid (CSG) to improve the damping performance of inter-area oscillations in CSG [28]. It is the first application of PMU measurements used as input to a continuous feedback control system in real power system. Results show that WADC provides significant improvement of damping inter-area modes oscillation. CSG's success implementation of WADC proves that real time control based on WAMS is effective in power system.

In summary, the main advantages of having WAMS and WADC are:

- Better understanding of power system dynamic behavior;
- Transmission capacity enhancement;
- Power system stability improvement;

- Real time monitoring and control;
- Higher observability of the system compared to local measurement control;
- Event recording and post-disturbance analysis;
- Power system investment planning based on feedback obtained during analysis of system dynamics.

### **1.3 Thesis Objectives**

The main objective of this thesis is to design inter-area oscillation damping stabilizer based on wide-area measurement system (WAMS). Two area power system equipped with the proposed wide-area controller will be implemented and simulated using real-time digital simulator (RTDS). The controller model will be a widely used lead lag structure. Modal analysis including controllability, observability and residue analysis will be carried out in order to get the best performance of wide area damping controller (WADC). The controller location is selected based on Controllability measurements, and the input signals to the controller are determined according to the participating factors. The input signals for the controller going to be a combination of signals from all machines participating on the concerned inter-area mode. Multi-machine two-area power system, equipped with local PSS on each area, will be used to test the performance of WADC. In order to provide wide area signals to the controller, Phasor measurement units (PMUs) will be considered in all machine buses.

Eigenvalue analysis and time domain simulation will be performed to the two area system in order to validate the performance of the controller. All modal analysis and non-

linear time domain simulations are carried out using MATLAB software. Same system setup will be implemented on Real Time Digital Simulator (RTDS®) where two different cases will be simulated; transient fault condition and huge droop or increase in loads.

## **1.4 Thesis Organization**

This thesis consists of 9 chapters.

**Chapter 1: Introduction** addresses power system oscillation problem in the complex and interconnected power systems. Then, conventional way to tackle these oscillations is highlighted. The new wide area damping control based on PMU technology is introduced as a proposed solution. This chapter ends with describing the motivation and the objectives of this thesis.

**Chapter 2: Literature Review** covers low frequency oscillations definition, identification and analysis. It presents the PSS as a conventional supplementary controller to damp out these oscillations. In this chapter, the recent development in WAMS technology using PMU is highlighted. Also, different designs for WADC based on this technology are presented here. Finally, introduction to RTDS and its applications in power systems are given.

**Chapter 3: Power System Modeling and Analysis** presents the models of the main components of the power system. This includes synchronous generator, excitation system and Power System Stabilizer. Then, linearized model of the power system is described. Finally, modal analysis is carried out to the linearized power system model.

**Chapter 4: Wide Area Damping Control Design** introduces the WADC structure that will be used in the thesis. In this chapter, local PSSs and WADC design are described. Phase compensation technique is utilized to calculate the controller parameters.

**Chapter 5: Design of Local PSS for Multimachine Two-Area System** considers the two area power system as a case study to analyze and design PSSs for the purpose of damping local area modes of oscillations.

**Chapter 6: Analysis and Design of WADC** considers the same two area power system that chapter 6 end up with as a case study to analyze and design WADC for the purpose of damping interarea mode of oscillations. Also, a comparison between local based PSS and WADC is presented in this chapter. Finally, the parameters of the proposed WADC is optimized using Particle Swarm Optimization (PSO) technique.

**Chapter 7: Real Time Implementation** presents the main and the interested part of the thesis, which is implementing the two area power system equipped with the proposed WADC at Real Time Digital Simulator (RTDS). Again, a comparison between local based PSS and WADC is presented. This chapter ends with a comparison between MATLAB simulations and RTDS simulations results.

**Chapter 8: Conclusion and Future Work** presents the main conclusions of the work presented in the thesis. Proposals for possible future work are presented.

## CHAPTER 2

# LITERATURE REVIEW

### 2.1 Low Frequency Oscillations

Power system stability has been recognized as an important problem for a secure system operation since the beginning of last century. Many major blackouts caused by power system instability have illustrated the importance of this phenomenon [124]. Power system stability is defined by [124] as *“the ability of an electric power system, for a given initial operating condition, to regain a state of operating equilibrium after being subjected to a physical disturbance, with most system variable bounded so that practically the entire system remains intact”*.

Generally, power system is a highly nonlinear system that is subjected to a wide range of disturbances including small disturbances in the form of load changes that occur frequently or sever nature such as a short circuit on a transmission line or loss of a large generator. The sever nature disturbances are commonly referred to as large disturbances which may lead to structural changes due to the isolation of the faulted elements. Power

system may be stable for a given disturbance and unstable for another. Therefore, the stability of the system, when subject to a disturbance, depends on the initial operating conditions and the nature of the disturbance.

Power system stability is basically a single problem; however, the various forms of instabilities, which a power system may experience, cannot be properly understood by treating it as such. Due to high dimensionality and complexity of power system stability problems, it is necessary to make suitable simplifying assumptions for analyzing specific types of problems using an appropriate degree of details system representation and analytical techniques.

The classification of power system stability proposed here is based on the following considerations:

- The physical nature of the resulting mode of instability as indicated by the main system variable in which instability can be observed.
- The size of the disturbance considered which influences the method of calculation and prediction of stability.
- The devices, processes and the time span that must be taken into consideration in order to assess stability.

Power system stability can be classified into different categories and subcategories as shown in Figure 2-1. The descriptions of the corresponding forms of stability phenomena are given in the following subsections.

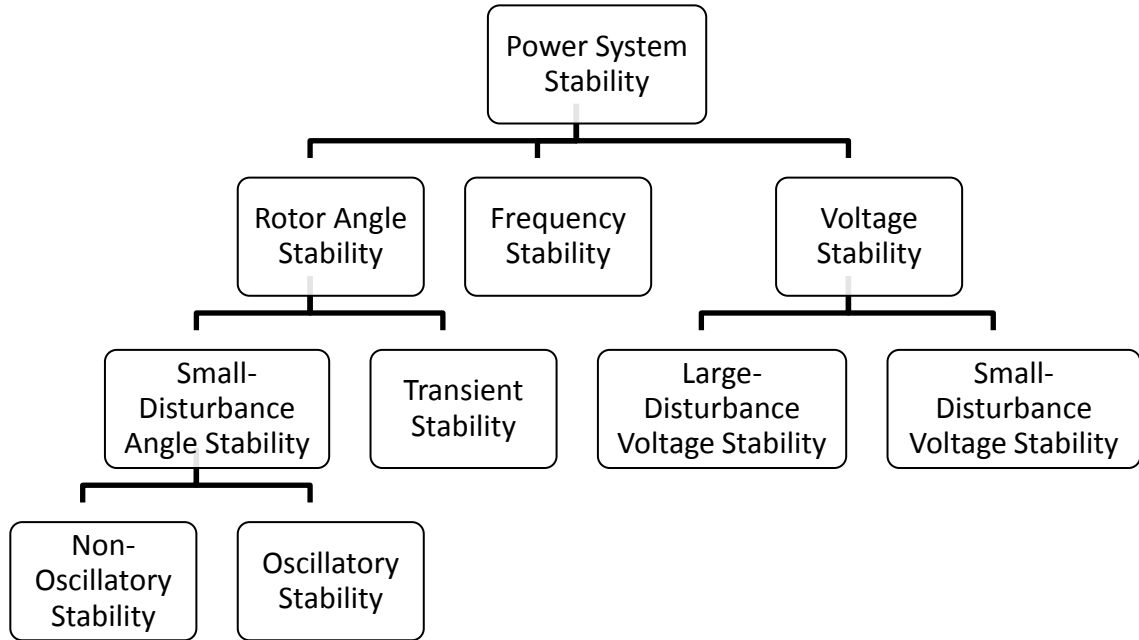


Figure 2-1: Classification of Power System Stability

Low frequency oscillation (LFO) is one of the earliest power system stability problems. LFOs are machine rotor angle oscillations having a frequency between 0.1-2.0 Hz [2]. The ability of machines of an interconnected power system to remain synchronism after being subjected to a small disturbance is known as small signal stability. These oscillations can be created by small disturbance in the system, such as changes in load. These small disturbances lead to a steady increase or decrease in machine rotor angle caused by the lack of synchronizing torque or because of rotor oscillations of increasing amplitude due to insufficient damping torque [1]. The LFOs can be classified as local and inter-area mode [11]. Local modes are associated with the swinging of the machine with respect to the rest of the power system with frequency range of 1-2 Hz. Inter-area modes are on the range of 0.1-0.7 Hz and are associated with swinging of many machines in one part of the system against machines in other parts.

The identification and analysis of LFOs are usually studied using small signal stability. There are different methods to find the dominant modes of inter-area oscillations. Eigenvalue based technique (Modal analysis) is a well-known technique and widely used in such analysis [2], [12]. The other more advanced techniques are measure data based methods such as Fourier algorithm [17], Prony algorithm [13], [15], [16], and Wavelet algorithm [14], [18]. These algorithms are a signal processing methods that have the ability to extract the oscillation information from the system.

Theses oscillations are conventionally damped out using power system stabilizer (PSS) which provide supplementary control action through the excitation system. Also, flexible ac transmission systems (FACTS) devices are used to maintain the voltage and enhance the stability of the system using reactive control [19], [20]. But these controllers usually use local measurements as inputs and cannot always be effective in damping out inter-area oscillations from the system. With WAMS technology, remote signals can be measured and transmitted anywhere in the system. So that designing a controller based on wide area measurements will not be a problem anymore. Recently, WAMS based controllers show promising results in damping inter-area oscillations. Section 2.3 provides more detail in WADC.

## **2.2 Power System Stabilizer**

Power system stabilizers (PSSs) have been extensively used as supplementary excitation controllers since 1960's to damp out the low frequency oscillations and enhance the overall system stability. The use of supplementary control added to the Automatic



Voltage Regulator (AVR) is a practical and economic way to supply additional damping to low frequency oscillations. The PSS extend the system stability limits by modulating generator excitation to provide damping to the oscillations of synchronous machine rotors relative to one another. PSS produces a component of torque in phase with rotor speed deviations in order to enhance the system damping [21]. Extensive researches have been conducted in such field as effect of PSS on power system stability, PSS input signals, PSS optimum locations and PSS tuning techniques [25].

Conventional PSS (CPSS) of lead-lag compensation type has been adopted by most utilities because of its simple structure, flexibility and ease to implementation. It consists of three blocks: a gain block, a washout block and a phase compensation block. The gain determines the amount of damping introduced by PSS and it should be set corresponding to the maximum damping. The washout block works as a high-pass filter. The lead/lag phase compensation block provides the required phase lead to compensate for the phase lag between the exciter input and the generator electrical torque [2]. The structure of lead-lag PSS used in this thesis is provided in chapter 4.

Several approaches and control methods have been applied to PSS design problem and its parameters tuning. Among them are pole placement [29]-[32], [59]-[63] ;  $H_\infty$  control design technique [64], linear matrix inequalities (LMI) [7], [66], [67] ,  $\mu$ -Synthesis [66], [68], [69] linear quadratic regulator (LQR) [70], [71] residue phase compensation, adaptive control [72]-[80] and the recent intelligent and optimization methods which includes; Genetic Algorithm [81]-[88], Tabu Search [89]-[92], Particle Swarm

Optimization [93]-[95], Simulated Annealing [96]-[99], Neural Networks [100]-[108], Fuzzy Logic [109]-[117], and evolutionary programming [118].

The selections of the most suitable locations for PSS and the control input signals are very important in the design of the control system. Optimal location of PSS and best selection of control input signal effect the performance of the PSS in damping out the oscillations. Several techniques have been proposed in the literature to determine the best location for PSSs. Participation factor method is one of the first methods in identifying the contribution of various generators in each mode [119]. Another technique is using sensitivity of PSS effect (SPE) as a criterion for determining the suitable location of PSSs [120]. Modal controllability and modal observability is also considered as a measure for determining the suitable location of PSSs and suitable signal as input of PSSs [121] and [122]. Other techniques used transfer function to locate the PSSs. In [123] transfer function residues are used to locate PSSs.

## **2.3 Wide-Area Damping Controller**

The increase in application of WAMS in power systems resulted in an increased in exploring effectiveness of wide area damping controller (WADC) to damp inter-area oscillations. Many researches achieved good results by applying remote signals from one or more distant locations of the power system to the controller [26]. It is found that if remote signals are applied, the system dynamic performance can be enhanced for inter-area oscillations.

The recent developments in WAMS technologies using phasor measurement units (PMUs) can deliver synchronous phasors and control signals at high speed. Location of PMUs is chosen such that the system observability is maximum. PMUs measure positive sequence voltages and currents of those locations. These measurements or signals are time synchronized using Global Positioning System (GPS) and then transmitted via telecommunication media (such as power line carrier, microwave links, or fiber-optic) to the controllers [27]. These signals are often referred to as global or wide-area signals to illustrate the fact that they contain valuable information about the whole system dynamics. In contrast to the local control signals which doesn't have sufficient observability of some of the inter-area oscillation modes. So, local signals may not be effective on damping inter-area modes. In order to damp out inter-area oscillation modes, signal with maximum observability is required for the controller and this signal can be from remote location or a combination of several signals from different locations [23], [24] and [9].

First real implementation of WADC has been developed and operated by China Southern Power Grid (CSG) [28]. The WADC uses modulation of two HVDC systems to damp out dominant inter-area oscillations. The controller was first operating in open-loop for half year, responding to various oscillations correctly. Recently, a close-loop field test of WADC had been conducted and result shows that WADC provides significant damping to inter-area modes.

Different designs for WADC were proposed in the literature; among them are modal analysis based, robust and optimal control techniques, adaptive methods and other

systematic procedure for designing WADC. Kamwa et al., [9] proposed a decentralized/hierarchical structure with two loop PSSs: a local loop that based on the machine rotor speed (simply CPSS); and a global loop that based on a differential frequency between two remote areas. Wide-area signals based PSS is used to provide additional damping to local ones. The proposed controller was tuned using sequential optimization procedure and applied on the Hydro-Quebec's existing power system. Simulation results show that WADC improved the dynamic performance of the system.

Modal analysis is very useful in determining the best controller locations and the proper selection of control inputs. An improved residue matrix is adapted in [23] for choosing the location of controller and input signals. The modes and the residues associated with inter-area oscillations are identified. Then, the placement and the stabilizing input of the controller are determined and finally the wide-area PSS parameters are designed using residue phase compensation method. Both modal analysis (eigenvalue analysis) and time domain simulation have shown that the inter-area modes are well damped with the proposed wide-area PSSs. Modal analysis has been also used in [24] to select the wide-area controller location and the signals combination based on largest controllability and observability for the concern inter-area mode. The proposed controller was validated in two-area power system and simulation results show that the controller is effective and robust for damping all oscillation modes.

Li et al., [42] analyzes the existing shortcoming of conventional PSS from the point of view of modal controllability, modal observability and zeros of transfer function. To overcome this problem, wide-area measurement is introduced as feedback signals to

improve the modal observability and thus damp the inter-area oscillation. Another wide-area PSS is proposed on [43]. In this paper, the wide-area PSS location, input signals and the design of controller were considered. Again modal analysis was used to determine the best location and the proper remote input signals. The controller was designed using phase compensation method. The designed control was tested on Kundurs' system and results proved the effectiveness of wide-area PSS in damping inter-area oscillations.

Optimal control techniques have been used recently in wide-area controller design. A linear matrix inequality (LMI) based design of wide-area controller is discussed in [45]. In this paper, the rotor speed of remote generator was used as a wide-area measurement signal added to the local PSS. The gains of the wide-area controller were obtained by solving (LMIs). Kundur's four-machine two-area system was used to test the performance of the wide-area damping controller. Results revealed that the wide-area control can improve the damping characteristics of power system and enhance power system stability. Another controller design method, employing LMI to design inter-area damping controller, is presented in [46]. Here, a reduced order state space model with dominant low frequency oscillation modes was obtained through system identification using dynamic response in power system. Then, a matrix inequality theorem is transformed into LMI form based on variable substitution. The design of the damping controller is converted to a cone complementarity problem subjecting to LMIs and solved by linearization iterative algorithm. Finally, the controller feedback gain matrix was obtained. Same Kundur's system was considered in order to test the performance of the controller and results show that the proposed method can well damp the inter-area low frequency oscillation.

$H_\infty$  - based robust control technique is used in [47] to design the wide-area PSS. This paper deals with the decentralized PSS which uses selected suitable wide-area PMU signals as supplementary inputs to achieve a better damping of specific inter-area modes. These wide-area signals are taken from network locations where the oscillations are well observable, and the PSS controller uses only those local and remote input signals in which the assigned single inter-area mode is most observable and it is located at a generator most effective in controlling that mode. Simulation studies on a 16-machine test system were conducted to investigate the effectiveness of proposed controllers during system disturbances. Results show that the controller using remote PMU signals contribute significantly to the damping of inter-area oscillations. Dotta et al., [48] propose a design of two-level control structured (decentralized and centralized) based on optimal control theorem. The decentralized (local) controller corresponding to the conventional PSS at the generators, ensure a minimum performance of the system. The centralized controller allows the optimization of the global system performance especially in situation where critical topological configurations required the retuning of the conventional PSS. The proposed two-level controller tested in the Southern/Southeastern Brazil equivalent system and results shown the effectiveness of the control scheme in damping the critical inter-area mode.

Adaptive concept gets recently involved in designing wide-area damping controller [50]-[53]. An adaptive supervisory controller (ASC) for robust stabilization of multi-machine power system is proposed in [50] and [51]. The controller uses the input signals from conveniently located PMUs in the system and dispatches control signals to available local controllers in the system. The output signals of ASC are added to the AVRs together with

the output signal from local PSSs. The ASC was designed by  $H^\infty$  robust design with pole-placement constraints and based on LMI approach. The performance and robustness of the controller were validated on a 4-machine 2-area test system and results show the system oscillations with the ASC in place are much better damped than without it. Another adaptive WADC is presented in [52]. This controller is based on generalized predictive control and model identification. The proposed WADC is implemented by adding its output signal to the excitation system of a selected generator. To identify the model of power system, a recursive least-squares algorithm (RLSA) with a varying forgetting factor is used. Based on this model, the generalized predictive control considering control output constraints is employed. The validity and effectiveness of the proposed adaptive WADC was evaluated by a simulation study on a two-area four-machine power system. The simulation results were compared with that of the conventional WADC. The comparison results show that the performance of the adaptive WADC to damp the inter-area oscillation is better than those of the conventional WADC under wide range of operating conditions and different disturbances.

An adaptive PSS tuning method for damping inter-area oscillation is presented in [53]. The main objective is to adaptively improve the observability of the PSS by utilizing a combination of remote and local PMU signals. To achieve optimal observability towards inter-area oscillations, the weighting factors of remote signals are adaptively adjusted and a relationship between the observability of inputs and active power transfer across a particular transmission line of interest is formulated under offline condition. Designs were conducted in MATLAB Simulink and simulations were executed using DiGSILENT Power Factor and PSS/E software. The proposed technique has

demonstrated to be better than the traditional local input based design by providing adequate damping over wider operation conditions.

Many researchs have been developed to design wide-area damping controller using systematic procedures [54]-[58]. A systematic design procedure for wide-area damping control systems is described in [54]. A centralized structure is proposed in this paper. The comparative strength of candidate input signals and the performance of output control signals at different locations with respect to inter-area modes were evaluated by geometric measures of controllability and observability. The synthesis of the robust MIMO controller is defined as a problem of mixed  $H_2/H_\infty$  output – feedback control with regional pole placement and was resolved by the LMI approach. This design method was tested on 39-bus New England system. Padhy et al., [55] present another systematic procedure for designing a wide-area centralized Takagi-Sugeno fuzzy controller to improve the angular stability of a multi-machine power system. The proposed fuzzy controller is designed by satisfying certain linear matrix inequality conditions, to stabilize the system at multiple operating points. The bilinear matrix inequality problem, encountered in Lyapunov-based stability criterion, has been converted into a convex optimization problem to eliminate iterative solution. The input-output control signals were selected by defining joint model controllability and observability index applying geometric approach. The proposed control scheme employs a global signal from the centralized controller to damp out the inter-area mode of oscillations, apart from the local controllers, which are assumed to be there to damp out the local mode of oscillations. The proposed control scheme has been implemented on three test systems. The combined



action of both the CPSS and the proposed TS fuzzy wide-area controller provided better performance than with only the local CPSS controllers.

Another systematic procedure is presented in [56] for design global power system stabilizers (GPSSs) based on collocated control to enhance the damping during inter-area oscillations. Here, the closed loop eigenvalues were excluded from a region of the complex plane by the collocated control algorithm guaranteeing that low frequency modes must be damped. The optimum locations for GPSSs were selected using controllability. The proposed design technique was applied on a 16-machine, 68-bus system and simulation results show that the control scheme is able to damp out inter-area oscillations following possible disturbances.

## **2.4 Modal Analysis as Design Technique**

Modal analysis or called eigenvalue analysis is a well-known technique that describes the behavior of the system based on linear model. It is true that power systems are highly non-linear, however under normal operations; system behavior can be approximated and linearized around an operating point [21]. When the linear model of the power system is available, eigenvalues and eigenvectors can be determined. The stability of the system can be analyzed by studying the eigenvalues. The system is stable if all of the eigenvalues are lie on the left-hand side of the imaginary axis of the complex plane, otherwise it is unstable. Also, eigenvalue analysis helps in identifying poorly damped electromechanical oscillation modes and type of these modes; local mode or inter-area mode. Additional

important information that can be determined from the eigenvalue analysis: are the oscillatory frequency and the damping ratio [2].

Eigen-analysis of the system model will produce eigenvalues and their corresponding right-eigenvectors and left-eigenvectors. The right-eigenvector long with system output matrix gives information about system observability which is used to select the controller signals. The left-eigenvector and system input matrix give information about system controllability [22]. Utilizing the right-eigenvector and the left-eigenvector information for certain oscillation mode will result on what is called participating factor (PF). The participating factor measures the contribution of each state variable of the system for certain oscillatory mode [23]. The combination of observability and controllability modes give system residues. Conventionally, local PSSs are located based on residue analysis of power system. So for certain oscillator mode, PSSs will be located at machines with largest residue.

Recently, new methods based on modal analysis were proposed to design WADC (or wide-area PSS) [23] and [24]. These methods select WADC location according to largest controllability. As well, the input signal for the controller going to be a combination signals from all machines participating on the concerned inter-area mode. Here, inputs from wide area locations are selected based on the most observable states.

## **2.5 Real Time Digital Simulator (RTDS)**

### **2.5.1 Introduction**

Power systems today are operating near their maximum limit and because of that networks are experiencing unusual generation and power flow patterns and unplanned congestion. Also, a lot of uncertainties regarding protection and control are introduced to the system. So, voltage, transient and dynamic stability analysis will be required to study the system and overcome these problems. Such analysis shall be done under realistic power system conditions. For this purpose, real-time power system simulators have been developed. The RTDS simulator is currently applied to many areas of development, testing and a lot of studies such as; system planning, protection and control, system operation and behavior, feasibility studies and for research and training purposes [33].

The RTDS is a real-time power system simulator that performs digital electromagnetic transient simulation. It is a super computer that performs real-time simulation using parallel computation. It is capable of performing time-domain simulation at real-time speed using time steps less than 50 microseconds [34]. Such fast computation let RTDS able to simulate power system phenomena in the range of 0 to 3 kHz with high accuracy and reliability.

A power system network to be simulated is constructed using a graphical user interface (GUI) software suit called RSCAD. This software has a large library containing many power system component and control models. The RSCAD software has different models, the main two modules are; Draft and Runtime [33]. The Draft module is used for

building the network and parameters entry. The Runtime module is used to control the operation of RTDS simulator. Using Runtime, user can performs a lot actions; such as starting and stopping of simulation, initiating system disturbances, changing some of the system set points, on-line monitoring and measuring of power system quantities, and other control functions.

All communication between the RTDS and workstation is carried out by a Workstation InterFace (WIF) card. An Inter-Rack Communication (IRC) card takes care of communication between the racks [35]. The RTDS at KFUPM consists of cubicle with four processor racks, two Giga Processor cards (GPCs).

### **2.5.2 RTDS Applications**

The RTDS simulator is currently applied to many areas of development, testing and a lot of studies such as; protection and control system, general AC and DC system operations and behavior, feasibility studies, and for demonstration and training purposes [35].

RTDS is very helpful in testing control systems where real time closed loop feedback is used. Controls performance can be tested under different conditions; from steady state to rare emergency operating conditions. The RTDS has been used by many clients to test different power system controls including; power system stabilizer (PSS), FACTS devices (STATCOM, UPFC, SSSC,...), Exciter and voltage regulators, TCSC series compensation, distributed generation (wind, solar, fuel cell,...), smart grid, HVDC, SVC, ... etc [35]. The closed loop interaction of the control system and the network model

provides insight on both the performance of the controller as well as its effect on the power system. Followings are some RTDS implementations for different designs of power system stabilizer (CPSS) and wide-area damping controller (WADC).

Ganesh and Swakshar presented work relating to wide-area controllers and their implementation on real-time digital simulator (RTDS®) [4], [36]-[38]. Reference [4] and [36] present the design and the Digital Signal Processor (DSP) implementation of a nonlinear optimal wide area controller on the RTDS®. The controller is based on adaptive critic designs and neural networks. The wide-area control system (WACS) consists of three neural networks; the critic neural network, the action network (WAC) and the model neural network (WAM). WACS is implemented on the Innovative Integration M67 DSP card and connected to the RTDS® through DSP-RTDS Interface. The power system dynamics quantities are estimated online by WAM using a feed-forward neural network. The DSP implementation of WACS was applied to the two area power system which is modeled using RTDS®. Simulation results show that WACS provides better damping of power system oscillations under small and large disturbances.

In reference [37], Ganech et al. considered the communication delays in designing measurement-based adaptive wide-area control system. The WACS is realized with single simultaneous recurrent neural network (SRN) which is used for both identification of power system dynamics and initiation of appropriate damping control signals. This WACS design was also implemented on the RTDS® and DSP platform. Simulation results show improvement in damping power system oscillations due to small and large disturbances over wide range operating conditions.

Programmable logic controller (PLC) was used in [38] as a platform for exploring advanced modeling and control methods including computational intelligence based techniques such as neural networks, particle swarm optimization (PSO) and many others. In this paper, the controller consists two neural networks; one for modeling and the other for control. The design and the implementation of the controller is implemented on a single PLC. The controller is a conventional power system stabilizer (CPSS) that is used for power system oscillation damping. The PLC control system (PLC-CPSS) is connected or interfaced to the RTDS®. RTDS® allows for the simulation of power system in real-time while connecting auxiliary control components to the simulation via analog I/O. Real-time simulation results showing that PLC is a suitable hardware platform for implementing advanced modeling and control techniques for industrial applications.

Palangapour et al., [39] presents wide-area monitoring and control using RTDS and Synchrophasor Vector Processor (SVP). This paper developed a real-time hardware test bed in order to analyze the transient stability of a simulated power system by using synchrophasors to visualize system stress across a transmission line with and without load-shedding schemes. The main tools used in this work consist of an RTDS, PMUs, a satellite-synchronized clock, and an SVP. The PMUs obtain wide-area measurements from the RTDS, and the SVP runs the wide-area control algorithm for implementing the remedial action schemes (RASs) for transient stability. The test system was simulated for normal and fault conditions; results show an improvement in transient stability.

Another RTDS application is presented in [40]. In this paper, particle swarm optimization (PSO) technique is applied to obtain the optimal parameters of PSSs for a power system

simulated in real-time. The PSO and PSSs are implemented in a single digital signal processor (DSP) card and the rest of the power system is simulated in RTDS. The whole tuning process is done with hardware in loop arrangement. Results show a successful implementation of PSO-tuned PSSs in real-time environment.

Modeling and simulation of power systems on three different simulation platforms are compared at reference [41]. The platforms are RSCAD/RTDS, PSCAD/EMTDC, and SIMULINK SimPowerSystems. The Kundur's two area power system with and without PSS is presented as a case study. Studies under steady state and transient for various operating conditions were carried out and results confirmed that RTDS is the most flexible and the efficient way to study power system.

## **CHAPTER 3**

# **POWER SYSTEM MODELING AND ANALYSIS**

### **3.1 Introduction**

In this chapter, models of the main components of power system are described. This includes synchronous generators, excitation systems and power system stabilizers. Following this, linearized model of power system is developed. Then, modal analysis is carried out, that includes participation factor, modal controllability and observability, and residues. Models of the power system that presented in this chapter will be used in nonlinear time domain simulation. likewise, modal analysis presented here will be used to design the controllers (local PSSs and WADC) that will be applied to the multi-machine two-area power system.



## 3.2 Power System Model

### 3.2.1 Synchronous Generator and Exciter Models

Synchronous generators form the main source of electric energy in power systems. The power system stability problem is largely one of keeping interconnected synchronous machines in synchronism. Therefore, accurate modeling of the dynamic performance of these generators are very important to study the power system stability [2]. The synchronous generator model used in this thesis is the 3<sup>rd</sup> order model. The model differential equations of  $i$ th machine can be written as [89]

$$\dot{\delta}_i = \omega_b(\omega_i - 1) \quad (3.1)$$

$$\dot{\omega}_i = \frac{1}{M_i}(P_{mi} - P_{ei} - D_i(\omega_i - 1)) \quad (3.2)$$

$$\dot{E}'_{qi} = \frac{1}{T'_{doi}}[E_{fdi} - E'_{qi} - (x_{di} - x'_{di})i_{di}] \quad (3.3)$$

Where  $\delta_i$  and  $\omega_i$  are the rotor angle and speed of the  $i$ th machine, respectively.  $M_i$  and  $D_i$  are machine inertia constant and damping coefficient of the  $i$ th machine, respectively;  $\omega_b$  is the synchronous speed;  $E'_{qi}$  is the internal voltage behind  $x'_{di}$ ;  $E_{fdi}$  is the equivalent excitation voltage;  $T'_{doi}$  is the time constant of excitation circuit;  $P_{mi}$  and  $P_{ei}$  are the input and output powers of the  $i$ th generator, respectively. The output power of the generator can be expressed in terms of the  $d$ -axis and  $q$ -axis components of the armature current,  $i$  and terminal voltage,  $V_i$  as

$$P_{ei} = V_{di}i_{di} + V_{qi}i_{qi} \quad (3.4)$$

Where

$$V_{di} = x_{qi} i_{qi} , \quad V_{qi} = E'_{qi} - x'_{di} i_{di} \quad (3.5)$$

Synchronous generators are usually equipped with exciter. The basic function of an excitation system is to provide direct current to the synchronous machine field winding. In addition, the excitation system performs control and protective functions essential to the satisfactory performance of the power system by controlling the field voltage and thereby the field current. The control functions include the control of voltage and reactive power flow, and the enhancement of system stability. The protective functions ensure that the capability limits of the synchronous machine, excitation system, and other equipment are not exceeded.

The exciter model used here is the standard IEEE type-ST1 as shown in Figure 3-1. It can be described as

$$\dot{E}_{fdi} = \frac{1}{T_{Ai}} [K_{Ai}(V_{refi} - V_i + u_{pssi}) - E_{fdi}] \quad (3.6)$$

and,

$$V_i = \sqrt{V_{di}^2 + V_{qi}^2} \quad (3.7)$$

Where  $K_{Ai}$  and  $T_{Ai}$  are the gain and time constant of the excitation system, respectively;  $V_i$  and  $V_{refi}$  are the terminal and reference voltages respectively;  $u_{pssi}$  is the PSS output signal.

### 3.2.2 Power System Stabilizer Structure

The basic function of a power system stabilizer is to add damping to the generator rotor oscillations by controlling its excitation using auxiliary stabilizing signals. A PSS is added to the automatic voltage regulator (AVR), which controls the generator stator terminal voltage. PSS uses stabilizing feedback signals such as shaft speed, terminal frequency and real power to change the input signal of the AVR. To provide damping, PSS must produce a component of electrical torque in phase with the rotor speed deviations.

A widely used conventional lead-lag PSS is considered in the feedback loop to generate a supplementary stabilizing signal  $u_{pss}$ , see Figure 3-1. As shown in the PSS block, the rotor speed deviation  $\Delta\omega$  is used as the input signal to the PSS;  $K_{PSS}$  is the stabilizer gain;  $T_w$  is the washout time constant.

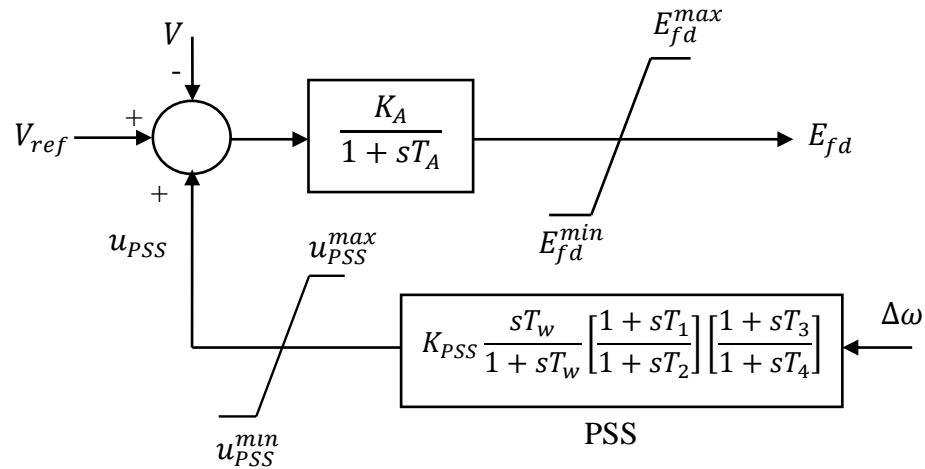


Figure 3-1: IEEE type-ST1 excitation system with PSS

### 3.3 Modal Analysis

To model the behavior of dynamic systems, a set of  $n$  first order nonlinear ordinary differential equations are used

$$\dot{x}_i = f_i(x_1, x_2, \dots, x_n; u_1, u_2, \dots, u_r; t) \quad i = 1, 2, \dots, n \quad (3.8)$$

Where  $n$  is the order of the system and  $r$  is the number of inputs. If the derivatives of the state variables are not explicit functions of time, (3.8) can be reduced to

$$\dot{\mathbf{x}} = \mathbf{f}(\mathbf{x}, \mathbf{u}) \quad (3.9)$$

$\mathbf{x}$ ,  $\mathbf{u}$  and  $\mathbf{f}$  denote column vectors of the form

$$\mathbf{x} = \begin{bmatrix} x_1 \\ x_2 \\ \vdots \\ x_n \end{bmatrix} \quad \mathbf{u} = \begin{bmatrix} u_1 \\ u_2 \\ \vdots \\ u_r \end{bmatrix} \quad \mathbf{f} = \begin{bmatrix} f_1 \\ f_2 \\ \vdots \\ f_n \end{bmatrix} \quad (3.10)$$

The state vector  $\mathbf{x}$  contains the state variables of the power system, vector  $\mathbf{u}$  contains the system inputs and  $\dot{\mathbf{x}}$  includes the derivatives of the state variables with respect to time.

The equation relating the outputs to the inputs and state variables can be written as

$$\dot{\mathbf{y}} = \mathbf{g}(\mathbf{x}, \mathbf{u}) \quad (3.11)$$

For the general state space system, the linearization of (3.9) and (3.11) about certain operating point  $\mathbf{x}_0$  and  $\mathbf{u}_0$  yield the linearized state space system

$$\Delta \dot{\mathbf{x}} = \mathbf{A} \Delta \mathbf{x} + \mathbf{B} \Delta \mathbf{u} \quad (3.12)$$

$$\Delta \mathbf{y} = \mathbf{C} \Delta \mathbf{x} + \mathbf{D} \Delta \mathbf{u} \quad (3.13)$$

Where  $\Delta \mathbf{x}$  is the  $n$  state vector increment,  $\Delta \mathbf{y}$  is the  $m$  output vector increment,  $\Delta \mathbf{u}$  is the  $r$  input vector increment,  $\mathbf{A}$  is the  $n \times n$  state matrix,  $\mathbf{B}$  is the  $n \times r$  input matrix,  $\mathbf{C}$  is the  $m \times n$  output matrix and  $\mathbf{D}$  is the  $m \times r$  feed-forward matrix. Specifically,  $\Delta \mathbf{x} = \mathbf{x} - \mathbf{x}_0$ ,  $\Delta \mathbf{y} = \mathbf{y} - \mathbf{y}_0$ ,  $\Delta \mathbf{u} = \mathbf{u} - \mathbf{u}_0$ .

Once the state space system for the power system is written in the linearized matrix form (3.12), the stability of the system can analyzed by calculating the eigenvalues  $\lambda_i$  of the matrix  $\mathbf{A}$ .

From previous section, the nonlinear equations (3.1)-(3.3) and (3.6) can be written as

$$\dot{\mathbf{x}} = \mathbf{f}(\mathbf{x}, \mathbf{U}) \quad (3.14)$$

Where  $\mathbf{x} = [\delta, \omega, E'_q, E_{fd}]^T$  and  $\mathbf{U}$  is the PSS output signals. In the design of electromechanical mode damping controllers, the linearized incremental models around a equilibrium point are usually employed. Figure 3-2 shows a block diagram of the  $i$ th machine in a multimachine power system. Where  $\mathbf{K}_{1ii}, \mathbf{K}_{1ij}, \dots, \mathbf{K}_{6ii}, \mathbf{K}_{6ij}$  are the linearized constant matrices.

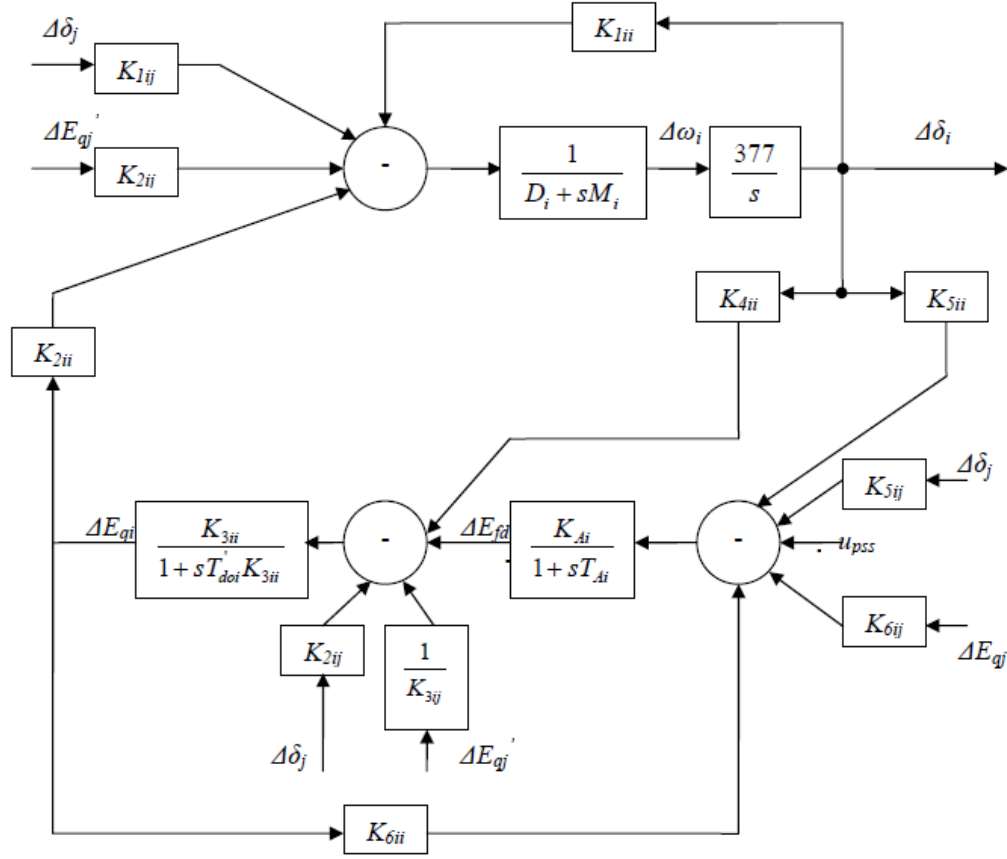


Figure 3-2: Linearized model of the  $i$ th machine in multimachine power system

The linearized state equation of power system with  $n$ -machines and  $m$ -stabilizers can be written as

$$\Delta \dot{\mathbf{x}} = \mathbf{A} \Delta \mathbf{x} + \mathbf{B} \mathbf{U} \quad (3.15)$$

Where  $\mathbf{A}$  is  $(4n \times 4n)$  matrix and  $\mathbf{B}$  is  $(4n \times m)$  matrix;  $\Delta \mathbf{x}$  is  $(4n \times 1)$  state vector and  $\mathbf{U}$  is  $(m \times 1)$  input vector.

### 3.3.1 Participation Factors and Mode Shape

Once the oscillatory modes have been identified and the modal matrices (right-eigenvector,  $\Phi_i$  and left-eigenvector,  $\Psi_i$ ) constructed, analysis is performed to find the specific rotor angle modes. These modes provide the largest contribution to the low frequency oscillations. Oscillatory modes can be identified by analyzing the right and left eigenvectors in conjunction with the participation factors.

A matrix called the participation factors matrix, denoted by  $P$ , provides a measure of association between the state variables and the oscillatory modes. It is defined as [2]

$$P = [P_1 \quad P_2 \quad \cdots \quad P_n] \quad (3.16)$$

With

$$P_i = \begin{bmatrix} p_{1i} \\ p_{2i} \\ \vdots \\ p_{ni} \end{bmatrix} = \begin{bmatrix} \Phi_{1i} \Psi_{i1} \\ \Phi_{2i} \Psi_{i2} \\ \vdots \\ \Phi_{ni} \Psi_{in} \end{bmatrix} \quad (3.17)$$

The element ( $p_{ki} = \Phi_{ki} \Psi_{ik}$ ) is called the participation factor, and gives a measure of the participation of  $k$ th state variable in the  $i$ th mode. The use of the participation factor will be used in analyzing the oscillatory modes of the tested power system.

The mode shape of the rotor-angle modes should be examined to confirm whether the particular mode is of local or inter-area type. Referring to the system state equation (3.12) and assuming that the system doesn't have input ( $\Delta u = 0$ )

$$\Delta \dot{x} = A \Delta x \quad (3.18)$$

Equation (3.18) cannot be used in the mode shape analysis. The problem is that the rate of change of each state variable is a linear combination of all the state variables. As the result of cross-coupling between the states, it is difficult to separate the parameters that influence certain oscillatory mode. In order to eliminate the cross-coupling between the state variables, a new state vector  $\mathbf{z}$  is consider and related to the original state vector  $\Delta\mathbf{x}$  by the following transformation

$$\Delta\mathbf{x} = \boldsymbol{\Phi}\mathbf{z} \quad (3.19)$$

$$\begin{bmatrix} \Delta x_1 \\ \Delta x_2 \\ \vdots \\ \Delta x_n \end{bmatrix} = [\boldsymbol{\Phi}_1 \quad \boldsymbol{\Phi}_2 \quad \dots \quad \boldsymbol{\Phi}_n] \begin{bmatrix} z_1 \\ z_2 \\ \vdots \\ z_n \end{bmatrix} \quad (3.20)$$

Where  $\boldsymbol{\Phi}$  is the modal matrix of  $\mathbf{A}$ . The variables  $\Delta x_1, \Delta x_2, \dots, \Delta x_n$  are the original state variables chosen to represent the dynamic of the system. The variables  $z_1, z_2, \dots, z_n$  are the transformed state variables such that each variable is associated with only one mode. In other words, the transformed variables are directly related to the modes. From (3.19), we can see that the right-eigenvector gives the mode shape, i.e., the relative activity of the state variables when a particular mode is excited. For example, the degree of activity of the state variable  $x_k$  in the  $i$ th mode is given by the element  $\Phi_{ki}$  of the right eigenvector  $\Phi_i$ .

### 3.3.2 Controllability, Observability and Residue

Expressing the linearized state space equations given in (3.12) and (3.13) in terms of the transformed variable  $\mathbf{z}$  defined by Equation (3.19) and rearranging them into a convenient, decoupled form yields



$$\dot{\mathbf{z}} = \mathbf{A} \mathbf{z} + \mathbf{B}' \Delta \mathbf{u} \quad (3.21)$$

$$\Delta \mathbf{y} = \mathbf{C}' \mathbf{z} + \mathbf{D} \Delta \mathbf{u} \quad (3.22)$$

Where

$$\mathbf{B}' = \mathbf{\Phi}^{-1} \mathbf{B} \quad (3.23)$$

$$\mathbf{C}' = \mathbf{C} \mathbf{\Phi} \quad (3.24)$$

The entries of matrix  $\mathbf{B}'$  relate the inputs to the oscillatory modes in the system. As a result, if the  $i$ th row is zero, the inputs have no effect on that mode and the mode is considered to be uncontrollable. Therefore,  $\mathbf{B}'$  is called the *mode controllability matrix*. On the other hand, the entries of matrix  $\mathbf{C}'$  relate the state variable  $z_i$  to the outputs of the system. Because of this, if the  $i$ th column is zero, the outputs do not contribute to that mode and the mode is considered to be unobservable. Hence,  $\mathbf{C}'$  is called the *mode observability matrix*.

For stability analysis of power systems, the eigenvalue analysis of the system state matrix is considered. However, for control design, open-loop transfer function between specific variables is used. To see how this is related to the state matrix and to the eigenproperties, the transfer function between the output and the input variables need to be obtained [2]. The transfer function representation of linearized model, assuming zero initial conditions, can be obtained by taking the Laplace transform of (3.12) and (3.13)

$$G(s) = \frac{\Delta y(s)}{\Delta u(s)} = \mathbf{C}(s\mathbf{I} - \mathbf{A})^{-1}\mathbf{B} + \mathbf{D} \quad (3.25)$$

Similarly, if the same transformation is applied to the transfer function representation given by (3.25), assuming zero feed-forward matrix  $\mathbf{D}$ , then (3.25) becomes

$$G(s) = \frac{\Delta y(s)}{\Delta u(s)} = \mathbf{C}\Phi(\mathbf{sI} - \mathbf{\Lambda})^{-1}\Psi\mathbf{B} \quad (3.26)$$

Since  $\mathbf{\Lambda}$  is a diagonal matrix,  $G(s)$  can be written as

$$G(s) = \sum_{i=1}^n \frac{R_i}{s - \lambda_i} \quad (3.27)$$

where

$$\mathbf{R}_i = \mathbf{C}\Phi_i\Psi_i^T\mathbf{B} \quad (3.28)$$

$R_i$  is known as the residue of the output variable  $y$  and the input variable  $u$  with regard to the  $i$ th mode.

### 3.4 Summary

Models of the main components of power system are briefly presented in this chapter. This includes synchronous generators, excitation systems and power system stabilizers. Modal analysis of linearized power system model was introduced. Physical interpretation of the power system model eigenvalues in the context of system stability was explained. Importance of the use of right eigenvectors and left eigenvectors in determine the participation factors and mode shape was addressed. Mode controllability and observability matrices, which are used in determine the controller's location and input signals, were introduced.

## **CHAPTER 4**

# **WIDE AREA DAMPING CONTROL DESIGN**

### **4.1 Introduction**

This chapter presents the design of WADC which uses wide area signals as additional measuring information from different part of the system. First section provides details of local PSSs design and the optimal locations of the PSSs. Second section of this chapter presents the wide area control system structure used in this thesis. The WADC placement technique and the method followed in selection of controller input signals combination are explained. Finally, controller parameters setting are tuned using the conventional residue-based method (or what is called phase compensation method).

### **4.2 Local PSSs Placement**

Conventionally, local PSSs are designed to damp out both local and interarea oscillations modes. Here, local PSS will be designed to damp out a specific local mode and the interarea modes will be left for WADC to deal with.

In the research area of power system angle stability, electromechanical oscillation modes correlated with rotor speed are of concern [23] and [24]. As known, there are  $n-1$  electromechanical oscillation modes in an  $n$ -machines system. Feedback signals are selected from the generator rotor speed signal  $\omega$ , while input signals are selected from the auxiliary control input signal  $u_{pss}$  of exciters given by PSSs. Since conventional PSSs adopt local machine signals, output feedback signals are obtained from control machines. Thus, the participation factor is introduced in order to take the selection of both feedback and control machines into account

$$p_{ki} = \Phi_{ki} \Psi_{ik} \quad (4.1)$$

According to the mode controllability and mode observability that introduced in the previous chapter, it is necessary to consider the mode controllability of the  $k$ th input signal  $u_{pss}$  as well as the mode observability of the  $k$ th machine output signals  $\omega$  with regard to the  $i$ th mode. To determine the best location of PSS, residue is considered as follows

$$R_{kk}^i = \mathbf{C}_k \Phi_i \Psi_i^T \mathbf{B}_k \quad (4.2)$$

$R_{kk}^i$  measures the relative participation of the  $k$ th machine in the  $i$ th mode based on the mode observability and mode controllability. Therefore, PSS should be placed on the  $k$ th machine which has a relatively greater residue with regard to the  $i$ th mode.

### **4.3 Design of Wide Area Damping Controller**

In most power systems, local oscillation modes are often well damped due to the installation of local PSS. On the other hand, interarea modes are lightly damped because the control inputs used by those PSSs are local signals and they are often lack of observability of certain interarea modes. Because of that, wide area controller which uses wide area measurements as inputs to enhance the damping of interarea oscillations. The proper placement and selection of control inputs are of vital important for achieving satisfactory performance of the damping control [23]. So location and selection of inputs are the two key factors in interarea damping controller design [24].

Figure 4-1 shows the WADC structure that is used in this thesis. In the proposed WADC system, selected stabilizing signals are measured by PMUs. These measurements or signals are time synchronized using GPS and then transmitted via telecommunication links (such as power line carrier, microwave links, or fiber optic) to the controller. Finally, the WADC provides the require control signal to the generator excitation system.

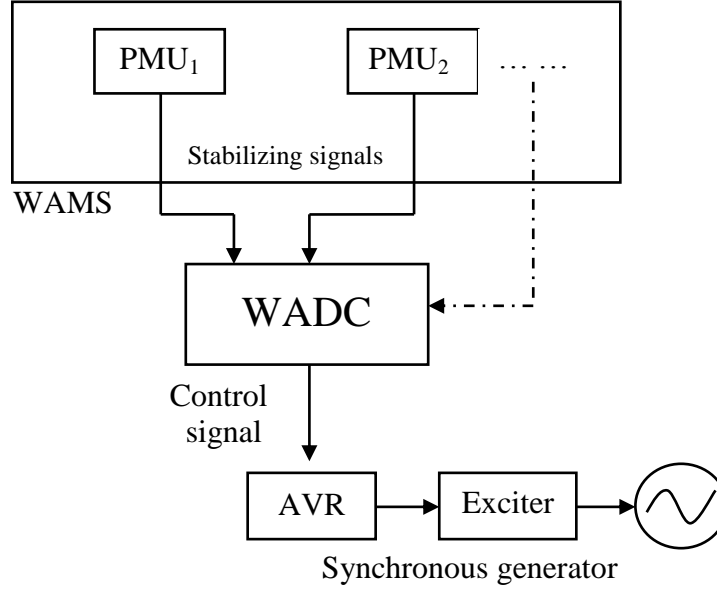


Figure 4-1: Wide Area Damping Control System Structure

In designing WADC, observation machines are selected due to the mode observability of their output signals while control machines are selected due to the mode controllability of their input signals with regard to concerned interarea modes. That means, when the output signal  $\omega$  of the  $j$ th machine has the maximum mode observability and the input signal  $u_{pss}$  of the  $k$ th machine has the maximum mode controllability with regard to the  $i$ th interarea mode, it is better to damp the  $i$ th mode by feeding back the  $\omega$  of the  $j$ th machine as an input to the WADC that located at  $k$ th machine. So, for WADC (4.2) can be rewritten here as

$$R_{jk}^i = \mathbf{C}_j \boldsymbol{\Phi}_i \boldsymbol{\Psi}_i^T \mathbf{B}_k \quad (4.3)$$

Controllability and observability measures can be introduced from (4.3)

$$Cont_{.ik} = |\boldsymbol{\Psi}_i \mathbf{B}_k| \quad (4.4)$$

$$Obse_{ji} = |\mathbf{C}_j \Phi_i| \quad (4.5)$$

Where  $Cont_{ik}$  is used to measure the mode controllability of mode  $i$  from the  $k$ th input and  $Obse_{ji}$  measures the mode observability of mode  $i$  from the  $j$ th output.

#### 4.3.1 WADC Placement

As  $Cont_{ik}$  measures the mode controllability of interarea mode  $i$  from the  $k$ th input, the input with the largest  $Cont.$  should be selected if we expect to control the  $i$ th interarea mode. I.e. the generator related with this input is the location of the WADC. So the WADC used to damp the  $i$ th mode can be located at generator with the maximum  $Cont.$  and this can be expressed by

$$\max_k |\Psi_i \mathbf{B}_k| \quad (4.6)$$

#### 4.3.2 WADC With a Combination Input Signal

Interarea oscillations appear as group of coherent generators swing against each other. Mode shape as discussed in chapter 4 can be determined by using eigenvalues analysis. Dominant generators participating in the oscillation of a specific mode can be gained according to the mode observability of the rotor speed with regard to this mode [23].

As  $Obse_{ji}$  measures the mode observability of interarea mode  $i$  from the  $j$ th output, the system output with the largest  $Obse.$  should be selected if we expect to observe the  $i$ th

mode. The input signals of WADC, generally being the rotor speed signals, can be written as

$$y_j = K_j \Delta \omega \quad (4.7)$$

$$= K_j C_\omega x \quad (4.8)$$

Where  $K_j$  is a selection vector,  $\Delta \omega$  is the column-vector of rotor speed and  $C_\omega$  is the corresponding output matrix. If  $\Delta \omega_k$  is selected in the  $j$ th output, then  $K_{jk}$  is 1 or -1. Otherwise,  $K_{jk}$  is zero.

In order to have better damping of an interarea oscillations, signals from both sides of the oscillating generator groups need to be introduced to the WADC. Therefore, the combination of the signals is used as input to the WADC. This provides both the amplitude and the relative phase of this oscillation. The number of signals from each group should be same to keep symmetric. Considering the PMUs in a practical system are not installed sufficiently, the total amount of signals fed back to WADC is constrained by  $M$ .

As summery of the above analysis, the objective function and its bound constraints are given by

$$\max_j = |K_j C_\omega \Phi_i| \quad (4.9)$$

$$s. t. K_{jk} = 0, 1 \text{ or } -1; \quad (4.10)$$

$$\sum_k |K_{jk}| \leq M; \quad (4.11)$$



$$\sum_{k \in group1} |K_{jk}| = \sum_{k \in group2} |K_{jk}| \quad (4.12)$$

#### 4.4 Controller Parameters Tuning

Assume that the controller is located at generator  $j$  having the largest controllability of the  $i$ th mode. The output  $\Delta\omega$  is fed back to the controller. In the condition of local PSS design,  $\Delta\omega$  is the rotor speed from the same generator  $j$ . While in the condition of WADC design, it is the combination of wide area rotor speed signals from different generators participating in that certain  $i$ th mode.

Figure 4-2 shows WADC block diagram connected to the generator exciter. The wide area damping system consists of i) WAMS block, where all concerned signals throughout the system are measured using PMUs, time stamped and transmitted to the controller, and ii) WADC, where the main control action signal is provided. WADC block consists of simple lead/lag compensation block and the main controller block which is responsible for selecting controller input signals combination and process the final wide area damping signal to the Lead/Lag compensation block.

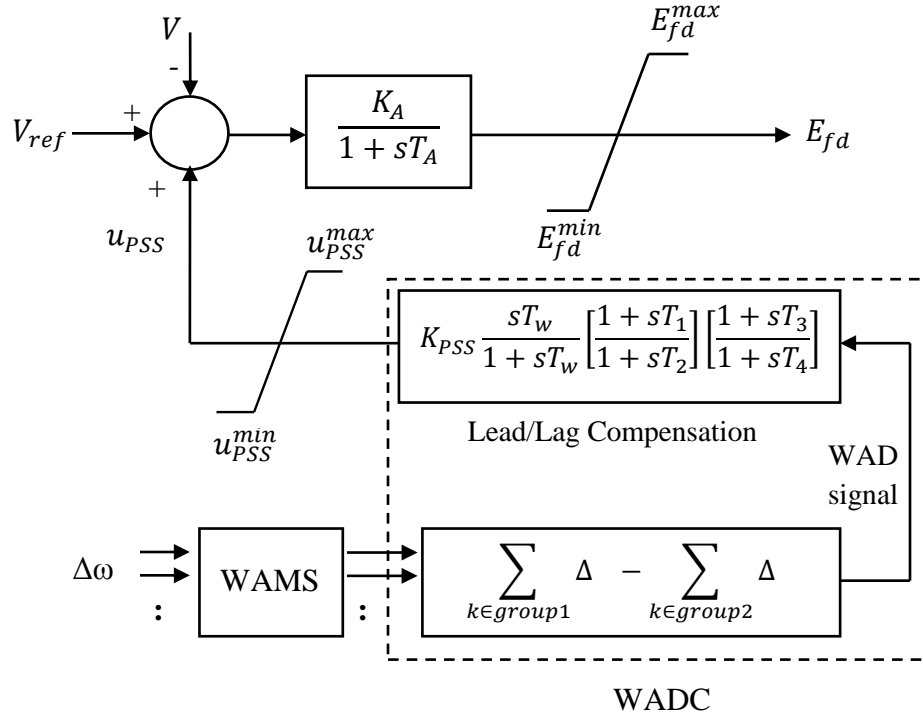


Figure 4-2: Wide Area Damping Controller

The design of WADC in this chapter is in accordance with the line of “measurement – identification – design”. The first stage is the measurement and as mentioned before it the function of WAMS. The second stage is to identify the oscillatory modes of concerned and to decide which signals combination will be involved in design stage. The last step is WADC parameters tuning. The phase compensation method is used here in WADC design. From Figure 4-2, the transfer function of Lead/Lag compensation block is

$$H(s)_j = K_{PSS} \frac{sT_w}{1+sT_w} \left[ \frac{1+sT_1}{1+sT_2} \right] \left[ \frac{1+sT_3}{1+sT_4} \right] \quad (4.13)$$

Where  $K_{PSS}$  is the constant gain of the controller.  $T_1, T_2, T_3$  and  $T_4$  are the time constants of lead/lag compensation block of the controller.  $T_w$  is the washout time constant (usually 5-10 sec.). The relationship of the eigenvalue  $\lambda_i$  and the transfer function  $H(s)_j$  is as following [24]

$$\partial \lambda_i / \partial K_{PSS} = \boldsymbol{\Psi}_i \mathbf{B}_k (\partial H_j(\lambda_i) / \partial K_{PSS}) \mathbf{C}_j \boldsymbol{\Phi}_i \quad (4.14)$$

For small values of gain  $K_{PSS}$ , (4.14) gives

$$\begin{aligned} \Delta \lambda_i &= \Delta K_{PSS} \boldsymbol{\Psi}_i \mathbf{B}_k (\partial H_j(\lambda_i) / \partial K_{PSS}) \mathbf{C}_j \boldsymbol{\Phi}_i \\ &= (\mathbf{C}_j \boldsymbol{\Phi}_i) (\boldsymbol{\Psi}_i \mathbf{B}_k) \Delta H_j(\lambda_i) \\ &= R_{jk}^i \Delta H_j(\lambda_i) \end{aligned} \quad (4.15)$$

Where  $R_{jk}^i$  is the residue defined in (4.3). The change of the eigenvalue should be directed towards the left-hand plan. This can be done by shaping the phase of  $H_j(s)$  using phase lead compensation. The required phase lead  $\varphi$  is given by

$$\varphi = \pi - \arg(R_{jk}^i) \quad (4.16)$$

Where  $\arg(R_{jk}^i)$  is the angle of the complex residue  $R_{jk}^i$ . Then  $T_1, T_2, T_3$  and  $T_4$  can be solved by

$$\alpha = \frac{1 - \sin(\varphi/2)}{1 + \sin(\varphi/2)}, \quad T_1 = T_3 = \frac{1}{\omega \sqrt{\alpha}}, \quad T_2 = T_4 = \alpha T_1 \quad (4.17)$$

Where  $\omega$  is the frequency of the concerned mode in rad/s. The controller gain  $K_{PSS}$  can be computed as a function of desired eigenvalues location  $\lambda_{i,des}$  as follow

$$K_{PSS} = \left| \frac{\lambda_{i,des} - \lambda_i}{R_{jk}^i H_j(\lambda_i)} \right| \quad (4.18)$$

## 4.5 Summary

Local PSS was designed using residue analysis which determines the best location of the controller to damp out the local oscillatory modes. For the WADC design, the optimal location of the controller was placed based on controllability measure. Then, the combination input signals to the WADC are selected based on participation of machines in the interested interarea mode. The last step in WADC design is parameters tuning such that the performance of the controller in damping inter area oscillations is enhanced. The phase compensation method was used here in to determine parameters setting which provide the require phase lead compensation in order to direct the eigenvalue towards the left-hand plan.

## **CHAPTER 5**

# **DESIGN OF LOCAL PSS FOR MULTIMACHINE**

## **TWO-AREA SYSTEM**

### **5.1 Introduction**

The main objective of chapter 5 is to analyze and design PSSs for the purpose of damping local modes of oscillations. A standard two area power system is considered here as a case study. Eigenvalues analysis (Modal analysis) is carried out on the test system to identify the nature of the oscillations; local or interarea modes. Additionally, out of the modal analysis, the required number of PSSs and their optimal locations can be determined. After that, the stabilizers parameters need to be tuned to improve stabilizers performance in damping the oscillations. Last section presents the nonlinear time domain simulation in order to observe the dynamic response of the system after applying local PSSs. Appendix B shows the details of modal analysis results taken from Matlab Workspace. However, relevant results will be discussed here.

## 5.2 Case Study

A 4-machine two area system which consists of two similar areas connected by a tie-line as shown in Figure 5-1 is considered. Each area consists of two coupled generating units, each having rating of 900 MVA and 20 kV. All four generating units are represented by the same dynamic model and equipped with fast static exciter. The system is operating with area-1 exporting approximately 400 MW to area-2. This system is considered as one of the benchmark models for performing studies on interarea oscillation because of its realistic structure and availability of system parameters [2]. Details of the system data including the dynamic generators model and exciter data used along with load flow result are given in Appendix A.

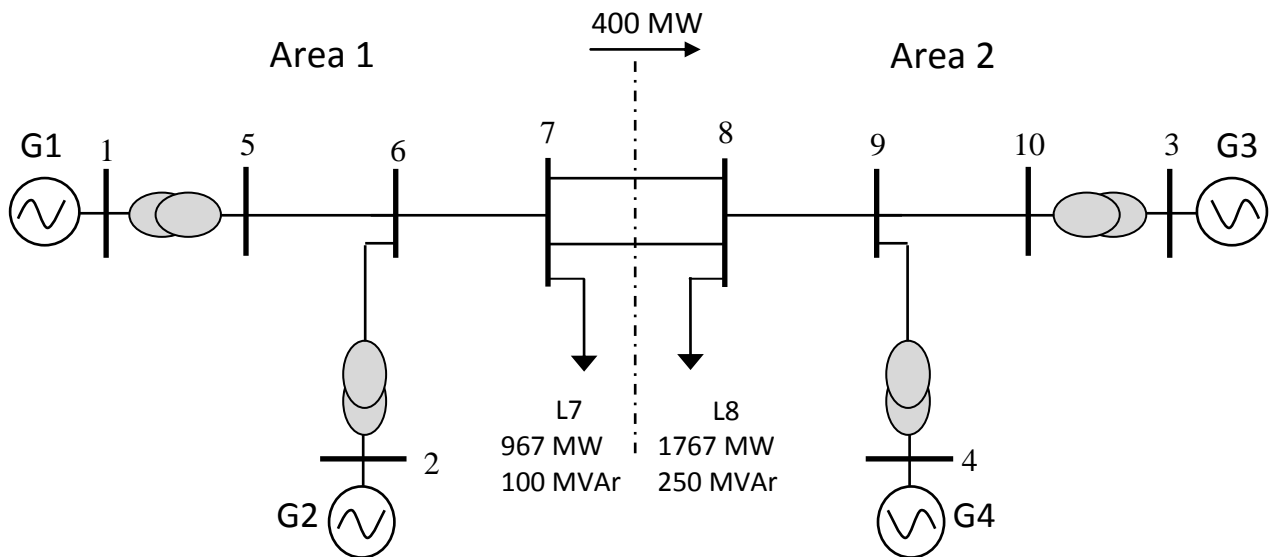


Figure 5-1: Two area four machine system

### 5.3 Modal Analysis

Modal analysis is carried out on the two area system to identify the oscillatory modes, mode shape and what are the dominant state variables that influence on each oscillatory mode. Moreover, the optimal location of local PSS in each area will be determined during the analysis.

The analysis here is carried out on the base case of loading condition given in Appendix A. The base system is the system without adding any PSSs or any other controller on the machines. So the size of the state matrix  $A$  is 16x16 which consists of 4 state variables per machine; three for the machine and one for the excitation system. The oscillation profile of the power system is simply the oscillatory modes information resultant from the eigenvalue analysis. From the oscillation profile, the oscillatory modes can be identified and their frequency and damping ratios are calculated. Table 5-1 shows the oscillatory modes results.

Table 5-1: Oscillatory modes of the system without control

Mode No.	Eigenvalue	Frequency Hz	Damping Ratio, $\zeta$
7	$-0.6349 \pm j 7.4525$	1.1861	0.0849
9	$-0.5275 \pm j 7.3083$	1.1632	0.0720
11	$0.1056 \pm j 4.0179$	0.6395	-0.0263

From Table 5-1, it is clear that one mode (mode-11) is unstable with a positive real part and negative damping ratio. The other two modes are stable with negative real parts and

positive damping ratios. Now further analysis need to be done to identify the type of oscillation and the dominant states in each oscillatory modes.

The participation factors shall be examined to determine the dominant states involved in each oscillatory modes. The participation factor magnitudes results for the oscillatory modes are given in Table 5-2. For mode-7, it can be seen that the participation factor of the rotor speed ( $\Delta\omega$ ) and rotor angle ( $\Delta\delta$ ) of generators G1 and G2 have the largest magnitudes. This indicates that these states have the greatest participation in this mode. In case of mode-9, generators G3 and G4 have the largest participation factor magnitudes and this indicates that these machines contribute more than the others during oscillations. Last part of Table 5-2 reveals that all machines are participating in mode-11. The previous information gives a clear indication on the type of oscillation (mode shape) for the three oscillatory modes; mode-7 is local oscillation mode in area 1, mode-9 is local oscillation mode in area 2 and mode-11 is interarea oscillation mode between area 1 and area 2.

Once the dominant states have been identified for each mode, the mode shape can be determined from the elements in the right-eigenvector corresponding to the state variables involved in the mode. The rotor angle right-eigenvector elements for the three modes are shown in Table 5-3. From the magnitude and the sign of the real part of the eigenvector entries, the mode shape can be determined. For mode-7, G1 has positive real part whereas G2 has negative one. This indicates that G1 rotate against G2 locally in area 1. Similarly, the second local oscillation of area 2 is between G3 and G4 as they have different real part signs. For the last mode, mode-11, it can be concluded that this is



interarea mode, since both G1 and G2 have same sign of real part and opposite to what G3 and G4 have. Table 5-4 summarized the results that can be concluded from the participation factors and mode shape analysis. Figure 5-2 and Figure 5-3 show the mode shapes corresponding to the rotor angle states for the two oscillatory modes, mode-7 and mode-9. It is clear from the mode shapes that these modes are local oscillation modes. On the other hand, Figure 5-4 shows mode-11 shape which indicates interarea oscillation between area 1 generators and area 2 generators.

Table 5-2: Participation factor magnitudes of oscillatory modes

<b>Mode 7</b>				
<b>Generator</b>	<b><math>\Delta\delta</math></b>	<b><math>\Delta\omega</math></b>	<b><math>\Delta E'_q</math></b>	<b><math>\Delta E_{fd}</math></b>
1	0.4913		0.0439	0.0006
2	0.5433		0.1350	0.0029
3	0.0205		0.0015	0.0000
4	0.0379		0.0081	0.0001
<b>Mode 9</b>				
<b>Generator</b>	<b><math>\Delta\delta</math></b>	<b><math>\Delta\omega</math></b>	<b><math>\Delta E'_q</math></b>	<b><math>\Delta E_{fd}</math></b>
1	0.0406		0.0032	0.0000
2	0.0180		0.0044	0.0002
3	0.4994		0.0398	0.0001
4	0.5196		0.1102	0.0023
<b>Mode 11</b>				
<b>Generator</b>	<b><math>\Delta\delta</math></b>	<b><math>\Delta\omega</math></b>	<b><math>\Delta E'_q</math></b>	<b><math>\Delta E_{fd}</math></b>
1	0.3096		0.0017	0.0000
2	0.2899		0.0077	0.0004
3	0.2286		0.0015	0.0004
4	0.1602		0.0324	0.0015

Table 5-3: Right-eigenvector elements (Corresponding to  $\Delta\delta$ )

<b>Mode 7</b>	
<b>Generator</b>	<b>Right Eigenvector Entry</b>
1	$0.0150 \mp j 0.0396$
2	$-0.0210 \pm j 0.0368$
<b>Mode 9</b>	
<b>Generator</b>	<b>Right Eigenvector Entry</b>
3	$0.0189 \mp j 0.0448$
4	$-0.0226 \pm j 0.0411$
<b>Mode 11</b>	
<b>Generator</b>	<b>Right Eigenvector Entry</b>
1	$-0.0530 \pm j 0.0914$
2	$-0.0456 \pm j 0.0846$
3	$0.0226 \mp j 0.0744$
4	$0.0226 \mp j 0.0487$

Table 5-4: Oscillatory modes shape for the system without control

<b>Mode</b>	<b>Damping Ratio, <math>\zeta</math></b>	<b>Mode Shape</b>
$-0.6349 \pm j 7.4525$	0.0849	G1 vs. G2
$-0.5275 \pm j 7.3083$	0.0720	G3 vs. G4
$0.1056 \pm j 4.0179$	-0.0263	G1&G2 vs. G3&G4

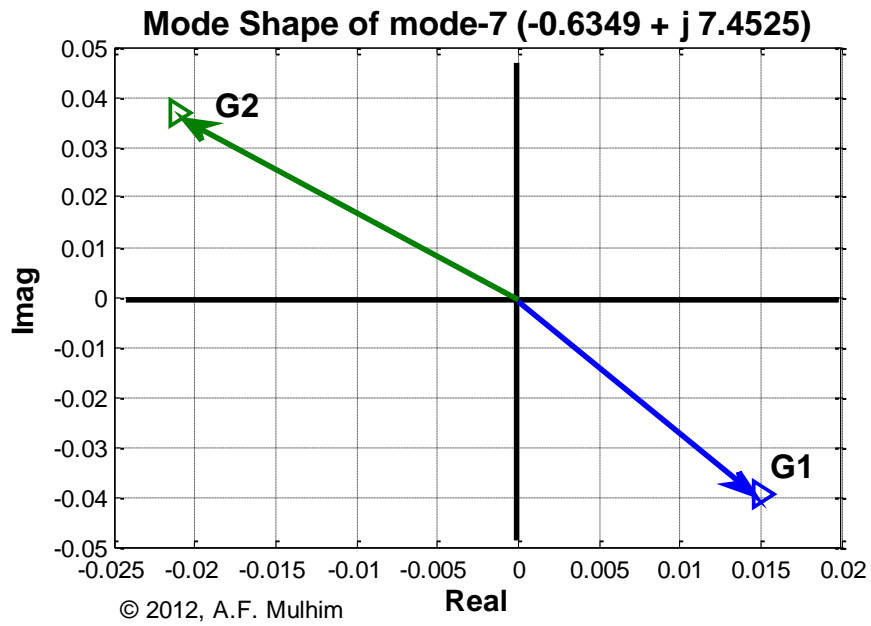


Figure 5-2: Mode shape of rotor angle (Mode-7) - System without control

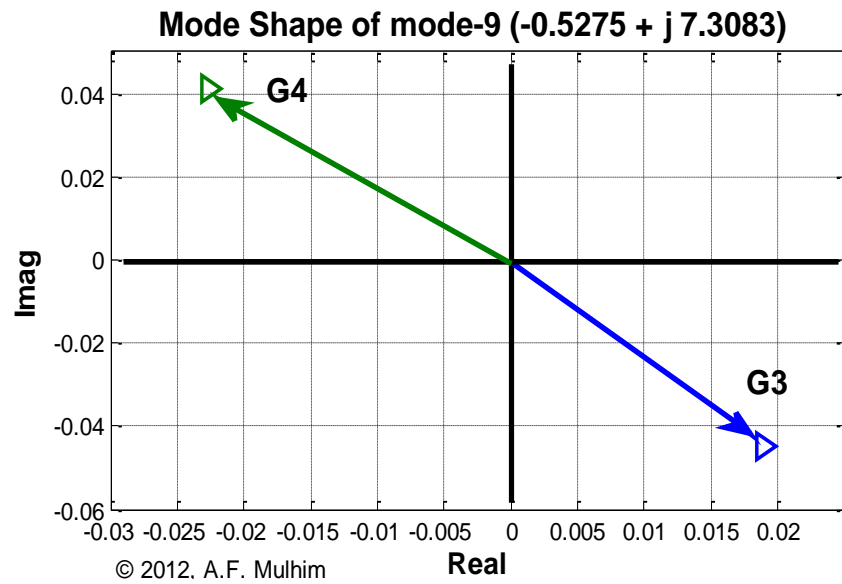


Figure 5-3: Mode shape of rotor angle (Mode-9) - System without control

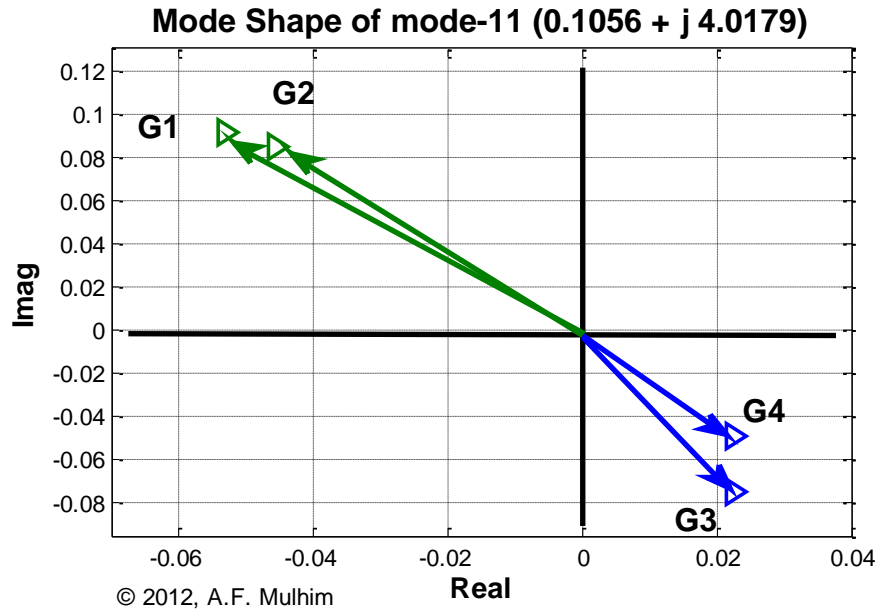


Figure 5-4: Mode shape of rotor angle (Mode-11) - System without control

Now, the interested oscillatory modes have been identified. The dominant machines and their state variables which highly participate in each mode are determined. The next section objective is to find out the number of PSSs required and their optimal locations in order to damp the oscillation in the system. Since this chapter focus on the analysis and design of local PSSs, only local oscillation modes will be considered here. The interarea oscillation mode will be considered in the next chapter where WADC is designed.

## 5.4 Local PSSs Design

### 5.4.1 Local PSSs Placement

To provide additional damping to the system, PSSs are added. Here, one PSS will be installed at each area. As mentioned, these stabilizers are local based and their objectives

are to enhance damping the local area oscillations only. Because of that, only local modes of oscillations will be considered in designing these stabilizers.

The local PSS can be located at the generator with the largest residue for the corresponding mode. So, calculating controllability measure and residue using previous section modal analysis are necessary to determine the location of PSS.

From participation factor results, Table 5-2, it can be seen that G2 has the largest PF among the others for mode-7. That means, this machine has more effect and can influence the oscillation on this mode more than the other machine in the same area. Similarly, for mode-9, where G4 has largest PF which indicates that this machine is the candidate place to install PSS to damp out area 2 oscillations. To support the previous discussion and confirm placing PSSs at G2 and G4 as optimal locations for damping local area oscillations, controllability measure and residue should be calculated. The controllability measures and residues of the four generators associated with local modes (mode-7 and mode-9) are shown in Figure 5-5 and Figure 5-6. It is clear that placing a PSS at G2 will improve damping the oscillations of Mode-7 since G2 has the largest residue in that mode. On the other local mode, G4 has the largest residue. So, the local PSSs should be located at G2 and G4 in order to get the best improvement in damping local area oscillations.

Additionally, to confirm the analysis, PSS is placed at each generator one by one and the eigenvalues and damping ratios are calculated. Typical values were chosen from reference [2] for the PSS parameters;  $K_{PSS}=10$ ,  $T_W=5$ ,  $T_1=T_3=0.1$  and  $T_2=T_4=0.05$ . Table

5-5 summarizes the results of placing PSS at each generator. The first column gives the PSS location. Column three and four contain the eigenvalue information followed by the damping ratio of that particular oscillatory mode. Results show that G2 is the best location to damp out the local area mode (Mode-7) with damping ratio of 0.2291. Whereas, the best place for PSS, to damp out the second local area mode (Mode-9), is G4 with damping ratio of 0.1952. As expected, eigenvalues and damping ratios results confirmed modal analysis results.

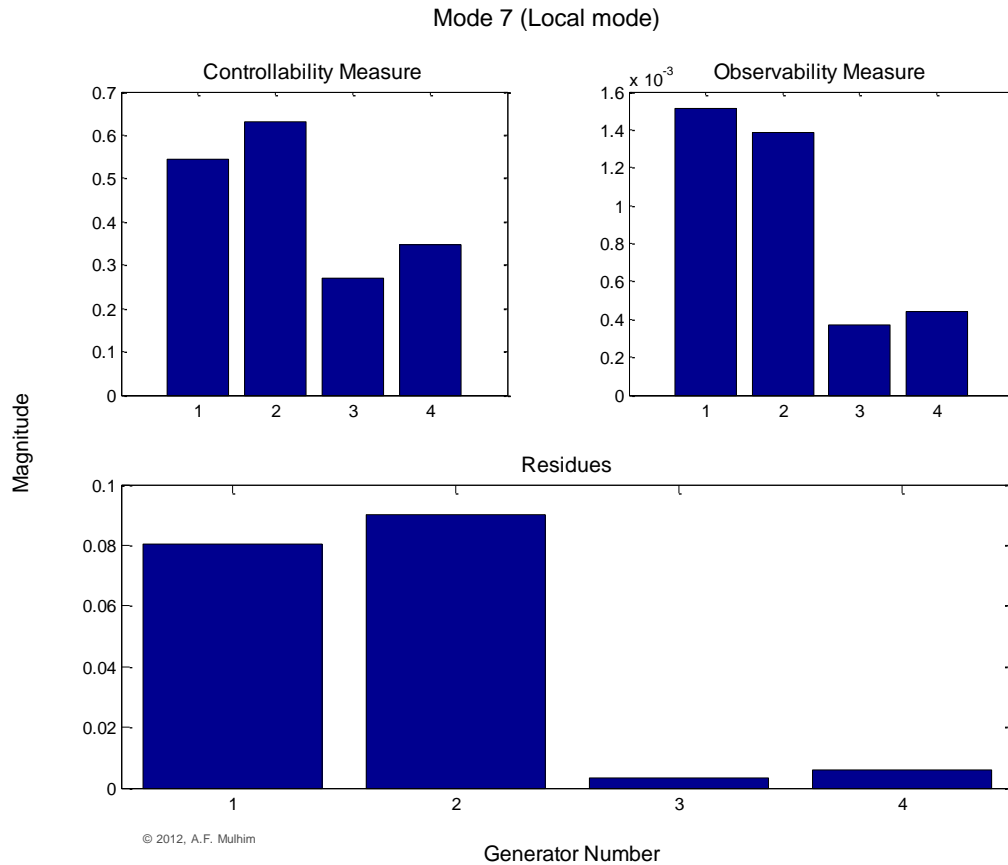


Figure 5-5: Controllability, observability and residue of Mode-7

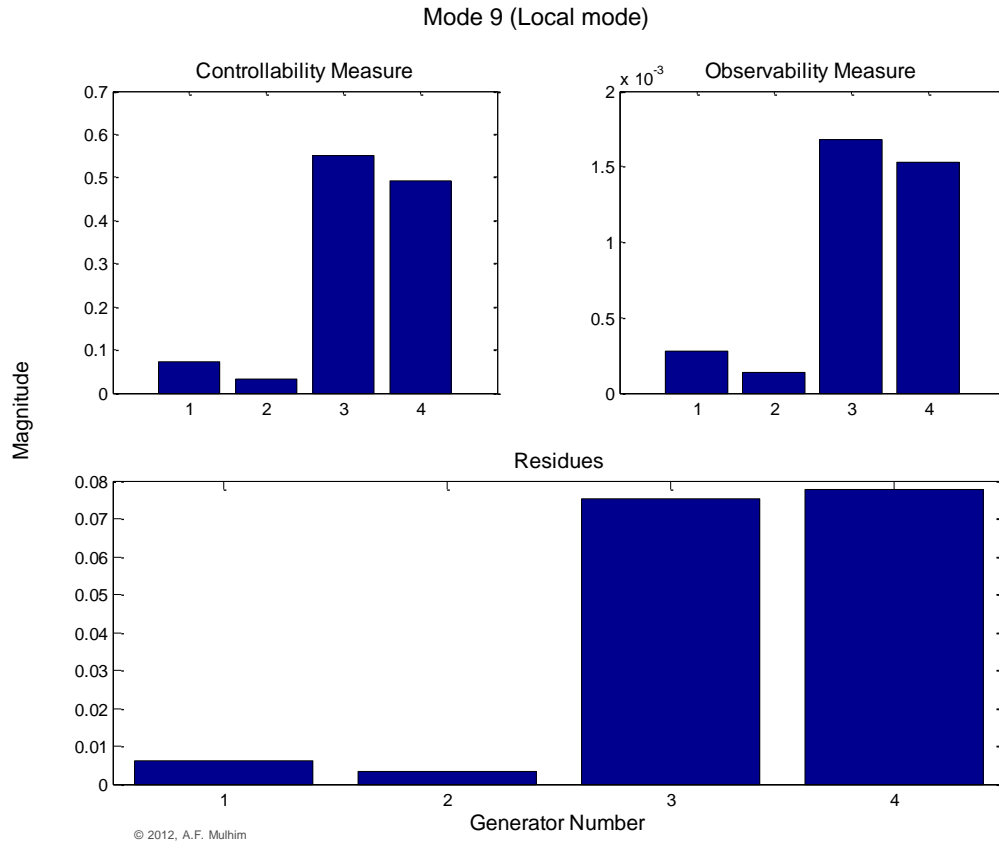


Figure 5-6: Controllability, observability and residue of Mode-9

Table 5-5: Oscillatory modes for the system with PSS

PSS Location	Mode	Eigenvalue	Damping Ratio
None	Mode 7 (Local-area1)	$-0.6349 \pm j 7.4525$	0.0849
	Mode 9 (Local-area2)	$-0.5275 \pm j 7.3083$	0.0720
	Mode 11 (Inter-area)	$0.1056 \pm j 4.0179$	-0.0263
G1	Mode 7 (Local-area1)	$-1.5322 \pm j 8.0049$	0.1880
	Mode 9 (Local-area2)	$-0.5353 \pm j 7.3161$	0.0730
	Mode 11 (Inter-area)	$-0.0392 \pm j 4.0048$	0.0098
G2	Mode 7 (Local-area1)	$-1.8546 \pm j 7.8797$	0.2291
	Mode 9 (Local-area2)	$-0.5317 \pm j 7.3118$	0.0725
	Mode 11 (Inter-area)	$-0.1663 \pm j 4.1116$	0.0404
G3	Mode 7 (Local-area1)	$-0.6304 \pm j 7.4451$	0.0844
	Mode 9 (Local-area2)	$-1.3940 \pm j 7.7761$	0.1765
	Mode 11 (Inter-area)	$-0.0014 \pm j 4.0394$	0.0004
G4	Mode 7 (Local-area1)	$-0.6279 \pm j 7.4397$	0.0841
	Mode 9 (Local-area2)	$-1.5466 \pm j 7.7721$	0.1952
	Mode 11 (Inter-area)	$-0.0301 \pm j 4.0704$	0.0074

### 5.4.2 PSSs Parameters Tuning

In order to get the best performance out of PSS, its parameters should be set carefully. As presented earlier, Phase Compensation method is used to calculate the PSS parameters. Again, only local oscillatory modes will be considered here during PSS parameters tuning.

Recall from equation (4.13), the transfer function of lead/lag compensation PSS was presented as

$$H(s)_j = K_{PSS} \frac{sT_w}{1+sT_w} \left[ \frac{1+sT_1}{1+sT_2} \right] \left[ \frac{1+sT_3}{1+sT_4} \right] \quad (5.1)$$

Using equations (4.16)-(4.18);  $K_{PSS}$ ,  $T_1$ ,  $T_2$ ,  $T_3$  and  $T_4$  can be calculated. Table 5-6 lists the information that is required to apply the above mentioned equations; mainly residues and eigenvalues of the concerned mode. By employing this information into equation (4.13), (4.16)-(4.18), local PSSs parameters can be determined. Table 5-7 shows the calculated parameters results for both local PSSs at G2 and G4.

Table 5-6: Information required to use phase compensation technique for local PSSs

Concerned Mode	Residue (at $G_i$ )	Eigenvalue $\lambda = \sigma \pm j\omega$	$\sigma$	$\omega$
Mode-7 Local Mode 1	-0.0707 +j 0.0557 (at $G_2$ )	-0.6349 ± j 7.4525	-0.6349	7.4525
Mode-9 Local Mode 2	-0.0593 +j 0.0504 (at $G_4$ )	-0.5275 ± j 7.3083	-0.5275	7.3083



Table 5-7: Local PSSs parameters

Location of PSS	$K_{PSS}$	$T_1$ & $T_3$	$T_2$ & $T_4$	$T_w$
G2	10.66	0.1885	0.0955	10
G4	11.68	0.1961	0.0955	10

To evaluate the effectiveness of placing two local PSSs (one at each area) with the new calculated parameters on the oscillatory modes, the new eigenvalues and damping ratios are determined. Table 5-8 shows the new oscillatory mode after PSSs are applied. It compares results of applying PSSs with reference [2] parameters and PSSs with the calculated phase lead compensation technique. It is clear that the oscillatory mode eigenvalues have been shifted to the left when PSSs are tuned using phase compensation method, and thus damping ratio improved accordingly.

Table 5-8: Oscillatory modes for the system with tuned PSSs at G2 and G4

Oscillatory Mode	Eigenvalue		Damping Ratio	
	Kundur [2]	Proposed	Kundur [2]	Proposed
Mode-7 Local Mode 1	-1.8921 $\pm j$ 7.9598	-1.8930 $\pm j$ 6.2886	0.2313	0.2882
Mode-9 Local Mode 2	-1.5027 $\pm j$ 7.6941	-2.1751 $\pm j$ 5.7087	0.1917	0.3560
Mode-11 Inter area Mode	-0.2642 $\pm j$ 4.2064	-0.5507 $\pm j$ 4.0233	0.0627	0.1356

## 5.5 Non-Linear Time Domain Simulation

Nonlinear time domain simulation was performed using the developed Matlab code to validate the damping performance of installing two local PSSs at G2 and G4. A 100 ms

three phase fault at bus 8 is considered. Figure 5-7 to Figure 5-23 show machines responses of the two area power system for such sever disturbance. It can be seen that system without PSSs experiences serious power oscillations. However, with implement of PSSs, at G2 and G4, such power oscillations are damped out. Furthermore, the performance of the PSSs, tuned by phase compensation technique, is greatly improved comparing to reference [2] and provide better damping characteristics to the power oscillations and thus enhance the dynamic stability of the power system. The nonlinear time domain simulation results confirm the conclusion drawn from modal analysis.

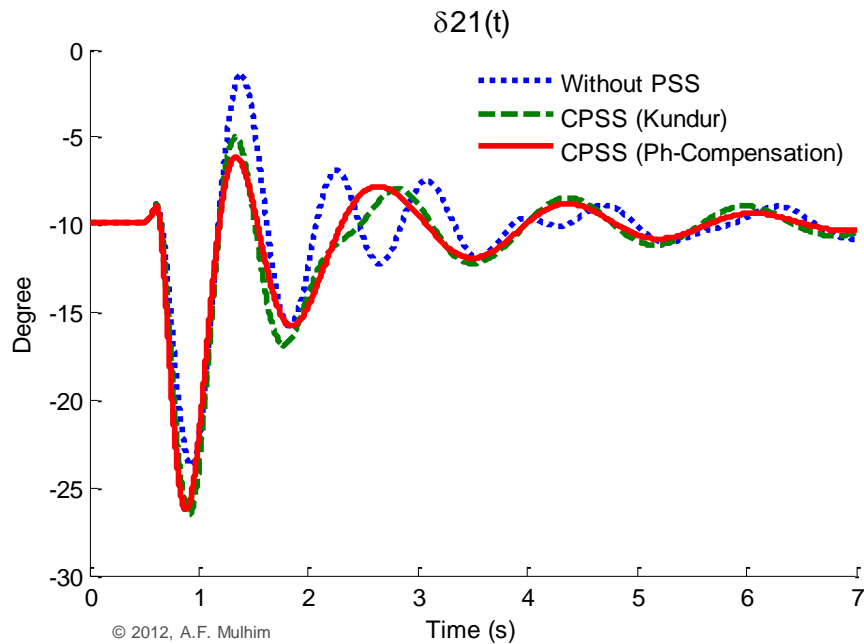


Figure 5-7: Rotor angle  $\delta_{21}$  response with local PSSs at G2 and G4

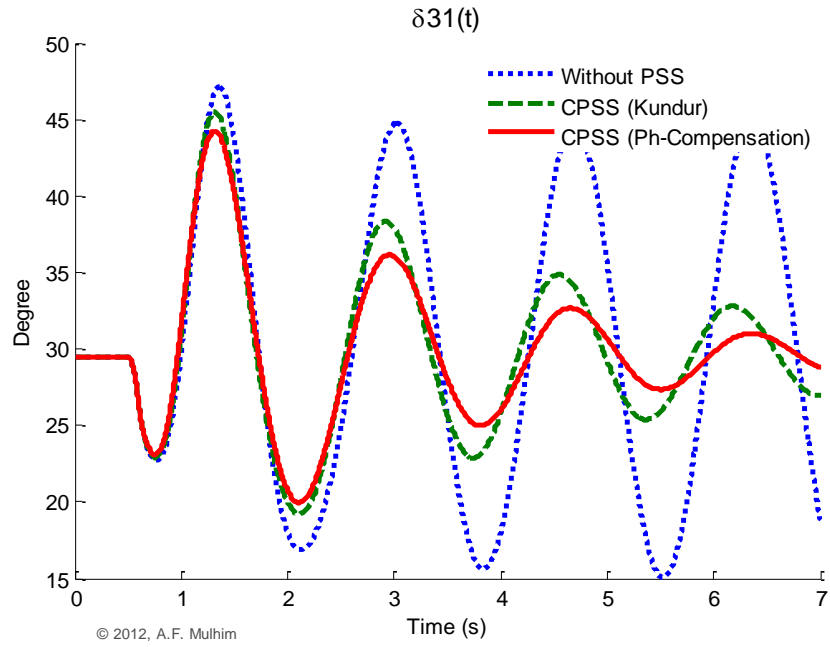


Figure 5-8: Rotor angle  $\delta_{31}$  response with local PSSs at G2 and G4

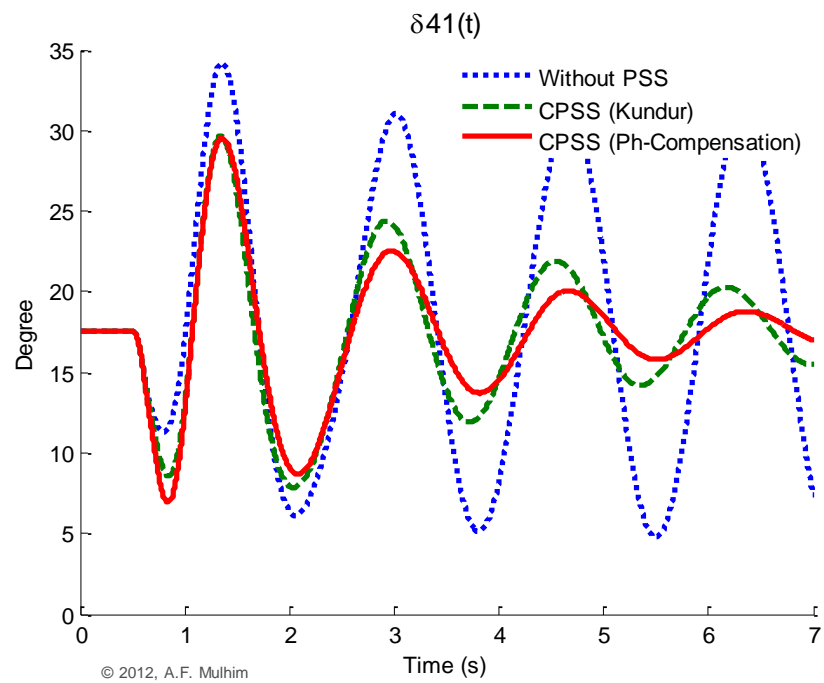


Figure 5-9: Rotor angle  $\delta_{41}$  response with local PSSs at G2 and G4

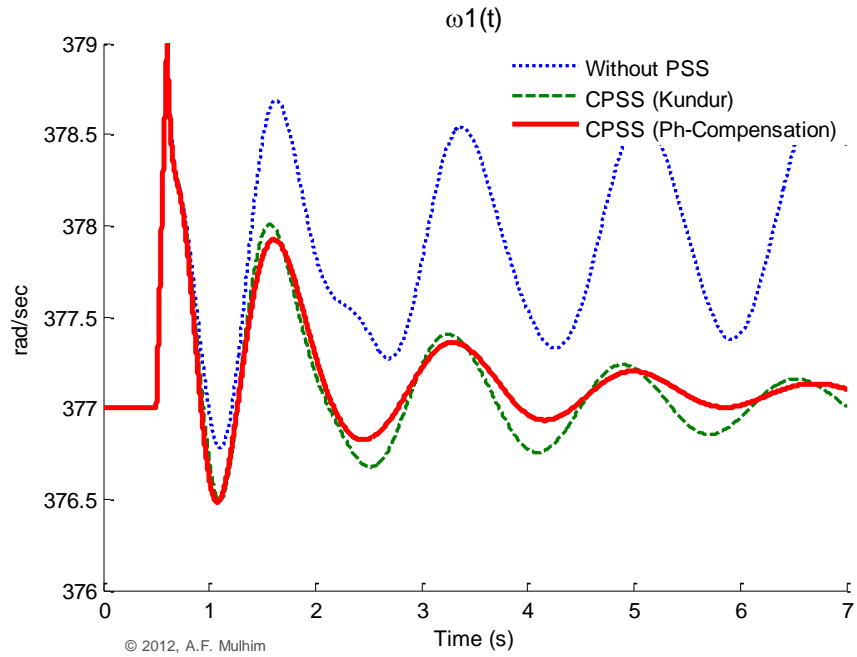


Figure 5-10: Rotor speed  $\omega_1$  response with local PSSs at G2 and G4

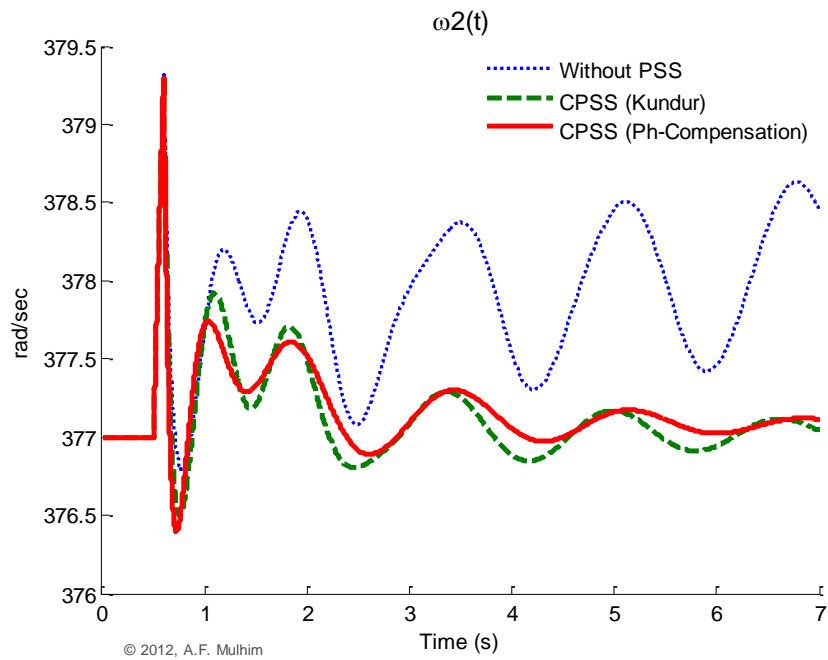


Figure 5-11: Rotor speed  $\omega_2$  response with local PSSs at G2 and G4

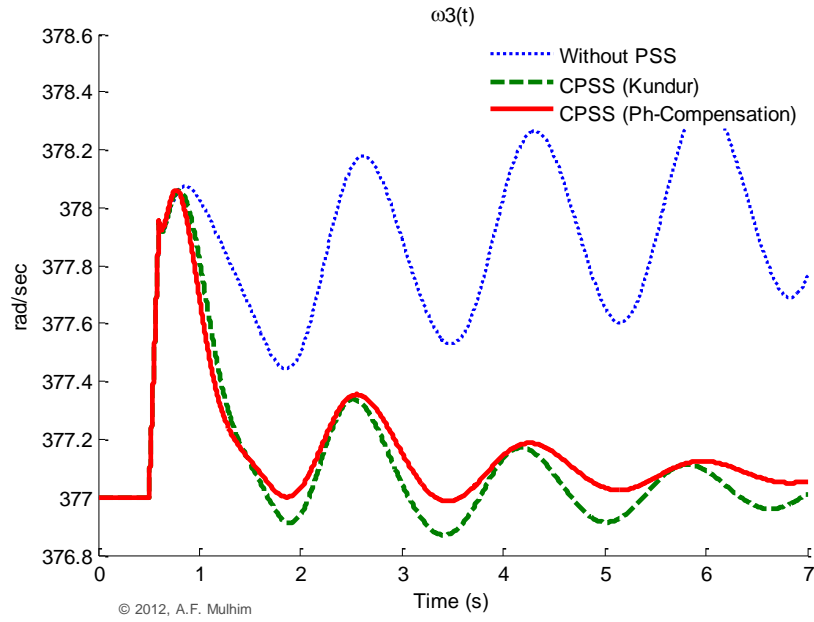


Figure 5-12: Rotor speed  $\omega_3$  response with local PSSs at G2 and G4

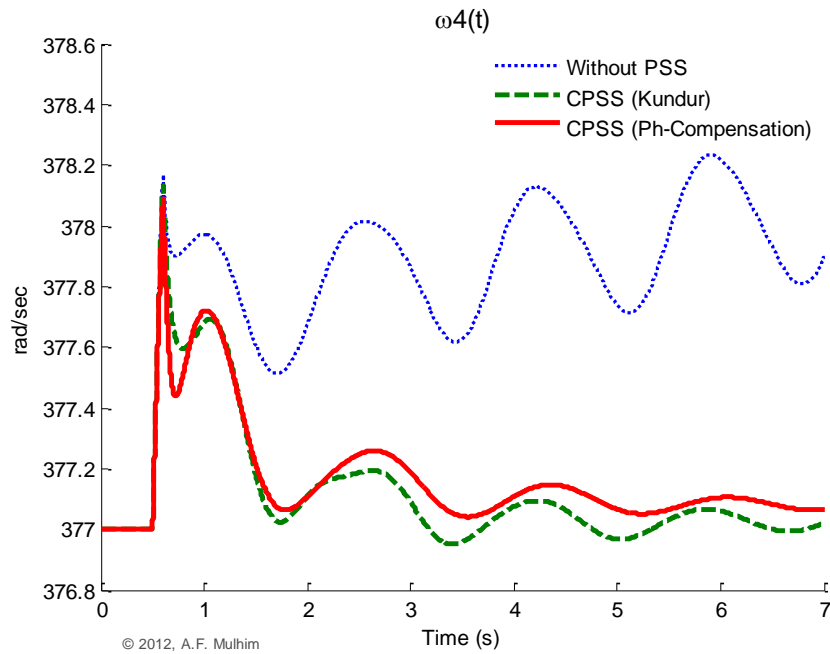


Figure 5-13: Rotor speed  $\omega_4$  response with local PSSs at G2 and G4

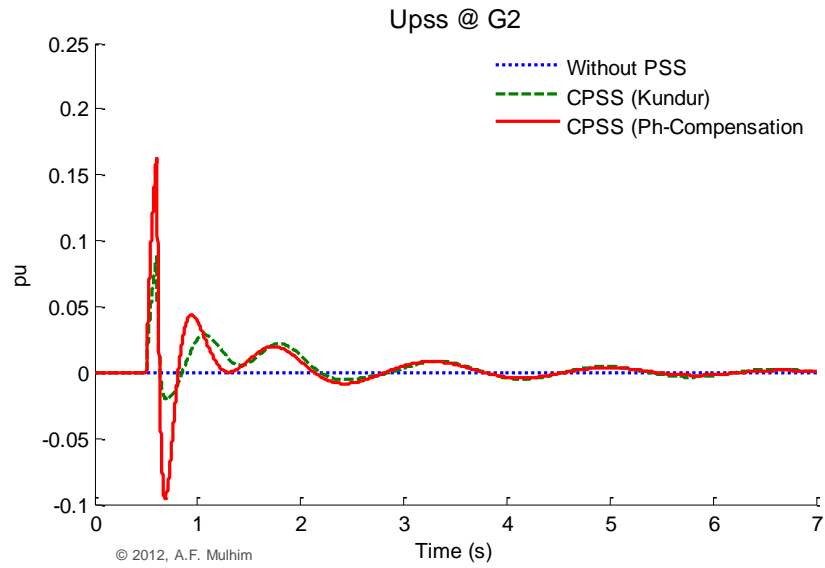


Figure 5-14: Control response of PSS at G2

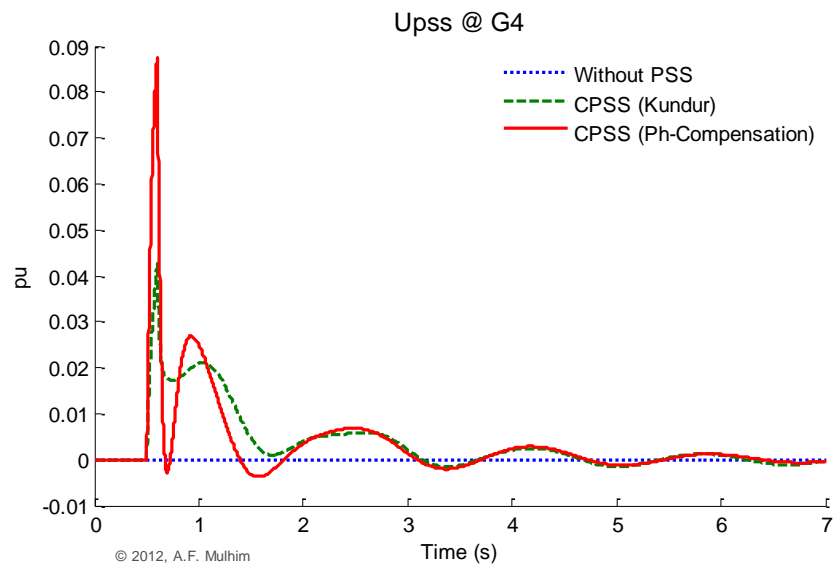


Figure 5-15: Control response of PSS at G4

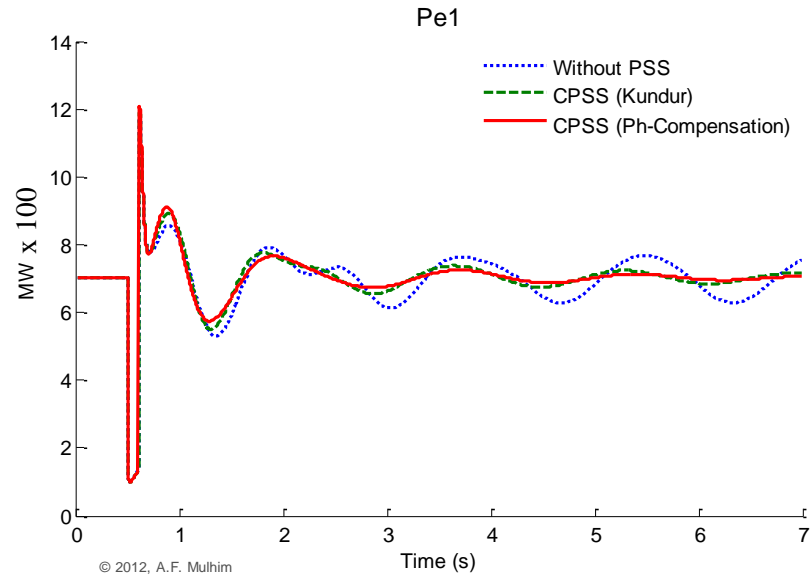


Figure 5-16: Electric power output  $P_{e1}$  response with local PSSs at G2 and G4

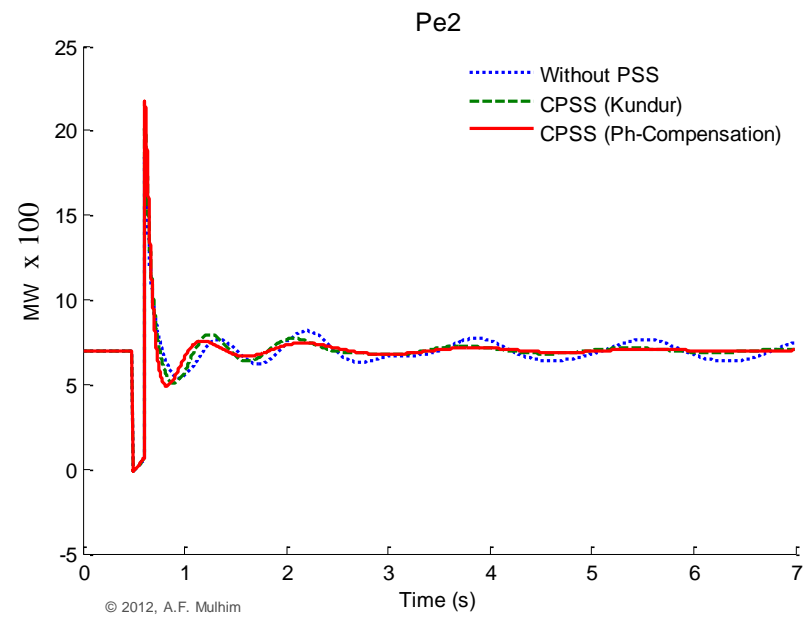


Figure 5-17: Electric power output  $P_{e2}$  response with local PSSs at G2 and G4

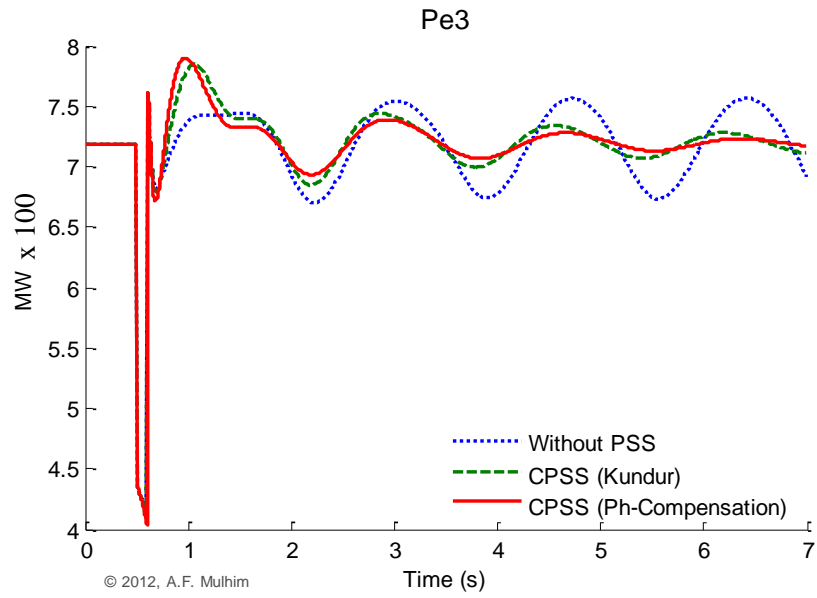


Figure 5-18: Electric power output  $P_{e3}$  response with local PSSs at G2 and G4

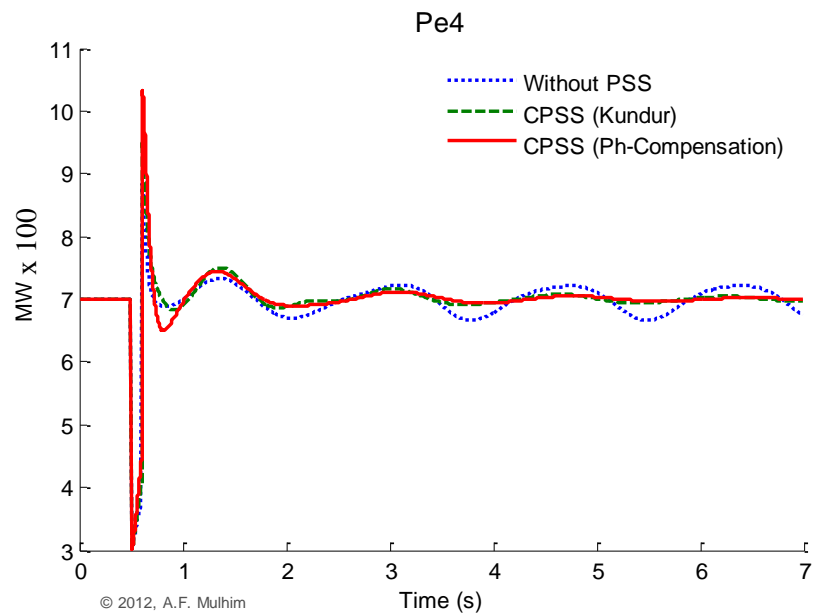


Figure 5-19: Electric power output  $P_{e4}$  response with local PSSs at G2 and G4



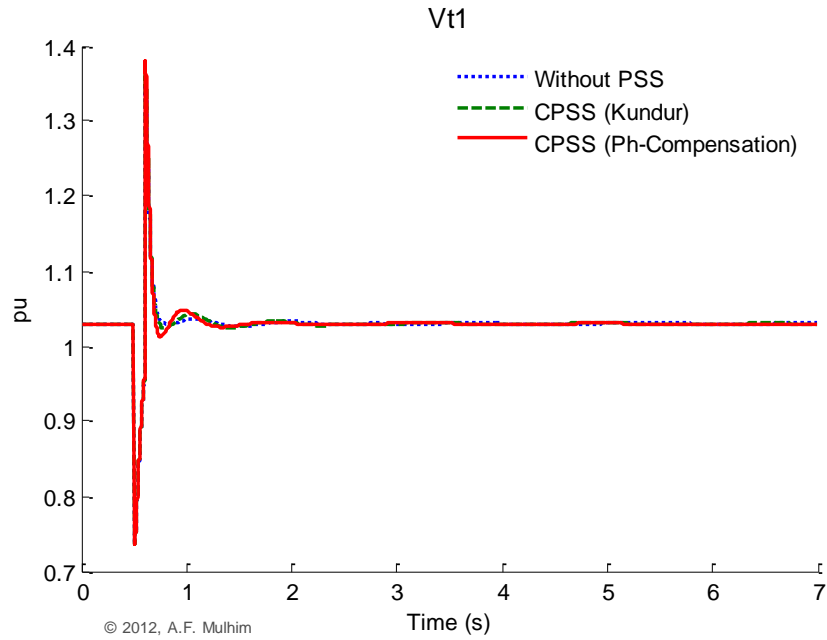


Figure 5-20: Terminal voltage  $V_{t1}$  response with local PSSs at G2 and G4

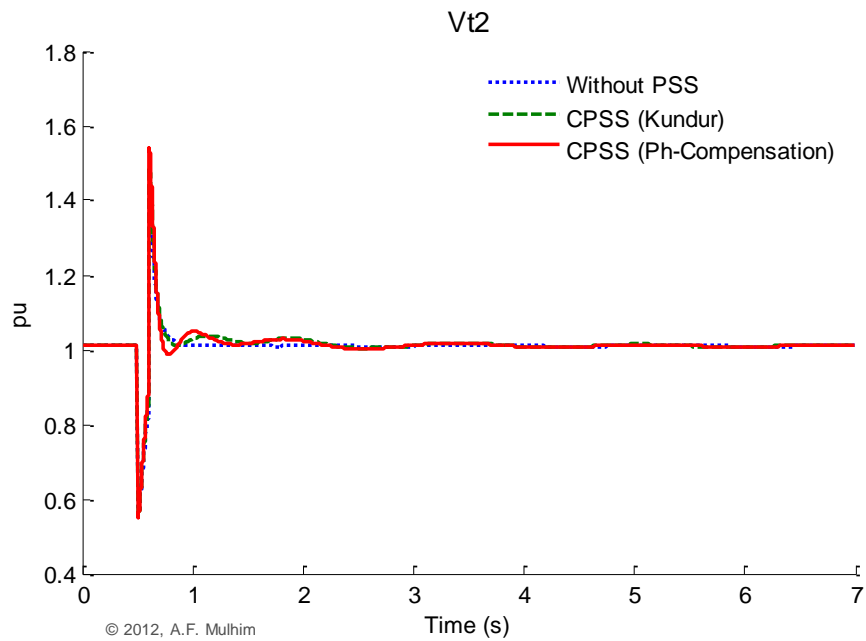


Figure 5-21: Terminal voltage  $V_{t2}$  response with local PSSs at G2 and G4

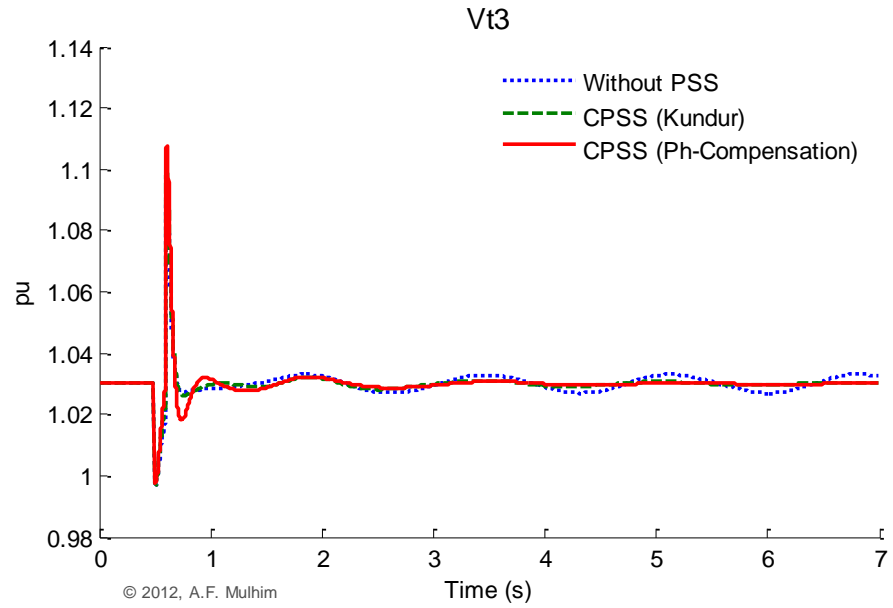


Figure 5-22: Terminal voltage  $V_{t3}$  response with local PSSs at G2 and G4

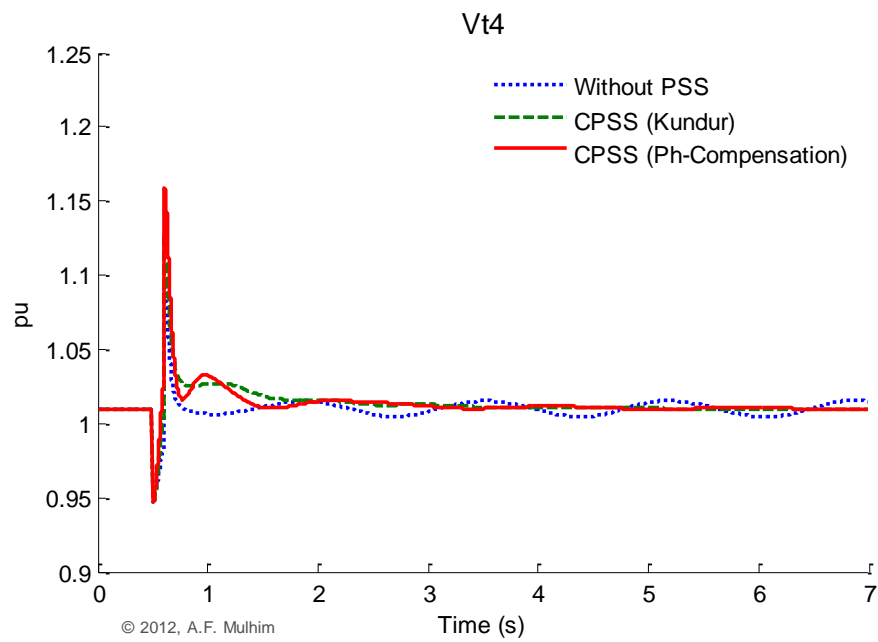


Figure 5-23: Terminal voltage  $V_{t4}$  response with local PSSs at G2 and G4

## 5.6 Summary

System analysis and control design were carried out on the considered two area power system. Modal analysis parameters included; eigenvalues, eigenvectors, PF, controllability and observability measures and residues were determined. From, modal analysis outcomes, type of oscillations modes were identified, and the PSSs were placed such that they provide better damping characteristics. After the local PSSs are located, their parameters were tuned using phase lead/lag compensation technique. Eigenvalues of the system are calculated after applying the tuned PSSs and results show that the eigenvalues are shifted to the left side of the plan. This indicates that damping is improved and the dynamic stability is enhanced accordingly. The last section of this chapter is the machines time domain simulation responses when the system is exposed to sever disturbance. Machine rotor angles, rotor speeds and the other parameters responses confirm the conclusion drawn from eigenvalues results.

## **CHAPTER 6**

# **ANALYSIS AND DESIGN OF WADC**

### **6.1 Introduction**

Similar to what have been done for the local PSSs, the aim here is to analyze and design the WADC to improve the performance of the control in damping out the interarea oscillation mode. Modal analysis is carried out on the test system to calculate the system eigenvalues, PF and controllability measures. Out of the modal analysis, location of the WADC is determined and the input signals combination are selected. Then, the WADC parameters are tuned using phase compensation technique. Next, the nonlinear time domain simulation results are presented in order to observe the dynamic response of the system after applying WADC. Appendix C shows the details of modal analysis results taken from Matlab Workspace. However, relevant results will be discussed here. Last section presents the comparison between the local based PSS and WADC performances when the controller is applied at only one pre selected machine. In addition to the typical parameters used for WADC, Particle Swarm Optimization (PSO) is used to tune the WADC parameters and output results of this are shown.

## 6.2 Case Study

The two area power system equipped with two local PSSs; one at each area, is considered here. The stabilizers are located at G2 and G4. Figure 6-1 shows the same two area system but equipped with WADC. One PMU is considered at each generator bus. This provide the access to measure all generators speeds in order to utilize these measurements in designing the WADC.

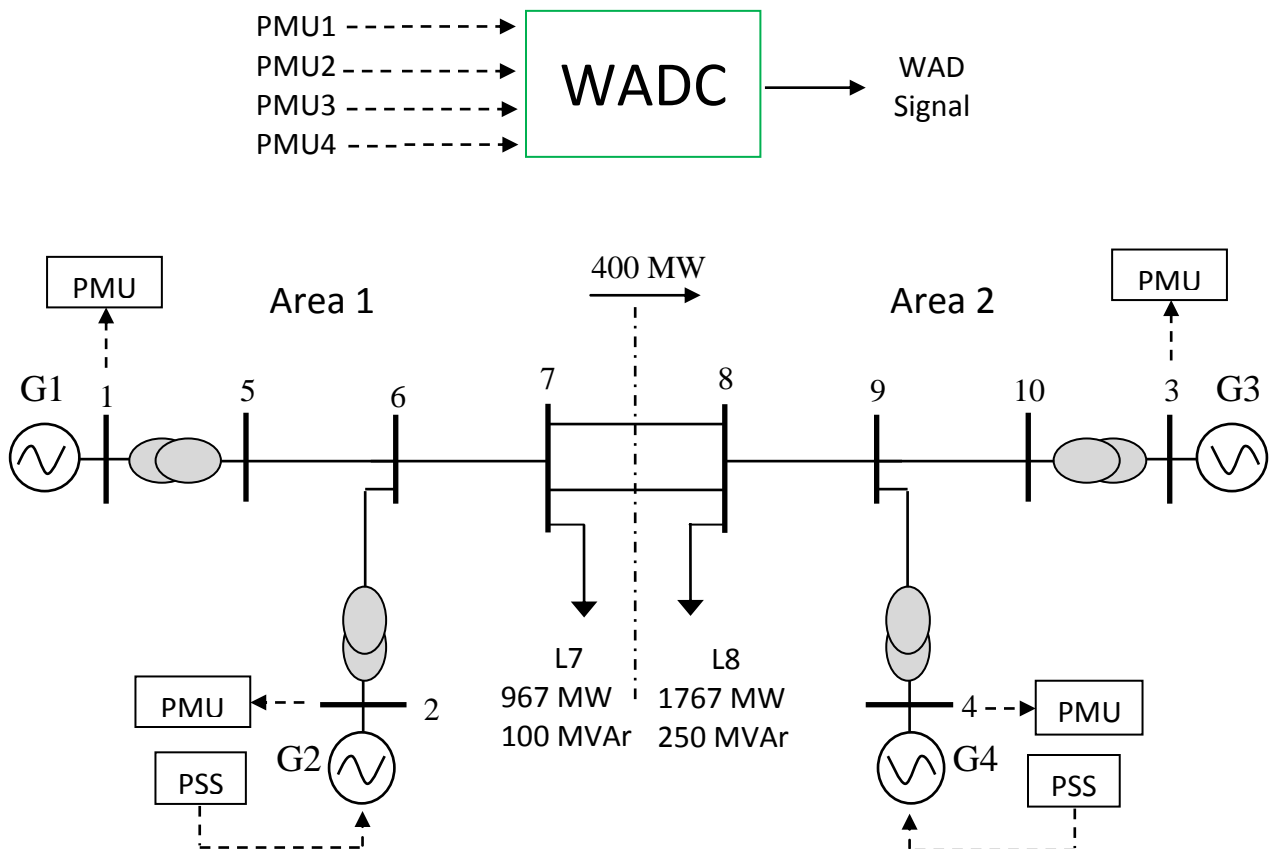


Figure 6-1: Two area four machine system equipped with WADC

### 6.3 Modal Analysis

After the local PSSs are added to the system at G2 and G4, modal analysis parameters should be calculated again. The reason of recalculating the modal analysis parameters is to locate the WADC and to select input signals based on the concerned interarea mode. Table 6-1 shows the last oscillatory modes resultant after the local PSSs are added to the system. In this chapter, the last mode in Table 6-1 (Interarea mode) will be considered in designing WADC.

Table 6-1: Oscillatory modes for the system with local PSSs

Parameters Used	PSSs Location	Eigenvalue	Mode	Damping Ratio	Frequency
Phase Lead Compensation	G2 & G4	-1.8930 ±j 6.2886	Area 1	0.2882	1.0009
		-2.1751 ±j 5.7087	Area 2	0.3560	0.9089
		-0.5507 ±j 4.0233	Interarea	0.1356	0.6403

Recall equation (4.3),

$$R_{jk}^i = C_j \Phi_i \Psi_i^T B_k \quad (6.1)$$

Controllability and observability measures can be introduced from (6.1) as

$$\text{Cont}_{ik} = |\Psi_i^T B_k| \quad (6.2)$$

$$\text{Obse}_{ji} = |C_j \Phi_i| \quad (6.3)$$

Where  $\text{Cont}_{ik}$  is used to measure the mode controllability of mode  $i$  from the  $k$ th input and  $\text{Obse}_{ji}$  measures the mode observability of mode  $i$  from the  $j$ th output.

Analysis results including; eigenvalues, oscillatory modes eigenvalues, PF, and controllability measure are given in Appendix C.

## 6.4 WADC Design

### 6.4.1 WADC Placement

The objective here is to locate the WADC such that it provides additional damping to the interarea mode of oscillations. As stated previously, that the generator with the maximum controllability measure related to the interarea mode, should be selected as the location of the WADC. So, the optimal location of WADC for effective damping of interarea oscillations is the generator with largest controllability measure. Table 6-2 and Figure 6-2 show the controllability measures of each generator in the interarea mode ( $-0.5507 \pm j 4.0233$ ).

Table 6-2: Controllability measure for interarea mode (normalized, 100 %)

<b>Controller Location</b>	<b>G1</b>	<b>G2</b>	<b>G3</b>	<b>G4</b>
Inter-area Mode	0.66.31	0.5029	0.6740	0.4644

The magnitude of the controllability measures of G1 and G3 are the largest comparing to the others. G1 has value of approximately 66 and G3 has slightly higher magnitude. So, it can be conclude that placing the WADC at G3 will be more effective on damping the interarea mode.

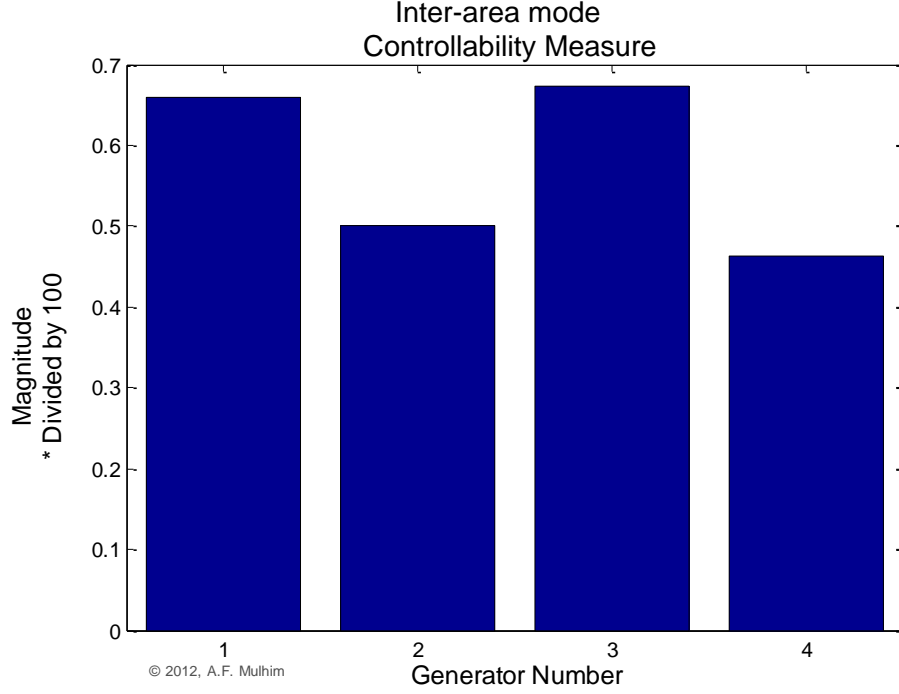


Figure 6-2: Interarea mode controllability measure

#### 6.4.2 WADC Input Signals Selection

The selection of the WADC input signals will be based on the machines that participating in the concerned interarea mode  $(-0.5507 \pm j 4.0233)$ . So, signals from both sides of the oscillating generator groups are introduced as a combination signal to the WADC. Here, the number of signals from each group going to be same to keep symmetric.

The selection vector  $\mathbf{K}$  was introduced to the system input equation

$$y_j = \mathbf{K}_j \Delta \omega \quad (6.4)$$

In this case, the number of signals is 4, the same as the number of generators participating in the interarea mode. So, the input signal is



$$\Delta\omega = \Delta(-\omega_1 - \omega_2 + \omega_3 + \omega_4) \quad (6.5)$$

And the selection vector  $\mathbf{K}$  can be determined

$$\mathbf{K} = [-1 \quad -1 \quad 1 \quad 1] \quad (6.6)$$

Thus, based on the previous analysis, it can be conclude that the WADC should be connected to G3 with input signals combination of  $\Delta(-\omega_1 - \omega_2 + \omega_3 + \omega_4)$ . So, the WADC block diagram can be shown as in Figure 6-3.

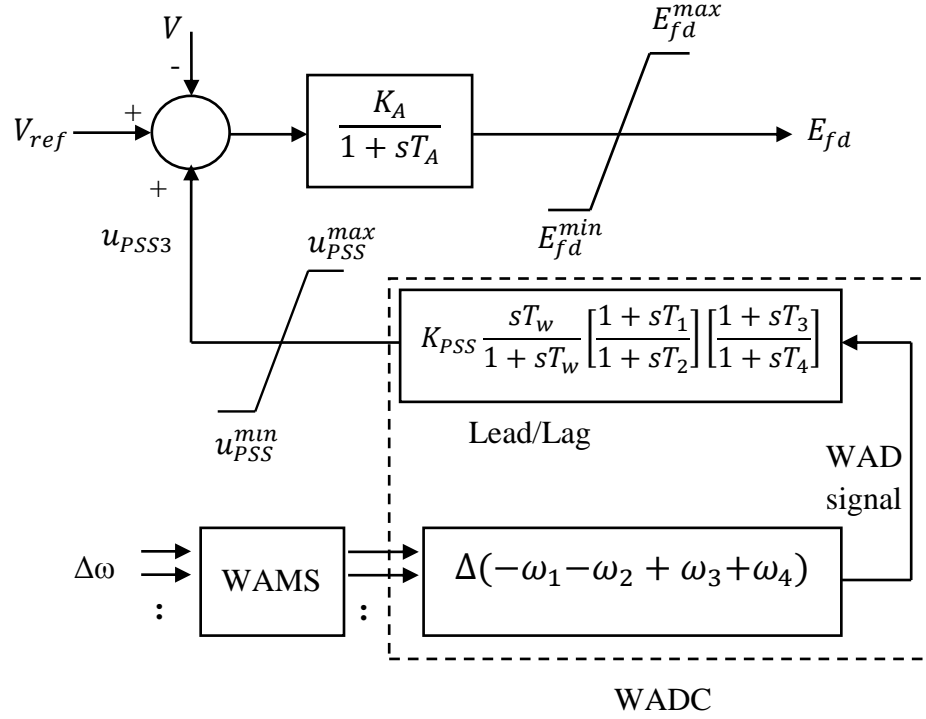


Figure 6-3: Wide Area Damping Controller connected to G3

### 6.4.3 WADC Parameters Tuning

In order to get the best performance out of the WADC, its parameters should be set carefully. As presented earlier, Phase Compensation method is used to calculate the

WADC parameters. Here, the interarea oscillatory mode  $(-0.5507 \pm j 4.0233)$  will be considered during the tuning process. Similar to the local PSSs parameters tuning, phase compensation technique is used here to calculate the WADC parameters.

Recall from chapter 5, the transfer function of lead/lag compensation is

$$H(s)_j = K_{PSS} \frac{sT_w}{1+sT_w} \left[ \frac{1+sT_1}{1+sT_2} \right] \left[ \frac{1+sT_3}{1+sT_4} \right] \quad (6.7)$$

And by using equations (4.16)-(4.18);  $K_{PSS}$ ,  $T_1$ ,  $T_2$ ,  $T_3$  and  $T_4$  can be calculated. Table 6-3 lists the information that is required to apply the above mentioned equations; mainly residues and eigenvalues of the concerned interarea mode. By employing this information into equation (4.13), (4.16)-(4.18), the WADC parameters can be determined. Table 6-4 shows the calculated parameters results.

Table 6-3: Information required to use phase compensation technique for WADC

Concerned Interarea Mode	Residue (at $G_i$ )	Eigenvalue $\lambda = \sigma \pm j\omega$	$\sigma$	$\omega$
$-0.5507 \pm j 4.0233$	$-0.0607 + j 0.0478$ (at $G_3$ )	$-0.5507 \pm j 4.0233$	-0.5507	4.0233

Table 6-4: WADC parameters

Location of WADC	$K_{PSS}$	$T_1$ & $T_3$	$T_2$ & $T_4$	$T_w$
G3	13.23	0.3492	0.1769	10

To evaluate the effectiveness of placing the WADC at G3 in addition to the two local PSSs (one at each area), the new eigenvalues and damping ratios are determined. Table 6-5 shows the new oscillatory mode after the WADC is applied. It compares results of applying WADC with the local PSSs. It is clear that applying WADC in addition to the local PSSs gives better performance in damping the interarea oscillation.

Table 6-5: Oscillatory modes for the system with local PSSs and WADC

Oscillatory Mode	Eigenvalue			Damping Ratio		
	Local PSS at G2&G4	Local PSS at G2,G3&G4	Local PSS at G2&G4/ WADC at G3	Local PSS at G2&G4	Local PSS at G2,G3&G4	Local PSS at G2&G4/ WADC at G3
<b>Mode-7</b>	-1.8930 $\pm j$ 6.2886	-1.9803 $\pm j$ 6.0329	-1.8786 $\pm j$ 6.1218	0.2882	0.3119	0.2934
<b>Mode-9</b>	-2.1751 $\pm j$ 5.7087	-2.9648 $\pm j$ 4.6124	-2.1598 $\pm j$ 3.5993	0.3560	0.5407	0.5145
<b>Mode-11</b>	-0.5507 $\pm j$ 4.0233	-0.6607 $\pm j$ 3.8143	-1.0714 $\pm j$ 2.8188	0.1356	0.1707	0.3553

## 6.5 Non-Linear Time Domain Simulation

Nonlinear time domain simulation was performed using Matlab to validate the performance of applying WADC at G3 in addition to the installed two local PSSs. A 100 ms three phase fault at bus 8 is considered.

Figure 6-4 to Figure 6-21 show machines responses of the two area power system for such severe disturbance. It can be seen that system without control experiences serious power oscillations. With implement of PSSs, at G2 and G4, such power oscillations are damped out slightly better than without applying any control. Furthermore, applying

three local PSSs at G2, G3 and G4 gives better results. Taking the last case and replacing the local PSS at G3 with the proposed WADC, this greatly improves the system responses comparing to the other cases. The WADC in addition to the local PSSs provide better damping characteristics to the power oscillations and thus enhance the dynamic stability of the power system. The nonlinear time domain simulation results confirm the conclusion drawn from eigenvalues analysis.

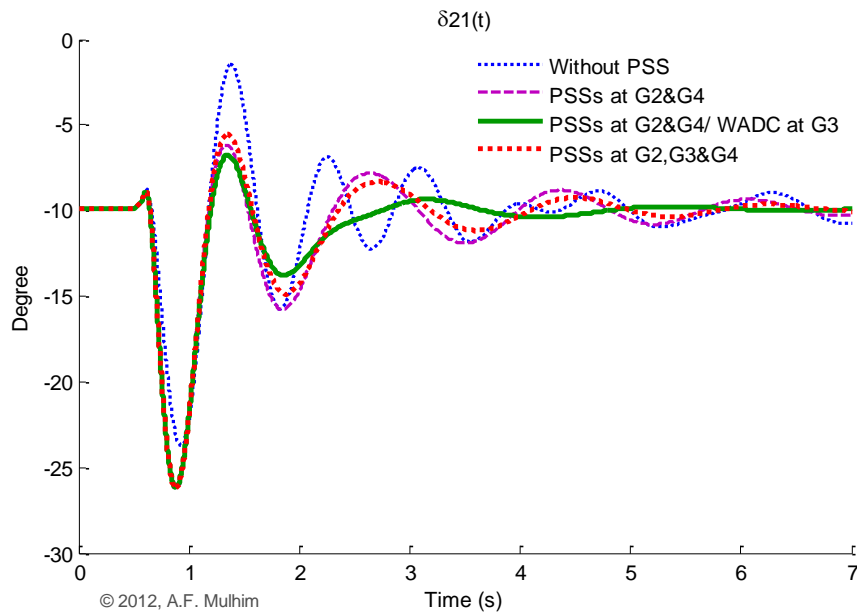


Figure 6-4: Rotor angle  $\delta_{21}$  response

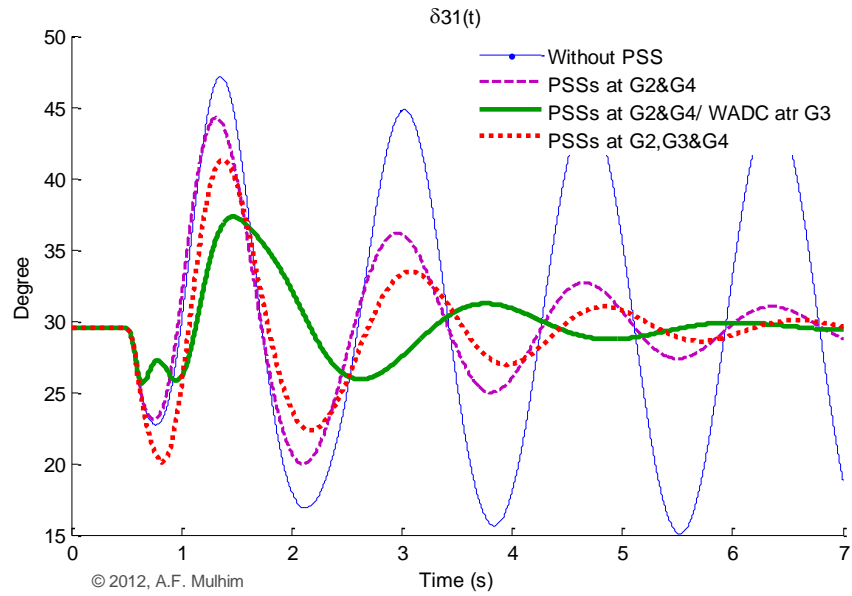


Figure 6-5: Rotor angle  $\delta_{31}$  response

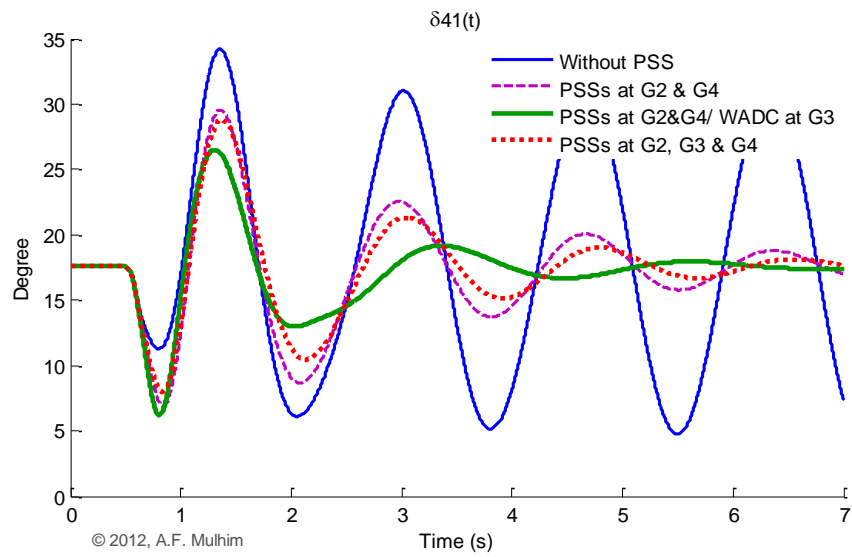


Figure 6-6: Rotor angle  $\delta_{41}$  response

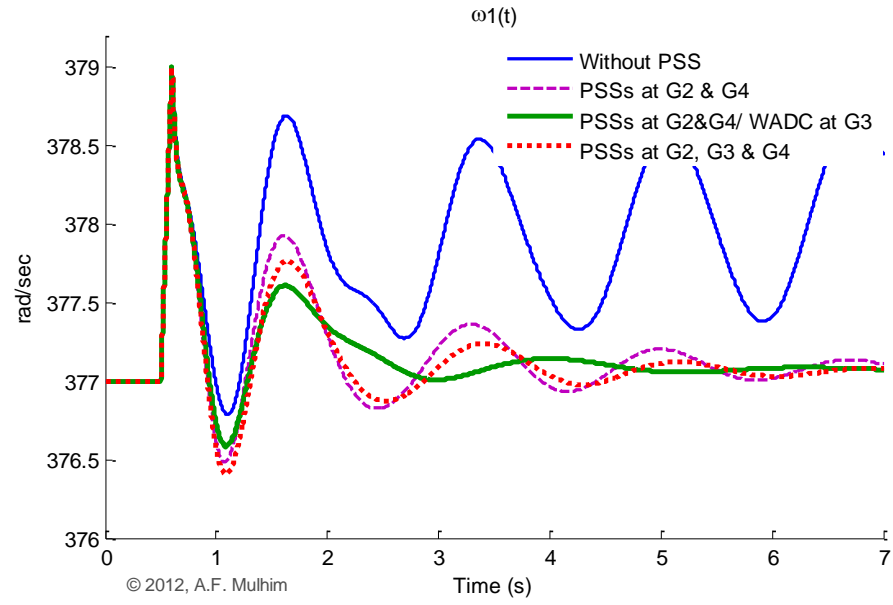


Figure 6-7: Rotor speed  $\omega_1$  response

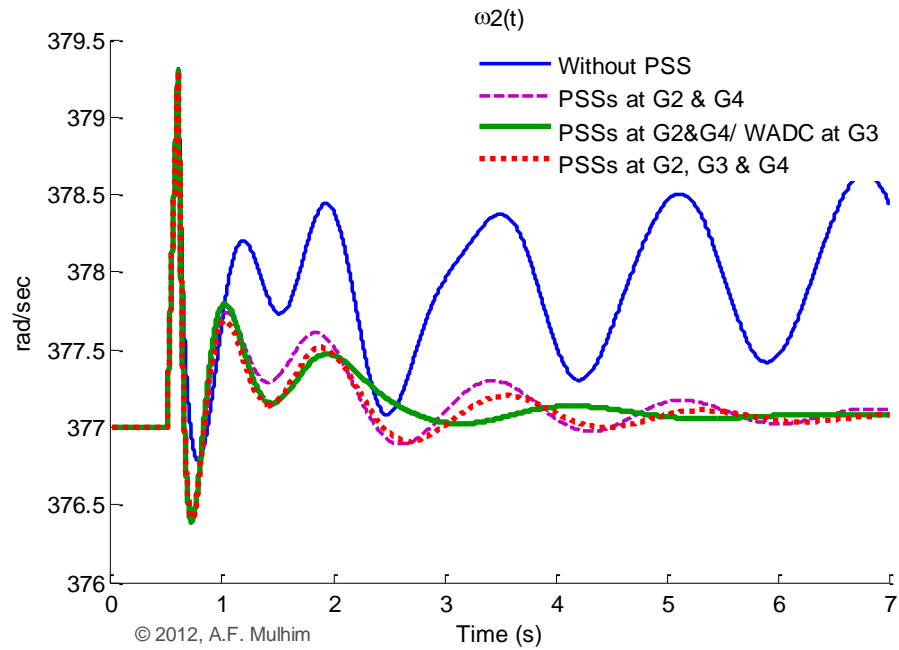


Figure 6-8: Rotor speed  $\omega_2$  response

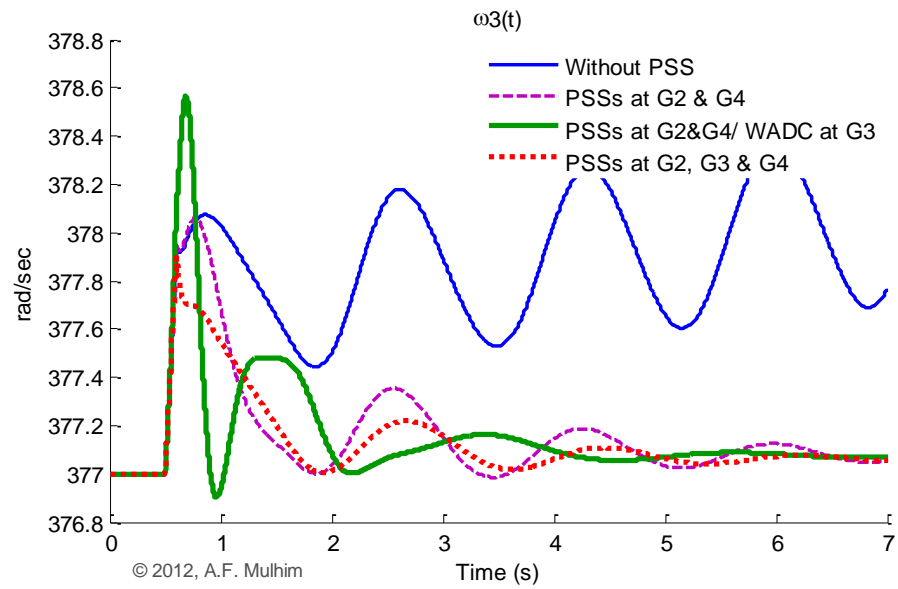


Figure 6-9: Rotor speed  $\omega_3$  response

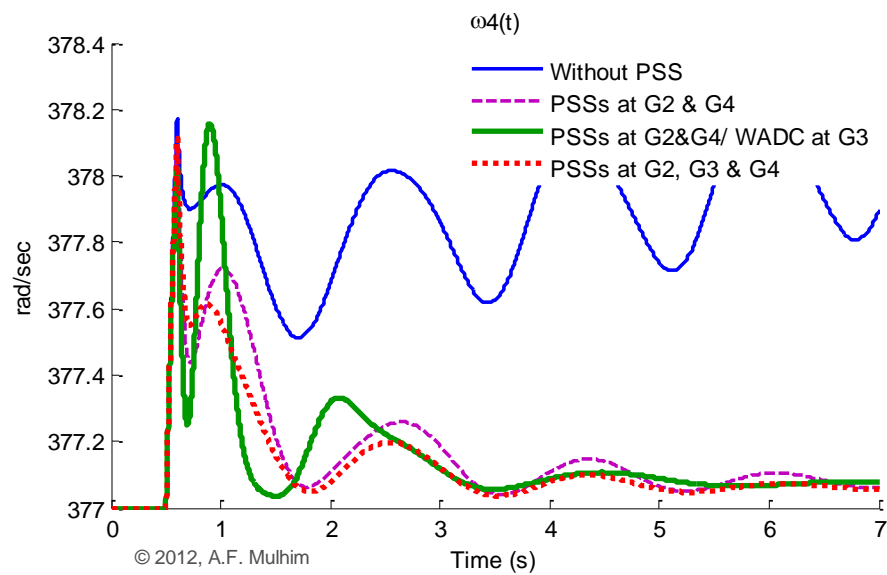


Figure 6-10: Rotor speed  $\omega_4$  response

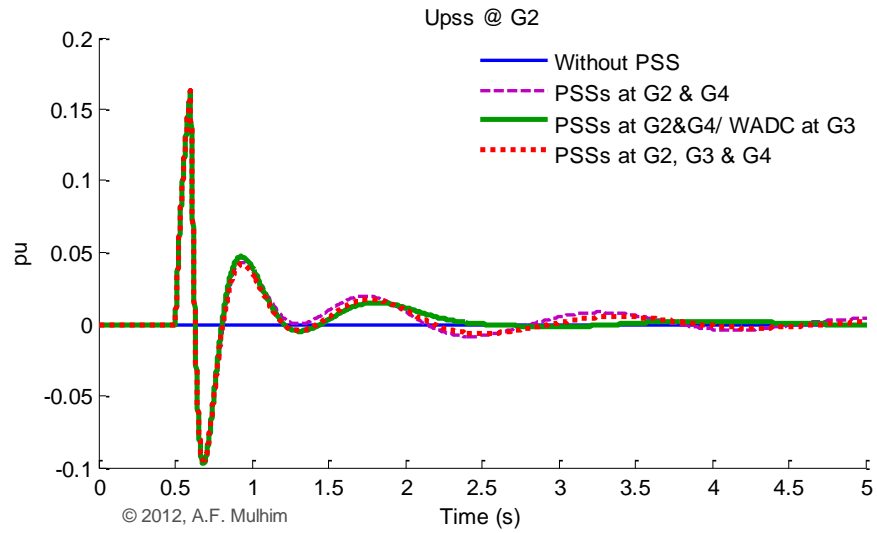


Figure 6-11: Control response at G2

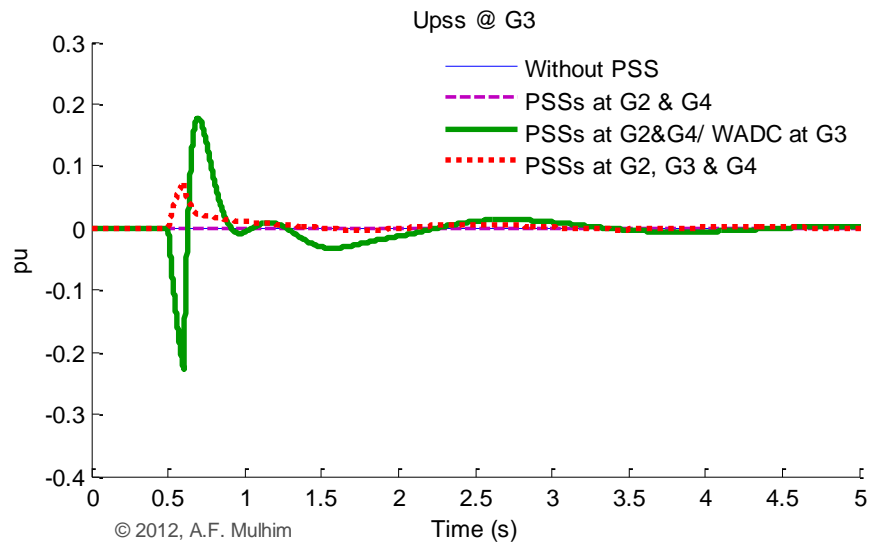


Figure 6-12: Control response at G3



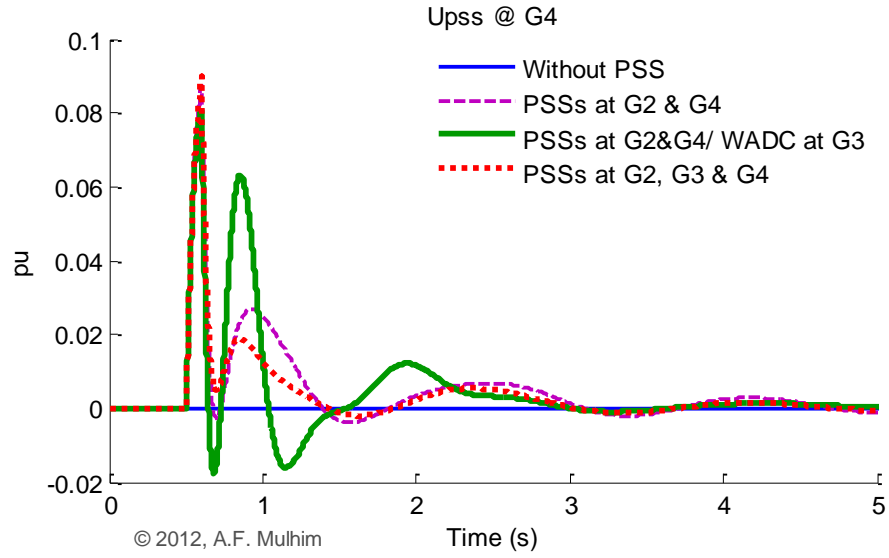


Figure 6-13: Control response at G4

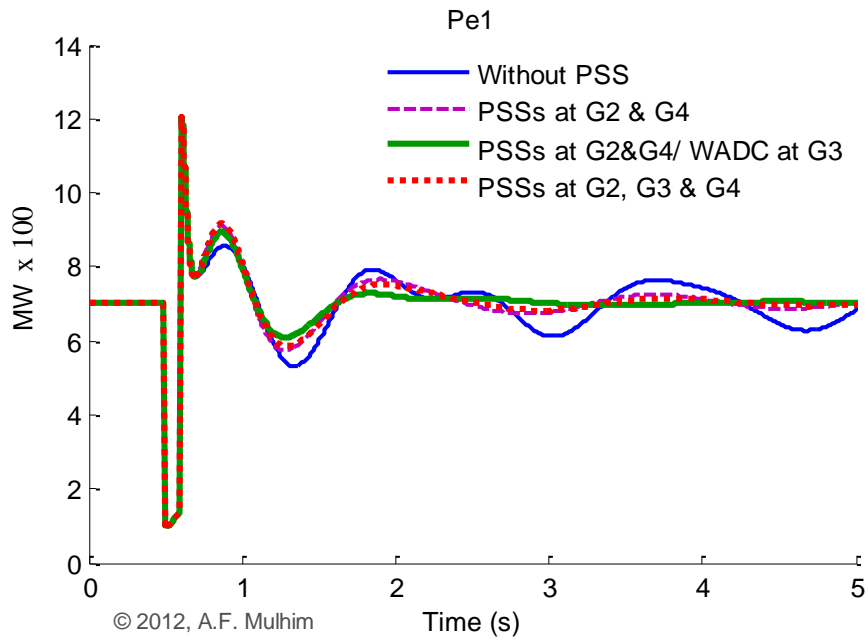


Figure 6-14: Electric power output  $P_{e1}$  response

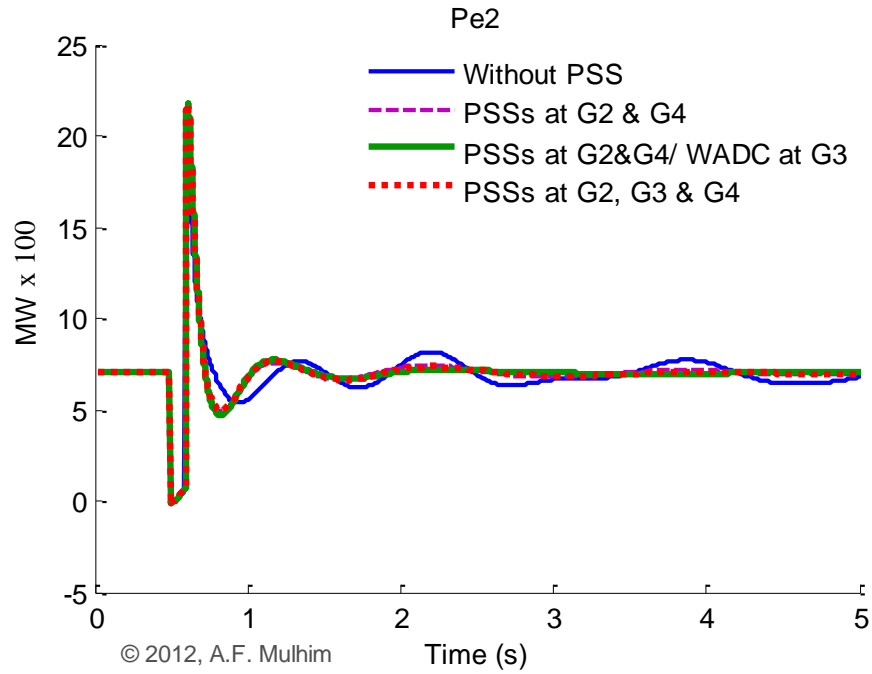


Figure 6-15: Electric power output  $P_{e2}$  response

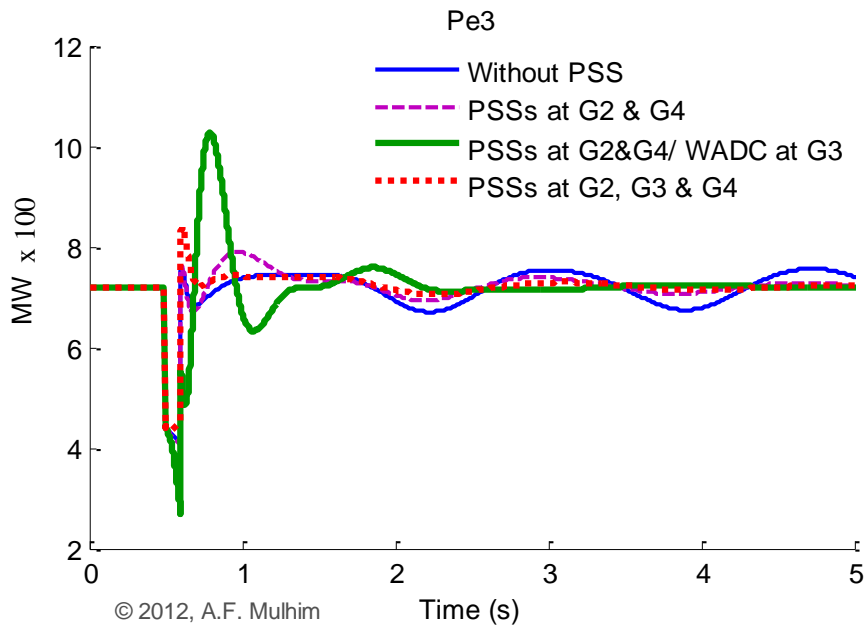


Figure 6-16: Electric power output  $P_{e3}$  response

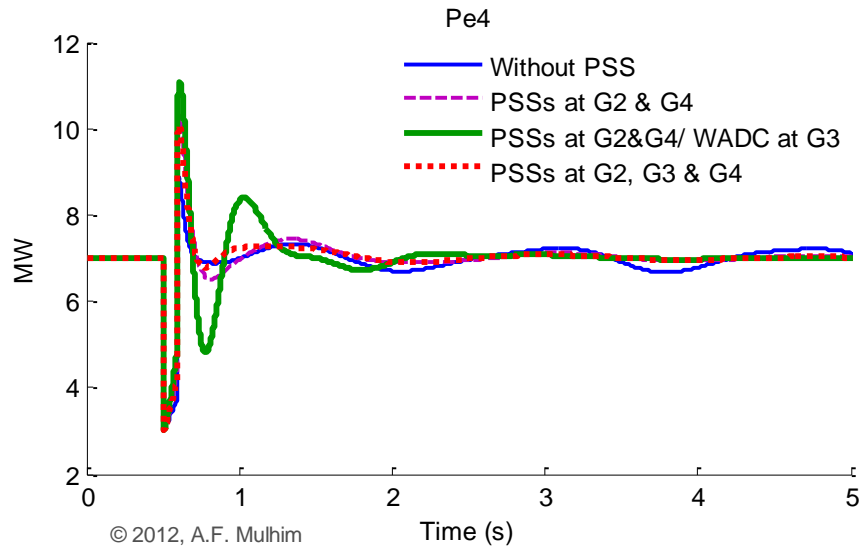


Figure 6-17: Electric power output  $P_{e4}$  response

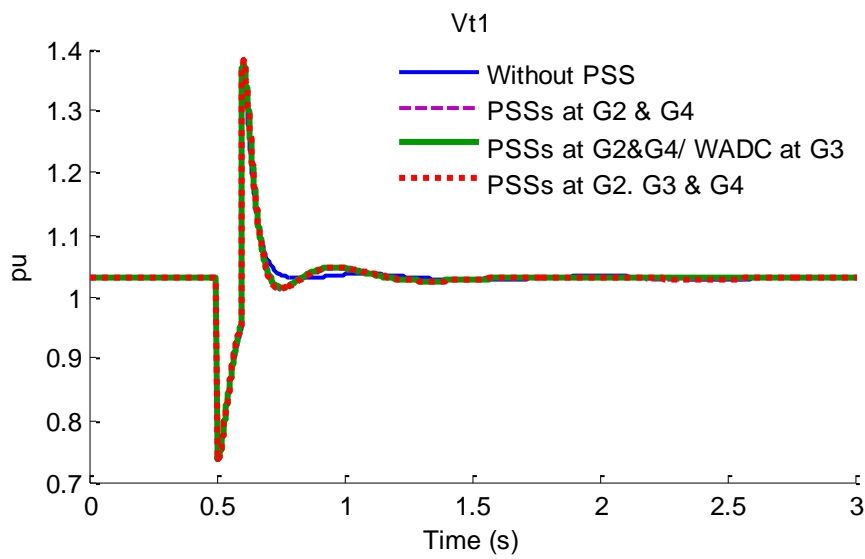


Figure 6-18: Terminal voltage  $V_{t1}$  response

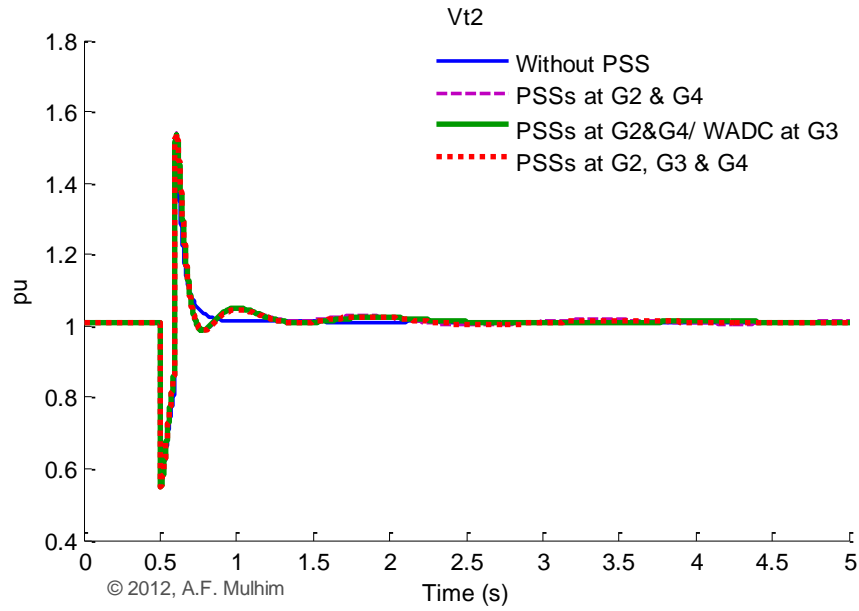


Figure 6-19: Terminal voltage  $V_{t2}$  response

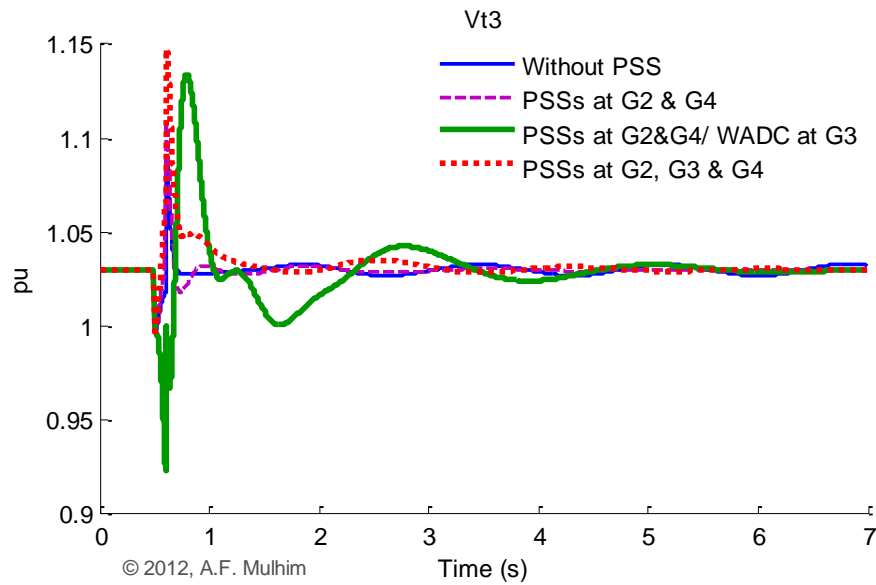


Figure 6-20: Terminal voltage  $V_{t3}$  response

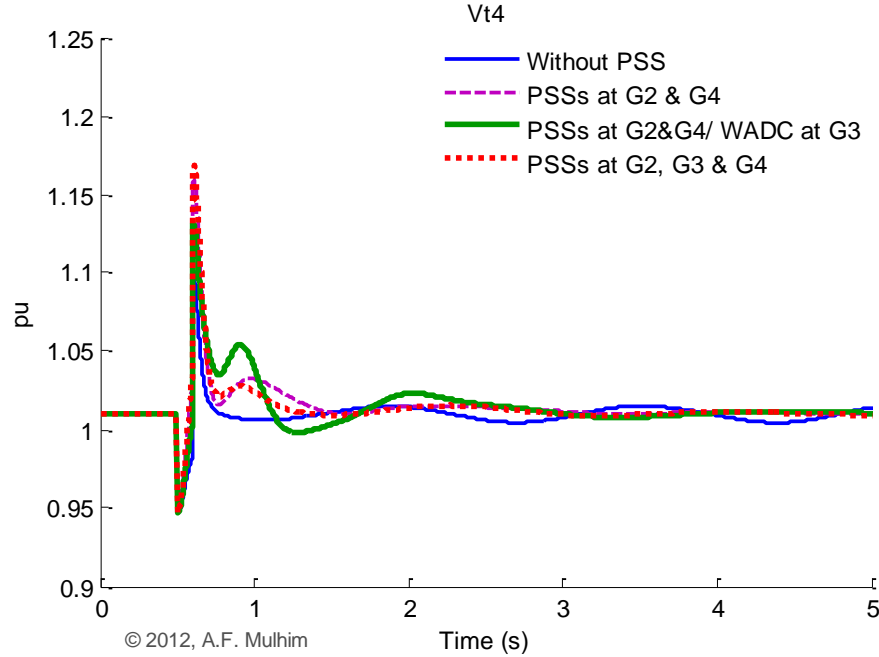


Figure 6-21: Terminal voltage  $V_{t4}$  response

## 6.6 Comparison Between Local Based PSS and WADC

A comparison is presented here between local based PSS and WADC considering that controller is applied at G3 only. The main objective, from applying the controller at only one machine, is to evaluate the performance of each controller alone. The comparison was done using typical controller parameters in the first part below. Then, PSO technique is applied to the WADC parameters in the second part.

### 6.6.1 Using Typical Values for The Controller Parameters

Typical values were chosen from reference [2] for the controller parameters;  $K_{PSS}=10$ ,  $T_w=5$ ,  $T_1=T_3=0.1$  and  $T_2=T_4=0.05$ . Table 6-6 summarizes the eigenvalue analysis results

of placing both controllers at G3, local based PSS and proposed WADC. Results show significant improvement in eigenvalues and damping ratios of the Interarea Mode plus the Local Mode 2 when the proposed WADC is applied to G3.

In addition to the eigenvalue analysis, nonlinear time domain simulations were performed using Matlab to compare the performance of applying WADC at G3 to the local based PSS. Again, a 100 ms three phase fault at bus 8 is considered. Figure 6-22 to Figure 6-30 show the machines responses for this case of simulation. . It is clearly that system oscillations are damped faster in case of applying WADC. Thus, system stability is significantly improved comparing to the local based PSS. Figure 6-22 to Figure 6-24 show the machines rotor angle responses with respect to G1. Figure 6-25 to Figure 6-28 present the rotor speed responses of the machines. The electric output power responses of G1 and G3 are given in Figure 6-29 and Figure 6-30.

Table 6-6: Oscillatory modes for the system with controller placed at G3

Oscillatory Mode	Eigenvalue		Damping Ratio	
	Local PSS	Proposed WADC	Local PSS	Proposed WADC
Local Mode 1	-0.5757 ±j 7.4982	-0.5778 ±j 7.4979	0.0766	0.0768
Local Mode 2	-1.4827 ±j 7.7808	-2.6007 ±j 8.3302	0.1872	0.2980
Inter area Mode	-0.0204 ±j 4.0284	-0.2966 ±j 4.1028	0.0051	0.0721

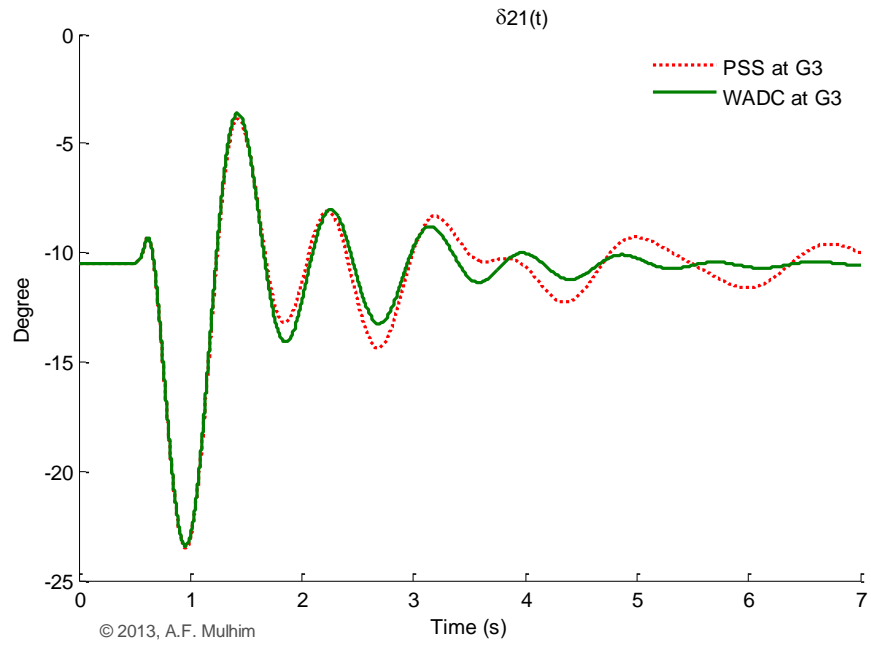


Figure 6-22: Rotor angle  $\delta_{21}$  response with controller placed at G3

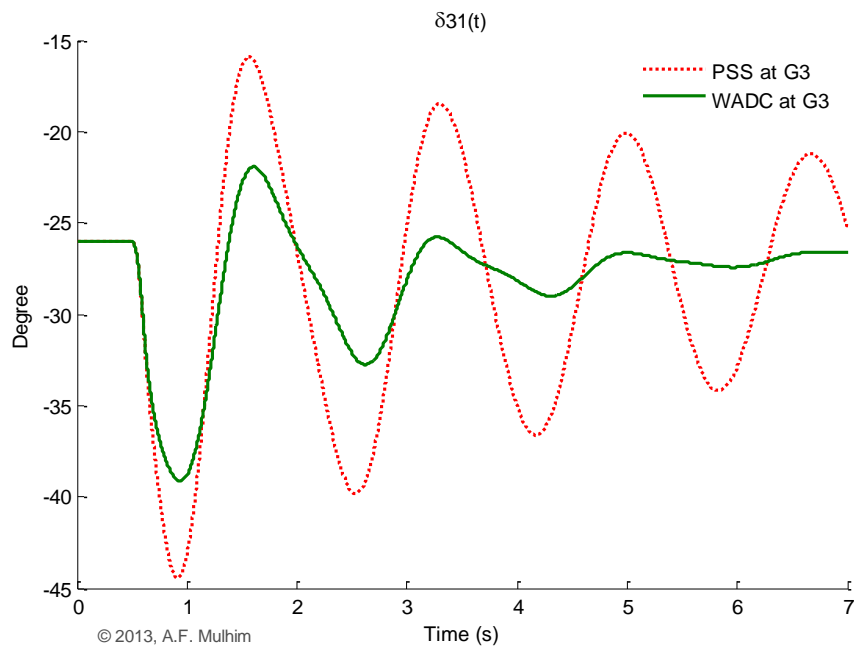


Figure 6-23: Rotor angle  $\delta_{31}$  response with controller placed at G3

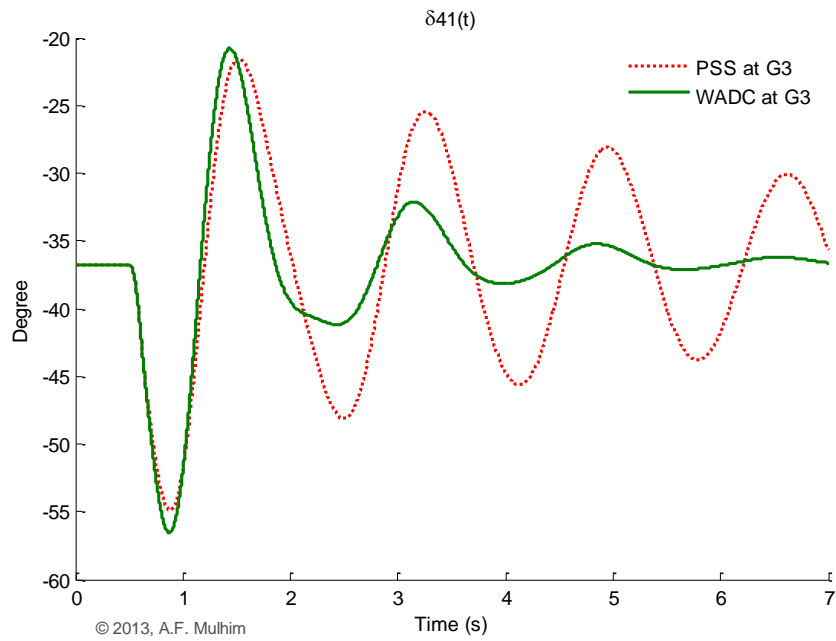


Figure 6-24: Rotor angle  $\delta_{41}$  response with controller placed at G3

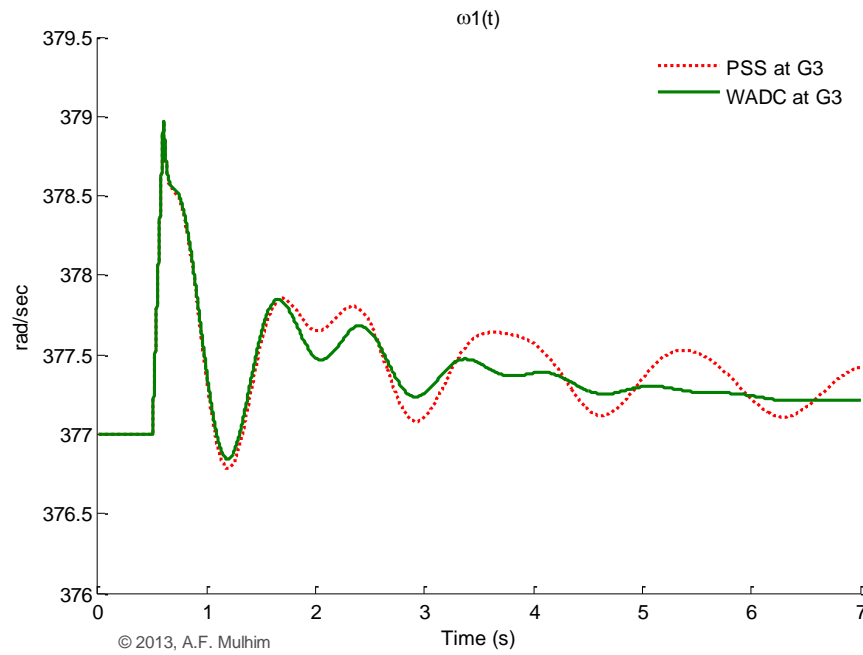


Figure 6-25: Rotor speed  $\omega_1$  response with controller placed at G3



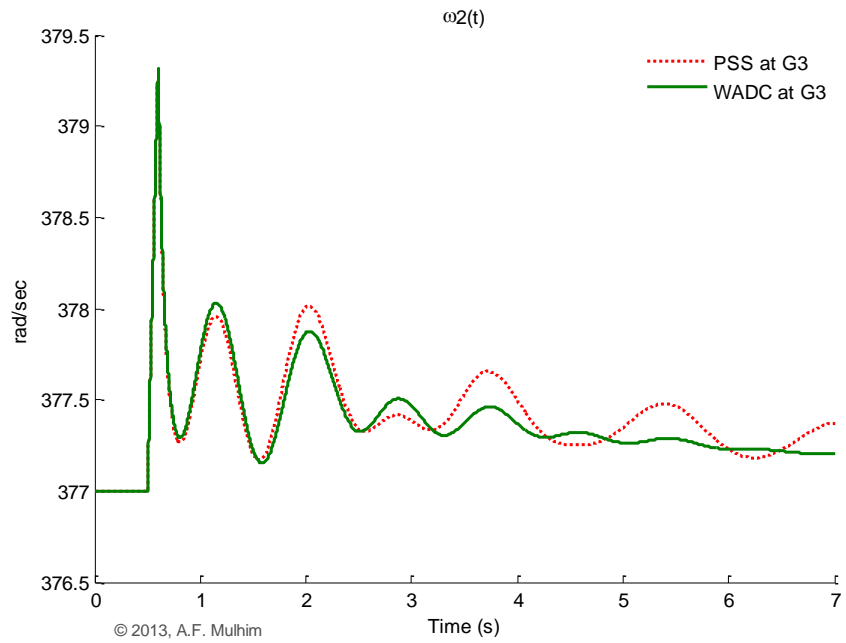


Figure 6-26: Rotor speed  $\omega_2$  response with controller placed at G3

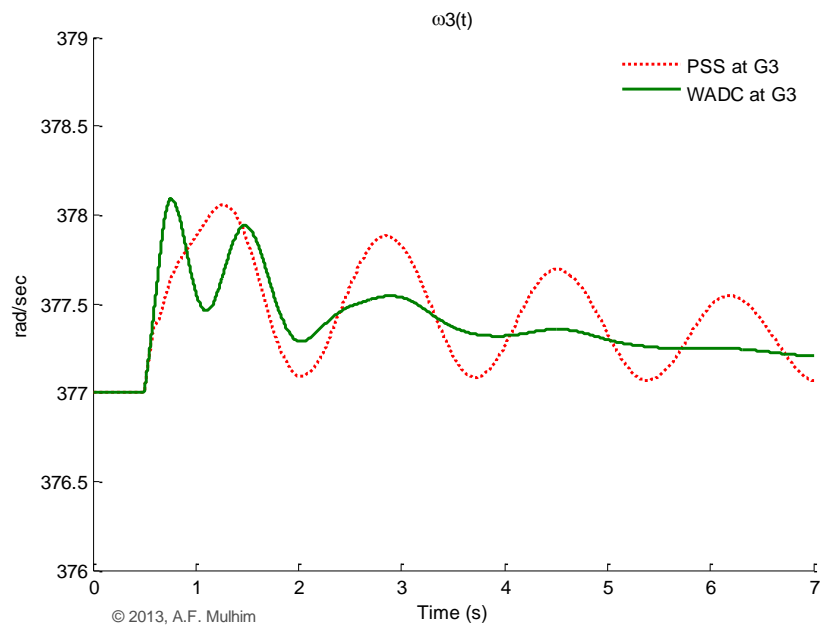


Figure 6-27: Rotor speed  $\omega_3$  response with controller placed at G3

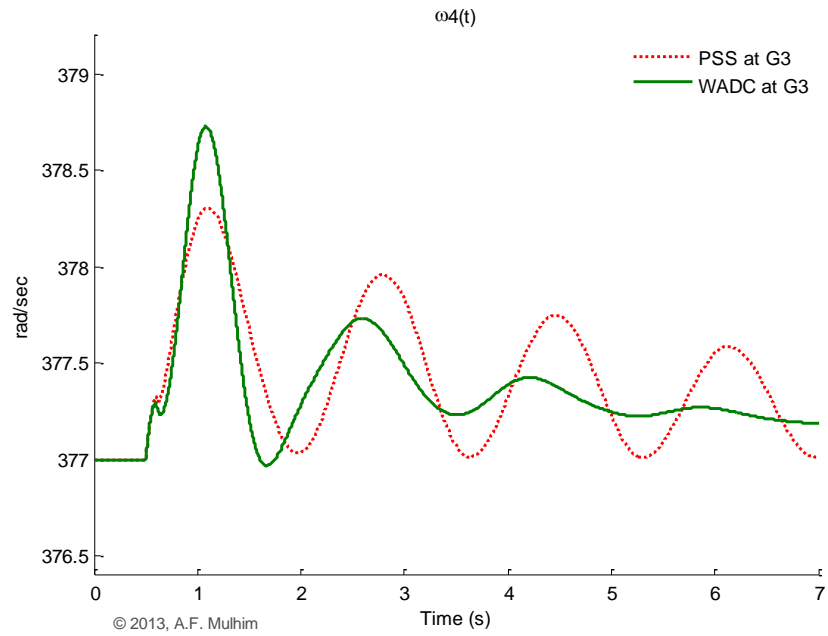


Figure 6-28: Rotor speed  $\omega_4$  response with controller placed at G3

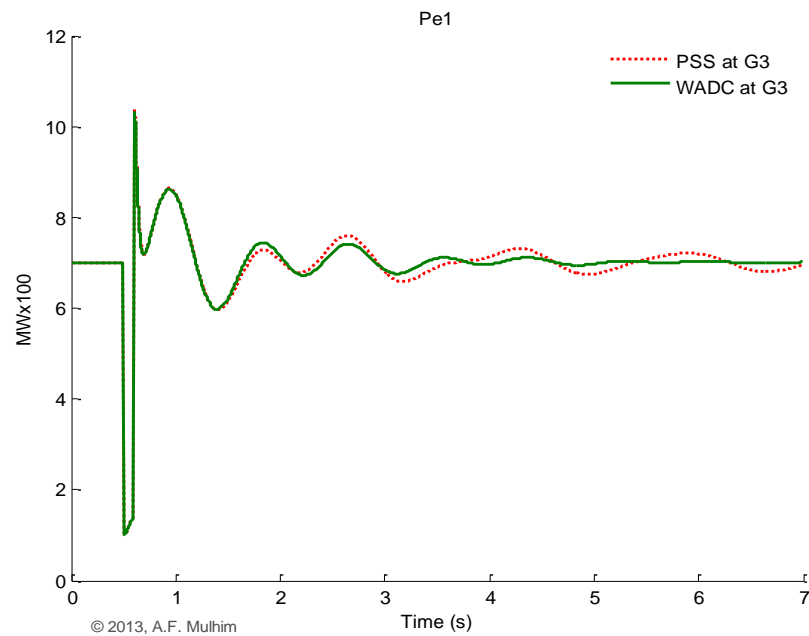


Figure 6-29: Electric power output  $Pe_1$  response with controller placed at G3

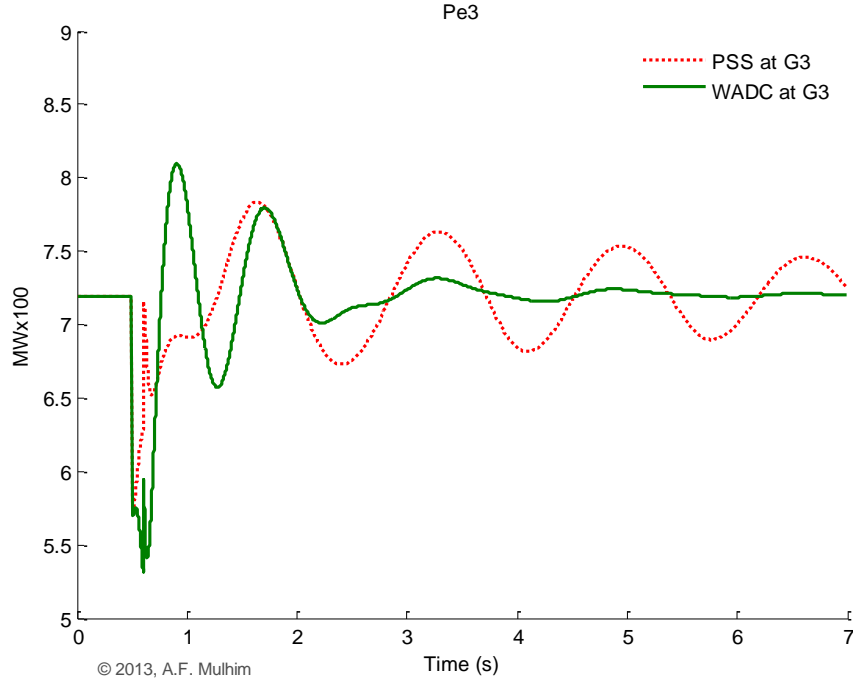


Figure 6-30: Electric power output Pe3 response with controller placed at G3

### 6.6.2 WADC Parameters Optimization Using PSO Technique

In order to get the best performance of the controller, its parameters should be set carefully and based on certain desired objective function. Particle swarm optimization (PSO) is used here to optimized the Lead/Lag block parameters ( $K_{PSS}$ ,  $T_1$ ,  $T_2$ ,  $T_3$  and  $T_4$ ). Details of the PSO technique will not be discussed here. For more information regard applying the PSO, refer to reference [95] from where all information is taken.

To increase the system damping of electromechanical (oscillatory) modes, eigenvalue-based objective function is considered as follows

$$J = \min[\zeta_i ; i \in \text{set of electromechanical modes}] \quad (6.8)$$

maximize  $J$

Where  $\zeta_i$  is the damping ratio of the  $i$ th eigenvalue. In the optimization process, it is aimed to maximize  $J$  in order to improve the damping characteristic of oscillatory mode. The problem constraints are the optimized parameters limits. So, the optimization problem will be as follow

Optimize  $J$  , Subject to

$$K_i^{\min} \leq K_i \leq K_i^{\max} \quad (6.9)$$

$$T_i^{\min} \leq T_i \leq T_i^{\max}$$

Typical range of the optimized parameters are used, [0.001-50] for  $K_i$  and [0.06-1.0] for time constants  $T_i$ . The time constant  $T_w$  is set as 10 sec. The PSO parameters are set as shown in Table 6-7.

Table 6-7: PSO Parameters

Maximum Iteration	100
Population size	50
$\alpha$ – set	0.99
$c_1, c_2$	2
No. of Interval	10
Inertia weight, $w$	0.9

WADC optimized parameters results are given in Table 6-8. The convergence of the objective function is shown in Figure 6-31. To evaluate the effectiveness of the optimized WADC on the oscillatory modes, the eigenvalues and damping ratios are determined. Table 6-9 shows the eigenvalue analysis results of the system with optimized WADC placed at G3. It is clear that the eigenvalues of both Local Mode 2 and Interarea Mode have been shifted to the left when the optimized WADC is applied.

Table 6-8: WADC optimized parameters

Location of WADC	K	T <sub>1</sub>	T <sub>2</sub>	T <sub>3</sub>	T <sub>4</sub>	T <sub>w</sub>
G3	39.0443	0.7371	0.6765	0.3650	0.5491	10

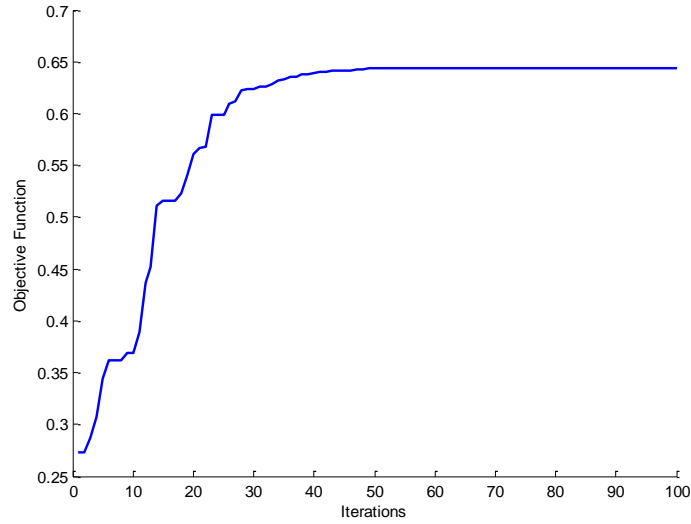


Figure 6-31: Convergence of the objective function

Table 6-9: Oscillatory modes for the system with optimized WADC placed at G3

Oscillatory Mode	Eigenvalue			Damping Ratio		
	Local PSS	Proposed WADC	PSO Optimized WADC	Local PSS	Proposed WADC	PSO Optimized WADC
Local Mode 1	-0.5757 ±j 7.4982	-0.5778 ±j 7.4979	-0.5778 ±j 7.4981	0.0766	0.0768	0.0768
Local Mode 2	-1.4827 ±j 7.7808	-2.6007 ±j 8.3302	-3.4247 ±j 12.1876	0.1872	0.2980	0.2705
Inter area Mode	-0.0204 ±j 4.0284	-0.2966 ±j 4.1028	-0.4478 ±j 4.3726	0.0051	0.0721	0.1019

Again, nonlinear time domain simulations were performed to validate the robustness of the optimized WADC. A 100 ms three phase disturbance is applied at Bus 8. System responses, after the PSO optimized WADC is applied, are shown in Figure 6-32 to Figure 6-38. Plots also shows comparison of optimized WADC responses to the responses obtained in the previous section that controller use typical value of WADC and local based PSS. It can be seen that the performance of the WADC after optimized its parameters, is greatly improved and provide much better damping characteristics to the power oscillations and thus enhance the dynamic stability of the power system.

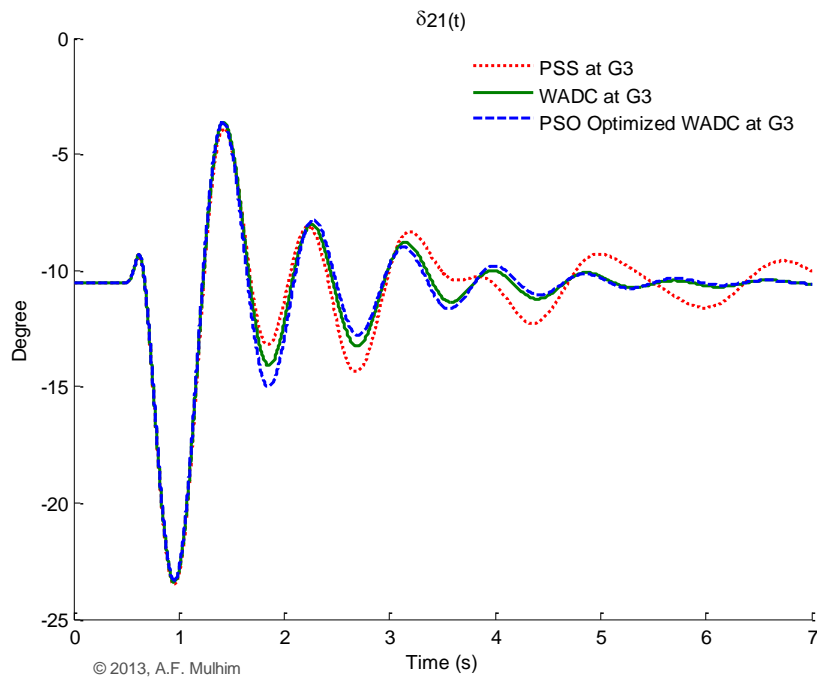


Figure 6-32: Rotor angle  $\delta_{21}$  response with controller placed at G3 (Optimized WADC)

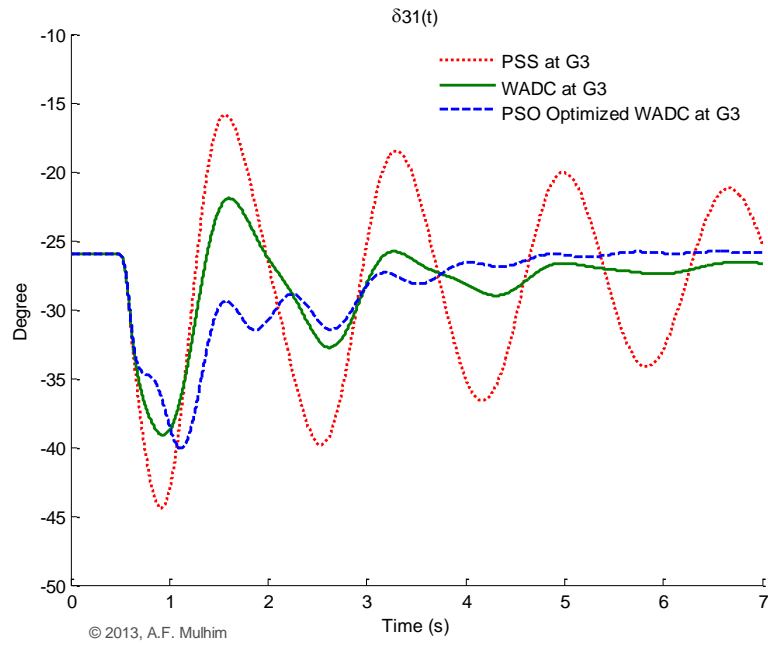


Figure 6-33: Rotor angle  $\delta_{31}$  response with controller placed at G3 (Optimized WADC)

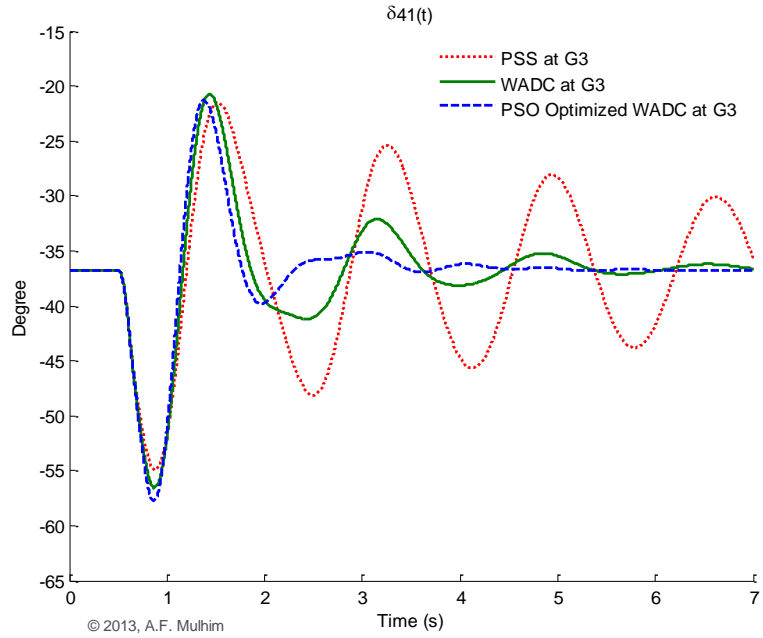


Figure 6-34: Rotor angle  $\delta_{41}$  response with controller placed at G3 (Optimized WADC)

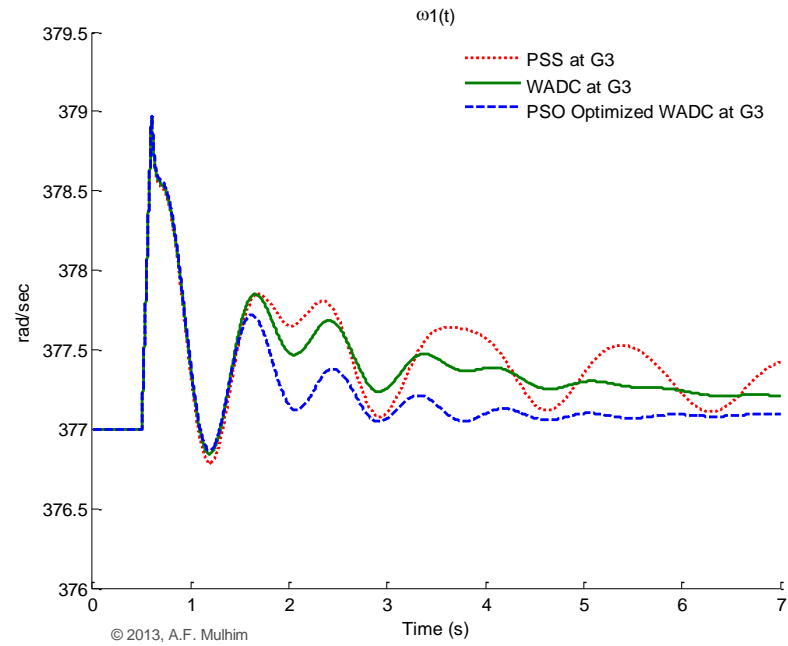


Figure 6-35: Rotor speed  $\omega_1$  response with controller placed at G3 (Optimized WADC)

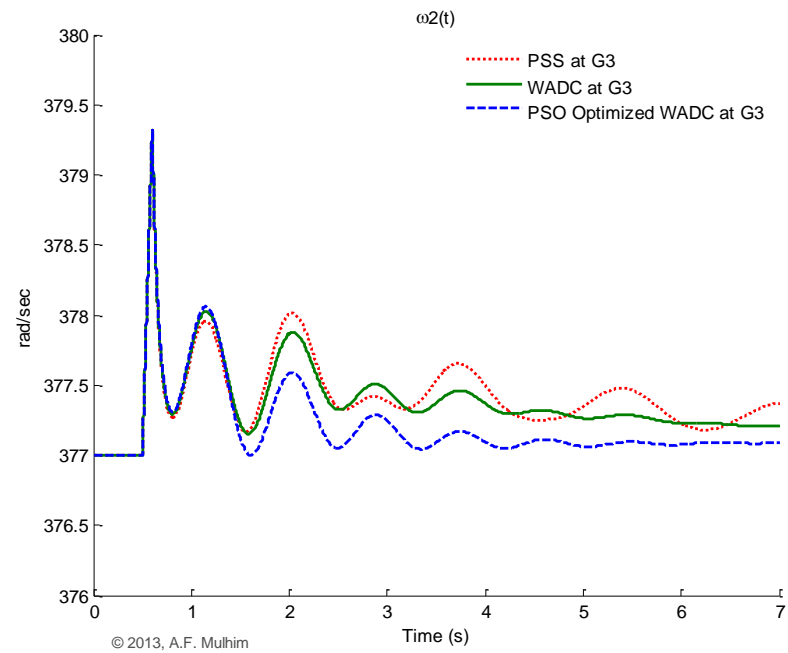


Figure 6-36: Rotor speed  $\omega_2$  response with controller placed at G3 (Optimized WADC)



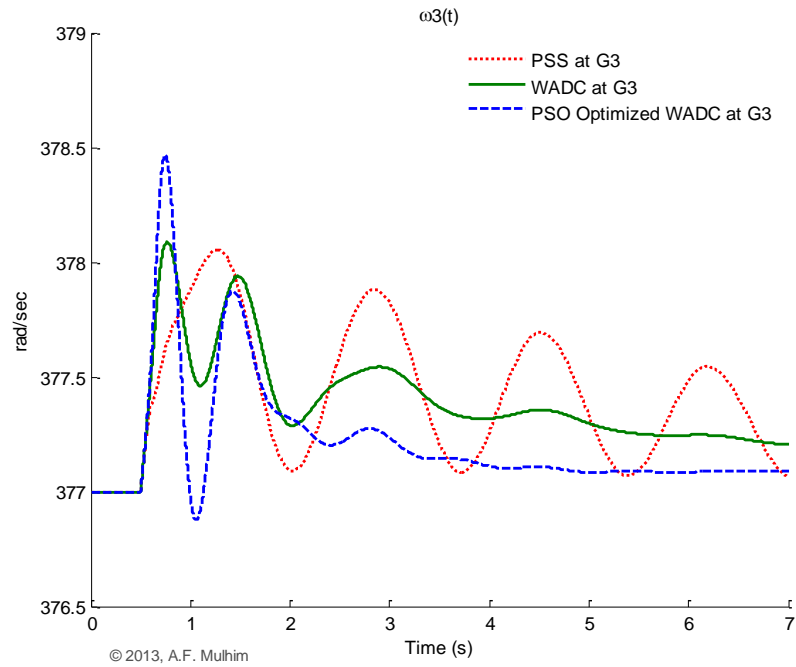


Figure 6-37: Rotor speed  $\omega_3$  response with controller placed at G3 (Optimized WADC)

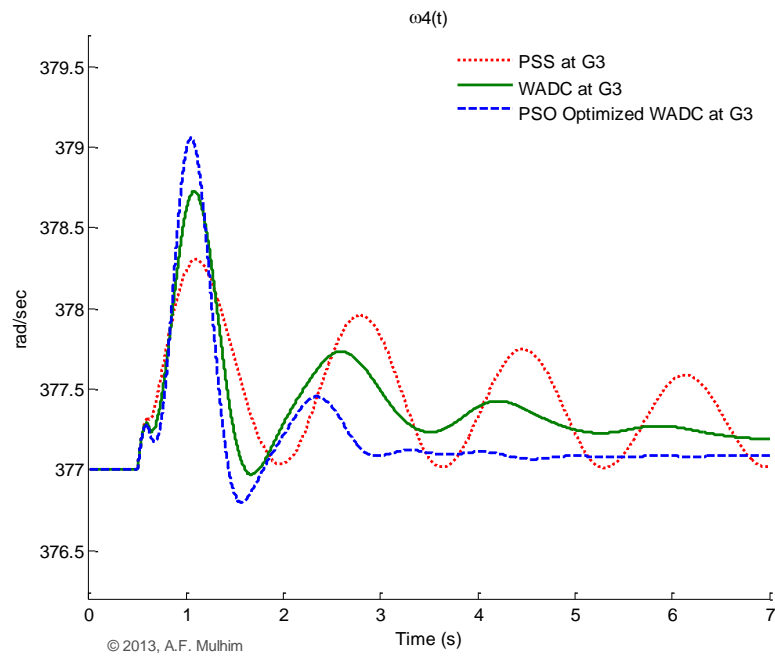


Figure 6-38: Rotor speed  $\omega_4$  response with controller placed at G3 (Optimized WADC)

## 6.7 Summary

System analysis and control design were carried out on the considered two area power system. Modal analysis parameters included; eigenvalues, eigenvectors, PF, and controllability measures were determined. From, modal analysis outcomes, the WADC placement is located. Results show that G3 is the best place to locate the control at, and that is because G3 has the largest controllability measure corresponding to interarea mode. The control input signals combination is identified based on  $\mathbf{K}$  vector selection which reflects the participation of the machines in the concerned interarea mode. After the WADC is located and their input signals combination are selected, control parameters were tuned using phase lead/lag compensation technique. Eigenvalues of the system are calculated after applying the proposed WADC at G3 and results show that the eigenvalues corresponding to the interarea mode are shifted to the left side of the plan. This indicates that interarea oscillations damping is improved and the dynamic stability is enhanced accordingly. Also, the time domain simulation responses were considered when the system is exposed to severe disturbance. Machine rotor angles, rotor speeds and the other parameters responses confirm the conclusion drawn from eigenvalues results. Finally, the WADC parameters were optimized using PSO and resulted system responses are shown and compared to the typical parameters WADC and local based PSS results.

## **CHAPTER 7**

# **REAL-TIME IMPLEMENTATION**

### **7.1 Introduction**

This chapter presents the experimental part of the research work, which is implementing the two area power system equipped with the proposed WADC at real-time platform simulator. First, an overview of the real-time simulator used (RTDS) is given. Then, a laboratory setup for the simulated power system is described. Two different scenarios are taking into consider; i) for fault disturbance case, and ii) for sudden load change. Finally, RTDS simulations are carried out when local based PSS and WADC are applied at G3, one each a time, for comparison purpose.

### **7.2 Real Time Digital Simulator (RTDS) Overview**

Dynamic stability analysis now a days is very important and essential to study the system and test the performance of protection and control systems. Such critical analysis shall be done under realistic power system conditions. Because of that, real-time power system

simulators have been developed [33]. RTDS<sup>®</sup> is one of the powerful simulators that can perform dynamic stability in realistic and fast manner.

The RTDS is a real-time power system simulator that performs digital electromagnetic transient simulation. It is a super computer that performs real-time simulation using parallel computation. It is capable of performing time-domain simulation at real-time speed using time steps less than 50 microseconds [34]. Such fast computation, let RTDS able to simulate power system phenomena in the range of 0 to 3 kHz with high accuracy and reliability.

The RTDS simulator consists of custom hardware and software, specifically designed to perform real time electromagnetic transient simulations. The RTDS simulator's fully digital parallel processing hardware architecture is capable of simulating complex networks using a typical time step of 50 microseconds. The simulator also allows for small time step sub-networks that operate with time steps in the range of 1-4 microseconds for simulation of fast switching power electronic devices. The hardware is bundled into modular units called racks that allow easy expansion of the simulator's computing capability as required [35].

The RTDS software is the link to the simulator hardware. The main elements of the software are the graphical user interface (GUI), RSCAD and the libraries of power and control system component models. RSCAD represents a family of software tools consisting of individual modules that accomplish the different tasks involved in operating the simulator. Through RSCAD, simulation projects and cases can be organized and

shared. RSCAD has the ability to; assemble circuit diagrams using predefined or user-defined power and control system component models; automate or interact with simulator operation, and analyze and post-process simulation results. So, power system network to be simulated is constructed RSCAD. This software has a large library containing many power system component and control models. The RSCAD software has different models, the main two modules are; Draft and Runtime [33]. The Draft module is used for building the network and parameters entry. The Runtime module is used to control the operation of RTDS simulator. Using Runtime, user can performs a lot actions; such as starting and stopping of simulation, initiating system disturbances, changing some of the system set points, on-line monitoring and measuring of power system quantities, and other control functions.

The RTDS simulator is currently applied to many areas of development, testing and a lot of studies such as; protection and control system, general AC and DC system operations and behavior, feasibility studies, and for demonstration and training purposes [35].

### **7.3 Laboratory Setup for RTDS Simulation**

In this section, the case study of the two area power system, with the complete control system designed in chapter 6, is considered. Control system includes local PSSs at G2 & G4 and WADC at G3. For the purpose of circuit components assembly and parameters entry, RSCAD/Draft module has been used. The Draft screen is divided into two sections; the library section and the circuit assembly section. Individual components icons are selected from the library and placed in the circuit assembly section.

Figure 7-1 shows the three phase diagram view of the synchronous generator model; including generator control systems (Governor, Exciter and PSS). Where the parameters can be easily set. Figure 7-2 to Figure 7-4 represent the block diagrams of the governor, the exciter and the PSS used in the model, respectively. Parameters used for the generators, governors, exciters and PSSs are given in Table D-1 to Table D-7 in Appendix D.

WAMS model, which consists of four PMUs; one at each generator bus, is shown in Figure 7-5. The PMU component is suitable for providing the symmetrical component information related to a pair of 3 sets of instantaneous values of voltage and current. Each PMU can be configured easily; by setting the voltages and currents measurements of the related bus as inputs to the PMU. In addition to symmetrical and zero sequence voltages and currents, PMU can measure frequency and rate of change of frequency. In the case study, frequencies were measured and speeds in rad/sec are calculated accordingly. These speeds signals are sent to the WADC as shown in Figure 7-6.

Final components to complete the system model are loads and transmission lines. The load and the basic components of transmission line models are shown in Figure 7-7. Loads and transmission lines parameters are given in Table D-8 and Table D-9 in Appendix D. Finally, a fault branch is connected to Bus 8 as shown in Figure 7-8, in order to simulate a short circuit at this point. The fault branch consists of a switch whose open resistance is very large and whose closed resistance is specified by the user. The type of fault, line-ground or line-line, is specified by the 'Type' parameter in the fault component configuration menu. With this, the system assembly is completed and ready to be run.

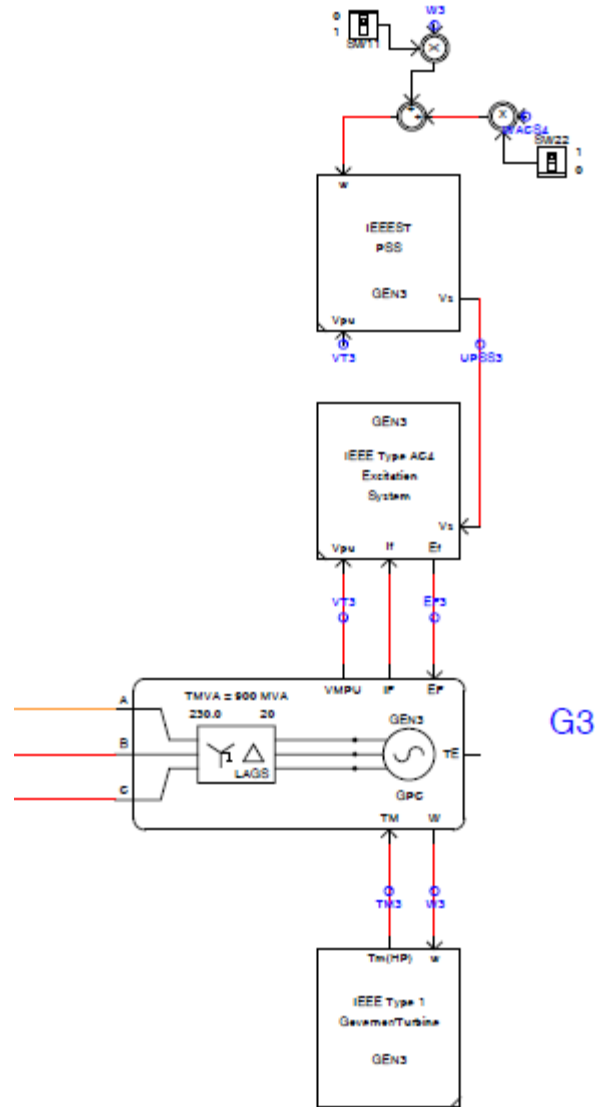


Figure 7-1: Synchronous generator Model in RSCAD

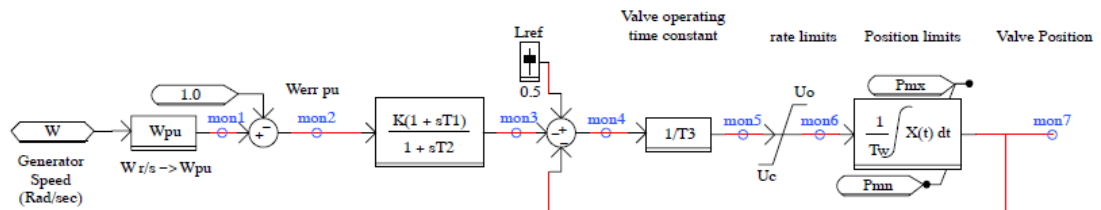


Figure 7-2: IEEE type 1 speed governor block diagram



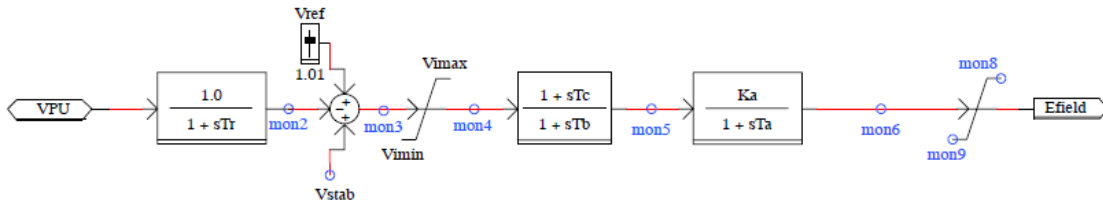


Figure 7-3: IEEE type AC4 exciter block diagram

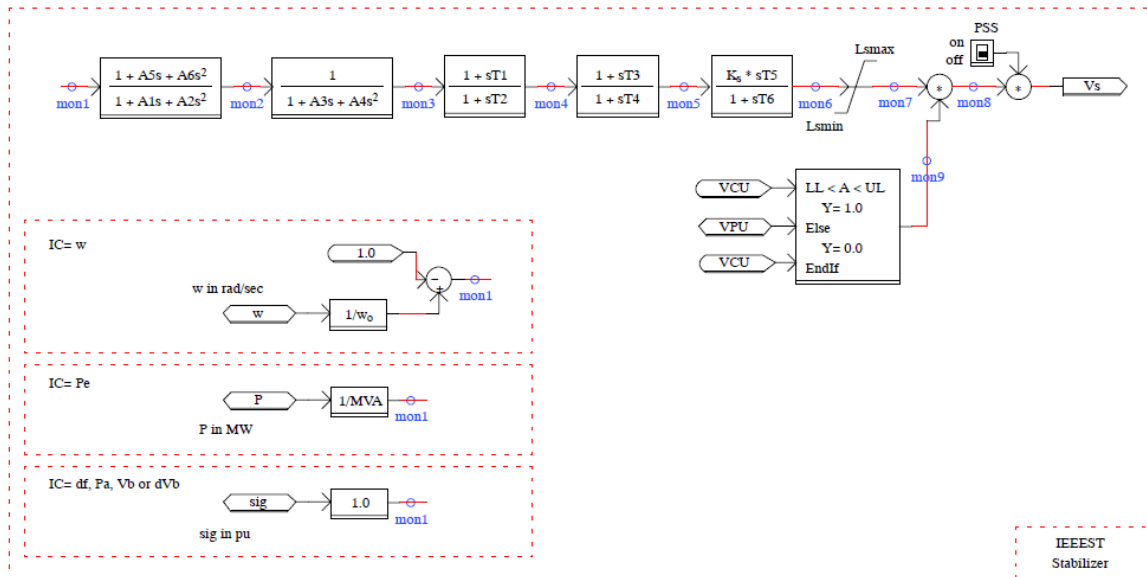


Figure 7-4: IEEE type ST stabilizer block diagram

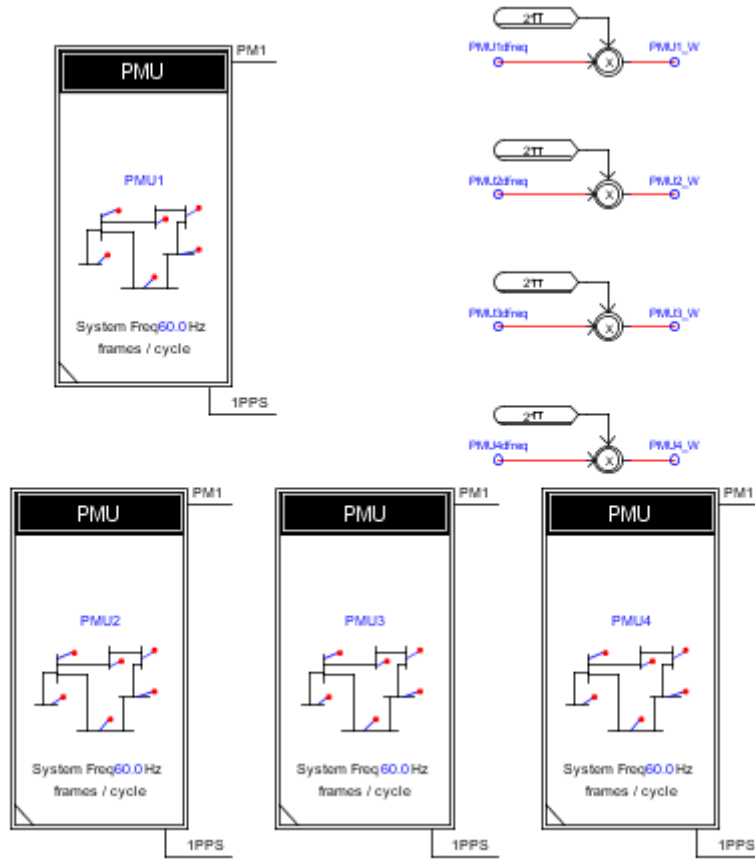


Figure 7-5: PMUs model in RSCAD

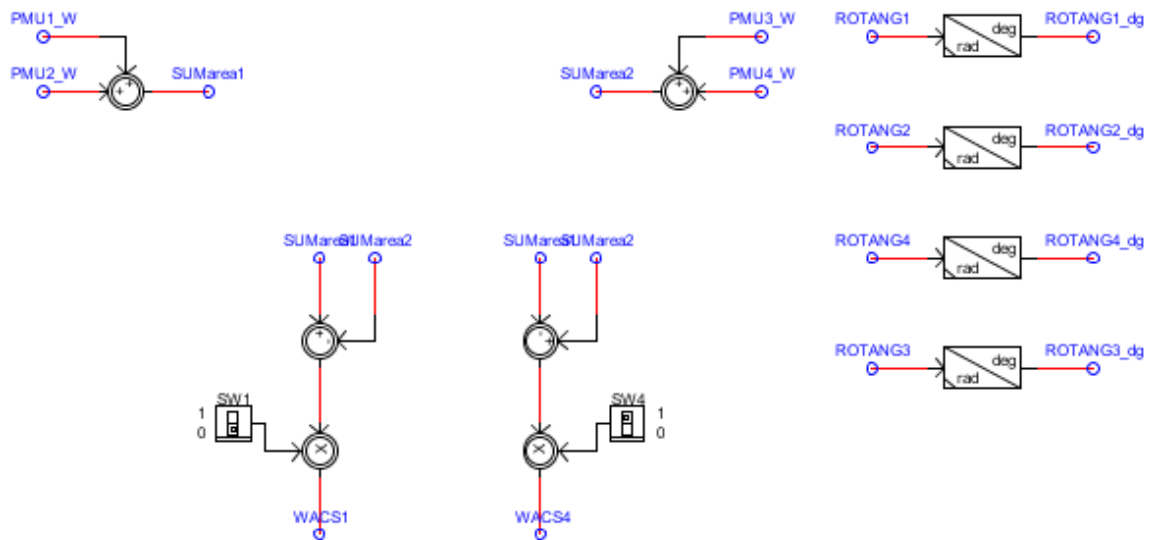


Figure 7-6: WADC scheme in RSCAD

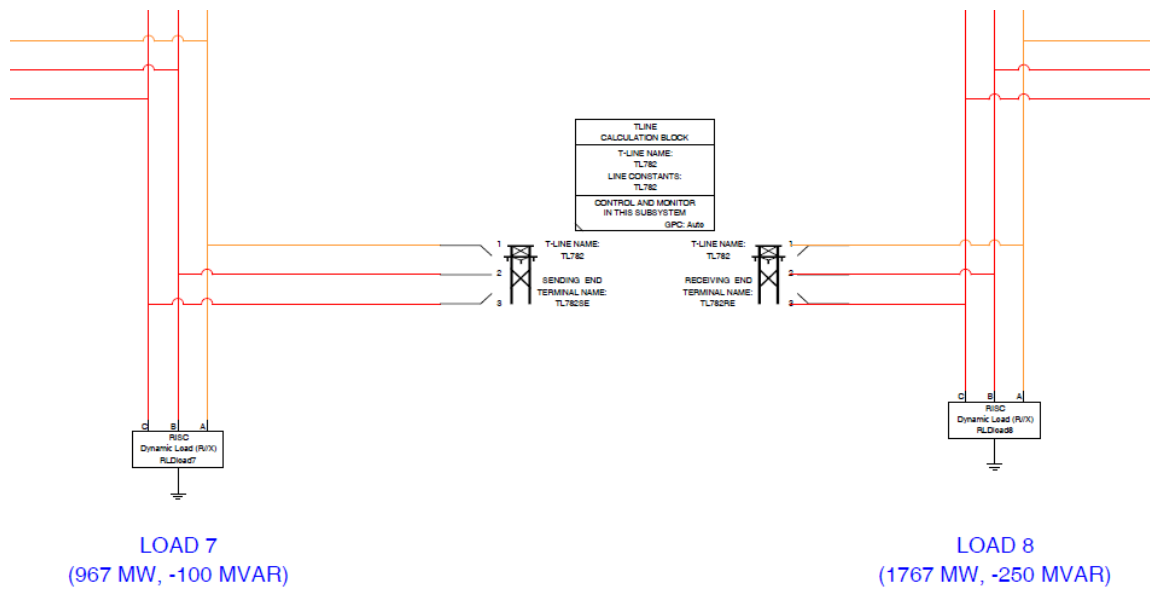


Figure 7-7: Load and transmission line models in RSCAD

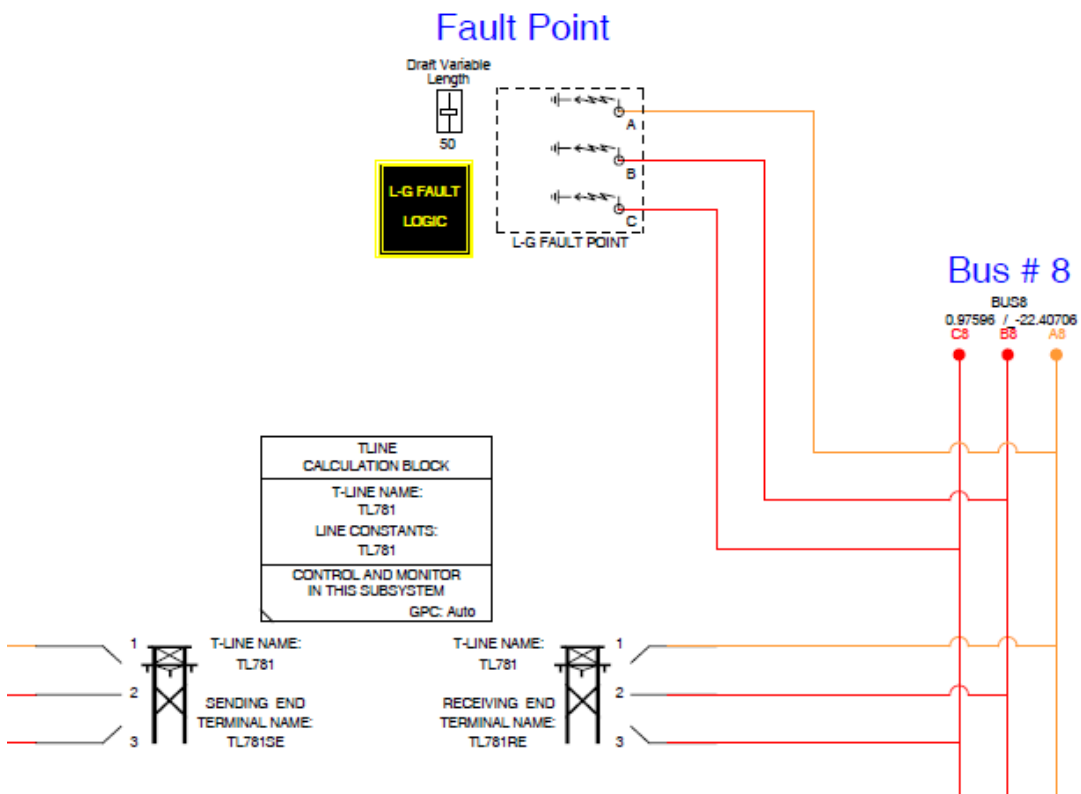


Figure 7-8: Fault point model at RSCAD (connected at Bus 8)

## 7.4 RTDS Simulation

Figure 7-9 shows the two area power system as modeled in RSCAD. To run the simulation, the circuit built in the previous section needs to be compiled first from RSCAD/Draft and then the case can be load into RSCAD/RunTime module. RunTime is used to control the simulation case being performed on the RTDS hardware. Simulation control; including start/stop commands, set point adjustment, fault application, etc. are performed through the RunTime Operator's Console [35]. Additionally, meters and plots can be created to monitor various system quantities such as bus voltages, line currents, generators rotor speed, generators power output, etc.

The system was simulated for two different cases; i) for transient fault, and ii) sudden change in loads. The simulation results are presented here in two means; first one is the usual plots of the system parameters response, and the other representation displays the on-line responses of some of the system parameters at the RunTime. Figure 7-10 shows graphical representation of the two-area power system RunTime module. This representation gives flexibility and easy interface with the system and allowed the user to select different form of results, such as numerical values, trends, plots, meters and other measurements display means. On-line flow of MW and MVAR can be shown also on each branch of the circuit.

Figure 7-10 shows the on-line normal operation case where around 400 MW and 16 MVAR are transferred across the tie line from area 1 to area 2. It is clear that the system is stable before applying any disturbance.

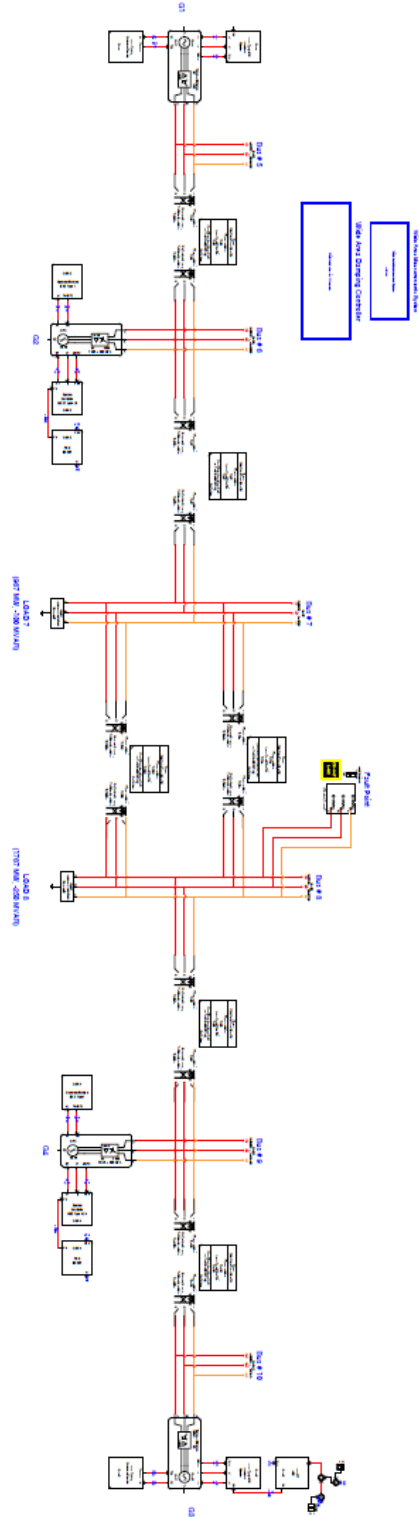


Figure 7-9: Two-area power system as modeled in RSCAD

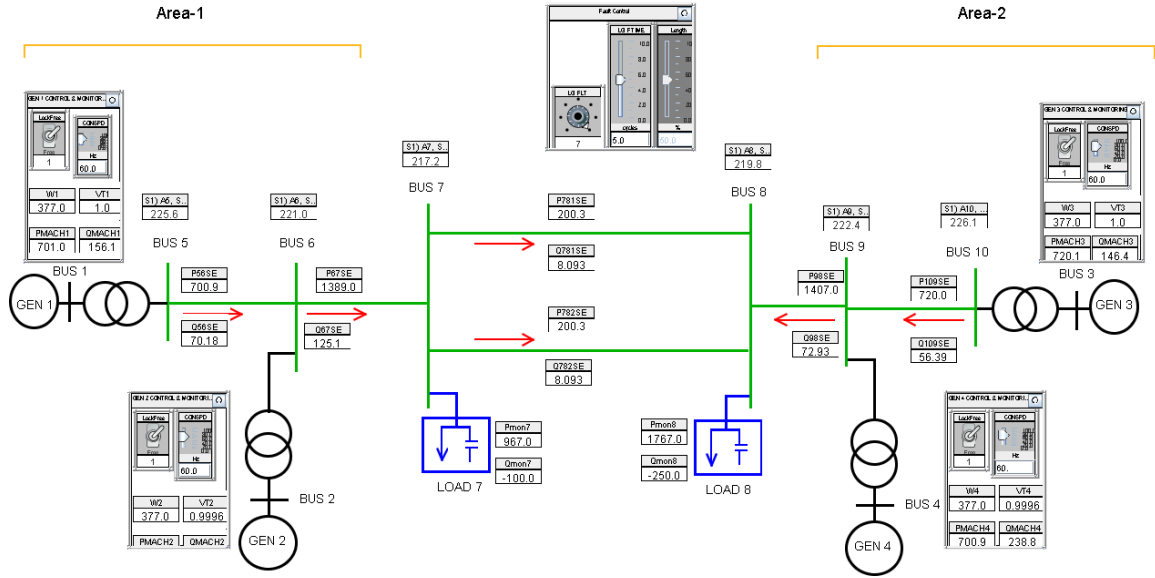


Figure 7-10: Two-area power system represented graphically at RunTime

## 7.4.1 Simulation Results

### 7.4.1.1 Case-1: Fault Disturbance

Here, the system was exposed to a severe disturbance in order to test the performance of the proposed WADC and its effectiveness in damping out the inter area oscillations. So, three phase fault was applied at Bus 8 for 5 cycles and system responses were plotted for the four control system designs (without controller; PSSs at G2 & G4; PSSs at G2, G3 & G4; PSSs at G2 & G4 and WADC at G3).

Figure 7-11 to Figure 7-14 show the rotor speed responses of all machines for different control system designs applied. It is clear from these figures that the local PSSs can stabilize the system. Moreover, the WADC provides better oscillations damping than the local based PSSs. Figure 7-15 shows the control signals action as result of 3-phase fault

applied at Bus 8. Figure 7-16 to Figure 7-19 show the electric power output responses of each machine. Again, responses indicated that the performance of the control system with WADC is improved and provide better damping action than the control with local PSSs. The MW transfer through the tie line during the fault is shown in Figure 7-24. This figure presents one tie line of the two parallel lines and each line transfer around 200 MW from area 1 to area 2. Figure 7-20 to Figure 7-23 show the voltages at each generator terminal.

The results show significant improvement in damping the inter area oscillation using combination of PSSs, one on each area and WADC installed based on the modal analysis of the system.

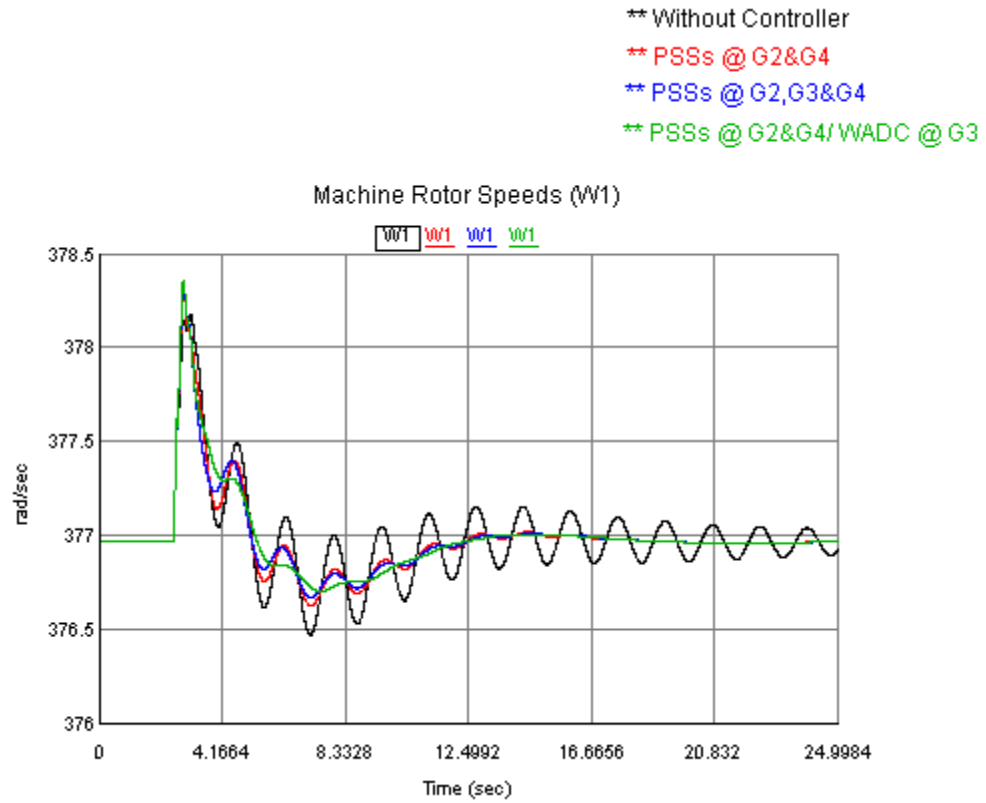


Figure 7-11: Rotor Speed response of G1 for a 3-phase fault at Bus 8 (RTDS)

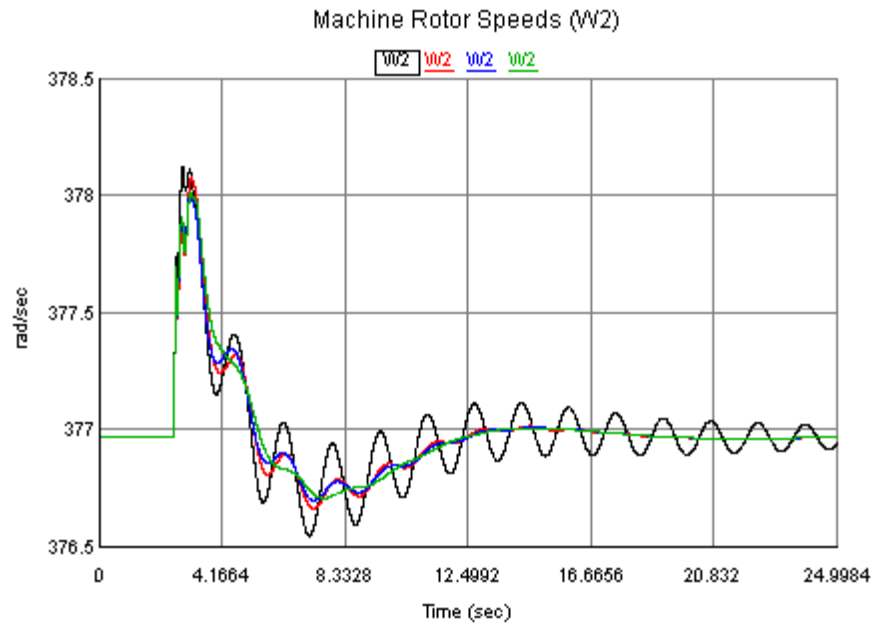


Figure 7-12: Rotor Speed response of G2 for a 3-phase fault at Bus 8 (RTDS)



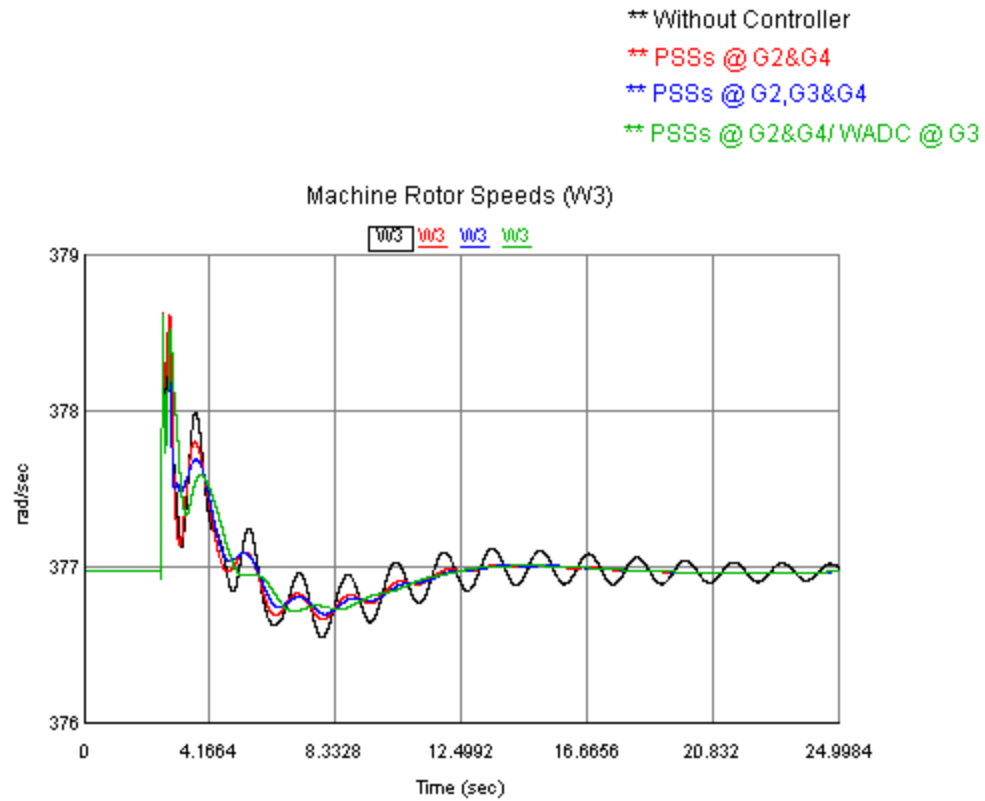


Figure 7-13: Rotor Speed response of G3 for a 3-phase fault at Bus 8 (RTDS)

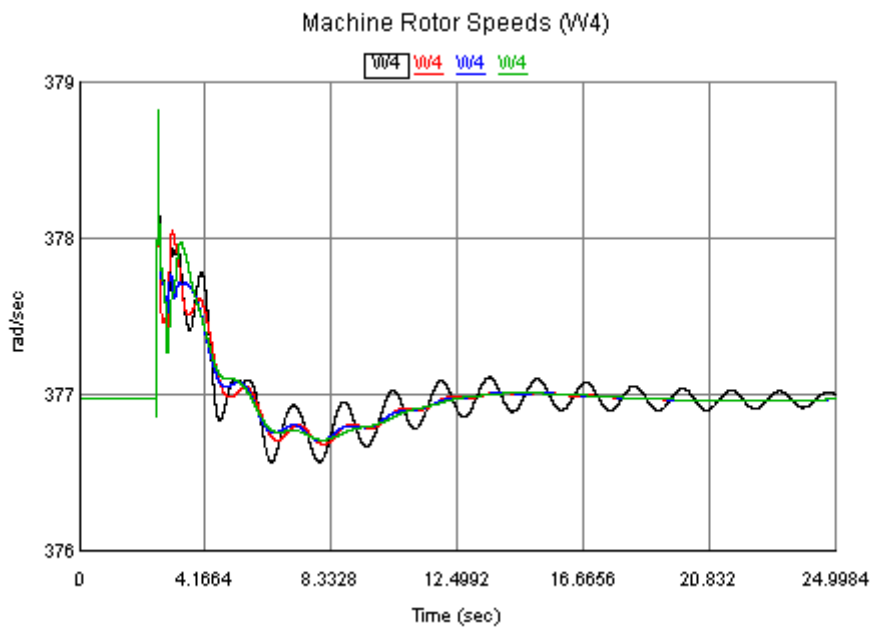


Figure 7-14: Rotor Speed response of G4 for a 3-phase fault at Bus 8 (RTDS)

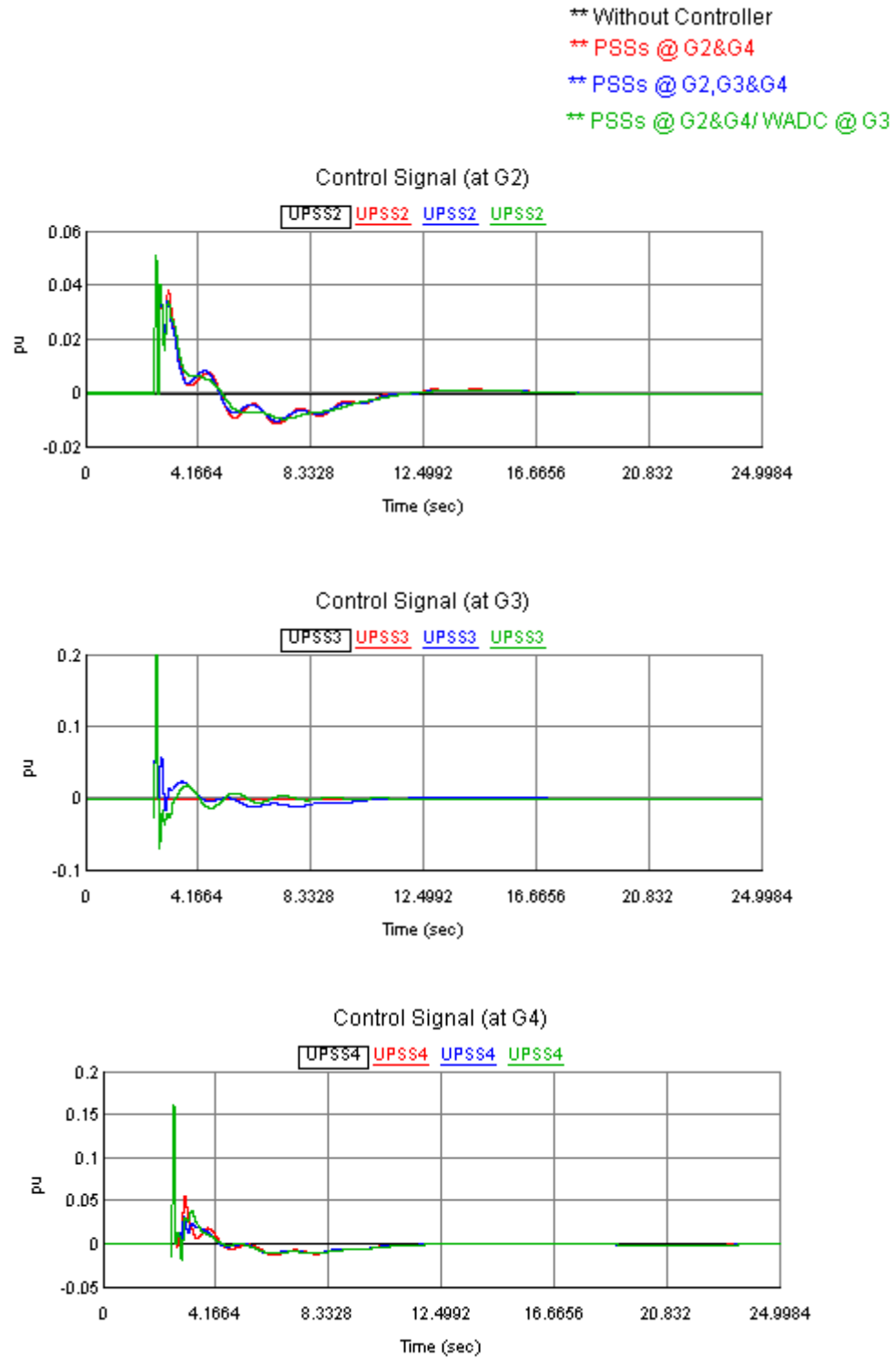


Figure 7-15: Control responses for 3-phase fault at Bus 8 (RTDS)

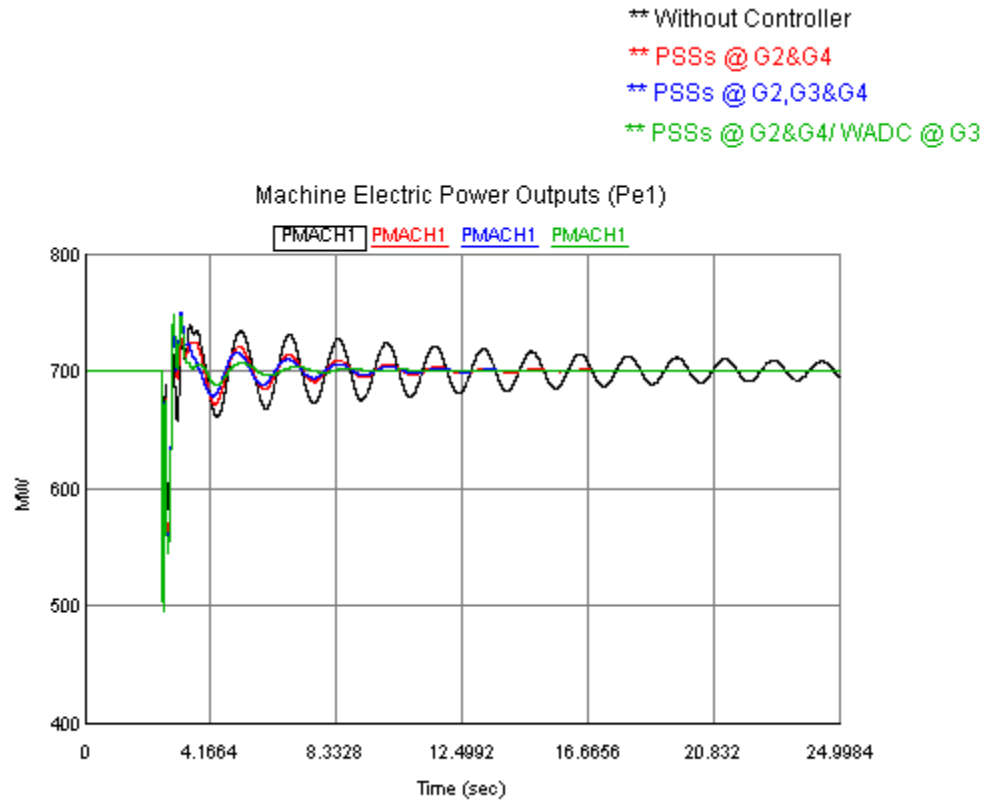


Figure 7-16: Electric power output response of G1 for 3-phase fault at Bus 8 (RTDS)

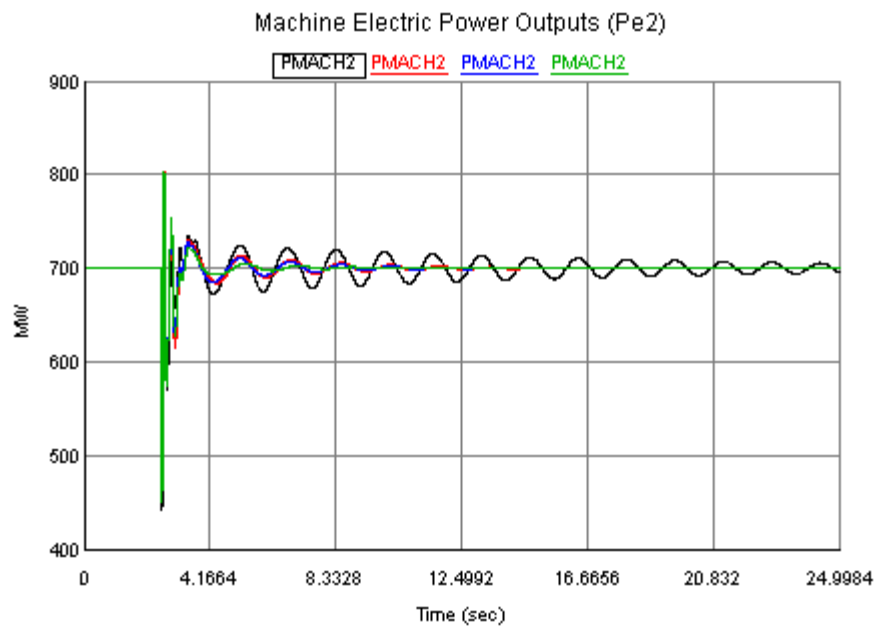


Figure 7-17: Electric power output response of G2 for 3-phase fault at Bus 8 (RTDS)

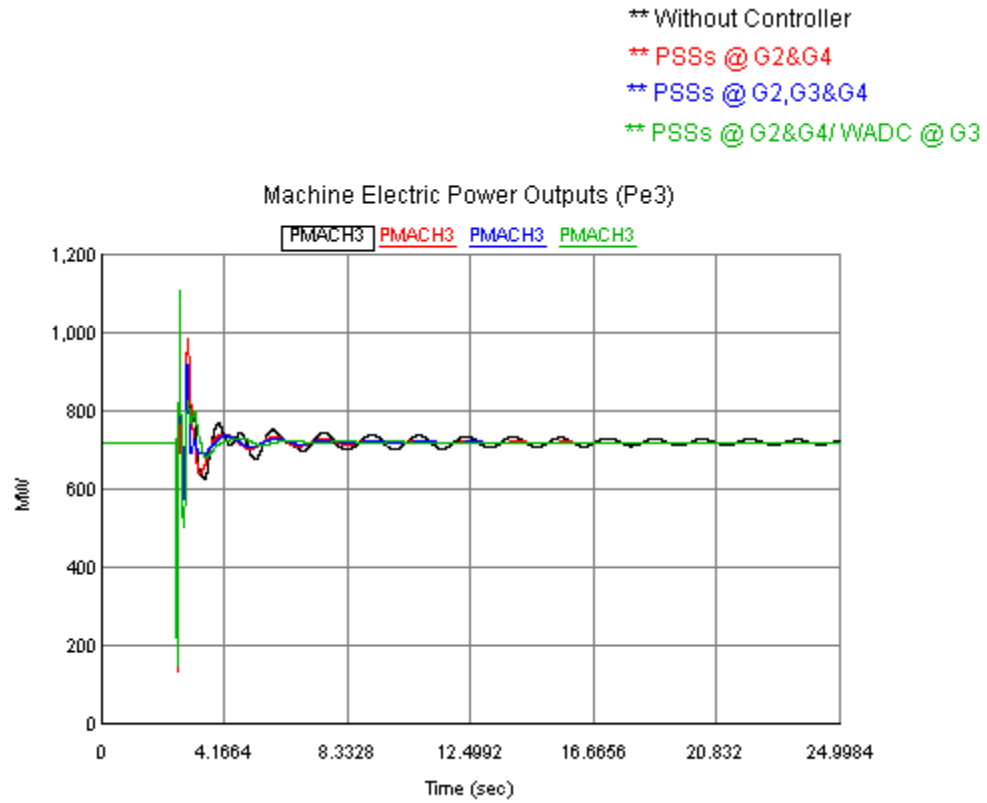


Figure 7-18: Electric power output response of G3 for 3-phase fault at Bus 8 (RTDS)

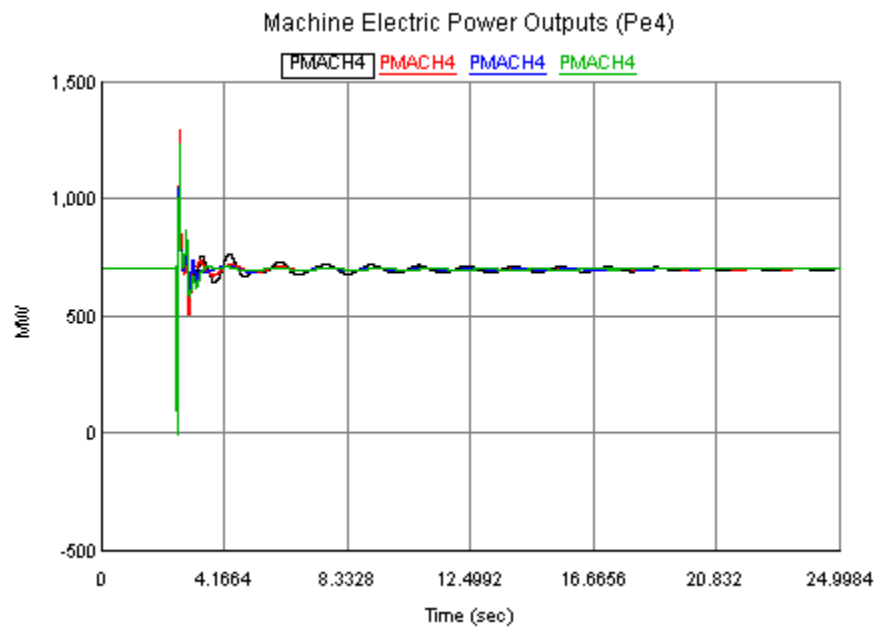


Figure 7-19: Electric power output response of G4 for 3-phase fault at Bus 8 (RTDS)

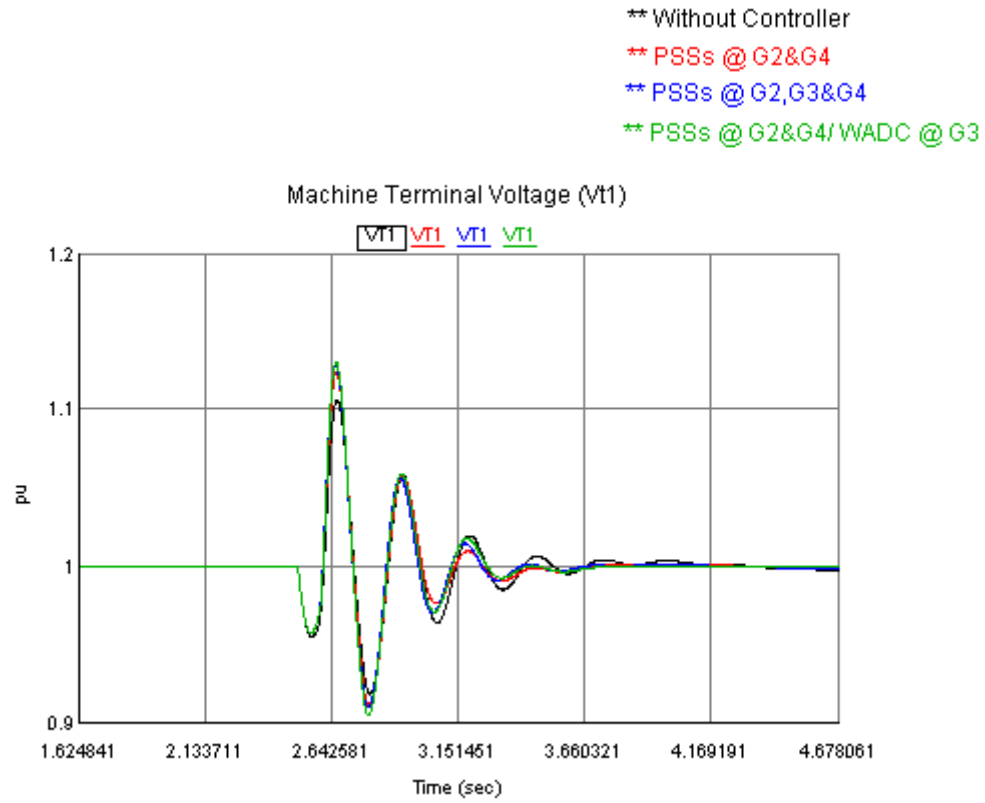


Figure 7-20: Terminal voltage response of G1 for 3-phase fault at Bus 8 (RTDS)

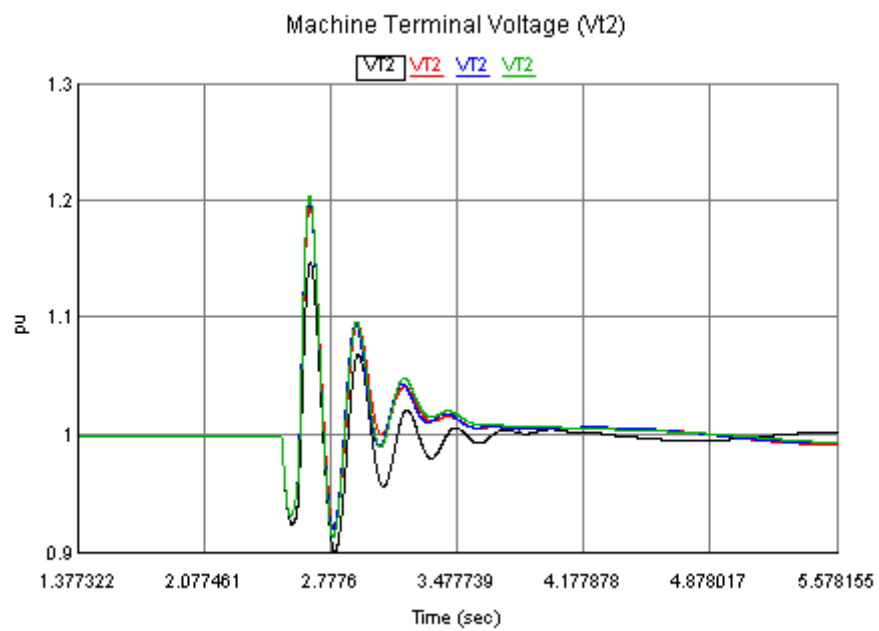


Figure 7-21: Terminal voltage response of G2 for 3-phase fault at Bus 8 (RTDS)

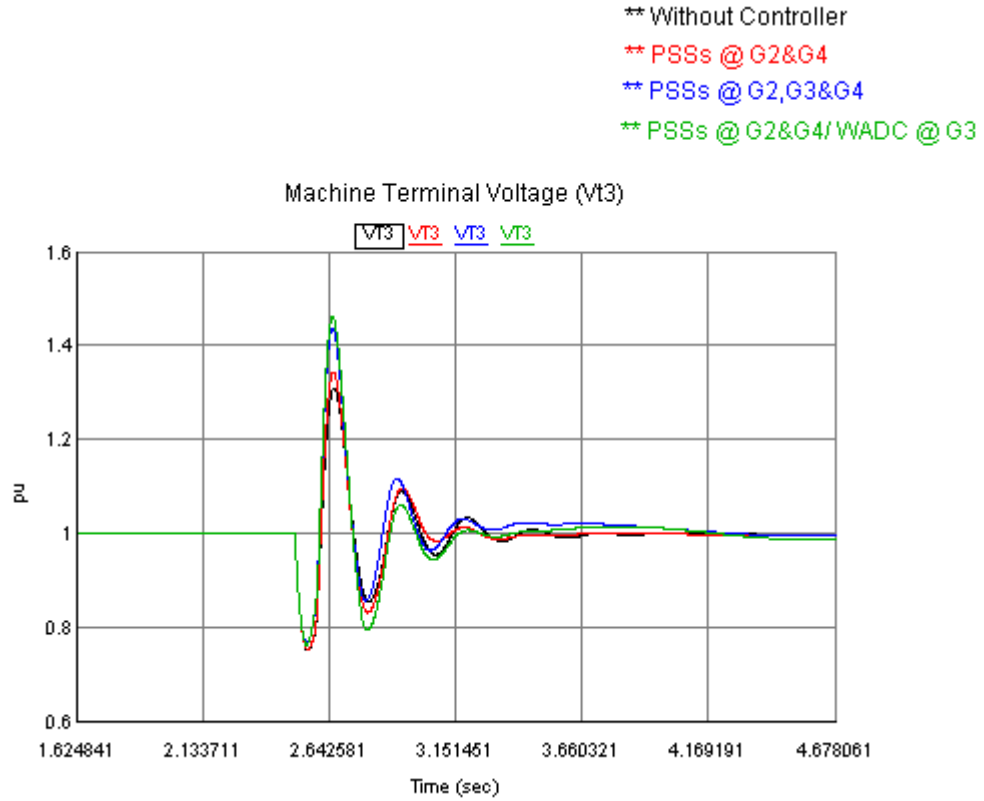


Figure 7-22: Terminal voltage response of G3 for 3-phase fault at Bus 8 (RTDS)

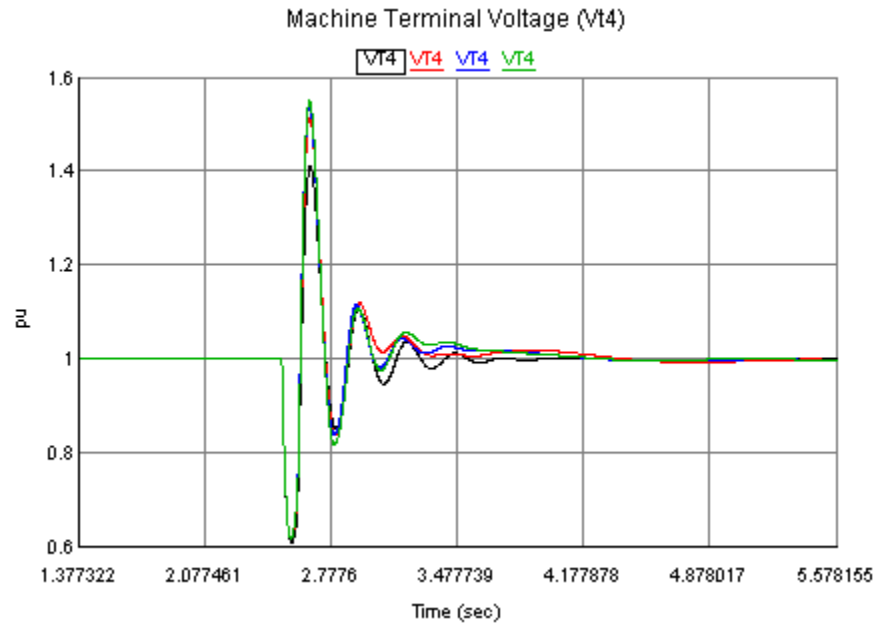


Figure 7-23: Terminal voltage response of G4 for 3-phase fault at Bus 8 (RTDS)

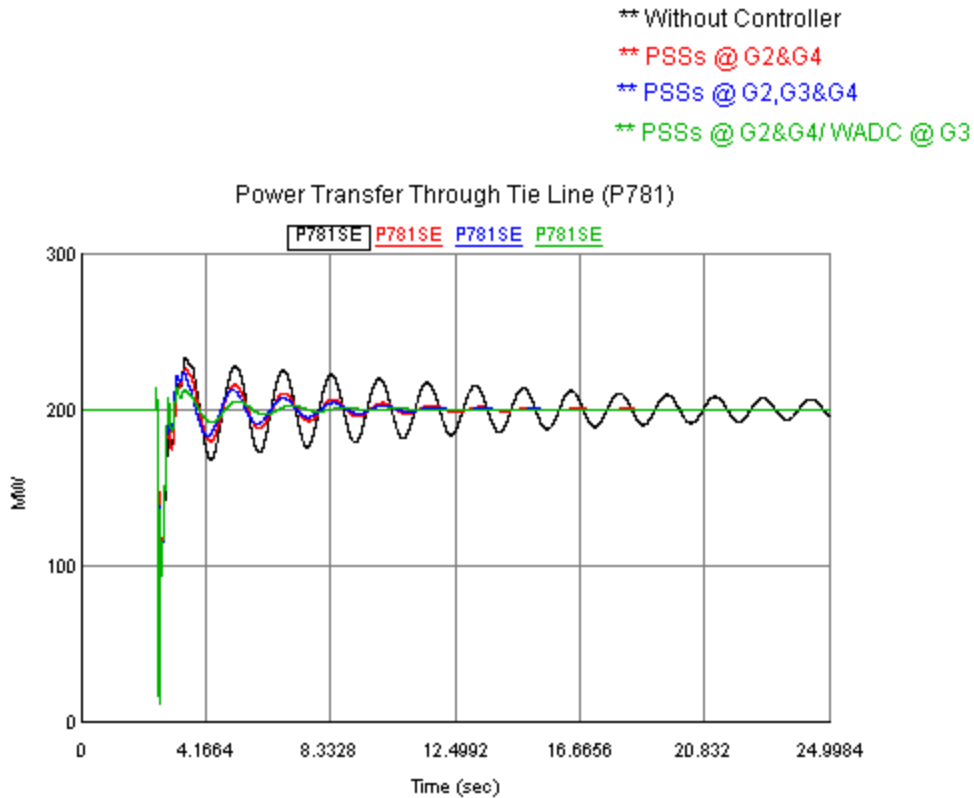


Figure 7-24: Power transfer across one of the tie lines for 3-phase fault at Bus 8 (RTDS)

#### 7.4.1.2 Case-2: Load Change Disturbance

In the second case, the system was tested for small disturbance such as load change. A sudden decreased in the LOAD 8 with amount of 60 MW was simulated. So the total power transfer from area 1 to area 2 becomes 340 MW plus the power losses in the transmission lines.

The rotor speed responses due to this decreased in LOAD 8 are shown in Figure 7-25 to Figure 7-28. Here, since this is considered to be small disturbance, the rotor speed oscillations are small comparing to short circuit case. Because of that, responses look

similar for all controllers applied. So the proposed WADC performance cannot be evaluated correctly by referring to rotor speed response of the machine. It is observable that there is a small steady state error in the speed response causing 0.079% change in the rotor speed. This as a result of the speed governors have a 5% droop setting.

However, this is not the case, if the electric power output of the machine or/and the power transfer through the system, are referred to. Figure 7-29 to Figure 7-32 show the electric power output responses of the machines for the decreased in LOAD 8. The difference in the controllers' performance can be noticed here. The oscillation damping using the WADC has better characteristic comparing to the other controllers. Same thing can be observed in Figure 7-33, where the oscillations in the power transfer through tie lines from area 1 to area 2 are damped faster using WADC controller.



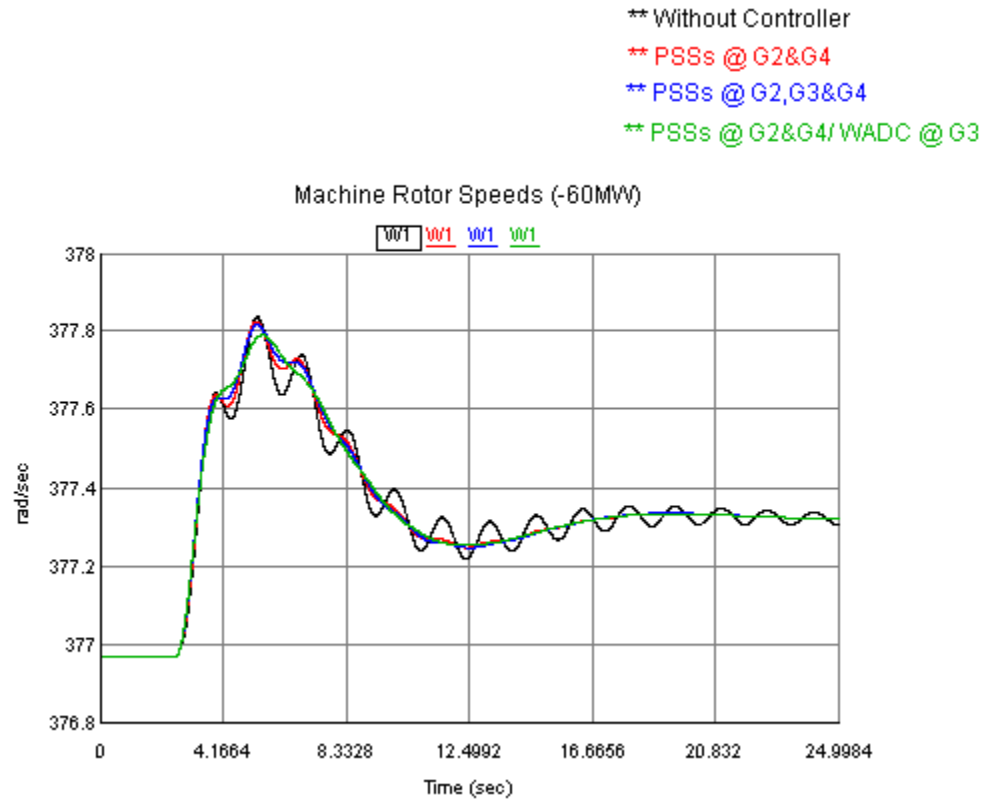


Figure 7-25: Rotor speed response of G1 for sudden decreased in LOAD 8 (RTDS)

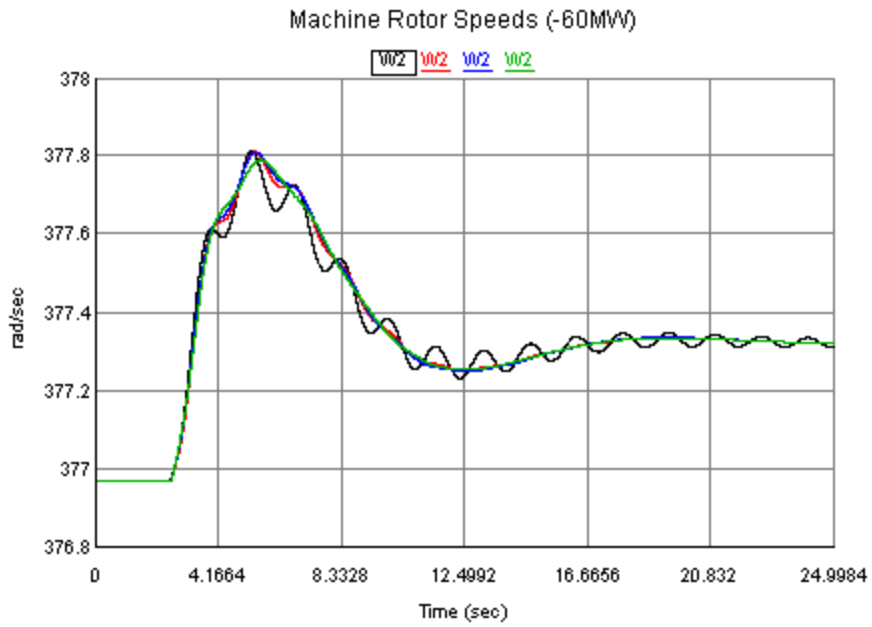


Figure 7-26: Rotor speed response of G2 for sudden decreased in LOAD 8 (RTDS)

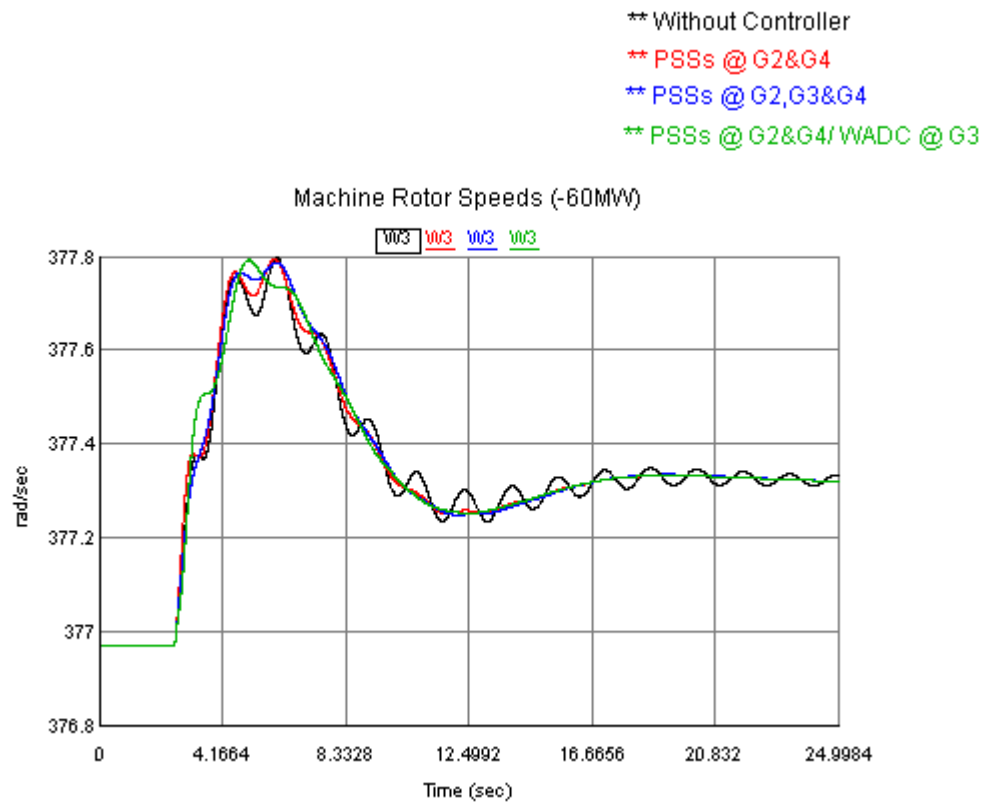


Figure 7-27: Rotor speed response of G3 for sudden decreased in LOAD 8 (RTDS)

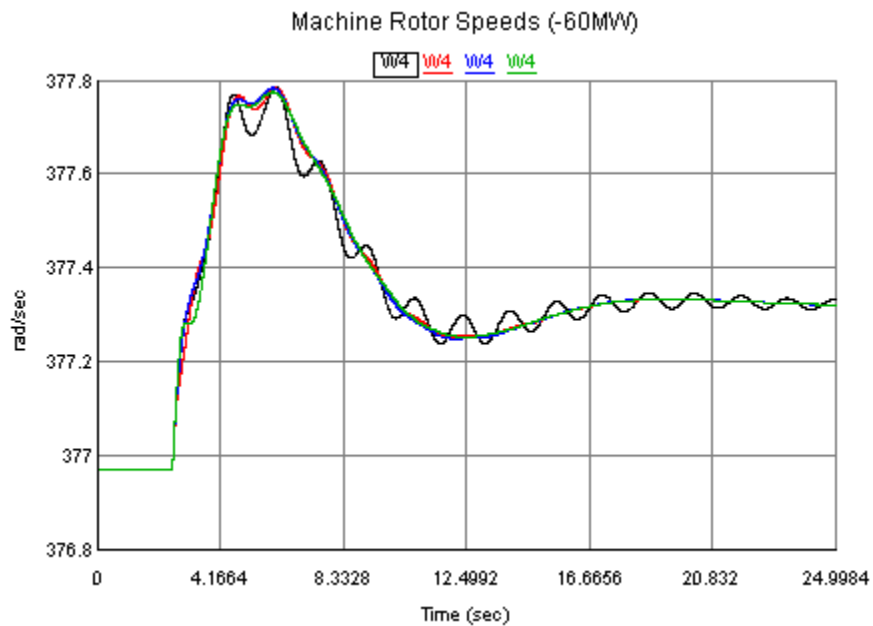


Figure 7-28: Rotor speed response of G4 for sudden decreased in LOAD 8 (RTDS)

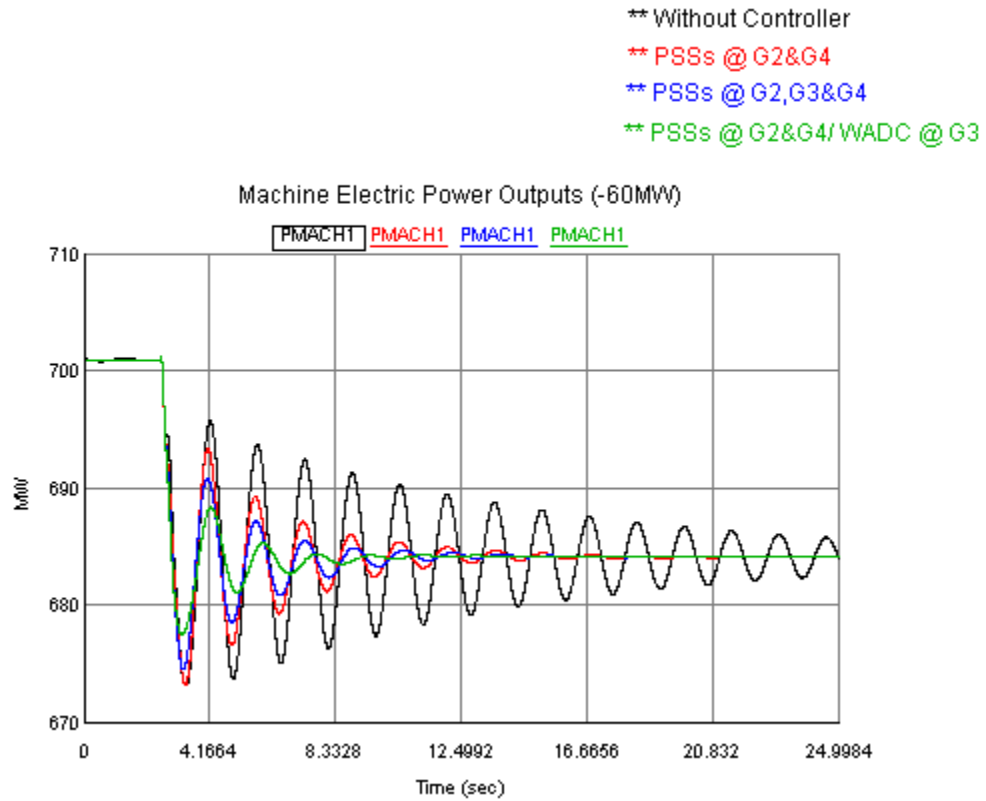


Figure 7-29: Electric power output response of G1 for sudden decreased in LOAD 8 (RTDS)

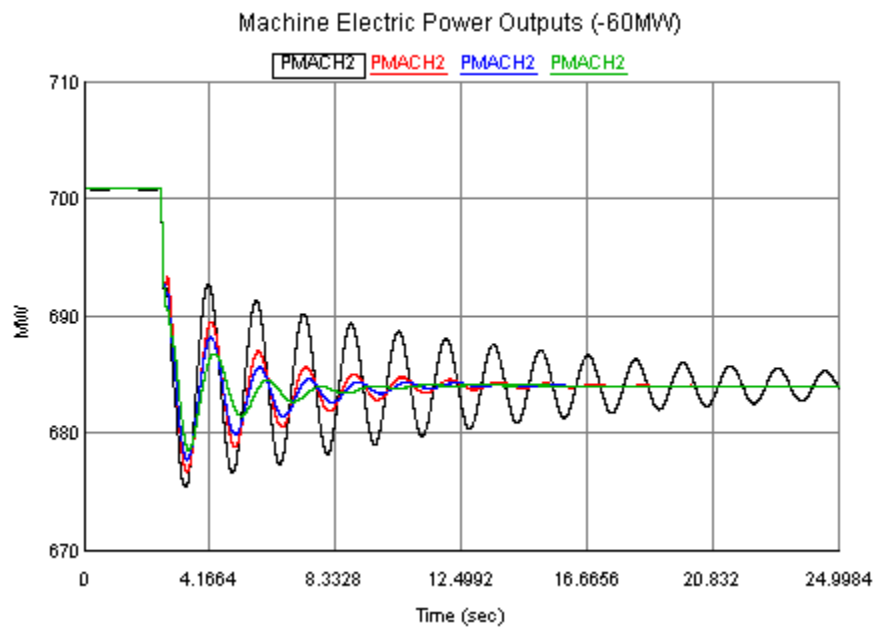


Figure 7-30: Electric power output response of G2 for sudden decreased in LOAD 8 (RTDS)

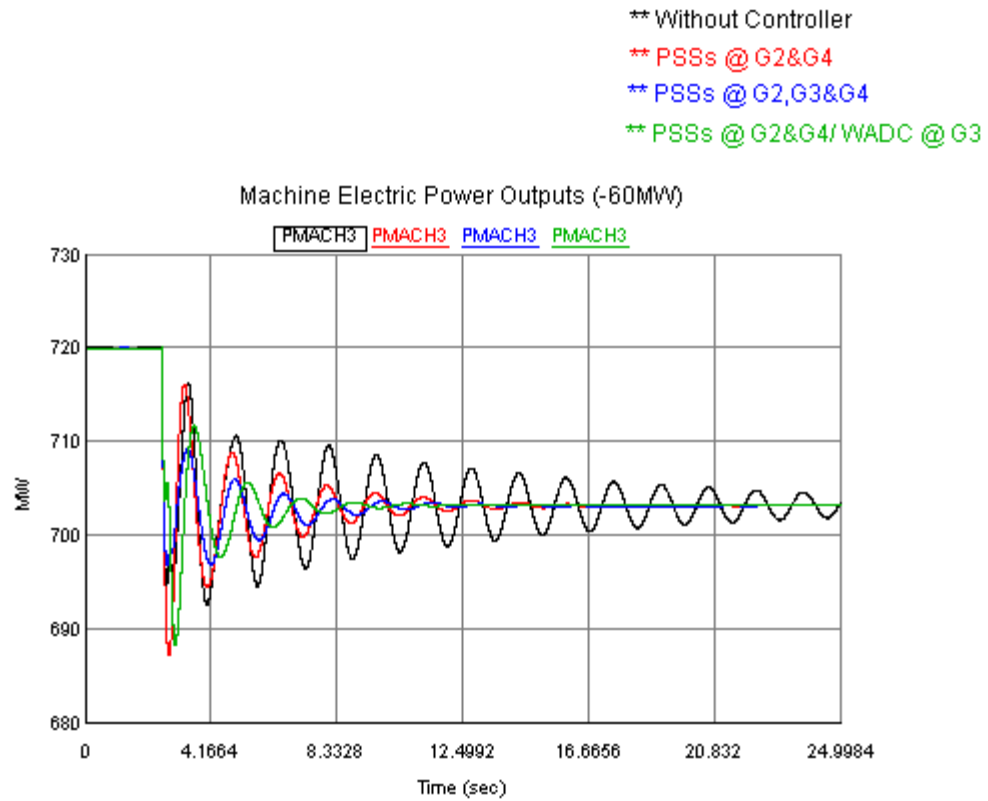


Figure 7-31: Electric power output response of G3 for sudden decreased in LOAD 8 (RTDS)

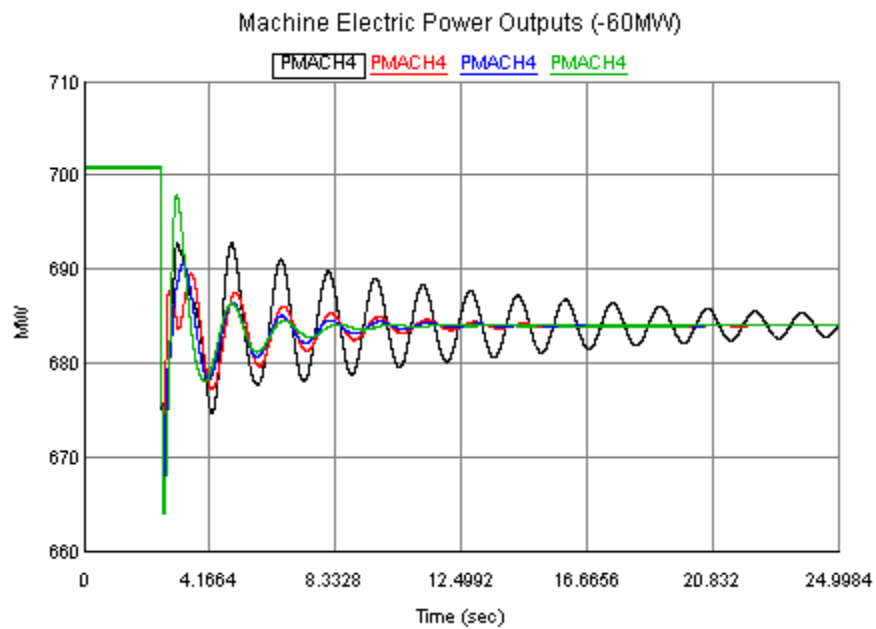


Figure 7-32: Electric power output response of G4 for sudden decreased in LOAD 8 (RTDS)

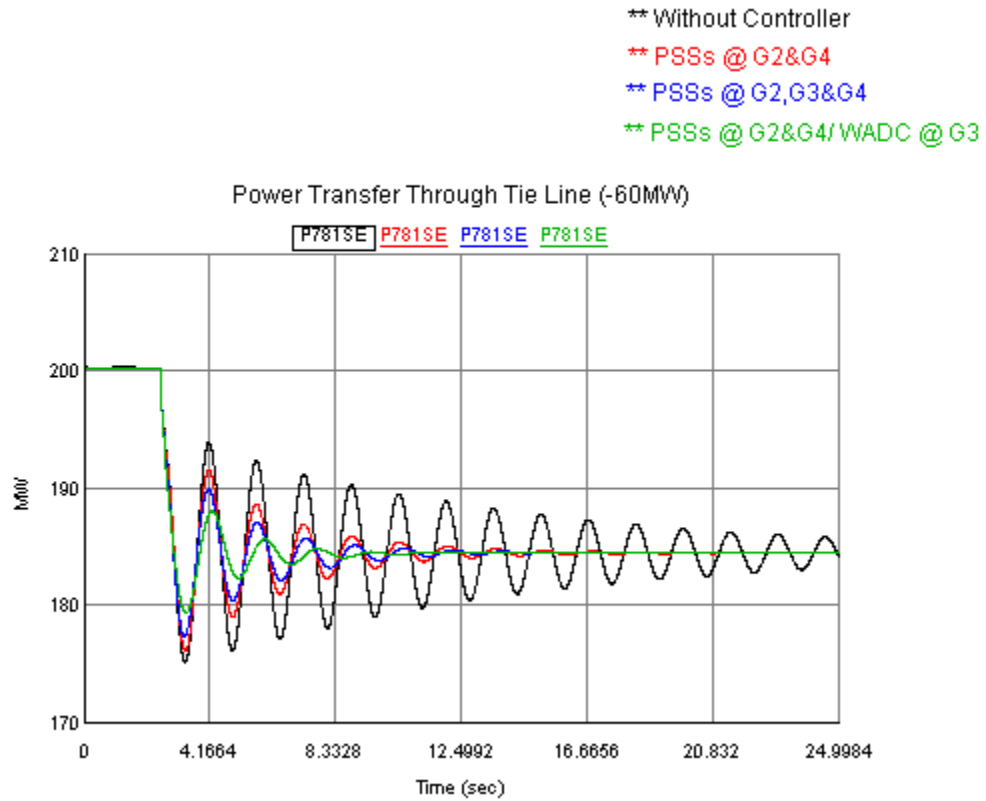


Figure 7-33: Power transfer across one of the tie lines for sudden decreased in LOAD 8  
(RTDS)

## 7.4.2 RUNTIME Interface (On-Line) Results

### 7.4.2.1 Case-1: Fault Disturbance

This section presents the same simulation results of previous section but in RunTime On-Line trends. Since space is limited in this graphical representation, only two parameters on-line results were selected to be displayed. The rotor speed of machine 1 and the power transfer through one of the tie-line are the selected two parameters.

3-phase transient fault was applied at Bus 8 for 5 cycles and On-Line simulation results are captured. This process was done for the system without any controller applied and also for the system with different control system combinations.

The responses of the system without controller are shown in Figure 7-34. Results show that the system experienced a severe oscillations and since there is no control system is acting, damping out these oscillations take long time. Placing local based PSSs, improve the damping characteristic and shorten the damping slightly as shown in Figure 7-35 and Figure 7-36. The significant enhancement in damping out the oscillations is observed, when the local PSS at G3 is replaced with the proposed WADC, see Figure 7-37. It is extremely cleared, from rotor speed of machine 1 and the power transfer through tie-line responses, which the proposed WADC contribute effectively in the total control action.

#### **7.4.2.2 Case-2: Load Change Disturbance**

Same amount of MW was dropped suddenly from LOAD 8 (60 MW). Simulation results are shown in Figure 7-38 to Figure 7-41. Again RunTime results confirmed that the performance of the proposed WADC is more robust than local based stabilizer.

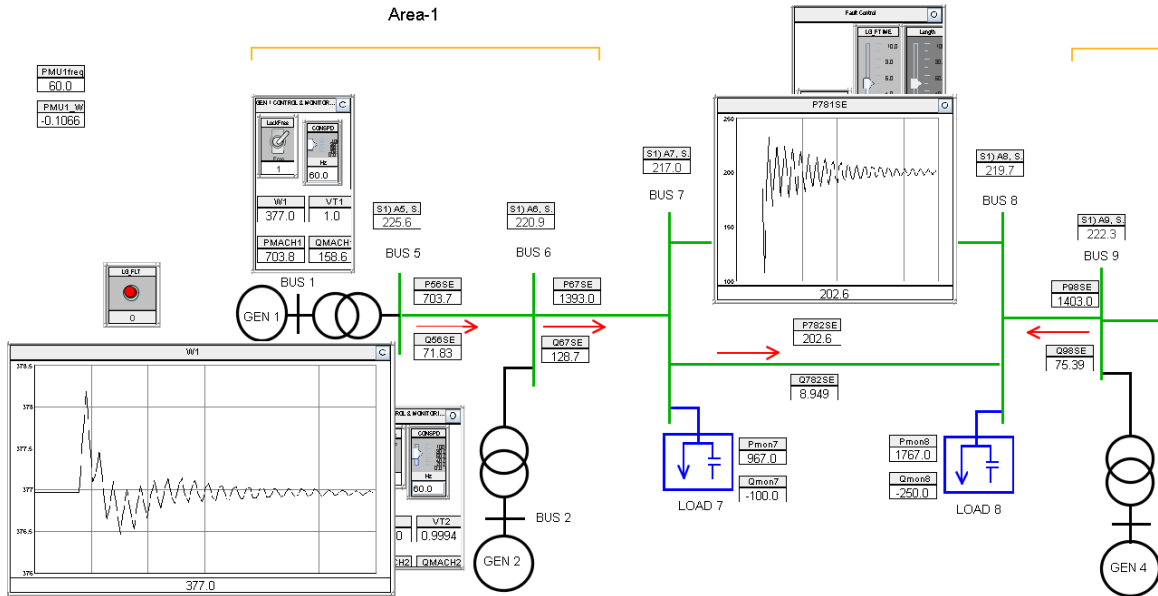


Figure 7-34: System responses for 3-phase fault at Bus 8 (without controller, RunTime interface)

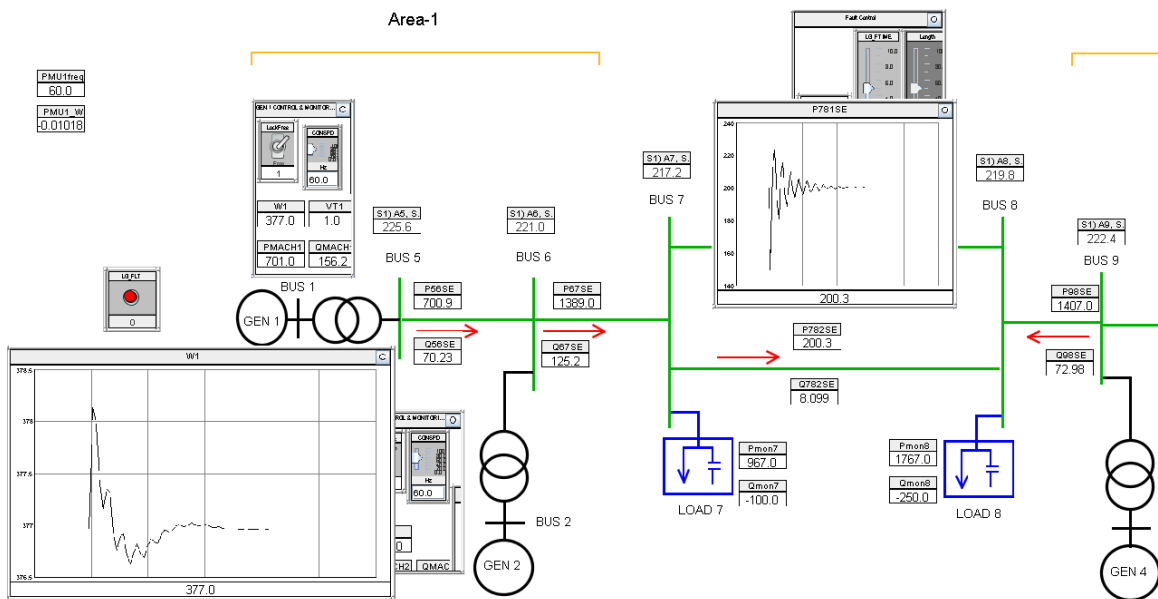


Figure 7-35: System responses for 3-phase fault at Bus 8 (with PSSs at G2 & G4, RunTime interface)

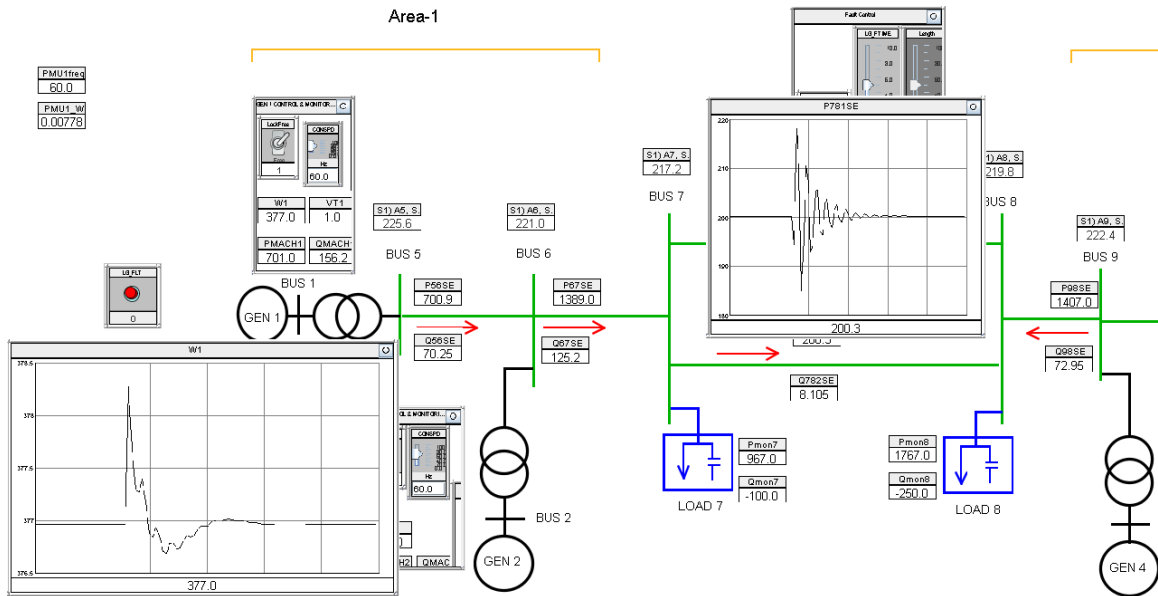


Figure 7-36: System responses for 3-phase fault at Bus 8 (with PSSs at G2, G3 & G4, RunTime interface)

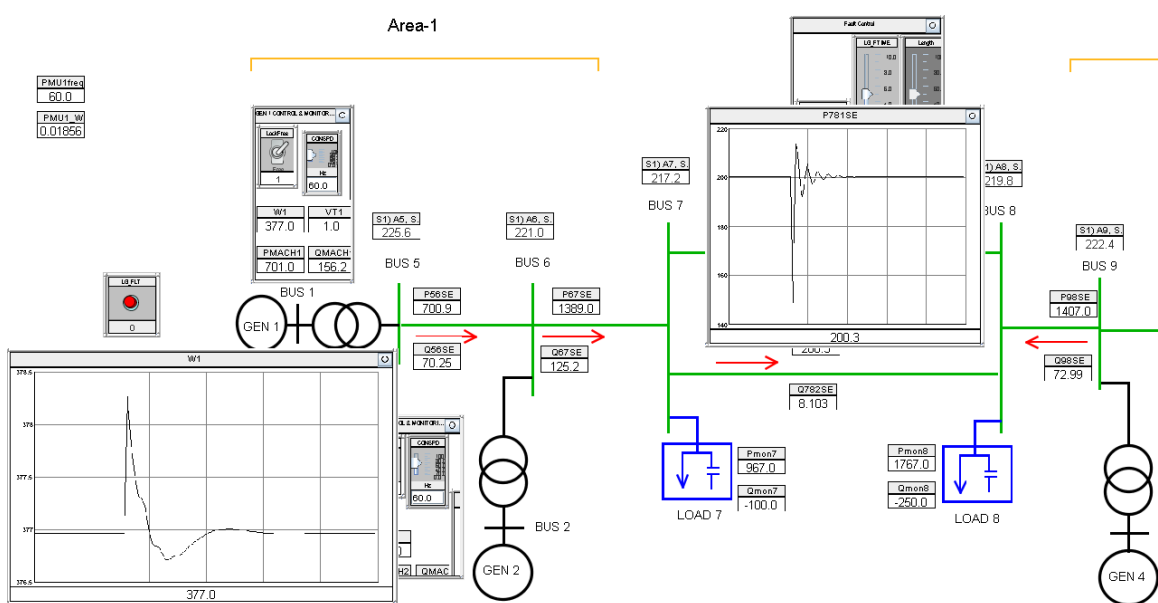


Figure 7-37: System responses for 3-phase fault at Bus 8 (with PSSs at G2 & G4 and WADC at G3, RunTime interface)



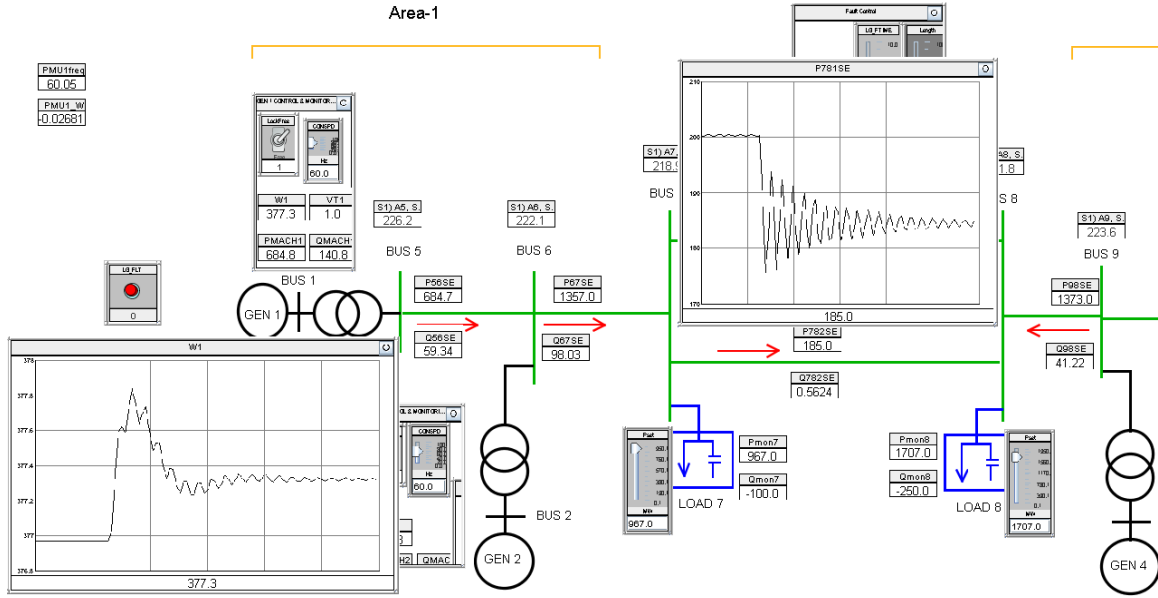


Figure 7-38: System responses for sudden decreased in LOAD 8 (without controller, RunTime interface)

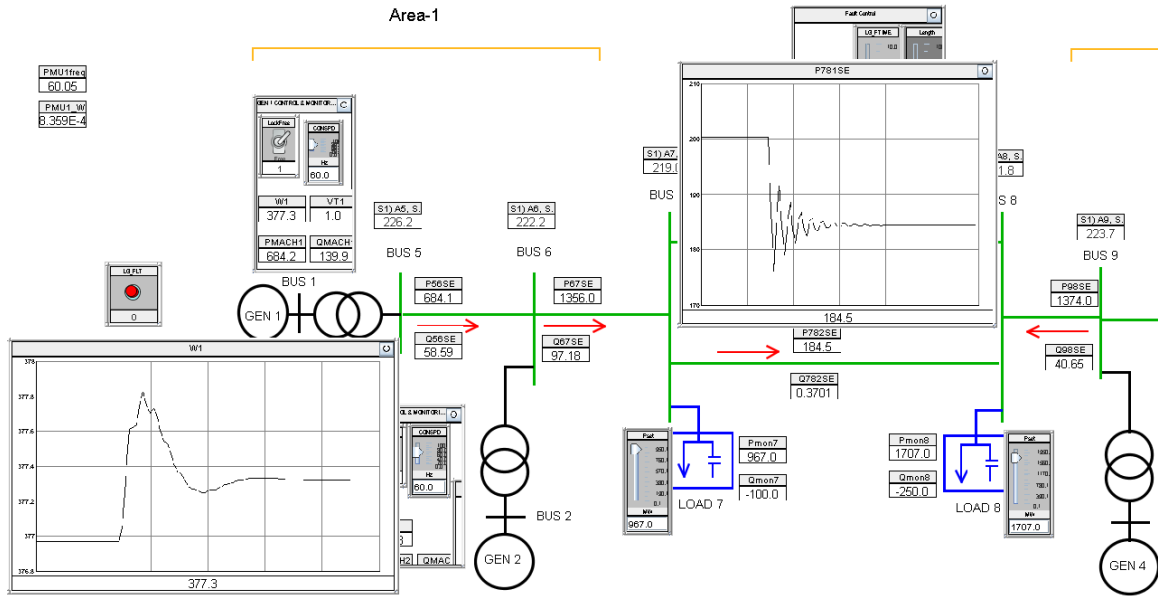


Figure 7-39: System responses for sudden decreased in LOAD 8 (with PSSs at G2 & G4, RunTime interface)

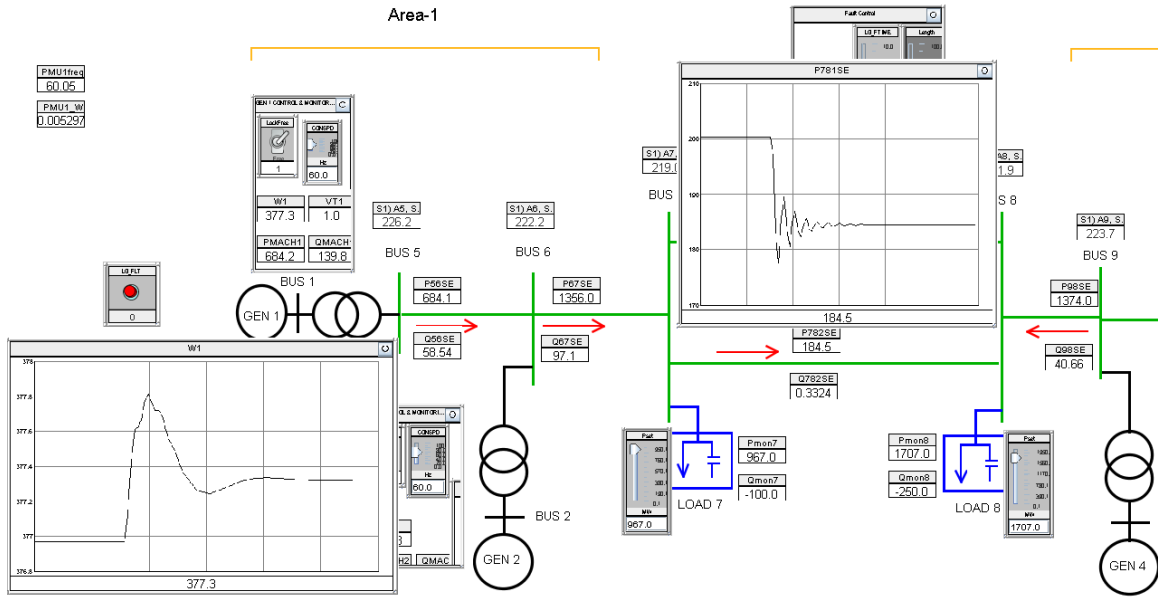


Figure 7-40: System responses for sudden decreased in LOAD 8 (with PSSs at G2, G3 & G4, RunTime interface)

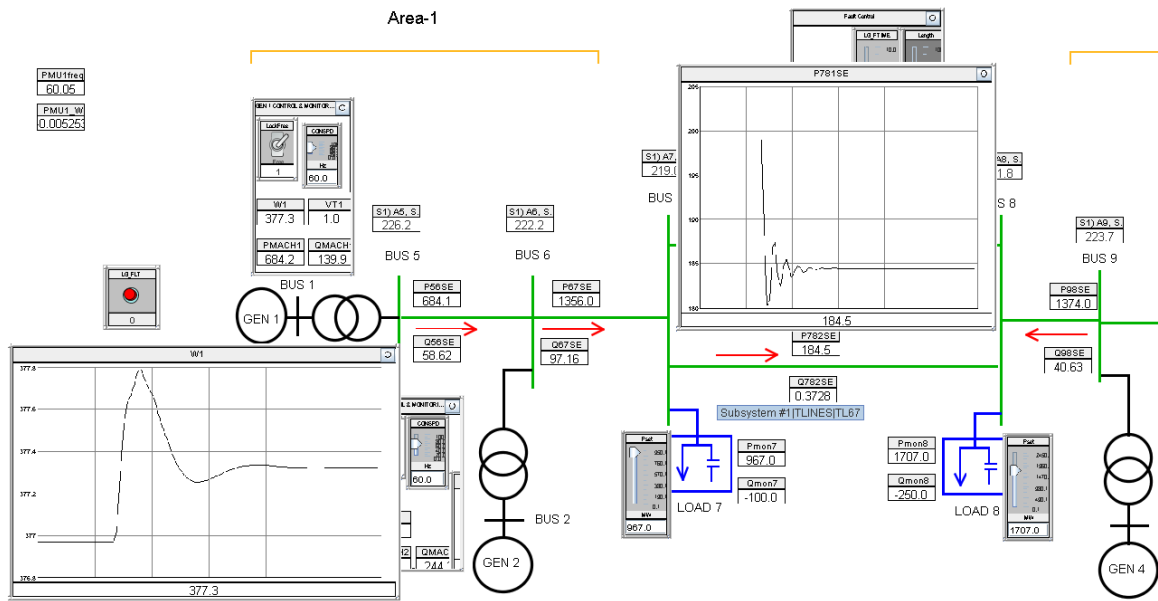


Figure 7-41: System responses for sudden decreased in LOAD 8 (with PSSs at G2 & G4 and WADC at G3, RunTime interface)

## **7.5 RTDS Comparison Between Local Based PSS and WADC**

A comparison is presented here between local based PSS and WADC considering that controller is applied at G3 only. The main objective, from applying the controller at only one machine, is to evaluate the performance of each controller alone. The comparison was done using typical controller parameters in the first part below. Then, WADC parameters which optimized using PSO technique in the previous chapter will be used in the second part.

### **7.5.1 Using Typical Values for The Controller Parameters**

Typical values were chosen from reference [2] for the controller parameters;  $K_{PSS}=10$ ,  $T_W=5$ ,  $T_1=T_3=0.1$  and  $T_2=T_4=0.05$ . As mentioned the controller is applied at G3 only to compare the system output responses of using local based PSS and WADC, one each a time. RTDS simulations were carried out for the case of three phase disturbance was applied at Bus 8 for 5 cycles.

Figure 7-42 to Figure 7-45 show the rotor speed responses of the machines. Figure 7-46 to Figure 7-48 show the machines electric power output. The power transfer through one of the tie lines is presented in Figure 7-49. It is clear from these figures that the local PSS can stabilize the system. Moreover, the WADC provides better oscillations damping than the local based PSS.

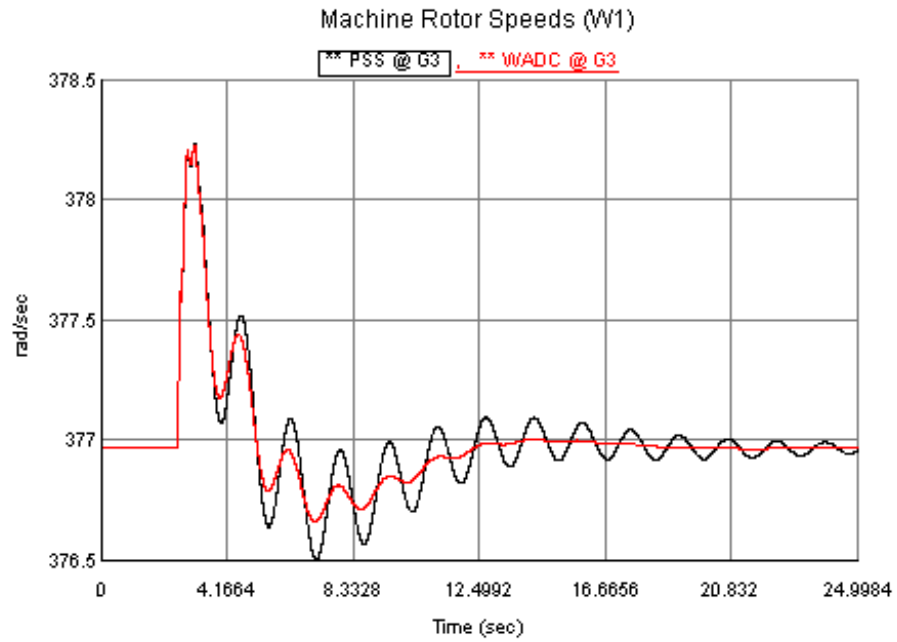


Figure 7-42: Rotor speed  $\omega_1$  response with controller placed at G3 (RTDS)

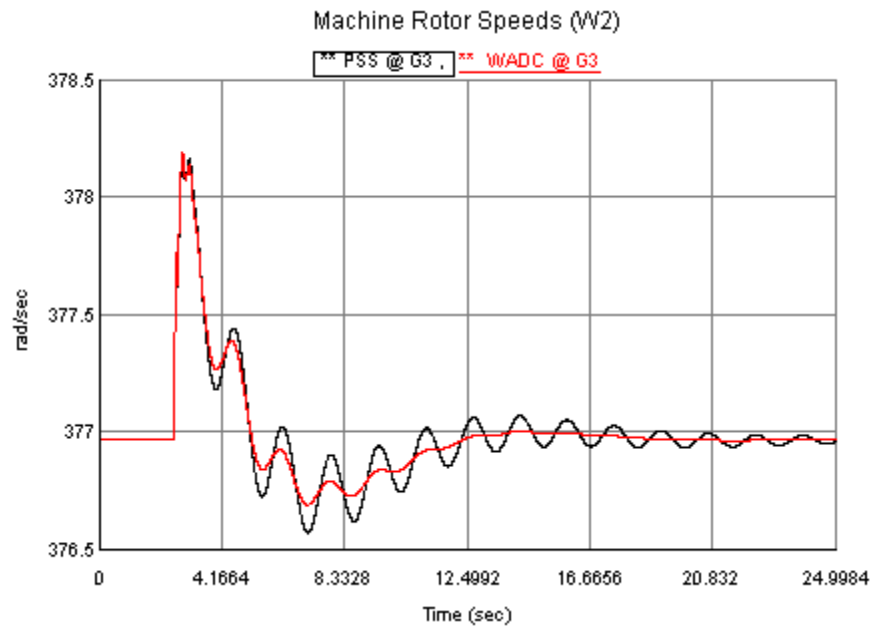


Figure 7-43: Rotor speed  $\omega_2$  response with controller placed at G3 (RTDS)

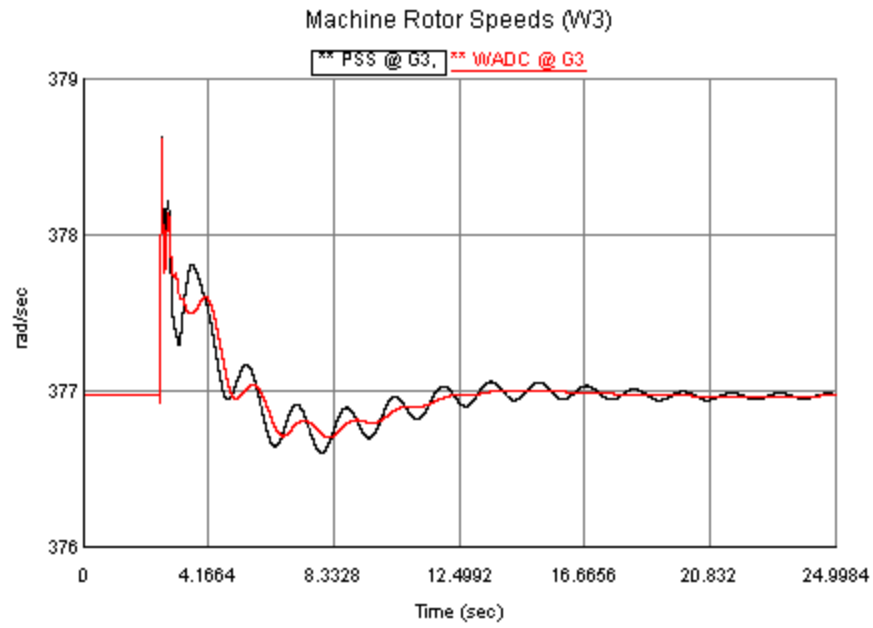


Figure 7-44: Rotor speed  $\omega_3$  response with controller placed at G3 (RTDS)

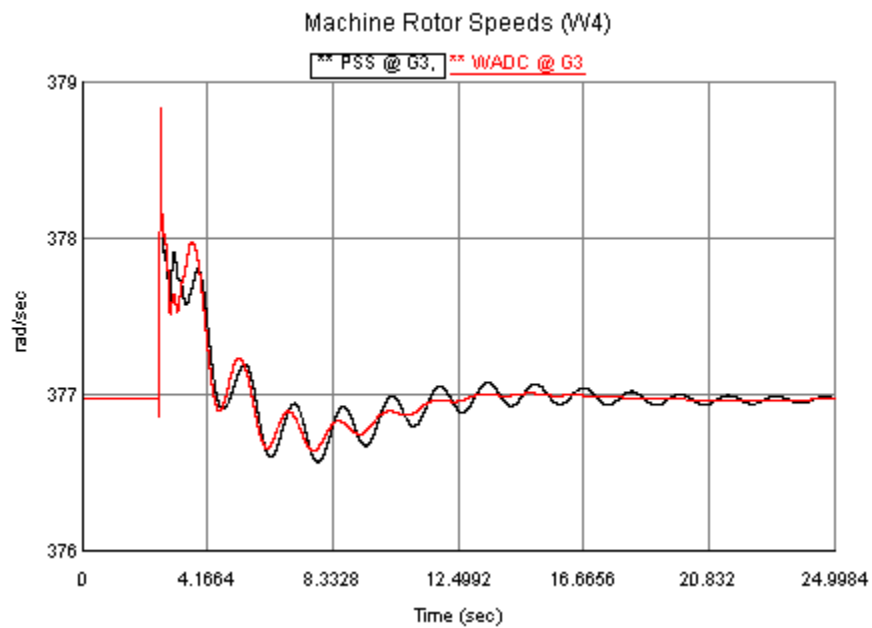


Figure 7-45: Rotor speed  $\omega_4$  response with controller placed at G3 (RTDS)

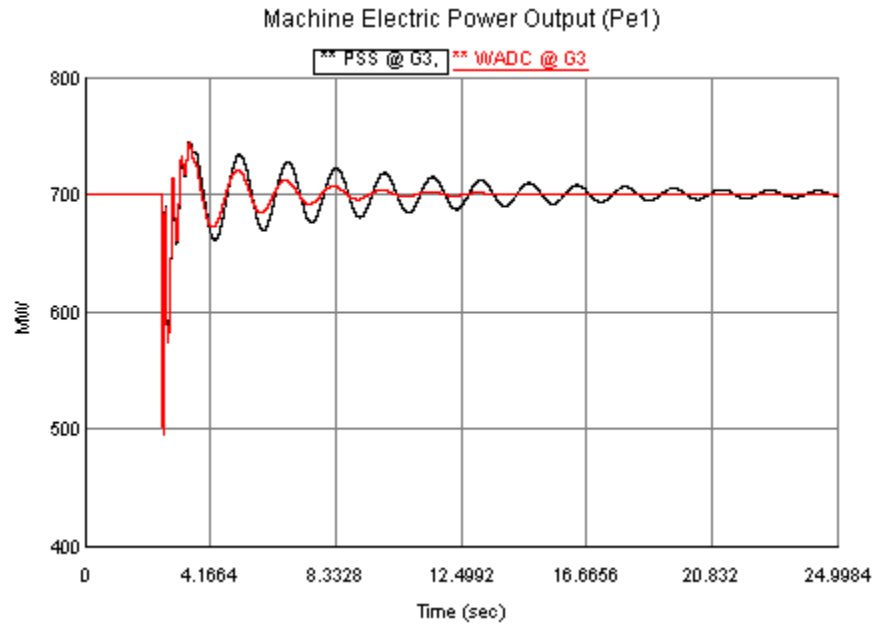


Figure 7-46: Electric power output Pe1 response with controller placed at G3 (RTDS)

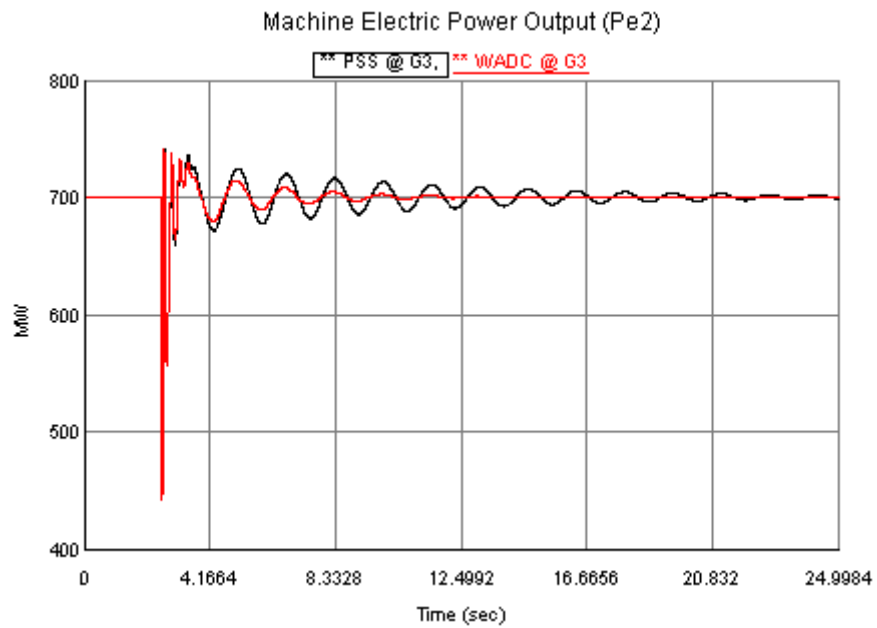


Figure 7-47: Electric power output Pe2 response with controller placed at G3 (RTDS)

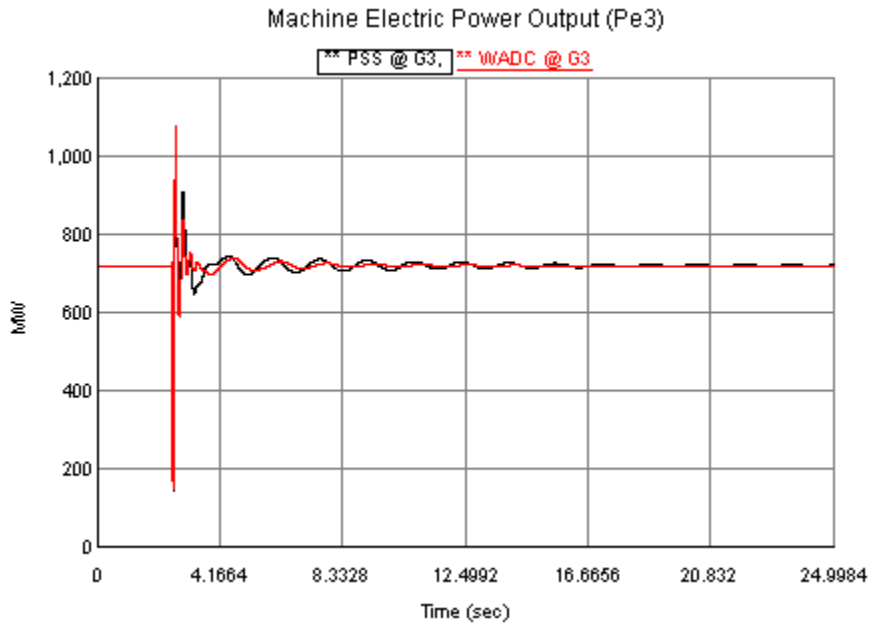


Figure 7-48: Electric power output Pe3 response with controller placed at G3 (RTDS)

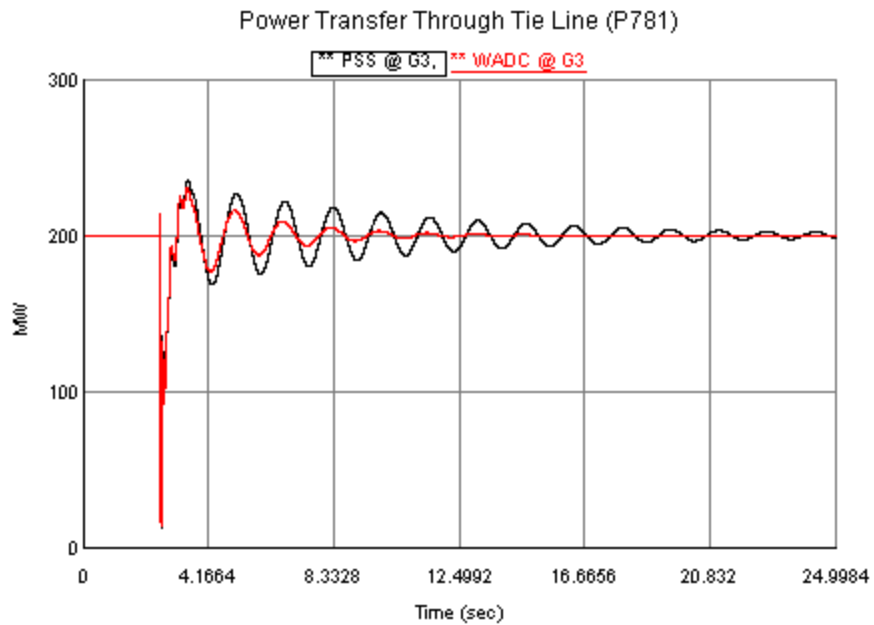


Figure 7-49: Power transfer through one of the tie lines response with controller placed at G3 (RTDS)

### 7.5.2 Using WADC Parameters Optimized By PSO Technique

The same optimized WADC parameters resulted from previous chapter is used here. The responses presented in Figure 7-50 to Figure 7-54, provide a promise results in the area of WADC parameters optimization. A slight enhancement can be notice in damping the oscillations after using optimized WADC.

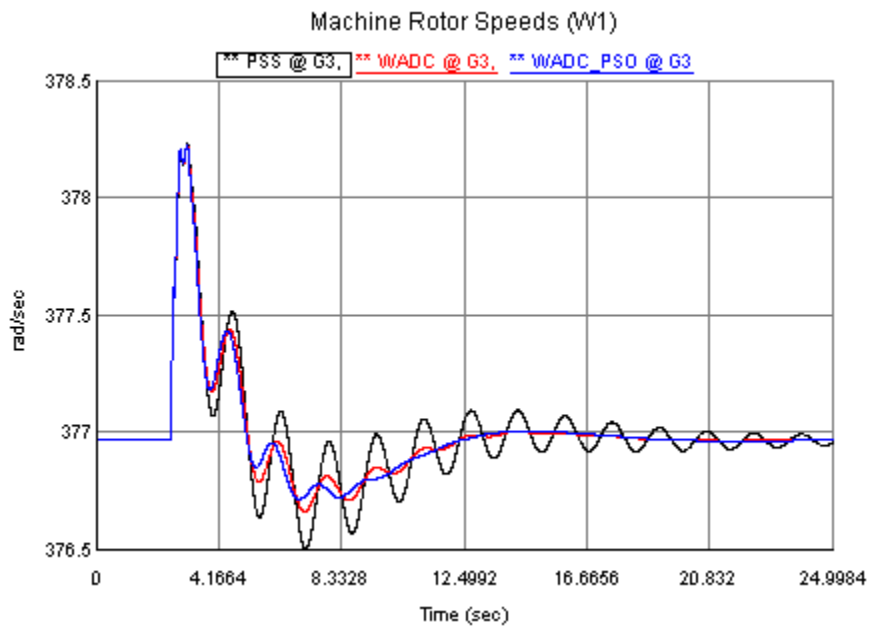


Figure 7-50: Rotor speed  $\omega_1$  response with controller placed at G3 (Optimized RTDS)



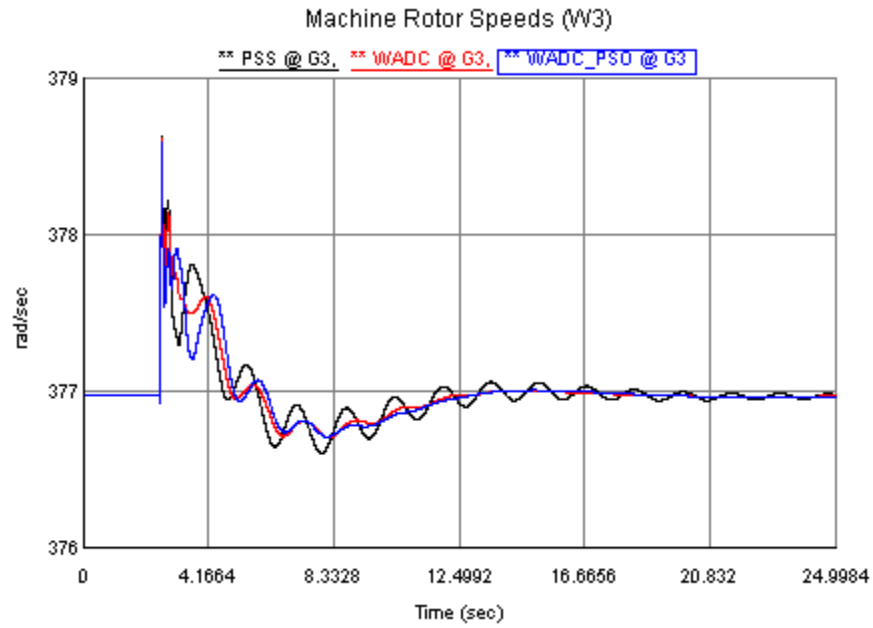


Figure 7-51: Rotor speed  $\omega_3$  response with controller placed at G3 (Optimized RTDS)

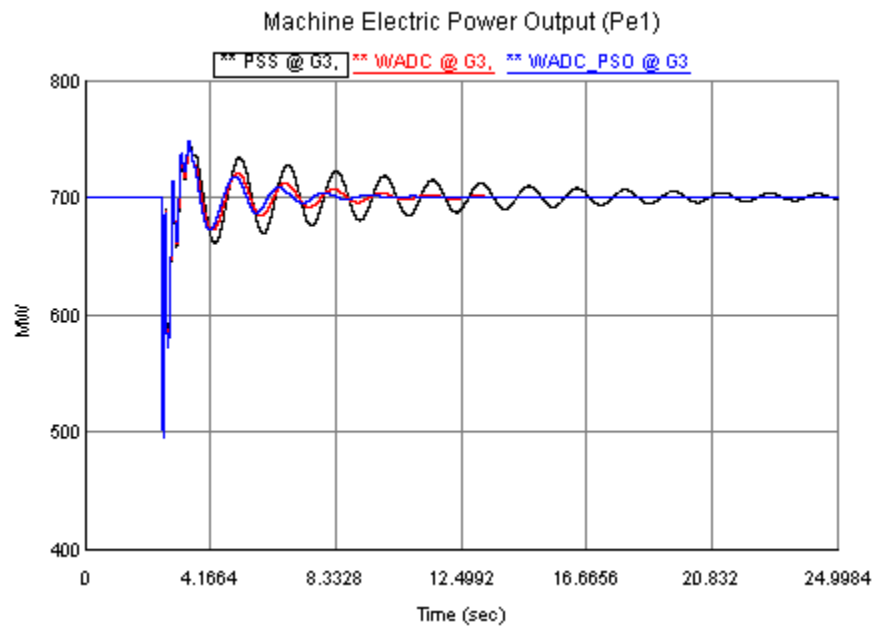


Figure 7-52: Electric power output  $P_{e1}$  response with controller placed at G3 (Optimized RTDS)

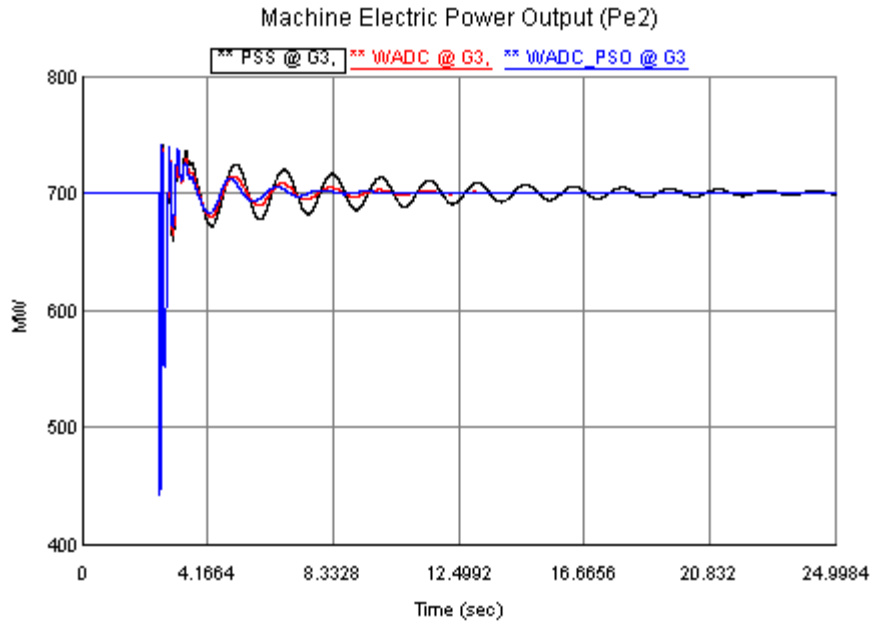


Figure 7-53: Electric power output Pe2 response with controller placed at G3 (Optimized RTDS)

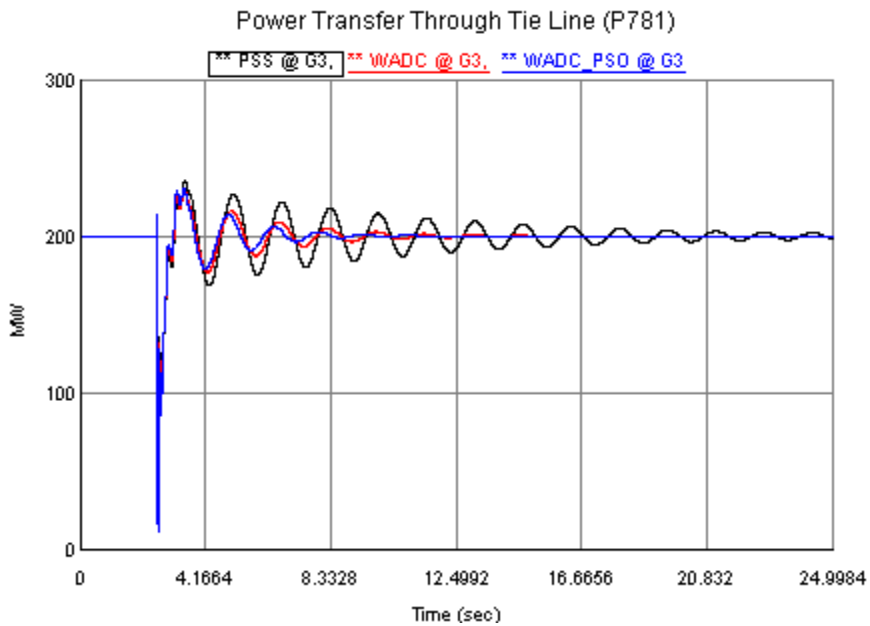


Figure 7-54: Power transfer through one of the tie lines response with controller placed at G3 (Optimized RTDS)

## **7.6 Comparison Between Simulation and RTDS Results**

In order to validate the proposed WADC design and to verify the accuracy of the system responses after applied the WADC controller, MATLAB simulations and RTDS simulations results are compared together. The previous section case is simulated here where the WADC controller is applied at G3 only. The recent PSO optimized parameters are used for both MATLAB and RTDS simulations.

Selected machines parameters are plotted for this comparison purpose as shown in Figure 7-55 to Figure 7-57. The electric power output responses of machines 1 and 3 ( $P_{e1}$  and  $P_{e3}$ ) are given in Figure 7-55 and Figure 7-56. Figure 7-57 shows the terminal voltage of machine 1 in pu. In view of the fact that the power system is modeled in very details in terms of dynamic perspective at RTDS, it can be seen that RTDS gives more practical and realistic results than the MATLAB. Although, both MATLAB Simulation and RTDS results are compatible to a certain extend.

In spite of the small difference, comparing results confirmed that the output results of the system with the proposed WADC are acceptable in terms of accuracy and correctness.

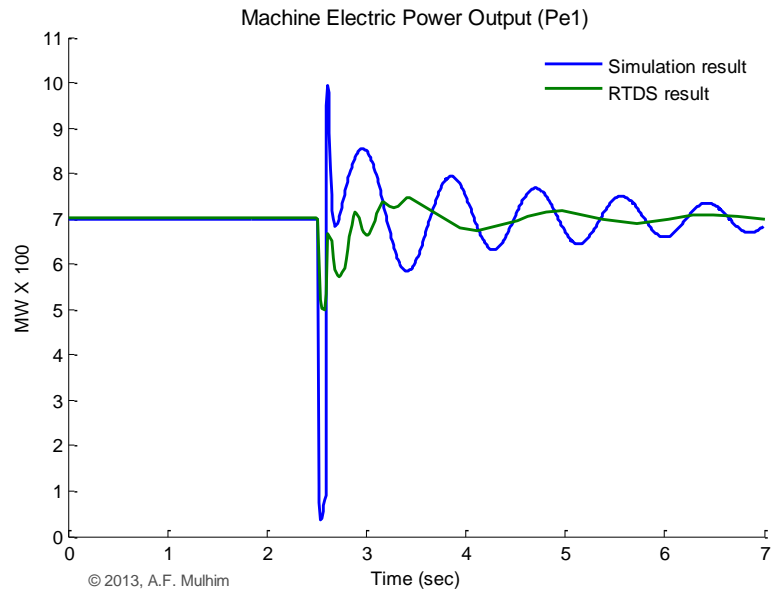


Figure 7-55: Electric power output Pe1 response with controller placed at G3 (MATLAB and RTDS)

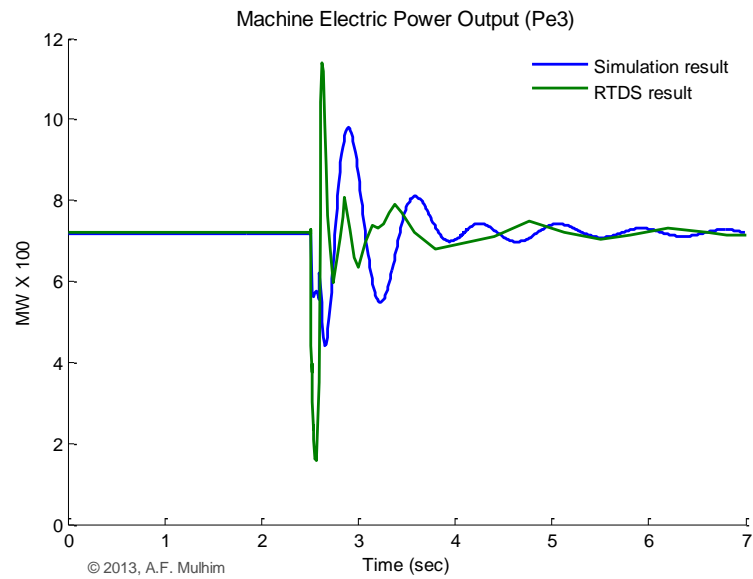


Figure 7-56: Electric power output Pe3 response with controller placed at G3 (MATLAB and RTDS)

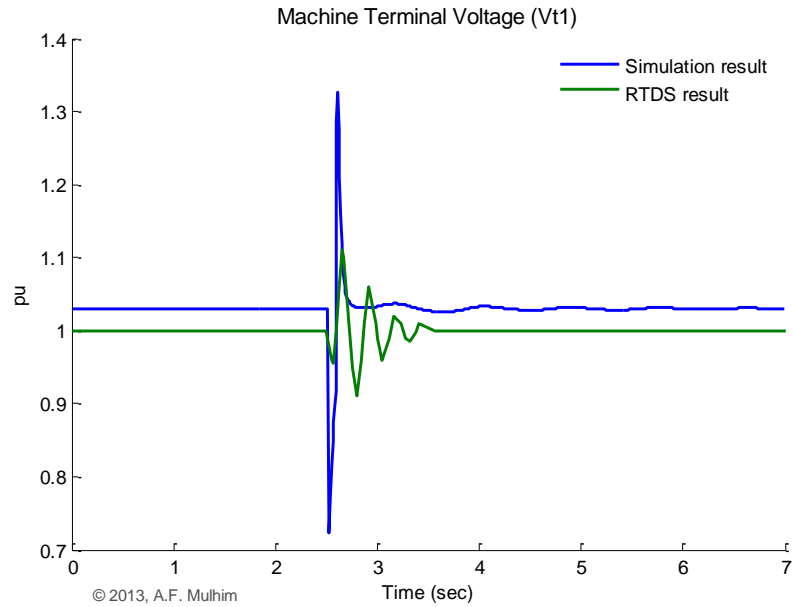


Figure 7-57: Terminal voltage  $V_{t1}$  response with controller placed at G3 (MATLAB and RTDS)

## 7.7 Summary

Real-time implementation of the system through RTDS has been presented in this chapter. The system with the proposed WADC was modeled using RSCAD/Draft module. Each component modeled dynamically using either IEEE standard models or different standard that's available in the RSCAD library.

Simulations were conducted for two different cases. The first one is when the system is subjected to transient fault (three phase fault). System responses for different control designs, confirmed that using combination of PSSs (one at each area) and WADC provide better damping characteristics comparing to the others.

The second case is for a sudden change in loads. Loosing 60 MW was simulated in this case such that the amount of MW transferred through the tie-line is reduced. Machines rotor speed responses for all control designs give almost same damping characteristic. However, the responses of machines electric power and power flow through system tie-line show that using WADC in the control system enhance the stability of the system and makes the performance of the controller more robust.

At the end of this chapter, a comparison between the local based PSS and WADC is presented for the case of the controller is applied at G3. Moreover, WADC parameters were optimized using PSO technique and results confirmed an improvement in the WADC performance. Finally, both simulations using MATLAB and RTDS are compared together and results confirmed the validity of the proposed WADC.

## **CHAPTER 8**

# **CONCLUSIONS AND FUTURE WORK**

### **8.1 Conclusions**

In this thesis, the effectiveness of wide area damping control system to enhance the power system stability has been investigated. The control system used consists mainly of the proposed WADC which based on wide area measurement signals and the conventional local based PSSs. The WADC structure used is simple lead-lag compensation block, where its stabilizing signals are measured by PMUs that are installed at different areas of the system. These measured signals are synchronized in time through GPS and transmitted via telecommunication links to the controller. The WADC was designed such that it focuses on stabilizing the interarea oscillations in the system while leaving local modes of oscillations to be controlled by local PSSs. Two-area multimachine power system was taken as a case study for this research.

The main contributions and conclusions of this research are summarized below:

- Modal analysis was carried out on the two area system and parameters including; eigenvalues, eigenvectors, PF, controllability and observability measures and residues were determined. From the analysis, two local based PSSs were concluded to be installed; one at each area. Moreover, stabilizers were located such that they provide better damping for local area oscillations and their parameters were tuned using phase compensation technique. After the local based PSSs are placed and their parameters are tuned, modal analysis of the system equipped with the stabilizers were carried out. Results show that the eigenvalues are shifted to the left side of the plan.
- To confirm that system stability is improved, a non-linear time domain simulation was conducted, where three phase short circuit is applied in the system. Simulation responses indicate that damping characteristic is improved and this confirmed the eigenvalue results.
- The WADC was designed for the purpose of enhancement the interarea mode of oscillations. Analysis was carried out to the power system to determine the best WADC location and the controller combination signals input. Based on the controllability measure corresponding to the interarea mode, it was found that G3 is the best place to locate the WADC at.
- For the controller input, the vector selection  $\mathbf{K}$  was defined to reflect the participation of the machines in the concerned interarea mode.
- After the WADC is located and their input signals combinations are selected, controller parameters were tuned using phase compensation technique.
- The performance of the designed WADC was investigated by applying three-phase short circuit at the tie-line and results show great improved in damping the inter-area mode. This can be seen from the calculated eigenvalues of the system which show that the eigenvalue corresponding to the interarea is shifted to the left side of the imaginary plan.



- The enhancement in the system stability can be also observed from the non-linear time domain simulation responses. Clearly, simulation results confirmed that applying the proposed WADC improve the damping characteristics and thus overall system stability enhanced accordingly.
- Comparing the machines mechanical parameters such as rotor angles and rotor speeds responses for the two considered control system cases; the local based control design (PSSs at G2, G3 and G4) and the WADC based control design (PSSs at G2 & G4 and WADC at G3), it can be concluded that using WADC in the control system providing more damping action than using local based PSS.
- In the experimental part of this thesis, the two area power system case study is implemented in Real-time simulator, that's RTDS. System components including; WADC and PMUs, were modeled at RSCAD/Draft module using the models available in the library. Two different cases were considered in the real-time simulation. First, when the system is subjected to fault disturbance at the tie-line (BUS 8) and the second case was simulating a sudden change in loads.
- Different controllers, that designed based on the previous chapters analysis, were considered in the simulation. System responses, for the case of applying three-phase fault at BUS8, confirmed that using combination of PSSs (one at each area) and WADC enhance the system stability and provide better damping characteristics comparing to the others. This is clear from the machines rotor speeds simulation results and the power transferred through the tie-line.
- Sudden decreased in the power transferred from area 1 to area 2 with amount of 60 MW was examined in the second case of the real-time simulation. Rotor speeds results revealed that both local based and wide-area based control designs give almost the same damping characteristics. That is because the load change is considered to be small disturbance compared to the sever three-phase short circuit. Even though, system stability enhancement can be noticed clearly from the machines electric power output responses and the responses of the power transferred through tie-line.

- PSO technique is used to optimized the proposed WADC parameters. Simulation results provide a promise results in the area of WADC parameters optimization.

## 8.2 Future Work

The research presented in this thesis study the effectiveness of WADC in improvement the damping of power system oscillations. The main objective is to design WADC using modal analysis and to implement the system with WADC in real-time simulator platform. The WADC structure used here is a simple lead-lag controller and the modal analysis was the basis of the design (WADC placement and inputs).

Although this research achieved their objectives and promising results were obtained using simple control structure and straight forward design procedure, there are many control structures and design techniques can be considered. Design includes the placement of the controller and the selection of the input signals. It mainly includes the following aspects;

- Wide area damping controller based on different control design techniques. This includes; pole placement,  $H_2/H_\infty$  approaches, linear matrix inequalities (LMI) technique, singular value decomposition ( $\mu$ -Synthesis), and others.
- Centralized/decentralized wide area control scheme for both local and inter-area damping.
- Wide area control schemes that using individual power electronics devices, such as HVDC, TCSC and SVC are very good research areas.

- Wide area damping controller parameters optimization techniques; Bacteria Foraging Optimization Algorithm (BFOA), Partial Swarm Optimization (PSO), and other heuristic search algorithms.
- Designing wide area damping controller considering the communication delays of the remote signals measured from the WAMS.
- Observability measurement in selecting the optimal input signals for the concerned oscillatory mode.
- Signal processing techniques in selecting the proper measured signals.
- Optimal PMU placement algorithms, such as dual search technique, bisecting search approach and simulated annealing method.
- Applications of wide area damping controllers in renewable systems such as photovoltaic (PV) plants and wind farms.
- Implementation of WADC on larger system with more than one tie line.

# APPENDICES

## Appendix A. 4-Machine Two Area System Data

\* The system base is 100 MVA with nominal voltage of 230 kV. Bus 1 is the slack bus.

### 1. Generators Data

Table A-1: Generator Dynamic Data

Gen.	$D$	$H$ (MW.s/MVA)	$X_d$ (pu)	$X_q$ (pu)	$X'_d$ (pu)	$X'_q$ (pu)	$T'_{do}$ (s)	$T'_{qo}$ (s)	$K_A$	$T_A$
1	0	55.575	0.2	0.19	0.033	0.061	8	0.4	200	0.01
2	0	55.575	0.2	0.19	0.033	0.061	8	0.4	200	0.01
3	0	58.5	0.2	0.19	0.033	0.061	8	0.4	200	0.01
4	0	58.5	0.2	0.19	0.033	0.061	8	0.4	200	0.01

### 2. Bus Data

Table A-2: System Bus Data

Bus no.	Type	Voltage (pu)	Angle	Generation		Load	
				P (MW)	Q (MVAR)	P (MW)	Q (MVAR)
1	1	1.03	0	0	0	0	0
2	2	1.01	0	700	0	0	0
3	2	1.03	0	719	0	0	0
4	2	1.01	0	700	0	0	0
5	3	1.00	0	0	0	0	0
6	3	1.00	0	0	0	0	0
7	3	1.00	0	0	0	967	100
8	3	1.00	0	0	0	1767	250
9	3	1.00	0	0	0	0	0
10	3	1.00	0	0	0	0	0

### 3. Transmission Lines Data

Table A-3: System Transmission Lines Data (in pu. value)

Line no.	From	To	R	X	B
1	1	5	0	0.0576	0.00
2	2	6	0	0.0625	0.00
3	3	10	0	0.0586	0.00
4	4	9	0	0.0850	0.088
5	5	6	0.0025	0.025	0.021875
6	6	7	0.001	0.01	0.00875
7	7	8	0.011	0.11	0.385
8	8	9	0.001	0.01	0.00875
9	9	10	0.0025	0.025	0.021875

### 4. Load Flow Results

Table A-4: System Load Flow Results

Bus no.	Voltage (pu)	Angle (Degree)	Generation		Load	
			P (MW)	Q (MVAR)	P (MW)	Q (MVAR)
1	1.03	0	699.94	179.56	0	0
2	1.01	-9.75	700	221.19	0	0
3	1.03	-27.15	719	169.71	0	0
4	1.01	-37.32	700	186.69	0	0
5	1.0073	-6.47	0	0	0	0
6	0.9803	-16.53	0	0	0	0
7	0.9649	-24.9	0	0	967	100
8	1.0092	-33.78	0	0	1767	250
9	0.9859	-44.06	0	0	0	0
10	0.9759	-52.43	0	0	0	0

## Appendix B. Modal Analysis Results (Base system)

### 1. System Eigenvalues:

```
-90.1250  
-89.8288  
-77.1767  
-66.1023  
-33.9804  
-23.1059  
-0.6349 + 7.4525i  
-0.6349 - 7.4525i  
-0.5275 + 7.3083i  
-0.5275 - 7.3083i  
0.1056 + 4.0179i  
0.1056 - 4.0179i  
-8.6475  
-9.1347  
0.0000 + 0.0000i  
0.0000 - 0.0000i
```

>>

### 2. System Oscillatory modes:

Eigenvalues	Damping Ratio	Freq.
0.1056 + 4.0179i	-0.0263	0.6395
-0.6349 + 7.4525i	0.0849	1.1861
-0.5275 + 7.3083i	0.0720	1.1632

>>

### 3. Participating Factors for Oscillatory modes:

```
PFmode =

    0.4913 + 0.0000i    0.0406 + 0.0000i    0.3096 + 0.0000i    0.1820
    0.4913 + 0.0000i    0.0406 + 0.0000i    0.3096 + 0.0000i    0.1820 - 0.0000i
   -0.0439 - 0.0000i   -0.0032 - 0.0000i    0.0017 + 0.0000i   -0.0000 + 0.0000i
   -0.0006 - 0.0000i   -0.0000 - 0.0000i   -0.0000 - 0.0000i    0.0000 - 0.0000i
    0.5433 + 0.0000i    0.0180 - 0.0000i    0.2899 - 0.0000i    0.2188 - 0.0000i
    0.5433 - 0.0000i    0.0180 - 0.0000i    0.2899 + 0.0000i    0.2188 - 0.0000i
   -0.1350 + 0.0000i   -0.0044 + 0.0000i   -0.0077 + 0.0000i    0.0000 - 0.0000i
    0.0029 - 0.0000i    0.0002 - 0.0000i    0.0004 + 0.0000i   -0.0000 + 0.0000i
    0.0205 - 0.0000i    0.4994 + 0.0000i    0.2286 - 0.0000i    0.2816
    0.0205 - 0.0000i    0.4994 - 0.0000i    0.2286 - 0.0000i    0.2816 - 0.0000i
   -0.0015 + 0.0000i   -0.0398 - 0.0000i   -0.0015 + 0.0000i    0.0000 + 0.0000i
    0.0000 + 0.0000i   -0.0001 - 0.0000i   -0.0004 + 0.0000i   -0.0000 - 0.0000i
    0.0379 + 0.0000i    0.5196 - 0.0000i    0.1602 + 0.0000i    0.3176 + 0.0000i
    0.0379 + 0.0000i    0.5196 + 0.0000i    0.1602 - 0.0000i    0.3176 - 0.0000i
   -0.0081 - 0.0000i   -0.1102 + 0.0000i    0.0324 + 0.0000i    0.0000 - 0.0000i
   -0.0001 - 0.0000i    0.0023 + 0.0000i   -0.0015 + 0.0000i    0.0000 + 0.0000i

>>
```

### 4. Right-Eigenvectors corresponding to Oscillatory modes:

```
>> VV(:,7:12)

ans =

    0.0150 - 0.0396i    0.0150 + 0.0396i    0.0102 - 0.0078i    0.0102 + 0.0078i   -0.0530 + 0.0914i   -0.0530 - 0.0914i
    0.0008 + 0.0004i    0.0008 - 0.0004i    0.0001 + 0.0002i    0.0001 - 0.0002i   -0.0010 - 0.0005i   -0.0010 + 0.0005i
    0.0041 + 0.0046i    0.0041 - 0.0046i    0.0004 + 0.0017i    0.0004 - 0.0017i    0.0012 + 0.0015i    0.0012 - 0.0015i
   -0.2532 + 0.1357i   -0.2532 - 0.1357i   -0.0783 - 0.0022i   -0.0783 + 0.0022i   -0.0761 + 0.0859i   -0.0761 - 0.0859i
   -0.0210 + 0.0368i   -0.0210 - 0.0368i   -0.0081 + 0.0042i   -0.0081 - 0.0042i   -0.0456 + 0.0846i   -0.0456 - 0.0846i
   -0.0007 - 0.0005i   -0.0007 + 0.0005i   -0.0001 - 0.0002i   -0.0001 + 0.0002i   -0.0009 - 0.0005i   -0.0009 + 0.0005i
   -0.0025 - 0.0160i   -0.0025 + 0.0160i    0.0021 - 0.0031i    0.0021 + 0.0031i    0.0007 - 0.0060i    0.0007 + 0.0060i
    0.9304              0.9304              0.1586 + 0.1399i    0.1586 - 0.1399i    0.1763 + 0.0600i    0.1763 - 0.0600i
    0.0014 + 0.0092i    0.0014 - 0.0092i    0.0189 - 0.0448i    0.0189 + 0.0448i    0.0226 - 0.0744i    0.0226 + 0.0744i
   -0.0002 + 0.0000i   -0.0002 - 0.0000i    0.0008 + 0.0004i    0.0008 - 0.0004i    0.0008 + 0.0002i    0.0008 - 0.0002i
   -0.0008 - 0.0007i   -0.0008 + 0.0007i    0.0040 + 0.0050i    0.0040 - 0.0050i    0.0056 - 0.0092i    0.0056 + 0.0092i
    0.0513 - 0.0199i    0.0513 + 0.0199i   -0.2622 + 0.1150i   -0.2622 - 0.1150i    0.3262 + 0.0868i    0.3262 - 0.0868i
    0.0002 - 0.0111i    0.0002 + 0.0111i   -0.0226 + 0.0411i   -0.0226 - 0.0411i    0.0226 - 0.0487i    0.0226 + 0.0487i
    0.0002 + 0.0000i    0.0002 - 0.0000i   -0.0008 - 0.0005i   -0.0008 + 0.0005i    0.0005 + 0.0002i    0.0005 - 0.0002i
    0.0032 + 0.0021i    0.0032 - 0.0021i   -0.0024 - 0.0164i   -0.0024 + 0.0164i    0.0027 - 0.0267i    0.0027 + 0.0267i
   -0.1391 + 0.1594i   -0.1391 - 0.1594i    0.9284              0.9284              0.8989              0.8989
```

## 5. Left-Eigenvectors corresponding to Oscillatory modes:

```

1.0e+002 *

Columns 1 through 7

    0.0252 + 0.0525i    2.5298 - 1.4897i    -0.0135 + 0.0356i    -0.0000 + 0.0000i    -0.0265 - 0.0587i    -2.8323 + 1.5817i    0.0156 - 0.0397i
    0.0252 - 0.0525i    2.5298 + 1.4897i    -0.0135 - 0.0356i    -0.0000 - 0.0000i    -0.0265 + 0.0587i    -2.8323 - 1.5817i    0.0156 + 0.0397i
    0.0130 + 0.0089i    0.4088 - 0.7016i    0.0007 + 0.0096i    0.0000 + 0.0000i    -0.0075 - 0.0070i    -0.3335 + 0.4124i    -0.0001 - 0.0071i
    0.0130 - 0.0089i    0.4088 + 0.7016i    0.0007 - 0.0096i    0.0000 - 0.0000i    -0.0075 + 0.0070i    -0.3335 - 0.4124i    -0.0001 + 0.0071i
    -0.0060 - 0.0134i    -1.2741 + 0.5333i    0.0049 - 0.0019i    0.0000 - 0.0000i    -0.0076 - 0.0130i    -1.2417 + 0.6793i    0.0072 - 0.0072i
    -0.0060 + 0.0134i    -1.2741 - 0.5333i    0.0049 + 0.0019i    0.0000 + 0.0000i    -0.0076 + 0.0130i    -1.2417 - 0.6793i    0.0072 + 0.0072i

Columns 8 through 14

    0.0000 - 0.0001i    0.0018 - 0.0109i    -0.5558 - 0.0439i    0.0057 - 0.0040i    0.0000 - 0.0000i    -0.0005 + 0.0170i    0.8583 - 0.0480i
    0.0000 + 0.0001i    0.0018 + 0.0109i    -0.5558 + 0.0439i    0.0057 + 0.0040i    0.0000 + 0.0000i    -0.0005 - 0.0170i    0.8583 + 0.0480i
    -0.0000 - 0.0000i    0.0201 + 0.0473i    2.3524 - 1.2078i    -0.0131 + 0.0290i    -0.0000 + 0.0000i    -0.0256 - 0.0492i    -2.4277 + 1.4969i
    -0.0000 + 0.0000i    0.0201 - 0.0473i    2.3524 + 1.2078i    -0.0131 - 0.0290i    -0.0000 - 0.0000i    -0.0256 + 0.0492i    -2.4277 - 1.4969i
    0.0000 - 0.0000i    0.0061 + 0.0135i    1.2817 - 0.5394i    -0.0048 + 0.0021i    -0.0000 + 0.0000i    0.0075 + 0.0130i    1.2340 - 0.6732i
    0.0000 + 0.0000i    0.0061 - 0.0135i    1.2817 + 0.5394i    -0.0048 - 0.0021i    -0.0000 - 0.0000i    0.0075 - 0.0130i    1.2340 + 0.6732i

Columns 15 through 16

    -0.0075 + 0.0077i    -0.0000 + 0.0000i
    -0.0075 - 0.0077i    -0.0000 - 0.0000i
    0.0122 - 0.0318i    0.0000 - 0.0000i
    0.0122 + 0.0318i    0.0000 + 0.0000i
    -0.0069 + 0.0068i    -0.0000 + 0.0000i
    -0.0069 - 0.0068i    -0.0000 - 0.0000i
>>

```

## 6. Controllability measure corresponding to Oscillatory modes:

```

CMode =

    -54.3628 - 0.0000i    63.2136 - 0.0000i    26.9411 - 0.0000i    -34.7979 - 0.0000i
         7.0991 + 0.0000i    -3.2444 + 0.0000i    -55.0807 + 0.0000i    49.1388 + 0.0000i
    23.8768 + 0.0000i    34.6392 + 0.0000i    -23.4653 + 0.0000i    -32.9635 + 0.0000i
         1.2069 + 0.0000i    -4.3095                1.2663                -2.2508

>>

```

## 7. Observability measure corresponding to Oscillatory modes:

```

OBmode =

    0.0015    0.0003   -0.0020   -0.0000
   -0.0014   -0.0001   -0.0018    0.0000
   -0.0004    0.0017    0.0016   -0.0000
    0.0004   -0.0015    0.0011    0.0000

>>

```



8. Residue measure corresponding to Local area Oscillatory modes:

```

Mode #

ans =

    7

res =

-0.0539 + 0.0594i    0.0611 - 0.0659i    0.0142 - 0.0035i    -0.0207 + 0.0092i
 0.0625 - 0.0504i   -0.0707 + 0.0557i   -0.0146 + 0.0013i    0.0219 - 0.0059i
 0.0039 - 0.0172i   -0.0046 + 0.0192i   -0.0023 + 0.0022i    0.0030 - 0.0040i
-0.0081 + 0.0194i    0.0093 - 0.0217i    0.0032 - 0.0021i   -0.0043 + 0.0041i

Mode #

ans =

    9

res =

-0.0045 + 0.0040i    0.0035 - 0.0028i   -0.0194 + 0.0045i    0.0205 - 0.0061i
 0.0036 - 0.0022i   -0.0028 + 0.0015i    0.0141 - 0.0007i   -0.0150 + 0.0017i
-0.0073 + 0.0216i    0.0062 - 0.0155i   -0.0553 + 0.0511i    0.0558 - 0.0583i
 0.0091 - 0.0200i   -0.0075 + 0.0143i    0.0581 - 0.0436i   -0.0593 + 0.0504i

```

## Appendix C. Modal Analysis Results (to Design WADC)

### 1. System Eigenvalues:

```
-91.5806  
-91.2473  
-78.2280  
-69.0443  
-26.5106  
-19.2184  
-11.4135 +10.6782i  
-11.4135 -10.6782i  
-9.7699 +11.7590i  
-9.7699 -11.7590i  
-1.8930 + 6.2886i  
-1.8930 - 6.2886i  
-2.1751 + 5.7087i  
-2.1751 - 5.7087i  
-0.5507 + 4.0233i  
-0.5507 - 4.0233i  
-6.8359 + 0.0371i  
-6.8359 - 0.0371i  
-1.0933  
-0.1011  
0.0000  
-0.0000  
-0.1852  
-50.0000  
-0.1000  
-0.1852  
-50.0000  
-0.1000
```

```
>>
```

## 2. System Oscillatory modes:

Eigenvalues	Damping Ratio	Freq.
-11.4135 +10.6782i	0.7302	1.6995
-9.7699 +11.7590i	0.6391	1.8715
-1.8930 + 6.2886i	0.2882	1.0009
-2.1751 + 5.7087i	0.3560	0.9086
-0.5507 + 4.0233i	0.1356	0.6403
-6.8359 + 0.0371i	1.0000	0.0059

## 3. Participating Factors for Oscillatory modes:

PFmode =

-0.0572 + 0.0000i	-0.0272 - 0.0000i	0.4161 + 0.0000i	0.2565 + 0.0000i	0.2724 - 0.0000i	-0.0014 - 0.0000i
-0.0572 - 0.0000i	-0.0272 - 0.0000i	0.4161 + 0.0000i	0.2565 - 0.0000i	0.2724 - 0.0000i	-0.0014 + 0.0000i
-0.0930 - 0.0000i	-0.0086 + 0.0000i	-0.1303 - 0.0000i	-0.1315 + 0.0000i	0.0322 - 0.0000i	0.1044 - 0.0000i
0.0761 + 0.0000i	0.0218 - 0.0000i	0.0022 + 0.0000i	0.0041 - 0.0000i	-0.0009 + 0.0000i	-0.0078 + 0.0000i
-0.0660 + 0.0000i	-0.0540 + 0.0000i	0.2593 - 0.0000i	0.3253 + 0.0000i	0.2940 - 0.0000i	0.0025 - 0.0000i
-0.0660 + 0.0000i	-0.0540 - 0.0000i	0.2593 - 0.0000i	0.3253 + 0.0000i	0.2940 - 0.0000i	0.0025 - 0.0000i
0.6691 - 0.0000i	0.5510 - 0.0000i	-0.1315 + 0.0000i	-0.1427 - 0.0000i	-0.1088 + 0.0000i	0.1847 + 0.0000i
-0.1100 + 0.0000i	-0.0667 + 0.0000i	0.0134 - 0.0000i	0.0213 + 0.0000i	-0.0018 - 0.0000i	-0.0138 - 0.0000i
-0.0464 - 0.0000i	-0.0439 + 0.0000i	0.3405 + 0.0000i	0.2675	0.2668 - 0.0000i	-0.0014 + 0.0000i
-0.0464 + 0.0000i	-0.0439 + 0.0000i	0.3405 + 0.0000i	0.2675 + 0.0000i	0.2668 + 0.0000i	-0.0014 - 0.0000i
0.0729 - 0.0000i	0.0039 - 0.0000i	-0.1031 - 0.0000i	-0.1144 - 0.0000i	0.0077 + 0.0000i	0.0930 + 0.0000i
0.0369 + 0.0000i	0.0345 - 0.0000i	0.0028 + 0.0000i	0.0037 + 0.0000i	-0.0008 - 0.0000i	-0.0069 - 0.0000i
-0.0316 - 0.0000i	-0.0821 - 0.0000i	0.2168 - 0.0000i	0.4279 + 0.0000i	0.0997 + 0.0000i	0.0140 - 0.0000i
-0.0316 + 0.0000i	-0.0821 - 0.0000i	0.2168 - 0.0000i	0.4279 - 0.0000i	0.0997 + 0.0000i	0.0140 + 0.0000i
0.4116 - 0.0000i	0.7552 + 0.0000i	-0.1136 + 0.0000i	-0.2297 + 0.0000i	0.0141 - 0.0000i	0.1535 - 0.0000i
-0.0693 - 0.0000i	-0.0883 - 0.0000i	0.0088 - 0.0000i	0.0206 - 0.0000i	-0.0036 - 0.0000i	-0.0113 + 0.0000i
0	0	0	0	0	0
0	0	0	0	0	0
0	0	0	0	0	0
-0.2481 - 0.0000i	-0.1716 + 0.0000i	-0.0101 + 0.0000i	-0.1051 - 0.0000i	0.1699 + 0.0000i	0.2145 + 0.0000i
0.2110 + 0.0000i	0.0855 - 0.0000i	0.1084 - 0.0000i	0.1920 + 0.0000i	0.0273 - 0.0000i	0.3972 + 0.0000i
0.8709 - 0.0000i	0.6009 + 0.0000i	-0.1125 + 0.0000i	-0.0996 + 0.0000i	-0.0827 + 0.0000i	0.1190 + 0.0000i
0	0	0	0	0	0
0	0	0	0	0	0
0	0	0	0	0	0
-0.1587 - 0.0000i	-0.2225 + 0.0000i	0.0163 + 0.0000i	-0.0381 + 0.0000i	0.1196 - 0.0000i	0.2065 - 0.0000i
0.1281 + 0.0000i	0.1534 - 0.0000i	0.0891 - 0.0000i	0.2101 - 0.0000i	0.0032 + 0.0000i	0.4085 - 0.0000i
0.6048 - 0.0000i	0.7660 - 0.0000i	-0.1053 + 0.0000i	-0.1453 + 0.0000i	-0.0412 - 0.0000i	0.1308 - 0.0000i

>>

#### 4. Controllability measure:

CO =

1.0e+006 \*

-0.0089 + 0.0000i	0.0127 + 0.0000i	0.0089 + 0.0000i	-0.0129 + 0.0000i
0.0092 + 0.0000i	-0.0097 + 0.0000i	0.0112 + 0.0000i	-0.0137 + 0.0000i
-0.0144 - 0.0000i	-0.0128 - 0.0000i	0.0148 - 0.0000i	0.0133 - 0.0000i
0.0191 - 0.0000i	0.0190 - 0.0000i	0.0152 - 0.0000i	0.0166 - 0.0000i
0.0089 + 0.0000i	0.0053 + 0.0000i	0.0098 + 0.0000i	0.0060 + 0.0000i
0.0050 - 0.0000i	0.0015 - 0.0000i	-0.0055 - 0.0000i	-0.0015 - 0.0000i
0.0003 - 0.0017i	-0.0018 + 0.0010i	0.0013 - 0.0007i	-0.0016 - 0.0003i
0.0003 + 0.0017i	-0.0018 - 0.0010i	0.0013 + 0.0007i	-0.0016 + 0.0003i
0.0005 + 0.0008i	0.0003 - 0.0017i	0.0003 - 0.0010i	-0.0013 + 0.0013i
0.0005 - 0.0008i	0.0003 + 0.0017i	0.0003 + 0.0010i	-0.0013 - 0.0013i
0.0002 - 0.0002i	-0.0002 + 0.0001i	0.0002 - 0.0000i	-0.0002 - 0.0000i
0.0002 + 0.0002i	-0.0002 - 0.0001i	0.0002 + 0.0000i	-0.0002 + 0.0000i
-0.0002 + 0.0002i	0.0003 - 0.0000i	0.0003 - 0.0000i	-0.0003 - 0.0001i
-0.0002 - 0.0002i	0.0003 + 0.0000i	0.0003 + 0.0000i	-0.0003 + 0.0001i
0.0000 - 0.0000i	-0.0000 - 0.0001i	-0.0000 + 0.0000i	0.0000 + 0.0001i
0.0000 + 0.0000i	-0.0000 + 0.0001i	-0.0000 - 0.0000i	0.0000 - 0.0001i
-0.0002 - 0.0001i	0.0002 + 0.0001i	0.0000 - 0.0002i	-0.0000 + 0.0003i
-0.0002 + 0.0001i	0.0002 - 0.0001i	0.0000 + 0.0002i	-0.0000 - 0.0003i
0.0000 + 0.0000i	0.0000 + 0.0000i	0.0000 + 0.0000i	0.0000 + 0.0000i
0.0000 + 0.0000i	-0.0000 + 0.0000i	-0.0000 + 0.0000i	0.0000 + 0.0000i
-1.9350 - 0.0000i	-9.9063 - 0.0000i	-1.8088 - 0.0000i	-8.8515 - 0.0000i
1.9350 + 0.0000i	9.9062 + 0.0000i	1.8088 + 0.0000i	8.8515 + 0.0000i
0	0	0	0
0	0	0	0
0	0	0	0
0	0	0	0
0	0	0	0
0	0	0	0

>>

## Appendix D. RTDS Power System Components Parameters

### 1. Synchronous Generator with Embedded Transformer:

\* Based on generator rated MVA (900 MVA)

Table D-1: Generator parameters

Parameter	Description	Value*
H	Inertia Constant	6.175 MWs/MVA
D	Synchronous Mechanical Damping	0 pu/pu
Xa	Stator Leakage Reactance	0.2 pu
Xd	D-axis: Unsaturated Reactance	1.8 pu
Xd'	D: Unsaturated Transient Reactance	0.3 pu
Xd''	D: Unsaturated Sub-Trans. Reactance	0.25 pu
Gfld	D: Real Component of Transfer Admit.	100.0 pu
Bfld	D: Imag Component of Transfer Admit.	100.0 pu
Xq	Q-axis Unsaturated Reactance	1.7 pu
Xq'	Q: Unsaturated Transient Reactance	0.55 pu
Xq''	Q: Unsaturated Sub-Trans. Reactance	0.25 pu
Ra	Stator Resistance	0.0025 pu
Tdo'	D: Unsat. Transient Open T Const.	8 sec
Tdo''	D: Unsat. Sub-Trans. Open T Const.	0.03 sec
Tqo'	Q: Unsat. Transient Open T Const.	0.4 sec
Tqo''	Q: Unsat. Sub-Trans. Open T Const.	0.05 sec

Table D-2: Transformer parameters

Parameter	Description	Value*
vtpri	Transformer Primary L-L RMS kV	230 kV
vtsec	Transformer Secondary L-L RMS kV	20 kV
dlagp	Delta Leads or Lags Primary 30 Deg.	Lags
TMVA	Transformer MVA rating	900 MVA
trpos	Positive Sequence Resistance:	0.0 pu
txpos	Positive Sequence Reactance:	0.15 pu
itzro	Is there a TRF zero sequence path ?	Yes
trzro	-- Zero Sequence Resistance:	0.0 pu
txzro	-- Zero Sequence Reactance:	0.1 pu
tloss	Shunt Conductance at TRF Primary:	0.0001 pu

2. IEEE Type 1 Speed Governor:

Table D-3: Speed governor parameters

Parameter	Description	Value
K	Constant K	20.000000
T1	Time Constant T1	0.01 sec
T2	Time Constant T2	0.001 sec
T3	Time Constant T3	0.025 sec
Uo	Upper Rate Limit	0.114 pu/sec
Uc	Lower Rate Limit	-1.139 pu/sec
Pmx	Upper Limit Pmax	1.07 pu
Pmn	Lower Limit Pmin	0.0000 pu
T4	Time Constant T4	0 sec
K1	Constant K1	0
K2	Constant K2	0.000000
T5	Time Constant T5	0.2 sec
K3	Constant K3	0.3
K4	Constant K4	0.000000
T6	Time Constant T6	6 sec
K5	Constant K5	0.3
K6	Constant K6	0.000000
T7	Time Constant T7	0.4 sec
K7	Constant K7	0.4
K8	Constant K8	0.000000

### 3. IEEE Type AC4 Excitation System:

Table D-4: Exciter parameters

Parameter	Description	Value
Gen	Generator Name	GEN1
Mon	Monitor Internal Variable	No
PSS	Include Stabalizer Input?	Yes
Vbs	Bus Voltage Input source	Vpu
Vb	Rated RMS Phase Voltage	11.548 kV
Vi	Initial Terminal Voltage	1.0 pu
Tr	Time Constant Tr	0.01 sec
Vimx	Maximum Limit Vi max	1.2 pu
Vimn	Minimum Limit Vi min	-1.2 pu
Tc	Lead Time Constant Tc	0 sec
Tb	lag Time Constant Tb	0 sec
Ka	Gain Ka	200
Ta	Time Constant Ta	0 sec
Vrmx	Maximum Limit Vr max	999 pu
Vrmn	Minimum Limit Vr min	-999 pu
Kc	Constant Kc	0
prtyp	Solve Model on card type:	GPC
Proc	Assigned Controls Processor	1
Pri	Priority Level	18

#### 4. IEEE Type ST PSSs:

Table D-5: PSS2 parameters

Parameter	Description	Value
Gen	Generator Name	GEN2
Mon	Monitor Internal Variable?	No
IC	Input Signal	w
HTZ	Generator Base angular Frequency	60.0 Hz
MVA	Generator MVA	900 MVA
Vbs	Bus Voltage Input source	Vpu
Vrate	Rated l-l rms bus voltage for 3 Phase	20
A1	Filter Constant A1	0
A2	Filter Constant A2	0
A3	Filter Constant A3	0
A4	Filter Constant A4	0
A5	Filter Constant A5	0
A6	Filter Constant A6	0
T1	Lead Time Constant T1 (1st leadlag)	0.1885 sec
T2	Lag Time Constant T2 (1st leadlag)	0.0955 sec
T3	Lead Time Constant T3 (2nd leadlag)	0.1885 sec
T4	Lag Time Constant T4 (2nd leadlag)	0.0955 sec
T5	Time Constant T5 (washout)	10 sec
T6	Time Constant T6 (washout)	10 sec
Ks	Gain (washout)	10.66
UL	Maximum Limit Lsmax	0.2 pu
LL	Minimum Limit Lsmin	-0.2 pu
Vcu	Output limiter Upper Limit	1.2 pu
Vcl	Output limiter Lower Limit	0.2 pu
prtyp	Solve Model on card type:	GPC
Proc	Assigned Controls Processor	1
Pri	Priority Level	21



Table D-6: PSS3 parameters

Parameter	Description	Value
Gen	Generator Name	GEN3
Mon	Monitor Internal Variable?	No
IC	Input Signal	w
HTZ	Generator Base angular Frequency	60.0 Hz
MVA	Generator MVA	900 MVA
Vbs	Bus Voltage Input source	Vpu
Vrate	Rated I-I rms bus voltage for 3 Phase	20
A1	Filter Constant A1	0
A2	Filter Constant A2	0
A3	Filter Constant A3	0
A4	Filter Constant A4	0
A5	Filter Constant A5	0
A6	Filter Constant A6	0
T1	Lead Time Constant T1 (1st leadlag)	0.3492 sec
T2	Lag Time Constant T2 (1st leadlag)	0.1769 sec
T3	Lead Time Constant T3 (2nd leadlag)	0.3492 sec
T4	Lag Time Constant T4 (2nd leadlag)	0.1769 sec
T5	Time Constant T5 (washout)	10 sec
T6	Time Constant T6 (washout)	10 sec
Ks	Gain (washout)	13.23
UL	Maximum Limit Lsmax	0.2 pu
LL	Minimum Limit Lsmin	-0.2 pu
Vcu	Output limiter Upper Limit	1.2 pu
Vcl	Output limiter Lower Limit	0.2 pu
prtyp	Solve Model on card type:	GPC
Proc	Assigned Controls Processor	1
Pri	Priority Level	35

Table D-7: PSS4 parameters

Parameter	Description	Value
Gen	Generator Name	GEN4
Mon	Monitor Internal Variable?	No
IC	Input Signal	w
HTZ	Generator Base angular Frequency	60.0 Hz
MVA	Generator MVA	900 MVA
Vbs	Bus Voltage Input source	Vpu
Vrate	Rated I-I rms bus voltage for 3 Phase	20
A1	Filter Constant A1	0
A2	Filter Constant A2	0
A3	Filter Constant A3	0
A4	Filter Constant A4	0
A5	Filter Constant A5	0
A6	Filter Constant A6	0
T1	Lead Time Constant T1 (1st leadlag)	0.1961 sec
T2	Lag Time Constant T2 (1st leadlag)	0.0955 sec
T3	Lead Time Constant T3 (2nd leadlag)	0.1961 sec
T4	Lag Time Constant T4 (2nd leadlag)	0.0955 sec
T5	Time Constant T5 (washout)	10 sec
T6	Time Constant T6 (washout)	10 sec
Ks	Gain (washout)	11.68
UL	Maximum Limit Lsmax	0.2 pu
LL	Minimum Limit Lsmin	-0.2 pu
Vcu	Output limiter Upper Limit	1.2 pu
Vcl	Output limiter Lower Limit	0.2 pu
prtyp	Solve Model on card type:	GPC
Proc	Assigned Controls Processor	1
Pri	Priority Level	27

5. Load Model:

Table D-8: Load parameters

Parameter	Description	Value	
		Load 7	Load 8
name	Component Name	RLDload7	RLDload8
type	Type of Load	RX	RX
btype	R & X in parallel ?	R//X	R//X
cc	P & Q Controlled by	Slider	Slider
gnd	Include Neutral Connection Point?	Yes	Yes
Vmeas	Bus Voltage Measurement	Internal	Internal
Vbus	Rated Line to Line Bus Voltage	230	230
Vmin	Minimum Bus Voltage(L-L)	0.8	0.8
constF	Assume Constant Freq	Yes	Yes
freq	Base Frequency	60	60
T	Time Constant for setting R, X values	0.01	0.01
Tm	Time Constant for measuring Vbus	0.003	0.003
Pinit	Initial Real Power	967	1767
Pmin	Minimum Real Power	0.1	0.1
Pmax	Maximum Real Power	1000	2000
Qinit	Initial Reactive Power	-100	-250
Qmin	Minimum Reactive Power	-200	-250
Qmax	Maximum Reactive Power	1000	1000
prtyp	Type of Processor Card	GPC	GPC

6. Transmission Line Model:

Table D-9: Trnsmission line data

Parameter	Value (in pu)					
	With base of 100 MVA and 230 kV					
	TL109	TL56	TL67	TL781	TL782	TL98
Number of Phases	3	3	3	3	3	3
Positive Seq. Series Resistance	0.0025	0.0025	0.001	0.022	0.022	0.0010
Positive Seq. Series Ind. React	0.025	0.025	0.01	0.22	0.22	0.01
Positive Seq. Shunt Cap. React	22.85	22.85	57.14	2.597	2.597	57.14
Zero Seq. Series Resistance	0.0025	0.0025	0.001	0.022	0.022	0.001
Zero Seq. Series Ind. React	0.075	0.075	0.03	0.66	0.66	0.03
Zero Seq. Shunt Cap. React	69.0	69.0	171.0	8.0	8.0	171.0

## BIBLIOGRAPHY

- [1] Prasertwong, K., Mithulanathan, N. and Thakur, D. (2010) "Understanding low frequency oscillation in power systems", *International Journal of Electrical Engineering Education*, vol. 47, 3: 248-262.
- [2] P. Kundur. *Power System Control and Stability*, New York: McGraw-Hill, Inc., 1994,
- [3] M. Aboul-Ela, A. Sallam, J. McCalley, and A. Fouad, "Damping controller design for power system oscillations using global signals," *IEEE Trans. Power Syst.*, vol. 11, pp. 767–773, May 1996.
- [4] S. Ray, G.K. Venayagamoorthy, "A wide area measurement based neurocontrol for generation excitation systems." *Engineering Applications of Artificial Intelligence* 22 (2009) 473–481.
- [5] A. G. Phadke, "Synchronized phasor measurements - a historical overview," In *Proc. IEEE/PES Transmission and Distribution Conference and Exhibition*, pp. 416-479, 2002.
- [6] Yuwa Chompoobutrgool, Luigi Vanfretti and Mehrdad Ghandhari," Survey on Power System Stabilizers Control and their Prospective Applications for Power System Damping using Synchrophasor-Based Wide-Area Systems," *European Transactions on Electrical Power*, Volume 21, Issue 8, pages 2098–2111, November 2011.
- [7] J. Chow, J. Sanchez-Gasca, H. Ren, and S. Wang, "Power system damping controller design using multiple input signals," *IEEE Control Syst. Mag.*, pp. 82–90, August 2000.
- [8] I. Kamwa, L. Gerin-Lajoie, and G. Trudel, "Multi-loop power system stabilizers using wide-area synchronous phasor measurements," *Proc. American Control Conference*, pp. 2963–2967, June 1998.
- [9] I. Kamwa, R. Grondin, and Y. Hebert, "Wide-Area Measurement based stabilizing control of large power systems - A decentralized/hierarchical approach," *IEEE Trans. Power Syst.*, vol. 16, no. 1, pp. 136–153, 2001.
- [10] I. Kamwa, A. Heniche, G. Trudel, M. Dobrescu, R. Grondin, and D. Lefebvre, "Assessing the technical value of FACTS-based wide-area damping control loops," *IEEE Power Eng. Soc. General Meeting*, 2005.
- [11] B. Pal and B. Chaudhuri. *Robust Control in Power Systems*, Springer Inc. New York, 2005.

- [12] G. Rogers, Power System Oscillations. Kluwer Academic Publishers Group, 2000.
- [13] S. Y. Sun, H.C. Shu and J.Dong, et al, "Analysis of low frequency oscillation mode based on PMU and Prony method," in Proc Electric Power Conference, 2008 pp. 1-4.
- [14] K. Mei, S.M. Rovnyak, C.M. Ong, "Dynamic Event Detection Using Wavelet Analysis", IEEE Power Engineering Society General Meeting, Montreal, Canada, 2006,
- [15] J. Sanchez-Gasca and J. Chow, "Performance comparison of three identification methods for the analysis of electromechanical oscillations," IEEE Trans. Power Syst., vol. 14, no. 3, pp. 995–1002, August 1999.
- [16] Tripath, P.; Srivastava, S.C.; Singh, S.N., "An improved Prony method for identifying low frequency oscillations using synchro-phasor measurements," ICEET, vol. 2, pp. 19-22, 2009.
- [17] K.M. EL-Naggar, "On-line measurement of low-frequency oscillations in power systems," Measurement, Volume 42, Issue 5, Pages 716-721, June 2009.
- [18] Samir Avdakovic, Amir Nuhanovic, Mirza Kusljugic, Mustafa Music, "Wavelet transform applications in power system dynamics," Electric Power Systems Research, Volume 83, Issue 1, February 2012, Pages 237-245.
- [19] M. A. Abido, "Analysis and assessment of STATCOM-Based damping stabilizers for power system stability enhancement" Electric Power Systems Research, Vol. 73, No. 2, February 2005, pp. 177-185.
- [20] Abdul-Malek, M.A.; Abido, M.A., "STATCOM based controller design using Particle Swarm Optimization for power system stability enhancement," IEEE International Symposium on Industrial Electronics (ISIE 2009), Seoul, Korea July 5-8, 2009, pp.1218 1223.
- [21] P. M. Anderson and A. A. Fouad, Power System Control and Stability. Ames, IA: Iowa State Univ. Press, 1977.
- [22] L. Rouco, "Eigenvalue-based Method for Analysis and Control of Power System Oscillations," IEE Colloquium on Power System Dynamics Stabilisation (Digest No. 1998/196 and 1998/278), Feb. 1998.
- [23] Ye Yuan; Yuanzhang Sun; Lin Cheng, "Determination of wide-area PSS locations and feedback signals using improved residue matrices," IEEE Asia Pacific Conference on Circuits and Systems, APCCAS 2008, pages 762 – 765.

- [24] Feng Xiao; Yuanzhang Sun; Fang Yang; Lin Cheng, "Inter-area damping controller design based on mode controllability and observability," International Power Engineering Conference, IPEC 2007, pages 95 – 99.
- [25] Ba-muqabel, A.A., and Abido, M.A., " Review of Conventional Power System Stabilizer Design Methods, " 2006 IEEE GCC Conference (GCC), 20-22 March.
- [26] Yang Zhang and Bose, A., "Design of Wide-Area Damping Controllers for Interarea Oscillations," IEEE TRANSACTIONS ON POWER SYSTEMS, VOL. 23, NO. 3, AUGUST 2008.
- [27] A. G. Phadke and J. S. Thorp, Synchronized Phasor Measurements and Their Applications, New York: Springer, 2008.
- [28] Li Peng, Wu Xiaochen, Lu Chao, Shi Jinghai, Hu Jiong, He Jingbo, Zhao Yong and Xu Aidong, "Implementation of CSG's Wide-Area Damping Control System: Overview and experience," Power Systems Conference and Exposition, 2009. PSCE '09. IEEE/PES, pp. 1-9, 15-18 March.
- [29] Chow JH (1988), "A pole-placement design approach for systems with multiple operating conditions," IEEE Proc. Decision Control. 2, 1272–1277.
- [30] Hasan Fayazi Boroujeni, Sayed Mojtaba Shirvani Boroujeni and Reza Hemmati "Robust PID power system stabilizer design based on pole placement and nonlinear programming methods," Indian J.Sci.Technol, April 2011, Vol. 4, Issue 4, pp: 456-461.
- [31] M. A. Abido, "Pole-placement technique for PSS and TCSC-based stabilizer design using simulated annealing," Electrical power and energy systems 22 (2000) 543-554.
- [32] M. Kashki, M.A. Abido, Y.L. Abdel-Magid, (2010), "Pole placement approach for robust optimum design of PSS and TCSC-based stabilizers using reinforcement learning automata," Electrical Engineering 91 (7), pp. 383-394, 2010.
- [33] Seung Tae Cha, Jacob Østergaard, Qiuwei Wu, F. Mara, "A real-time simulation platform for power system operation", International Power Engineering Conference - IPEC , pp. 909-914, 2010.
- [34] G. Jackson, U.D. Annakkage, A. M. Gole, D. Lowe, and M.P. McShane, "A Real-Time Platform for Teaching Power System Control Design", Proceedings of International Conference on Power Systems Transients, IPST, Montreal, Canada, June 19-23, 2005.
- [35] RTDS web site; <http://www.rtds.com>.

- [36] G. K. Venayagamoorthy and S. Ray, "A neural network based optimal wide area control for a power system", in IEEE IAS Annual Meeting, Hong Kong, October 2–6, 2005.
- [37] S. Ray and G. K. Venayagamoorthy, "Real-Time Implementation of a Measurement based Adaptive Wide Area Control System Considering Communication Delays", in IET Proceedings on Generation, Transmission and Distribution, 2008.
- [38] Parrot C, Venayagamoorthy GK, "Real-Time Implementation of Intelligent Modeling and Control Techniques on a PLC Platform", IEEE Industry Applications Society Annual Meeting, Edmonton, AB, Canada, October 5-9, 2008, pp. 1-7.
- [39] Palangapour P, Mitra P, Ray S, Vanayagamoorthy GK, "DSP-Based PSO Implementation for Online Optimization of Power System Stabilizers:, Adaptive Hardware and Systems, Netherlands, June 22-25, 2008, pp. 379-384.
- [40] Anurag Srivastava, Krishnanjan Gubba Ravikumar and Greg Zweigle, " Wide-area monitoring and control using the real time digital simulator and a synchrophasor vector processor", European Transactions on Electrical Power, European Transactions on Electrical Power, Volume 21, Issue 4, pages 1521–1530, May 2011.
- [41] Vanayagamoorthy GK, "Comparison of Power System Simulation Studies on Different Platforms-RSCAD, PSCAD/EMTDC, and Simulink SimPowerSystems", International Conference on Power Systems, Operation and Planning, Praia, Cape Verde, May 22-26, 2005, pp. 38-41.
- [42] Zhuxin Li, Bonian Shi and Yingduo Han, "A novel inter-area oscillation damping design based on wide area measurements", IEEE Asia Pacific Conference on Circuits and Systems, Macao, Nov. 30 – Dec. 3, 2008, pp. 773-776.
- [43] Y. Xia, R. Yuan, Z. Zhang and W. Hu, "Damping Inter-area Modes of Oscillations and Improving Transmission Capacity Using Global PSS", International Conference on Energy and Environment Technology, ICEET '09, Guilin, Guangxi, Oct. 16-18, 2009, pp. 107-110.
- [44] P. Korba, V. Kanzkins and M. Larsson," Power System Stabilizer With Synchronized Phasor Measurements", 17th Power System Computational Conference, Stockholm, Sweden, August 22-26, 2011.
- [45] H. Wu, Qi Wang and X. Li, "PMU-Based Wide Area Damping Control of Power Systems", Joint International Conference on Power System Technology and IEEE Power India Conference, 2008, pp. 1-4.

- [46] Ke Luo, Yutian Liu and Hua Ye, "Damping Controller Design Based on Wide Area Measurement", Asia-Pacific Power and Energy Engineering Conference (APPEEC), Chengdu, March 28-31, 2010.
- [47] Erlich, I., Hashmani, A. and Shewarega, F., „Selective Damping of Inter Area Oscillations Using Phasor Measurement Unit (PMU) Signals“, PowerTech 2011 conference on June 19-23, 2011, Trondheim , NTNU.
- [48] Daniel Dotta, Aguinaldo S. e Silva, and Ildemar C. Decker, "Wide-Area Measurements Based Two-Level Control Design Considering Signal Transmission Delay", IEEE Transactions on Power Systems, Feb. 2009, pp. 208 – 216.
- [49] Zhiyuan Duan, Chengxue Zhang, Zhijian Hu and Tao Ding, "Design for multi-machine power system damping controller via particle swarm optimization approach", International Conference on Sustainable Power Generation and Supply, Nanjing, April 6-7, 2009.
- [50] Zhijian Hu and Milanovic, J.V., "Damping of Inter-area Oscillations by WAM Based Supplementary Controller", IEEE Power Engineering Society General Meeting, Tampa, FL, June 24-28, 2007.
- [51] Zhijian Hu, "H $\infty$  control of inter-area oscillations based on WAMs considering signals transmission delay", 2nd IEEE Conference on Industrial Electronics and Applications (ICIEA) 2007, Harbin, May 23-25, 2007.
- [52] Yao, W., Jiang, L., Wen, J.Y., Cheng, S.J. and Wu, Q.H., "An adaptive wide-area damping controller based on generalized predictive control and model identification", IEEE Power & Energy Society General Meeting, Calgary, AB, July 26-30, 2009.
- [53] Peng, J.C.-H., Nair, N.-K.C., Maryani, A.L. and Ahmad, A., "Adaptive Power System Stabilizer tuning technique for damping inter-area oscillations", IEEE Power and Energy Society General Meeting, Minneapolis, MN, July 25-29, 2010.
- [54] Yang Zhang, and Anjan Bose, "Design of Wide-Area Damping Controllers for Interarea Oscillations", IEEE Trans. Power Syst., vol. 23, no. 3, pp. 1136-1143, Aug. 2008.
- [55] Padhy, B. P., Srivastava, S. C. And Verma, N. K., "Robust Wide-Area TS Fuzzy Output Feedback Controller for Enhancement of Stability in Multimachine Power System", IEEE Systems Journal, vol. PP, no. 99, pp. 1-10, Sep. 2011.
- [56] Jing Ma, Tong Wang, Zengping Wang, Jie Wu and Thorp, J.S., "Design of global power systems stabilizer to damp interarea oscillations based on wide-area collocated control technique", IEEE Power and Energy Society General Meeting, San Diego, CA, July 24-29, 2011.



- [57] Li Chunyan, Chen Xiangyi and Ma Zhanjun, "Design a Wide-area PSS for damping inter-area low-frequency oscillation", the 5th IEEE Conference on Industrial Electronics and Applications (ICIEA), Taichung, June 15-17, 2010.
- [58] Chen Xiangyi, Li Chunyan, Ma Zhanjun and Zhou Weijing, "Wide-area PSS design considering the time-delay of feedback signals", International Conference on Power System Technology (POWERCON), Hangzhou, Oct. 24-28, 2010.
- [59] H. Othman and et al., "On the design of robust power system stabilizers," IEEE Proc of 28th conf on Dec. & control, pp. 1853-1857, December 1989.
- [60] Y. Yu, and Q. Li, "Pole-placement power system stabilizers design of an unstable nine-machine system," IEEE Trans. Pr Sys., vol. 5, no. 2, pp. 353-358, May 1990.
- [61] Fleming R. J., Mohan M. A., and Parvatism K., "Selection of parameters of stabilizers in multimachine power systems," Power Apparatus and Systems, IEEE Trans., vol. 100, no. 5, pp. 2329-2333, 1981.
- [62] Lefebvre S., "Tuning of stabilizers in multimachine power systems," Power Apparatus and Systems, IEEE Trans., vol. 102, no. 2, pp. 290-299, 1983.
- [63] A. Chandra, O.P. Malik, and G.S. Hope, "A self-tuning controller for the control of multi-machine power systems," IEEE Trans. on Power Systems, vol. 3, no. 3, pp. 1065-1071, August 1988.
- [64] M. Klein, L.X. Le, G.J. Rogers, S. Farrokhpay, and N.J. Balu, " $H_{\infty}$  damping controller design in large power systems," IEEE Trans. on Power Systems, vol. 10, no. 1, pp. 158-166, Feb. 1995.
- [65] H. Shu, and T. Chen, "Robust digital design of PSSs," IEEE Proc. of American control conf., Albuquerque, New Mexico, pp. 1953-1957, June 1997.
- [66] G. Boukarim, S. Wang, J. Chow, G. Taranto, and N. Martins, "A comparison of classical, robust, and decentralized control designs for multiple power system stabilizers," IEEE Trans. Power Syst., vol. 15, no. 4, pp. 1287-1292, November 2000.
- [67] F. E. Scavoni, and et al., "Design of robust power system controllers using linear matrix inequalities," 2001 IEEE Porto Power Tech Conf. 10th – 13th Sep., Porto, Portugal.
- [68] T. Senjyu, R. Kuninaka, N. Urasaki, H. Fujita, and T. Funabashi, "Power system stabilization based on robust centralized and decentralized controllers," in Proc. IEEE 7th International Power Eng. Conf. IPEC, 2005.
- [69] Folly, K.A.; Magidimisa, M., "Power Systems Stabilization Considering System Uncertainties", IEEE Power Engineering Society Inaugural Conference and Exposition in Africa, pp. 249 – 255, 2005.

- [70] G. Radman, "Design power system stabilizer based on LQG/LTR formulations," Industry Applications Society Annual Meeting, Conf. Record of the 1992 IEEE, vol. 2, pp. 1787-1792, 4-9 Oct., 1992.
- [71] M. Nambu, and Y. Ohsawa, "Development of an advance power system stabilizer using a strict linearization approach," IEEE Trans. Power Systems, vol. 11, no. 2, pp. 813-818, May 1996.
- [72] Shahab Mehraeen, Sarangapani Jagannathan and Mariesa L. Crow, "Power System Stabilization Using Adaptive Neural Network-Based Dynamic Surface Control", IEEE Transactions on Power Systems, vol. 26, no. 2, pp. 669 – 680, May 2011.
- [73] L. Cai and I. Erlich, "Simultaneous Coordinated Tuning of PSS and FACTS Damping Controllers in Large Power Systems," IEEE Trans. Power Syst., Vol. 20, no. 1, pp. 294–300, Feb. 2005.
- [74] N. Hosseinzadeh, & A. Kalam, "A direct adaptive fuzzy PSS," IEEE Trans. Energy Con., vol. 14, no. 4, pp. 1564-1571, December 1999.
- [75] J. Lu, & et al., "A fuzzy logic-based adaptive PSS for multi-machine systems," IEEE, pp. 111-115, 2000.
- [76] J. Lu, & et al., "A fuzzy logic-based adaptive PSS for multi-machine systems," EPSR 60 (2001) 115-121.
- [77] A. M. Sharaf, & et al., "A self adjusting PSS," IEEE Proc of Canadian conf on Elec. & computer engineering, Edmonton, Canada, pp. 1298-1303, May 1999
- [78] T. Abdelazim, & O. P. Malik, "An adaptive PSS using on-line self-learning fuzzy systems," IEEE, pp. 1715-1720, 2003.
- [79] J. Ritonja, & et al., "Design of an adaptive PSS," IEEE, ISIE'99-Bled, Slovenia, pp. 1306-1311, 1999.
- [80] W. Gu, "System damping improvement using adaptive PSS," IEEE Proc of Canadian conf on Elec. & computer engineering, Edmonton, Canada, pp. 1245-1247, May 1999.
- [81] Y.L. Abdel-Magid, M. Bettayeb, M.M. Dawoud, "Simultaneous Stabilization of Power Systems using Genetic Algorithms" in IEE Proceedings Generation Transmission Distribution, Vol. 144, No. 1, Pp. 39- 44, 1977.
- [82] Y. L. Abdel-Magid, & M. A. Abido, "Optimal multiobjective design of robust PSSs using genetic algorithms," IEEE Trans. Power Sys., vol. 18, no. 3, pp. 1125-1132, August 2003.
- [83] A. Andreoiu, & K. Bhattacharya, "Lyapunov's method based genetic algorithm for multi-machine PSS tuning," IEEE, pp. 1495-1500, 2002.

- [84] Y. L. Abdel-Magid, & et al., "Power system output feedback stabilizer design via genetic algorithms," IEEE conf. publication no. 446, pp. 56-62, September 1997.
- [85] A. Hasanovic, & A. Feliachi, "Genetic algorithm based inter-area oscillation damping controller design using matlab," IEEE, pp. 1136-1141, 2002.
- [86] M. A. Abido, & Y. L. Abdel-Magid, "Coordinated design of a PSS and an SVC-based controller to enhance power system stability," EPSR 25 (2003) 695-704.
- [87] Y. L. Abdel-Magid, M. A. Abido, S. Al-Baiyat, and A. H. Mantawy, "Simultaneous Stabilization of Multimachine Power System via Genetic Algorithms," IEEE Trans. On Power Systems, vol. 14, no. 4, pp. 1428-1439, Nov 1999.
- [88] Y. L. Abdel-Magid, M. A. Abido, and A. H. Mantawy, "Robust Tuning of Power System Stabilizers in Multimachine Power Systems," IEEE Trans. On Power System, vol. 15, no. 2, pp. 735-740, May 2000.
- [89] M. A. Abido, and Y. L. Abdel-Magid, "Eigenvalue assignments in multimachine power systems using tabu search algorithm," Computer and Electrical engineering 28 (2002) 527-545.
- [90] S. Dechanupaprittha, and I. Ngamroo, "Design of robust power system stabilizers in multimachine power system using tabu search algorithm," IEEE International Conf. On Industrial Technology, 2002. IEEE ICIT '02, vol. 1, pp. 291-296, 11-14 Dec. 2002.
- [91] M. A. Abido, and Y. L. Abdel-Magid, "Robust design of electrical power-based stabilizers using tabu search," IEEE Power Engineering Society Summer Meeting, vol. 3, pp. 1573-1578, 15-19 July 2001.
- [92] . A. Abido, and Y. L. Abdel-Magid, "Robust design of multimachine power system stabilisers using tabu search algorithm," IEE Proceedings - Generation Transmission and Distribution, vol. 147, no. 6, pp. 387-394, Nov. 2000.
- [93] M. Soliman, E. H. E. Bayoumi, and M. F. Hassan, "PSO - Based Power System Stabilizer for Minimal Overshoot and Control Constraints", Journal of Electrical Engineering, Vol. 59, No. 3, Pp. 153-159, 2008.
- [94] M. A. Abido, "Particle swarm optimization for multi-machine PSS design," IEEE Power Engineering Society Summer Meeting, vol. 3, pp. 1346-1351, 2001.
- [95] M. A. Abido, "Optimal design of PSSs using particle swarm optimization," IEEE Trans. on Energy Conversion, vol. 17, no. 3, pp. 406-413, September 2002.
- [96] M. A. Abido, "Pole-placement technique for PSS and TCSC-based stabilizer design using simulated annealing," Electrical power and energy systems 22 (2000) 543-554.

- [97] M. A. Abido, "An efficient heuristic optimization technique for robust PSS design," *EPSR* 58 (2001) 53-62.
- [98] M. A. Abido, "Simulated annealing based approach to PSS and FACTS based stabilizer tuning," *Electrical power and energy systems* 22 (2000) 247-258.
- [99] M. A. Abido, "Robust design of multimachine PSSs using simulated annealing," *IEEE Trans. on Energy Conversion*, vol. 15, no. 3, pp. 297-304, September 2000.
- [100] Y. Hsu, & C. Chen, "Tuning of PSSs using an artificial neural network," *IEEE Trans. on Energy Conversion*, vol. 6, no. 4, pp. 612-619, December 1991.
- [101] Y. Zhang, & et al., "An artificial neural network based adaptive PSS," *IEEE Trans. on Energy Conversion*, vol. 8, no. 1, pp. 71-77, March 1993.
- [102] M. A. Abido, & Y. L. Abdel-Magid, "Radial basis function network based PSSs for multi-machine power systems," *IEEE International Conf. Vol. 2*, pp. 622-626, 1997.
- [103] R. Segal, & et al., "Radial basis function network adaptive PSS," *IEEE Trans. on Power Systems*, vol. 15, no. 2, pp. 722-727, May 2000.
- [104] R. Segal, & et al., "A self-tuning PSS based on artificial neural network," *Electrical power and energy systems* 26 (2004) 423-430.
- [105] W. Liu, G.K. Venayagamoorthy, and D.C. Wunsch, "Adaptive neural network based PSS design," *IEEE Proceedings of the International Joint Conference on Neural Networks*, vol. 4, pp. 2970-2975, 20-24 July 2003.
- [106] P. Shamsollahi, & O. P. Malik, "Design of a neural adaptive PSS using dynamic back-propagation method," *Electrical power and energy systems* 22 (2000) 29-34.
- [107] Y. Park, M. Choi, and K.Y. Lee, "A wide range operation power system stabilizer design with neural networks using power flow characteristics," *IEEE International Conf. on Intelligent Systems Applications to Power Systems, Proceedings, ISAP '96.*, pp. 294-298, 1996.
- [108] P. Pugliese, R. Sbrizzai, M. Trovato, and M. La Scala, "Intelligent control of inter-area oscillations in power systems," *8th Mediterranean Electrotechnical Conference, MELECON '96*, vol. 2, pp. 737-741, 13-16 May 1996.
- [109] Soon Kiat Yee, and J.V. Milanovic, "Fuzzy Logic Controller for Decentralized Stabilization of Multimachine Power Systems," *IEEE Transactions on Fuzzy Systems*, vol. 16, no. 4, pp. 971-981, August 2008.
- [110] H. A. Toliyat, and et al., "Design of augmented fuzzy logic power system stabilizers to enhance power systems stability," *IEEE Trans. Energy Con.*, vol. 11, no. 1, pp. 97-103, March 1996.

- [111] P.V. Etingov, and N.I. Voropai, "Application of Fuzzy Logic PSS to Enhance Transient Stability in Large Power Systems," International Conference on Power Electronics, Drives and Energy Systems, 2006. PEDES '06, New Delhi, 12-15 Dec. 2006.
- [112] Y. Lee, and et al., "Design of single-input fuzzy logic control PSS," IEEE Proc of TENCON'02, pp.1901-1904, 2002.
- [113] J. Lu, & et al., "A fuzzy logic-based adaptive PSS for multimachine systems," Electric power systems research 60 (2001) 115-121.
- [114] M. A. Abido, and Y. L. Abdel-Magid, "A hybrid neuro-fuzzy power system stabilizer for multimachine power systems," IEEE Transactions on Power Systems, vol. 13, no. 4, pp. 1323 – 1330, Nov. 1998.
- [115] M. A. Abido, and Y. L. Abdel-Magid, "Tuning of a fuzzy logic power system stabilizer using genetic algorithms," IEEE International Conference on Evolutionary Computation, Indianapolis, IN, 13-16 April 1997.
- [116] K.A. El-Metwally, and O.P. Malik, "Fuzzy logic power system stabiliser," IEE Proceedings Generation, Transmission and Distribution, vol. 142, no. 3, pp. 277 – 281, May 1995.
- [117] M. Ramirez-Gonzalez, and O.P. Malik, "Simplified Fuzzy Logic Controller and Its Application as a Power System Stabilizer," 15th International Conference on Intelligent System Applications to Power Systems, 2009. ISAP '09. Curitiba, 8-12 Nov. 2009.
- [118] M. A. Abido, and Y. L. Abdel-Magid, "Optimal design of power system stabilizers using evolutionary programming," IEEE Trans. Energy Con, vol. 17, no. 4, pp. 429-436, December 2002.
- [119] Y. Y. Hsu and C. L. Chen, "Identification of optimum location for stabilizer applications using participation factors", Proc. IEE, Vol. 134, Pt.C, No.3, pp. 238-244, 1987.
- [120] E. Z. Zhou, O. P. Malik and G. S. Hope, "Theory and method for selection of power system stabilizer location", IEEE Trans. On Energy Conversion, Vol. EC-6, pp. 170-176, 1991.
- [121] A. M. A. Hamdan, "An investigation of the significance of singular value decomposition in power system dynamics", International Journal of Electric Power and Energy Systems, Vol. 21, No.6, pp. 417-427, 1999.
- [122] A. M. A. Hamdan, "Use of SVD for power system stabilizer signal selection", Electric Machines and Power Systems, Vol. 21, No.2, p 229-240, 1993.

- [123] J. C. Castro and C. S. D. Araujo, "Frequency domain analysis of oscillatory modes in decentralized control systems", *Automatica*, Vol. 34, No. 12, pp. 1647-1998.
- [124] P. Kundur, J. Paserba, et al., "Definition and Classification of Power System Stability," *IEEE Transactions on Power Systems*, vol. 19, no.2. May 2004, pp. 1387-1401.

## **VITAE**

Name: Abdulmohsen Fahad Al-Mulhim

Nationality: Saudi

Date of Birth: January 13, 1982

Email: Abdulmohsen.mulhim.1@hotmail.com

Address: Dammam, Saudi Arabia

Academic Background: Bachelor of Science (B.S.) degree in Electrical Engineering from King Fahd Univedrsity of Petroleum & Minerals (KFUPM), Dhahran, Saudi Arabia in 2004.

Working Experience: Joined Saudi Aramco in November 2004